



ISSN 2686-7575 (Online)

# ТОНКИЕ ХИМИЧЕСКИЕ ТЕХНОЛОГИИ

## Fine Chemical Technologies

- | Theoretical Bases of Chemical Technology
- | Chemistry and Technology of Organic Substances
- | Chemistry and Technology of Medicinal Compounds and Biologically Active Substances
- | Biochemistry and Biotechnology
- | Synthesis and Processing of Polymers and Polymeric Composites
- | Chemistry and Technology of Inorganic Materials
- | Analytical Methods in Chemistry and Chemical Technology
- | Mathematical Methods and Information Systems in Chemical Technology

**17(2)**

**2022**

[www.finechem-mirea.ru](http://www.finechem-mirea.ru)





ISSN 2686-7575 (Online)

# ТОНКИЕ ХИМИЧЕСКИЕ ТЕХНОЛОГИИ

Fine  
Chemical  
Technologies

- | Theoretical Bases of Chemical Technology
- | Chemistry and Technology of Organic Substances
- | Chemistry and Technology of Medicinal Compounds and Biologically Active Substances
- | Biochemistry and Biotechnology
- | Synthesis and Processing of Polymers and Polymeric Composites
- | Chemistry and Technology of Inorganic Materials
- | Analytical Methods in Chemistry and Chemical Technology
- | Mathematical Methods and Information Systems in Chemical Technology

Tonkie Khimicheskie Tekhnologii =  
Fine Chemical Technologies  
**Vol. 17, No. 2, 2022**

Тонкие химические технологии =  
Fine Chemical Technologies  
**Том 17, № 2, 2022**

<https://doi.org/10.32362/2410-6593-2022-17-2>  
[www.finechem-mirea.ru](http://www.finechem-mirea.ru)

**Tonkie Khimicheskie Tekhnologii =  
Fine Chemical Technologies  
2022, vol. 17, no. 1**

The peer-reviewed scientific and technical journal Fine Chemical Technologies highlights the modern achievements of fundamental and applied research in the field of fine chemical technologies, including theoretical bases of chemical technology, chemistry and technology of medicinal compounds and biologically active substances, organic substances and inorganic materials, biochemistry and biotechnology, synthesis and processing of polymers and polymeric composites, analytical and mathematical methods and information systems in chemistry and chemical technology.

**Founder and Publisher**

Federal State Budget

Educational Institution of Higher Education

“MIREA – Russian Technological University”

78, Vernadskogo pr., Moscow, 119454, Russian Federation.

Publication frequency: bimonthly.

The journal was founded in 2006. The name was Vestnik MITHT until 2015 (ISSN 1819-1487).

**The journal is included into the List of peer-reviewed science press of the State Commission for Academic Degrees and Titles of the Russian Federation.**

**The journal is indexed:**

SCOPUS, DOAJ, Chemical Abstracts, Science Index, RSCI, Ulrich’s International Periodicals Directory

**Editor-in-Chief:**

**Alla K. Frolkova** – Dr. Sci. (Eng.), Professor, MIREA – Russian Technological University, Moscow, Russian Federation. Scopus Author ID 35617659200, ResearcherID G-7001-2018, <http://orcid.org/0000-0002-9763-4717>,

[frolkova\\_a@mirea.ru](mailto:frolkova_a@mirea.ru)

**Deputy Editor-in-Chief:**

**Valery V. Fomichev** – Dr. Sci. (Chem.), Professor, MIREA – Russian Technological University, Moscow, Russian Federation. Scopus Author ID 57196028937, <http://orcid.org/0000-0003-4840-0655>,

[fomichev@mirea.ru](mailto:fomichev@mirea.ru)

**Executive Editor:**

**Sergey A. Durakov** – Cand. Sci. (Chem.), Associate Professor, MIREA – Russian Technological University, Moscow, Russian Federation, Scopus Author ID 57194217518, ResearcherID AAS-6578-2020, <http://orcid.org/0000-0003-4842-3283>,

[durakov@mirea.ru](mailto:durakov@mirea.ru)

**Editorial staff:**

Managing Editor Cand. Sci. (Eng.) Galina D. Seredina  
Science editors Dr. Sci. (Chem.), Prof. Tatyana M. Buslaeva  
Dr. Sci. (Chem.), Prof. Anatolii A. Ischenko  
Dr. Sci. (Eng.), Prof. Valery F. Kornushko  
Dr. Sci. (Eng.), Prof. Anatolii V. Markov  
Dr. Sci. (Chem.), Prof. Yuri P. Miroshnikov  
Dr. Sci. (Chem.), Prof. Vladimir A. Tverskoy

Desktop publishing

Larisa G. Semernya

86, Vernadskogo pr., Moscow, 119571, Russian Federation.

Phone: +7(495) 246-05-55 (#2-88)

E-mail: [seredina@mirea.ru](mailto:seredina@mirea.ru)

The registration number ПИ № ФС 77–74580 was issued in December 14, 2018 by the Federal Service for Supervision of Communications, Information Technology, and Mass Media of Russia

The subscription index of *Pressa Rossii*: **36924**

**Тонкие химические технологии =  
Fine Chemical Technologies  
2022, том 17, № 1**

Научно-технический рецензируемый журнал «Тонкие химические технологии» освещает современные достижения фундаментальных и прикладных исследований в области тонких химических технологий, включая теоретические основы химической технологии, химию и технологию лекарственных препаратов и биологически активных соединений, органических веществ и неорганических материалов, биохимию и биотехнологию, синтез и переработку полимеров и композитов на их основе, аналитические и математические методы и информационные системы в химии и химической технологии.

**Учредитель и издатель**

федеральное государственное бюджетное

образовательное учреждение высшего образования

«МИРЭА – Российский технологический университет»

119454, РФ, Москва, пр-кт Вернадского, д. 78.

Периодичность: один раз в два месяца.

Журнал основан в 2006 году. До 2015 года издавался под названием «Вестник МИТХТ» (ISSN 1819-1487).

**Журнал входит в Перечень ведущих рецензируемых научных журналов ВАК РФ.**

**Индексируется:**

SCOPUS, DOAJ, Chemical Abstracts,  
РИНЦ (Science Index), RSCI,  
Ulrich’s International Periodicals Directory

**Главный редактор:**

**Фролкова Алла Константиновна** – д.т.н., профессор, МИРЭА – Российский технологический университет, Москва, Российская Федерация. Scopus Author ID 35617659200, ResearcherID G-7001-2018, <http://orcid.org/0000-0002-9763-4717>,

[frolkova\\_a@mirea.ru](mailto:frolkova_a@mirea.ru)

**Заместитель главного редактора:**

**Фомичёв Валерий Вячеславович** – д.х.н., профессор, МИРЭА – Российский технологический университет, Москва, Российская Федерация. Scopus Author ID 57196028937, <http://orcid.org/0000-0003-4840-0655>,

[fomichev@mirea.ru](mailto:fomichev@mirea.ru)

**Выпускающий редактор:**

**Дураков Сергей Алексеевич** – к.х.н., доцент, МИРЭА – Российский технологический университет, Москва, Российская Федерация, Scopus Author ID 57194217518, ResearcherID AAS-6578-2020, <http://orcid.org/0000-0003-4842-3283>,

[durakov@mirea.ru](mailto:durakov@mirea.ru)

**Редакция:**

Зав. редакцией к.т.н. Г.Д. Середина  
Научные редакторы д.х.н., проф. Т.М. Буслева  
д.х.н., проф. А.А. Ищенко  
д.т.н., проф. В.Ф. Корнюшко  
д.т.н., проф. А.В. Марков  
д.х.н., проф. Ю.П. Мирошников  
д.х.н., проф. В.А. Тверской

Компьютерная верстка

Л.Г. Семерня

119571, Москва, пр. Вернадского, 86, оф. Л-119.

Тел.: +7(495) 246-05-55 (#2-88)

E-mail: [seredina@mirea.ru](mailto:seredina@mirea.ru)

Регистрационный номер и дата принятия решения о регистрации СМИ: ПИ № ФС 77-74580 от 14.12.2018 г. СМИ зарегистрировано Федеральной службой по надзору в сфере связи, информационных технологий и массовых коммуникаций (Роскомнадзор)

Индекс по Объединенному каталогу «Пресса России»: **36924**

## Editorial Board

**Andrey V. Blokhin** – Dr. Sci. (Chem.), Professor, Belarusian State University, Minsk, Belarus. Scopus Author ID 7101971167, ResearcherID AAF-8122-2019 <https://orcid.org/0000-0003-4778-5872>  
[blokhin@bsu.by](mailto:blokhin@bsu.by).

**Sergey P. Verevkin** – Dr. Sci. (Eng.), Professor, University of Rostock, Rostock, Germany. Scopus Author ID 7006607848, ResearcherID G-3243-2011, <https://orcid.org/0000-0002-0957-5594>,  
[sergey.verevkin@uni-rostock.de](mailto:sergey.verevkin@uni-rostock.de).

**Konstantin Yu. Zhizhin** – Corresponding Member of the Russian Academy of Sciences (RAS), Dr. Sci. (Chem.), Professor, N.S. Kurnakov Institute of General and Inorganic Chemistry of the RAS, Moscow, Russian Federation. Scopus Author ID 6701495620, ResearcherID C-5681-2013, <http://orcid.org/0000-0002-4475-124X>,  
[kyuzhizhin@igic.ras.ru](mailto:kyuzhizhin@igic.ras.ru).

**Igor V. Ivanov** – Dr. Sci. (Chem.), Professor, MIREA – Russian Technological University, Moscow, Russian Federation. Scopus Author ID 34770109800, ResearcherID I-5606-2016, <http://orcid.org/0000-0003-0543-2067>,  
[ivanov\\_i@mirea.ru](mailto:ivanov_i@mirea.ru).

**Carlos A. Cardona** – PhD (Eng.), Professor, National University of Columbia, Manizales, Colombia. Scopus Author ID 7004278560, <http://orcid.org/0000-0002-0237-2313>,  
[ccardonaal@unal.edu.co](mailto:ccardonaal@unal.edu.co).

**Oskar I. Koifman** – Corresponding Member of the RAS, Dr. Sci. (Chem.), Professor, President of the Ivanovo State University of Chemistry and Technology, Ivanovo, Russian Federation. Scopus Author ID 6602070468, ResearcherID R-1020-2016, <http://orcid.org/0000-0002-1764-0819>,  
[president@isuct.ru](mailto:president@isuct.ru).

**Elvira T. Krut'ko** – Dr. Sci. (Eng.), Professor, Belarusian State Technological University, Minsk, Belarus. Scopus Author ID 6602297257,  
[ela\\_krutko@mail.ru](mailto:ela_krutko@mail.ru).

**Anatolii I. Miroshnikov** – Academician at the RAS, Dr. Sci. (Chem.), Professor, M.M. Shemyakin and Yu.A. Ovchinnikov Institute of Bioorganic Chemistry of the RAS, Member of the Presidium of the RAS, Chairman of the Presidium of the RAS Pushchino Research Center, Moscow, Russian Federation. Scopus Author ID 7006592304, ResearcherID G-5017-2017,  
[aiv@ibch.ru](mailto:aiv@ibch.ru).

**Aziz M. Muzafarov** – Academician at the RAS, Dr. Sci. (Chem.), Professor, A.N. Nesmeyanov Institute of Organoelement Compounds of the RAS, Moscow, Russian Federation. Scopus Author ID 7004472780, ResearcherID G-1644-2011, <https://orcid.org/0000-0002-3050-3253>,  
[aziz@ineos.ac.ru](mailto:aziz@ineos.ac.ru).

## Редакционная коллегия

**Блохин Андрей Викторович** – д.х.н., профессор Белорусского государственного университета, Минск, Беларусь. Scopus Author ID 7101971167, ResearcherID AAF-8122-2019 <https://orcid.org/0000-0003-4778-5872>  
[blokhin@bsu.by](mailto:blokhin@bsu.by).

**Верёвкин Сергей Петрович** – д.т.н., профессор Университета г. Росток, Росток, Германия. Scopus Author ID 7006607848, ResearcherID G-3243-2011, <https://orcid.org/0000-0002-0957-5594>,  
[sergey.verevkin@uni-rostock.de](mailto:sergey.verevkin@uni-rostock.de).

**Жижин Константин Юрьевич** – член-корр. Российской академии наук (РАН), д.х.н., профессор, Институт общей и неорганической химии им. Н.С. Курнакова РАН, Москва, Российская Федерация. Scopus Author ID 6701495620, ResearcherID C-5681-2013, <http://orcid.org/0000-0002-4475-124X>,  
[kyuzhizhin@igic.ras.ru](mailto:kyuzhizhin@igic.ras.ru).

**Иванов Игорь Владимирович** – д.х.н., профессор, МИРЭА – Российский технологический университет, Москва, Российская Федерация. Scopus Author ID 34770109800, ResearcherID I-5606-2016, <http://orcid.org/0000-0003-0543-2067>,  
[ivanov\\_i@mirea.ru](mailto:ivanov_i@mirea.ru).

**Кардона Карлос Ариэль** – PhD, профессор Национального университета Колумбии, Манизалес, Колумбия. Scopus Author ID 7004278560, <http://orcid.org/0000-0002-0237-2313>,  
[ccardonaal@unal.edu.co](mailto:ccardonaal@unal.edu.co).

**Койфман Оскар Иосифович** – член-корр. РАН, д.х.н., профессор, президент Ивановского государственного химико-технологического университета, Иваново, Российская Федерация. Scopus Author ID 6602070468, ResearcherID R-1020-2016, <http://orcid.org/0000-0002-1764-0819>,  
[president@isuct.ru](mailto:president@isuct.ru).

**Крутько Эльвира Тихоновна** – д.т.н., профессор Белорусского государственного технологического университета, Минск, Беларусь. Scopus Author ID 6602297257,  
[ela\\_krutko@mail.ru](mailto:ela_krutko@mail.ru).

**Мирошников Анатолий Иванович** – академик РАН, д.х.н., профессор, Институт биоорганической химии им. академиков М.М. Шемякина и Ю.А. Овчинникова РАН, член Президиума РАН, председатель Президиума Пушкинского научного центра РАН, Москва, Российская Федерация. Scopus Author ID 7006592304, ResearcherID G-5017-2017,  
[aiv@ibch.ru](mailto:aiv@ibch.ru).

**Музафаров Азиз Мансурович** – академик РАН, д.х.н., профессор, Институт элементоорганических соединений им. А.Н. Несмеянова РАН, Москва, Российская Федерация. Scopus Author ID 7004472780, ResearcherID G-1644-2011, <https://orcid.org/0000-0002-3050-3253>,  
[aziz@ineos.ac.ru](mailto:aziz@ineos.ac.ru).

**Ivan A. Novakov** – Academician at the RAS, Dr. Sci. (Chem.), Professor, President of the Volgograd State Technical University, Volgograd, Russian Federation. Scopus Author ID 7003436556, ResearcherID I-4668-2015, <http://orcid.org/0000-0002-0980-6591>, [president@vstu.ru](mailto:president@vstu.ru).

**Alexander N. Ozerin** – Corresponding Member of the RAS, Dr. Sci. (Chem.), Professor, Enikolopov Institute of Synthetic Polymeric Materials of the RAS, Moscow, Russian Federation. Scopus Author ID 7006188944, ResearcherID J-1866-2018, <https://orcid.org/0000-0001-7505-6090>, [ozerin@ispm.ru](mailto:ozerin@ispm.ru).

**Tapani A. Pakkanen** – PhD, Professor, Department of Chemistry, University of Eastern Finland, Joensuu, Finland. Scopus Author ID 7102310323, [tapani.pakkanen@uef.fi](mailto:tapani.pakkanen@uef.fi).

**Armando J.L. Pombeiro** – Academician at the Academy of Sciences of Lisbon, PhD, Professor, President of the Center for Structural Chemistry of the Higher Technical Institute of the University of Lisbon, Lisbon, Portugal. Scopus Author ID 7006067269, ResearcherID I-5945-2012, <https://orcid.org/0000-0001-8323-888X>, [pombeiro@ist.utl.pt](mailto:pombeiro@ist.utl.pt).

**Dmitrii V. Pyshnyi** – Corresponding Member of the RAS, Dr. Sci. (Chem.), Professor, Institute of Chemical Biology and Fundamental Medicine, Siberian Branch of the RAS, Novosibirsk, Russian Federation. Scopus Author ID 7006677629, ResearcherID F-4729-2013, <https://orcid.org/0000-0002-2587-3719>, [pyshnyi@niboch.nsc.ru](mailto:pyshnyi@niboch.nsc.ru).

**Alexander S. Sigov** – Academician at the RAS, Dr. Sci. (Phys. and Math.), Professor, President of MIREA – Russian Technological University, Moscow, Russian Federation. Scopus Author ID 35557510600, ResearcherID L-4103-2017, [sigov@mirea.ru](mailto:sigov@mirea.ru).

**Alexander M. Toikka** – Dr. Sci. (Chem.), Professor, Institute of Chemistry, Saint Petersburg State University, St. Petersburg, Russian Federation. Scopus Author ID 6603464176, ResearcherID A-5698-2010, <http://orcid.org/0000-0002-1863-5528>, [a.toikka@spbu.ru](mailto:a.toikka@spbu.ru).

**Andrzej W. Trochimczuk** – Dr. Sci. (Chem.), Professor, Faculty of Chemistry, Wrocław University of Science and Technology, Wrocław, Poland. Scopus Author ID 7003604847, [andrzej.trochimczuk@pwr.edu.pl](mailto:andrzej.trochimczuk@pwr.edu.pl).

**Aslan Yu. Tsvadze** – Academician at the RAS, Dr. Sci. (Chem.), Professor, A.N. Frumkin Institute of Physical Chemistry and Electrochemistry of the RAS, Moscow, Russian Federation. Scopus Author ID 7004245066, ResearcherID G-7422-2014, [tsiv@phyche.ac.ru](mailto:tsiv@phyche.ac.ru).

**Новаков Иван Александрович** – академик РАН, д.х.н., профессор, президент Волгоградского государственного технического университета, Волгоград, Российская Федерация. Scopus Author ID 7003436556, ResearcherID I-4668-2015, <http://orcid.org/0000-0002-0980-6591>, [president@vstu.ru](mailto:president@vstu.ru).

**Озерин Александр Никифорович** – член-корр. РАН, д.х.н., профессор, Институт синтетических полимерных материалов им. Н.С. Ениколопова РАН, Москва, Российская Федерация. Scopus Author ID 7006188944, ResearcherID J-1866-2018, <https://orcid.org/0000-0001-7505-6090>, [ozerin@ispm.ru](mailto:ozerin@ispm.ru).

**Пакканен Тапани** – PhD, профессор, Департамент химии, Университет Восточной Финляндии, Йоенсуу, Финляндия. Scopus Author ID 7102310323, [tapani.pakkanen@uef.fi](mailto:tapani.pakkanen@uef.fi).

**Помбейро Армандо** – академик Академии наук Лиссабона, PhD, профессор, президент Центра структурной химии Высшего технического института Университета Лиссабона, Португалия. Scopus Author ID 7006067269, ResearcherID I-5945-2012, <https://orcid.org/0000-0001-8323-888X>, [pombeiro@ist.utl.pt](mailto:pombeiro@ist.utl.pt).

**Пышный Дмитрий Владимирович** – член-корр. РАН, д.х.н., профессор, Институт химической биологии и фундаментальной медицины Сибирского отделения РАН, Новосибирск, Российская Федерация. Scopus Author ID 7006677629, ResearcherID F-4729-2013, <https://orcid.org/0000-0002-2587-3719>, [pyshnyi@niboch.nsc.ru](mailto:pyshnyi@niboch.nsc.ru).

**Сигов Александр Сергеевич** – академик РАН, д.ф.-м.н., профессор, президент МИРЭА – Российского технологического университета, Москва, Российская Федерация. Scopus Author ID 35557510600, ResearcherID L-4103-2017, [sigov@mirea.ru](mailto:sigov@mirea.ru).

**Тойкка Александр Матвеевич** – д.х.н., профессор, Институт химии, Санкт-Петербургский государственный университет, Санкт-Петербург, Российская Федерация. Scopus Author ID 6603464176, ResearcherID A-5698-2010, <http://orcid.org/0000-0002-1863-5528>, [a.toikka@spbu.ru](mailto:a.toikka@spbu.ru).

**Трохимчук Анджей** – д.х.н., профессор, Химический факультет Вроцлавского политехнического университета, Вроцлав, Польша. Scopus Author ID 7003604847, [andrzej.trochimczuk@pwr.edu.pl](mailto:andrzej.trochimczuk@pwr.edu.pl).

**Тсвадзе Аслан Юсупович** – академик РАН, д.х.н., профессор, Институт физической химии и электрохимии им. А.Н. Фрумкина РАН, Москва, Российская Федерация. Scopus Author ID 7004245066, ResearcherID G-7422-2014, [tsiv@phyche.ac.ru](mailto:tsiv@phyche.ac.ru).

**CONTENTS**

**СОДЕРЖАНИЕ**

**Theoretical Bases  
of Chemical Technology**

*Frolkova A.K., Frolkova A.V., Raeva V.M.,  
Zhuchkov V. I.*

Features of distillation separation  
of multicomponent mixtures

87

**Теоретические основы  
химической технологии**

*Фролкова А.К., Фролкова А.В., Раева В.М.,  
Жучков В.И.*

Особенности ректификационного разделения  
многокомпонентных смесей

**Chemistry and Technology  
of Medicinal Compounds  
and Biologically Active Substances**

*Polivanova A.G., Solovieva I.N., Botev D.O.,  
Yuriev D.Y., Mylnikova A.N., Oshchepkov M.S.*

Bifunctional gallium cation chelators

107

**Химия и технология лекарственных  
препаратов и биологически  
активных соединений**

*Поливанова А.Г., Соловьёва И.Н., Ботев Д.О.,  
Юрьев Д.Ю., Мыльникова А.Н., Ощепков М.С.*

Бифункциональные хелаторы к катиону галлия

*Ha A.C., Nguyen Ch.D.P., Le T.M.*

Screening medicinal plant extracts for xanthine  
oxidase inhibitory activity

131

*Ha A.C., Nguyen Ch.D.P., Le T.M.*

Screening medicinal plant extracts for xanthine  
oxidase inhibitory activity

## Biochemistry and biotechnology

*Pashkov E.A., Korotyshcheva M.O., Pak A.V., Faizuloev E.B., Sidorov A.V., Poddubikov A.V., Bystritskaya E.P., Dronina Yu.E., Solntseva V.K., Zaiceva T.A., Pashkov E.P., Bykov A.S., Svitich O.A., Zverev V.V.*  
Investigation of the anti-influenza activity of siRNA complexes against the cellular genes *FLT4*, *Nup98*, and *Nup205* *in vitro*

140

## Synthesis and Processing of Polymers and Polymeric Composites

*Dulina O.A., Eskova E.V., Tarasenko A.D., Kotova S.V.*  
Influence of various factors on surface properties of elastomeric materials based on nitrile butadiene rubbers

152

*Kirshanov K.A., Gervald A.Yu., Toms R.V., Lobanov A.N.*  
Obtaining phthalate substituted post-consumer polyethylene terephthalate and its isothermal crystallization

164

## Chemistry and Technology of Inorganic Materials

*Kornilov A.D., Grigoriev M.S., Savinkina E.V.*  
Comparison of the rare earth complexes iodides and polyiodides with biuret

172

## Биохимия и биотехнология

*Пашков Е.А., Коротышева М.О., Пак А.В., Файзулов Е.Б., Сидоров А.В., Поддубиков А.В., Быстрицкая Е.П., Дронина Ю.Е., Солнцева В.К., Зайцева Т.А., Пашков Е.П., Быков А.С., Свитич О.А., Зверев В.В.*  
Исследование противогриппозной активности комплексов миРНК против клеточных генов *FLT4*, *Nup98* и *Nup205* на модели *in vitro*

## Синтез и переработка полимеров и композитов на их основе

*Дулина О.А., Еськова Е.В., Тарасенко А.Д., Котова С.В.*  
Влияние различных факторов на поверхностные свойства эластомерных материалов на основе бутадиен-нитрильных каучуков

*Киришанов К.А., Гервальд А.Ю., Томс Р.В., Лобанов А.Н.*  
Получение фталатзамещенного вторичного полиэтилентерефталата и изучение его изотермической кристаллизации

## Химия и технология неорганических материалов

*Корнилов А.Д., Григорьев М.С., Савинкина Е.В.*  
Сравнение иодидов и полииодидов комплексов редкоземельных элементов с биуретом

**THEORETICAL BASES OF CHEMICAL TECHNOLOGY**

**ТЕОРЕТИЧЕСКИЕ ОСНОВЫ ХИМИЧЕСКОЙ ТЕХНОЛОГИИ**

---

ISSN 2686-7575 (Online)

<https://doi.org/10.32362/2410-6593-2022-17-2-87-106>



UDC 554.015+661.7

RESEARCH ARTICLE

## Features of distillation separation of multicomponent mixtures

**Alla K. Frolkova**✉, **Anastasiya V. Frolkova**, **Valentina M. Raeva**, **Valery I. Zhuchkov**

*MIREA – Russian Technological University (M.V. Lomonosov Institute of Fine Chemical Technologies), Moscow, 119571 Russia*

✉ Corresponding author, e-mail: [frolkova@gmail.com](mailto:frolkova@gmail.com)

### Abstract

**Objectives.** To improve the process of developing energy-efficient flowsheets for the distillation separation of multicomponent aqueous and organic mixtures based on a comprehensive study of the phase diagram structures, including those in the presence of additional selective substances.

**Methods.** Thermodynamic-topological analysis of phase diagrams; modeling of phase equilibria in the AspenTech software package using the equations of local compositions: Non-Random Two Liquid and Wilson; computational experiment to determine the column parameters for separation flowsheets of model and real mixtures of various nature.

**Results.** The fractionation conditions of the origin multicomponent mixture due to the use of sharp distillation, pre-splitting process, extractive distillation with individual and binary separating agents were revealed. The columns operation parameters and the energy consumption of the separation flowsheets ensuring the achievement of the required product quality with minimal energy consumption were determined.

**Conclusions.** Using the original methods developed by the authors earlier and based on the generalization of the results obtained, new approaches to the synthesis of energy-efficient multicomponent mixtures separation flowsheets were proposed. The provisions that form the methodological basis for the development of flowsheets for the separation of multicomponent mixtures and supplement the standard flowsheet synthesis plan with new procedures were formulated.

**Keywords:** distillation, technological flowsheet, phase diagram structure, separatrix manifold, extractive distillation

**For citation:** Frolkova A.K., Frolkova A.V., Raeva V.M., Zhuchkov V.I. Features of distillation separation of multicomponent mixtures. *Tonk. Khim. Tekhnol. = Fine Chem. Technol.* 2022;17(2):87–106 (Russ., Eng.). <https://doi.org/10.32362/2410-6593-2022-17-2-87-106>

НАУЧНАЯ СТАТЬЯ

# Особенности ректификационного разделения МНОГОКОМПОНЕНТНЫХ СМЕСЕЙ

А.К. Фролкова<sup>✉</sup>, А.В. Фролкова, В.М. Раева, В.И. Жучков

МИРЭА – Российский технологический университет (Институт тонких химических технологий им. М.В. Ломоносова), Москва, 119571 Россия

<sup>✉</sup>Автор для переписки, e-mail: frolokova@gmail.com

## Аннотация

**Цели.** Совершенствование процесса разработки энергоэффективных схем ректификационного разделения многокомпонентных водных и органических смесей на основе комплексного исследования структуры фазовой диаграммы, в том числе в присутствии селективных дополнительных веществ.

**Методы.** Термодинамико-топологический анализ фазовых диаграмм; моделирование фазовых равновесий в программном комплексе AspenTech с использованием уравнений локальных составов Non-Random Two Liquid, Вильсона; вычислительный эксперимент по определению параметров работы колонн схем разделения модельных и реальных смесей разной природы.

**Результаты.** Выявлены условия фракционирования исходной многокомпонентной смеси за счет использования промежуточного заданного разделения, предварительного расслаивания, экстрактивной ректификации с индивидуальными и бинарными разделяющими агентами. Определены параметры работы колонн и энергозатраты схем разделения, обеспечивающие достижение требуемого качества продуктов при минимальных энергозатратах.

**Выводы.** С использованием разработанных ранее авторами оригинальных методик и на основе обобщения полученных результатов предложены новые подходы к синтезу энергоэффективных схем разделения многокомпонентных смесей. Сформулированы положения, которые составляют методологическую основу разработки принципиальных схем разделения многокомпонентных смесей и дополняют типовой план синтеза схем новыми процедурами.

**Ключевые слова:** ректификация, технологическая схема, структура фазовой диаграммы, сепаратрическое многообразие, экстрактивная ректификация

**Для цитирования:** Фролкова А.К., Фролкова А.В., Раева В.М., Жучков В.И. Особенности ректификационного разделения многокомпонентных смесей. *Тонкие химические технологии*. 2022;17(2):87–106. <https://doi.org/10.32362/2410-6593-2022-17-2-87-106>

## INTRODUCTION

The development of technology for the production and isolation of organic substances is a complex scientific and technical task. The specificity of its solution is due to the complexity of the resulting mixtures, the nonlinearity of the dependencies of the mixture properties on the composition, and the presence of alternative process structuring options. One of the key problems is the polyvariance of technological solutions at each of the stages (chemical transformation and separation stages) of technology development (Fig. 1) [1–4].

The most energy-consuming processes in organic petrochemical synthesis technologies and in related industries are the processes of distillation separation of mixtures aimed at isolating required quality products, unreacted raw materials, additional substances, etc.

Figure 2 shows a flowchart describing the relationship between the various stages of the separation flowsheet synthesis procedure.

The determining role is assigned to the mixture physicochemical properties study, which determine the structure of the phase equilibrium diagram (SPED)

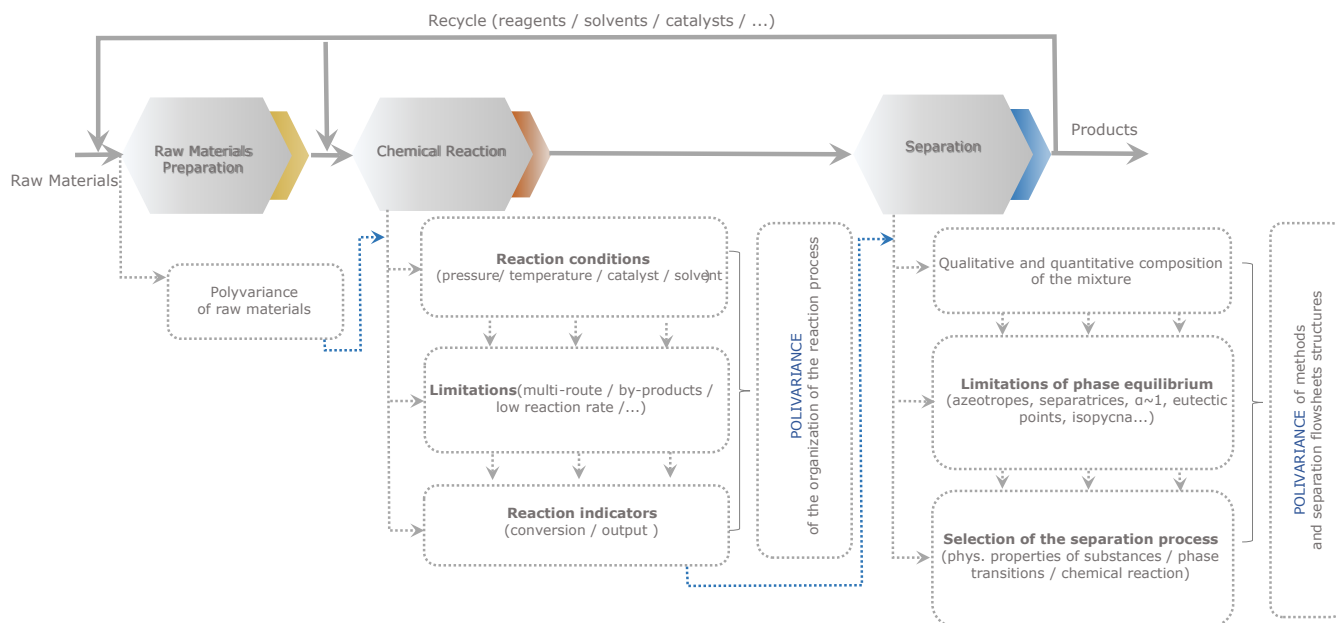


Fig. 1. Main stages of the organic compound production technology development.

(liquid–vapor, liquid–liquid, liquid–liquid–vapor). Data on the diagram structure and the system behavior when external parameters change (for example, pressure) underlie the choice of separation methods that can potentially be used in the flowsheets. Further, possible separation flowsheets are synthesized, and the structure of the latter directly depends on the belonging of the point of composition of the mixture to the specific distillation subregion (or splitting area) in the diagram. Moreover, the process from which separation begins is selected (conventional distillation, splitting, addition of separating

agents (SA), etc.). For multicomponent mixtures, essentially, we are talking about methods of its fractionation—separation into parts containing fewer components, which allow us to use a large amount of accumulated information about the separation features of binary and triple systems.

At the next stage, it is possible to discriminate between individual options, for example, by the number of devices in the flowsheet, the limitations inherent in a particular method or separation mode. In this case, qualitative criteria and heuristic rules are used for the formation of a set of alternative

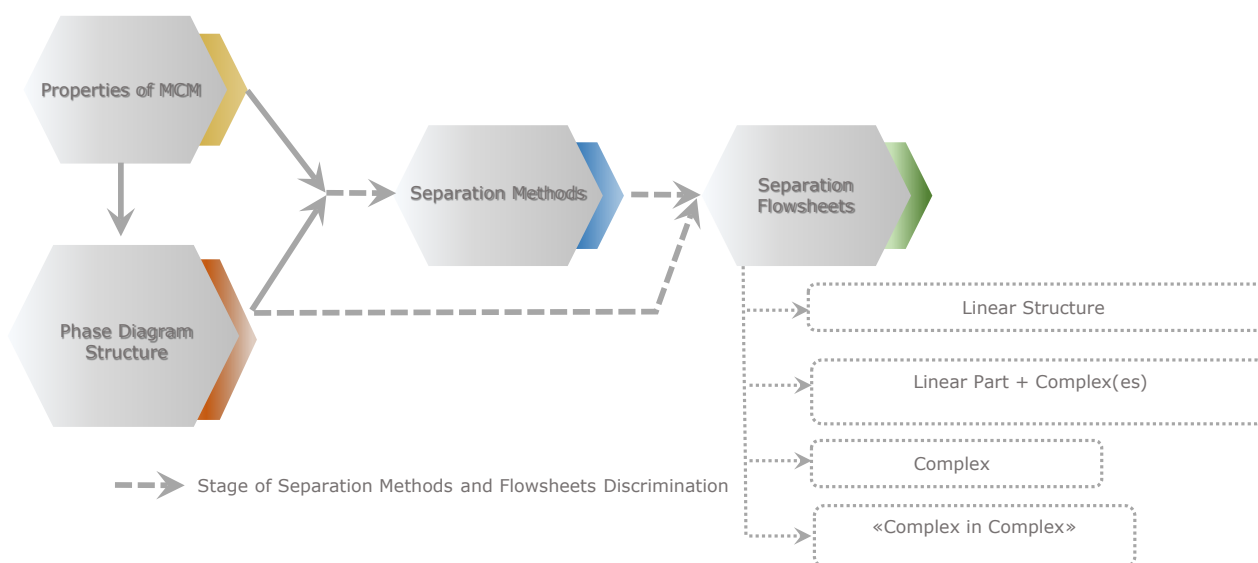


Fig. 2. Flowchart of the procedure for the synthesis of technological distillation flowsheets.

flowsheets that are subject to comparison by the selected criterion. These flowsheets can have a linear structure (a direct sequence of devices) or contain separation complexes as elements [5–7]. A characteristic feature of separation complexes is the presence of reverse (recycle) flows. There are virtually no qualitative criteria for screening flowsheets at this stage. According to the results of work [6], preference should be given to a simpler variant in structure (without feedbacks or with a minimum number of recycling flows). The final choice of the separation flowsheet is carried out only after simulating the processes and determining the device design and operating parameters (parametric optimization stage).

This algorithm in an enlarged form reflects a typical plan for the synthesis of basic technological distillation flowsheets (TDFS) [3], forms the basis of engineering research and has powerful information support in the form of modern software systems based on phase equilibria and processes mathematical modeling methods and on the use of extensive databases of physicochemical, thermodynamic data, and model parameters. The scientific and technical literature predominantly presents studies of binary and ternary mixtures [8–16], less often quaternary mixtures [17–21]. Review works [22, 23] are also devoted to the separation of binary and ternary mixtures, in particular, extractive distillation (ED). At the same time, quite a few multicomponent systems with internal azeotropes have been found [24–30].

The information presented in the appendices to [5] partially reflects the existing picture of the study of systems containing a different number of components (Table 1).

Usually, one method of separating a specific composition mixture and a fixed structure flowsheet is

proposed, which is subject to parametric optimization. In rare cases, alternative separation methods and all possible separation flowsheet structures are considered. Since distillation is the main method for separation in large-scale production of basic organic and petrochemical synthesis in related industries, we will consider this method in the future, which, despite its energy intensity, dominates in modern chemical technologies. The development of fundamental TDFS is based on the achievements of the scientific school of Professor L.A. Serafimov, created at the M.V. Lomonosov Moscow State Academy of Fine Chemical Technology in the 1960s and 1970s and has not lost the relevance of his research at the present time.

The synthesis of a TDFS set is based on the thermodynamic-topological analysis of the SPED [1, 3], the principle of redistribution of composition fields between separation areas [3, 5], the already mentioned standard plan containing the stages and procedures for the development of possible TDFS. This work is devoted to improving the procedures for developing and creating energy-efficient flowsheets for the distillation separation of multicomponent aqueous and organic mixtures based on a comprehensive study of the initial system phase diagram structure, as well as the properties of derived systems containing selective additional substances (SA). The choice of complex  $n$ -component systems as objects (where  $n$  takes values of 4 and higher) dictates the need to create new methods for studying multidimensional phase diagrams and the use of complex structure flowsheets representing a combination of a linear part and complexes with recycling flows, several functional complexes, and complexes in a complex.

Multicomponent systems (MCS), on the one hand, are closest in their properties to real

**Table 1.** Ratios of the number of publications devoted to the separation of mixtures with different numbers of components (based on materials [5])

Number of components in mixture	Number of systems studied	Number of separation variants suggested
2	70 (48.3%)	187 (72.5%)
3	43 (29.7%)	37 (14.3%)
≥ 4	32 (22.0%)	34 (13.2%)
Total	145 (100%)	258 (100%)

mixtures formed at different chemical production stages, which increases the practical value of the recommendations being developed. On the other hand, the MCS phase diagrams and their thermodynamic transformations have a number of features that distinguish them into a MCS class, which is determined by the composition space multidimensionality. It can be stated [31–33] that ternary mixtures occupy an intermediate position between binary and quaternary ones and in some cases it is impossible to extend the known laws of constructing phase diagrams of ternary systems to systems with a large number of components. This is confirmed by the new approaches to the study of the internal space of composition simplices of four- and five-component systems, developed by us [32]. A technique for studying the internal space of phase diagrams of  $n$ -component systems based on the analysis of the simplex two-dimensional boundary space structure was created. This technique has been successfully tested on the example of fifteen quaternary and four five-component systems containing substances of different classes and characterized by different complexity of phase behavior: the presence of azeotropes of different compositions and types, including those five with internal singular points. In particular, previously unknown quaternary azeotropes have been predicted in the ethyl acetate–ethanol–hexane–water and ethanol–chloroform–cyclohexane–water systems. In the latter, the presence of azeotrope is confirmed by our own field experiment. Using the example of the acetone–methyl acetate–chloroform–cis-dichloroethylene system, the specificity of the formation of a two-dimensional separatrix in a tetrahedron in the absence of a closed contour on a two-dimensional scan of the simplex is shown: some of the boundary elements of the separatrix coincide with the edges of the tetrahedron.

The study of the evolution of vapor–liquid equilibrium (VLE) diagrams of acetone–chloroform–ethanol–water systems (appearance/disappearance of a quaternary azeotrope of the saddle type, ternary nodal azeotrope) and chloroform–ethanol–cyclohexane–water systems (appearance/disappearance of a quaternary azeotrope of the node type) [34] demonstrates the possibilities of directional transformation of phase diagram structures with varying pressure and the creation of more favorable conditions for the separation of complex mixtures.

This article provides an overview of the authors' current work, as well as presents new results that illustrate certain provisions of the methodology for the synthesis of basic TDFS mixtures containing four or more components.

## RESULTS AND DISCUSSION

The study of the problem of separation of complex chemically inert multicomponent mixtures allows us to identify a number of fundamental points that complement to varying degrees the algorithm for the synthesis of flowsheets described in [3]. Most of the systems considered contain components, including homologues belonging to different classes of organic compounds, and water. These systems are characterized by the presence of azeotropes of different composition, separatrix manifolds of different structures (simplex, complex), and regions of two- and three-phase splitting. With a complex structure of the phase diagram, the elements of the TDFS most often are not single columns, but separation functional complexes based on one or different special separation techniques [1, 3, 5].

For the separation of mixtures of different compositions belonging to different distillation regions, a promising technique is the fractionation of the initial multicomponent mixture already at the first stage (in the first apparatus of the flowsheet). We have considered the following methods of fractionation of initial mixtures: 1) organizing a sharp distillation (absence of components distributed between distillate and bottom products) [35–39]; 2) preliminary splitting the mixture (in the case of a favorable arrangement of liquid–liquid tie-lines, which allows obtaining compositions of equilibrium layers in different regions of distillation); 3) use of ED in the presence of SA, selective with respect to the group of initial components [40, 41].

The possibility of implementing these MCS fractionating methods depends on the specifics of the system phase behavior and the initial mixture composition. The use of the sharp distillation at the first distillation stage is limited to system classes in which there are no internal separating surfaces, as well as areas of compositions of the initial mixture favorable for such separation [35]. This type of fractionation has shown its advantage over the modes of the direct and indirect sequences in the industrial mixtures separation flowsheets for the production of cyclohexanone [42, 43], methyl isobutyl ketone [36], and acetic anhydride [37, 38], as well as in the various solvents regeneration processes [36, 37].

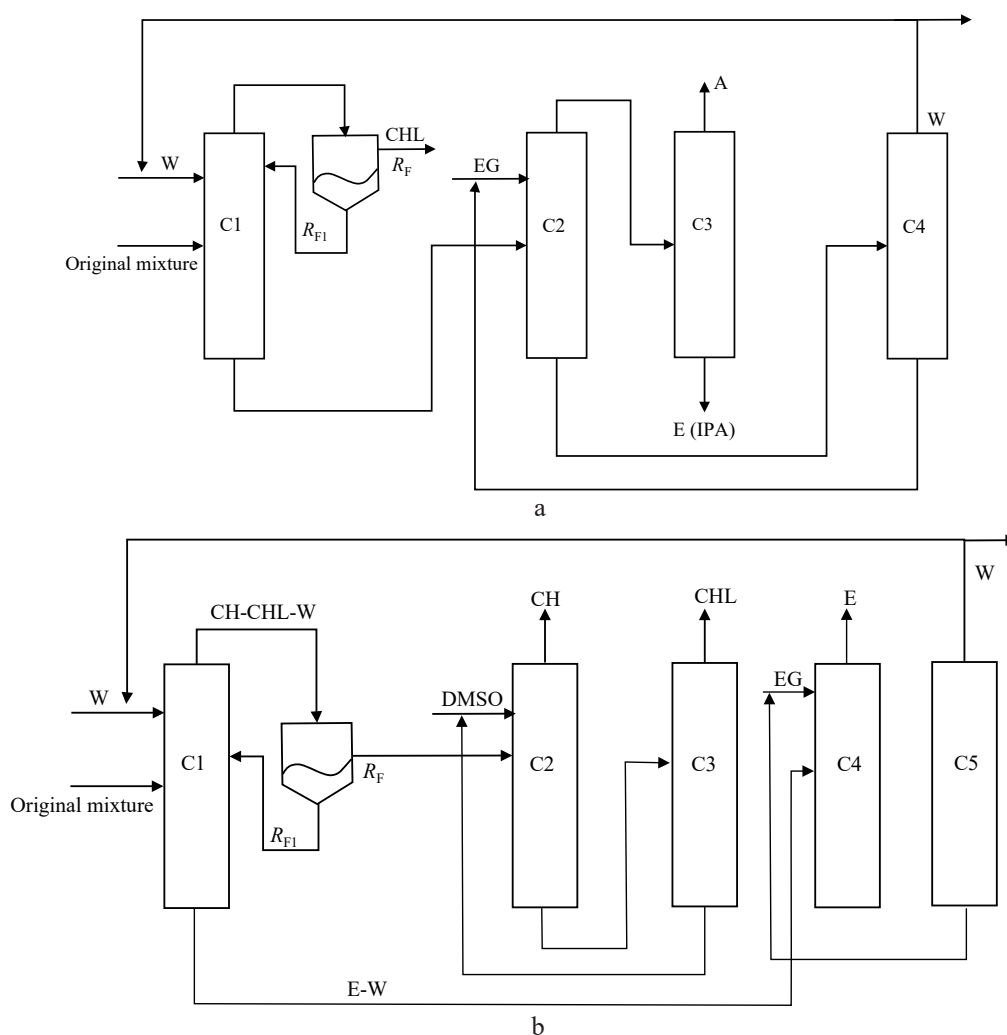
The use of preliminary fractionation due to the mixture splitting is associated with the liquid–liquid and liquid–vapor equilibrium peculiarities. The use of this technique is advisable if, as a result of separation, one or more components are almost in full in one of the equilibrium layers. The mutual arrangement

of separating manifolds and splitting simplices plays an important role. As an example, the separation of a mixture of solvents water–cyclohexanone–dichloroethane–butanol-1–dimethylformamide can be given here [20]. Water forms azeotropes with almost all components, however, when splitting the mixture of the composition supplied for separation, this component is present in the organic layer in impurity quantities that do not affect further separation. The mixture is separated in conventional distillation columns, with the exception of a cyclohexanone–dimethylformamide pair forming a positive azeotrope.

The use of SA, selective with respect to a group of components in the ED process or forming a heteroazeotrope with a group of components in heteroazeotropic (extractive-heteroazeotropic) distillation, is also an effective mixture fractionation method. It is advisable to use this technique when none of the listed above methods can be implemented. Most often, this situation is observed for systems characterized by a complex structure of the VLE diagram. The presence of water in the initial mixture, which increases the volatility of some components relative to others, allows it to be used

as a solvent for the (auto)extractive, heteroazeotropic or extractive-heteroazeotropic distillation process [44–47]. Figure 3 shows the separation flowsheets of a number of mixtures listed above, and Table 2 shows the static parameters of the columns and energy consumption in the columns and flowsheets.

If the size and localization of the splitting area in a quaternary system does not allow isolating all the components in flowsheets combining distillation and liquid splitting, then it is possible to apply an ED of an aqueous mixture with a specially selected SA. This SA should be selective with respect to azeotrope-forming components, and its introduction does not increase the splitting area in the derivative system separable mixture + SA [40]. An example is the ED of a mixture of methanol (M)–*tert*-butyl alcohol (TBA)–methyl *tert*-butyl ether (MTBE)–water (W), the phase diagram of which is characterized by the presence of three azeotropes and a separatrix manifold (Fig. 4). The separation of the M–TBA–MTBE–W mixture is proposed to be carried out in a flowsheet consisting of two-column ED complexes and a distillation column (Fig. 5).



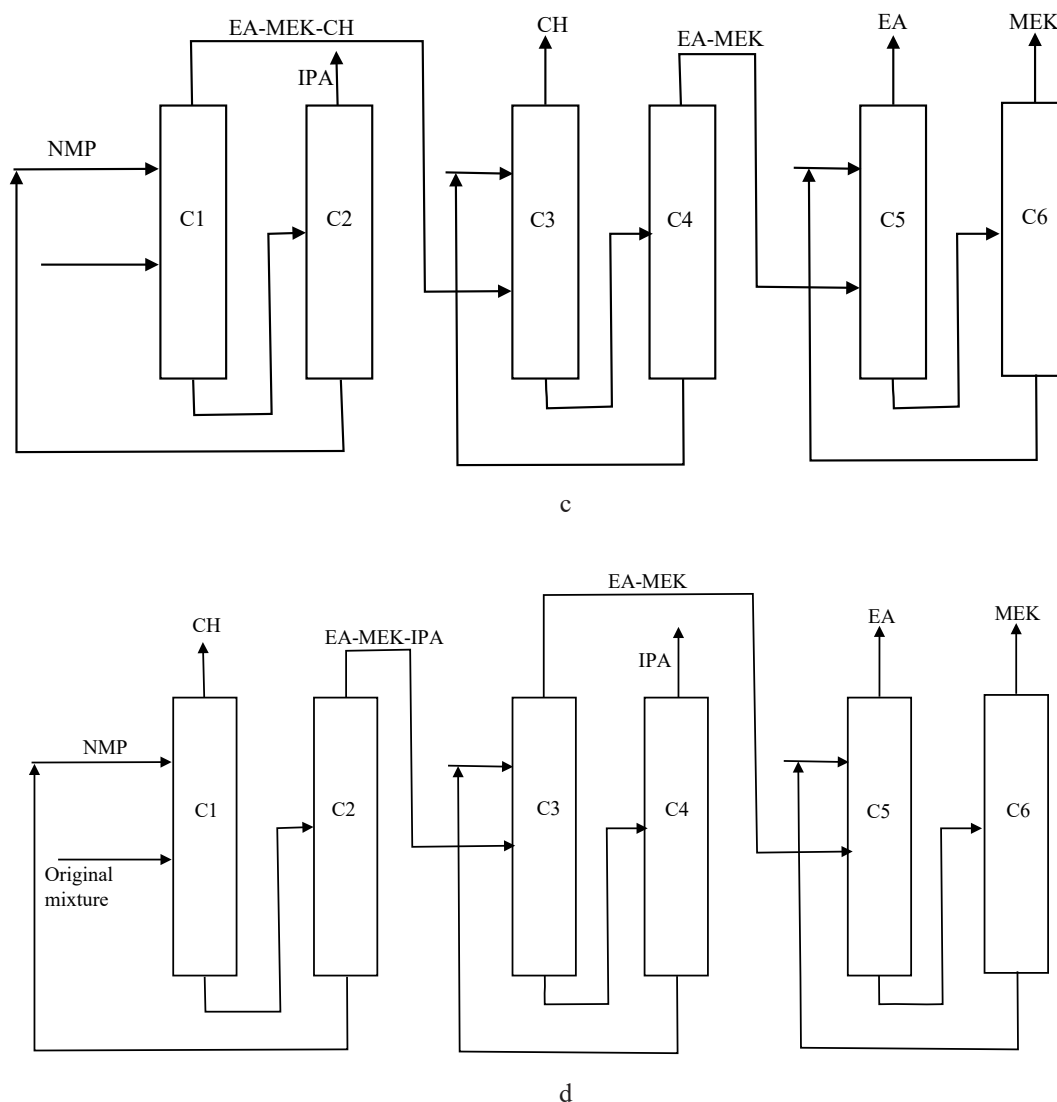


**Fig. 3.** Separation flowsheets for mixtures: (a) acetone (A)–chloroform (CHL)–ethanol (E) (isopropanol (IPA))–water (W); (b) chloroform (CHL)–ethanol (E)–cyclohexane (CH)–water (W); (c)–(d) ethyl acetate (EA)–methyl ethyl ketone (MEK)–cyclohexane (CH)–isopropanol (IPA) (EG is ethylene glycol, DMSO is dimethyl sulfoxide, NMP is *N*-methylpyrrolidone). C1–C6 are distillation columns;  $R_n$  and  $R_f$  are flows of equilibrium liquid phases from the decanter).

When separating quaternary systems containing more than three binary azeotropes, it is possible to use different agents at different stages of ED separation [40, 41]. For ED ternary aqueous mixtures of organic solvents, it is usually recommended to use dimethyl sulfoxide (DMSO), glycerin, or diols [48–53]. For the separation of a mixture of methanol (M)–*tert*-butyl alcohol (TBA)–methyl *tert*-butyl ether (MTBE)–water (W) industrial solvents, DMSO, and ethylene glycol (EG) are considered. The flowsheet shown in Fig. 5 provides for the introduction of a single DMSO or EG agent into the ED columns (columns C1, C4), as well as the use of these agents in different ED columns.

The component separation sequence in the flowsheet is determined by the nature of the SA's effect on the relative volatility of substances in the derived five-component system. According to the data of the M(1)–MTBE(2)–TBA(3)–W(4)–SA VLE systems, the relative volatility of the  $\alpha_{ij}$  components was calculated at 101.32 kPa, depending on the amounts of injected SA. In the presence of both agents, concentration of the organic solvents mixture in the distillate of the ED column is predicted. For example, when the flow rate is  $F:F_{SA} = 1:1$  (kmol/kmol) we have the ratio of values  $\alpha_{ij}$ :  $\alpha_{12}$  (0.95)  $<$   $\alpha_{34}$  (1.2)  $<$   $\alpha_{13}$  (3.0)  $<$   $\alpha_{23}$  (3.2)  $<$   $\alpha_{14}$  (3.8)  $<$   $\alpha_{24}$  (4.0), for EG, and  $\alpha_{12}$  (0.55)  $<$   $\alpha_{13}$  (1.2)  $<$   $\alpha_{34}$  (2.5)  $<$   $\alpha_{23}$  (2.8)  $<$   $\alpha_{14}$  (3.0)  $<$   $\alpha_{24}$  (6.8), for DMSO. An increase in the

**Table 2.** Operation parameters and energy consumption ( $Q$ ) of the distillation columns for the flowsheets presented in Fig. 3 (the amount of the original mixture is 100 kmol/h, the original composition of the mixture corresponds to the azeotropic, for the chloroform–ethanol–cyclohexane –water system, an equimolar composition was analyzed)

Column ( $P^*$ , kPa)	Stages number	FS <sub>orig(SA)</sub> <sup>**</sup>	$R^{***}$	$Q$ , kW	Column ( $P^*$ , kPa)	Stages number	FS <sub>orig(SA)</sub> <sup>**</sup>	$R^{***}$	$Q$ , kW
Flowsheet (a) in Fig. 3 for a system with ethanol, the SA amount in C1 (water) is 180 kmol/h; in C2 (ethylene glycol) – 100 kmol/h					Flowsheet (a) in Fig. 3 for a system with isopropyl alcohol, the SA amount in C1 (water) is 180 kmol/h; in C2 (ethylene glycol) – 100 kmol/h				
C1	30	19 (9)	0.9	488.6	C1	30	16 (10)	0.8	489.4
C2	20	12 (3)	0.5	1172.3	C2	20	17 (5)	2.8	2081.3
C3	35	23	8.6	4262.7	C3	25	16	6.6	2403.0
C4	7	4	0.1	2849.1	C4	7	4	0.2	2848.5
Total energy consumption				8772.7	Total energy consumption				7821.9
Flowsheet (b) in Fig. 3: the SA amount in C1 (water) is 110 kmol/h; in C2 (DMSO) – 70 kmol/h; in C4 (ethylene glycol) – 170 kmol/h									
C1	10	7 (3)	0.2	512.1	C4	16	10 (3)	0.6	869.9
C2	14	8 (4)	0.4	469.5	C5	13	6	0.4	2704.2
C3	11	5	0.4	466.2	Total energy consumption				5021.9
Flowsheet (c) in Fig. 3: the SA amount ( <i>N</i> -methylpyrrolidone) in C1 is 300 kmol/h; in C3 – 194 kmol/h (cyclohexanol); in C5 – 57.93 kmol/h					Flowsheet (d) in Fig. 3: the SA amount ( <i>N</i> -methylpyrrolidone) in C1 is 200 kmol/h; in C3 – 212.7 kmol/h (cyclohexanol); in C5 – 57.93 kmol/h				
C1 (50)	30	19 (5)	1.4	2327.6	C1	29	16 (5)	1.6	2685.4
C2	16	5	0.8	2050.5	C2	15	6	1.0	962.7
C3 (50)	20	11 (3)	3.9	1793.5	C3 (50)	37	26 (5)	1.2	1791.0
C4	13	5	0.7	1199.8	C4	12	5	0.8	1173.9
C5 (50)	29	14 (6)	0.4	324.6	C5 (50)	29	14 (6)	0.4	324.6
C6	17	8	0.6	408.5	C6	17	8	0.6	408.5
Total energy consumption				8104.5	Total energy consumption				6046.1

\* The pressure in the columns is 101.32 kPa, except for the values given in parentheses;

\*\* FS<sub>orig(SA)</sub> is a feed stage of original mixture (separating agent);

\*\*\* Reflux ratio.

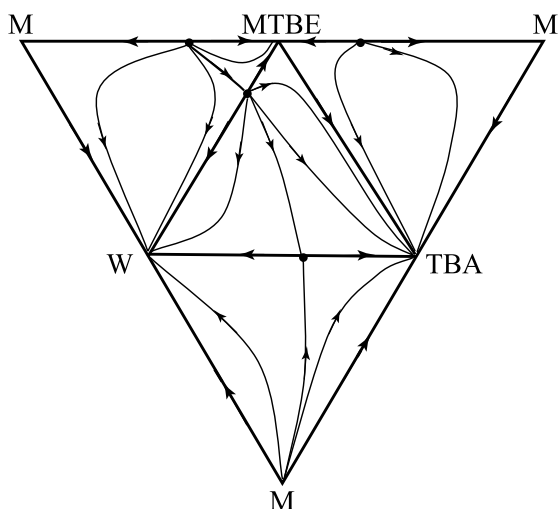


**Fig. 4.** Phase diagram of methanol (M)–*tert*-butyl alcohol (TBA)–methyl-*tert*-butyl ether (MTBE)–water (W) system at atmospheric pressure.

consumption of agents affects  $\alpha_{ij}$  differently: in the case of EG,  $\alpha_{12}$ ,  $\alpha_{34}$  increase and  $\alpha_{23}$ ,  $\alpha_{24}$  decrease, and the values of  $\alpha_{13}$  and  $\alpha_{14}$  increase to  $F:F_{SA} \approx 1:1$  and then go down. In the case of DMSO, a similar effect is observed for other pairs of components:  $\alpha_{12}$ ,  $\alpha_{14}$ , and  $\alpha_{34}$  increase,  $\alpha_{13}$  and  $\alpha_{23}$  decrease, and  $\alpha_{24}$  first increases, then decreases. The complex nature of the influence of agents on  $\alpha_{ij}$  leads to inversions of the relative volatility of the components when the flow rate of agents changes. The purpose of the ED of the quaternary mixture is the dehydration of organic solvents, achieved at different costs of EG and DMSO (Tables 3–6).

Then, ED is used to separate the azeotropic M–MTBE mixture (column C4, Fig. 5). With the introduction of EG, methanol is predicted to be obtained in the distillate of the ED column, and MTBE—in the case of DMSO introduction. For the ratio  $F:F_{SA} = 1:1$  (kmol/kmol), the relative volatility values are:  $\alpha_{12} = 1.4$  for EG and  $\alpha_{21} = 2.3$  for DMSO.

Since both EG and DMSO can be used in ED, it is possible to compare four variants of ED, differing in sets of agents for columns C1 and C4: 1) EG, EG, 2) DMSO, DMSO, 3) EG, DMSO, and 4) DMSO, EG. The calculation results of static parameters for the operation of the flowsheet columns necessary for this comparison are given in Tables 3–6. Accepted designations of the parameters of the columns:  $N$  is the total efficiency, theoretical stages (t.s.);  $N_F/N_{SA}$  are the numbers of the stages of the feed of the initial mixture and SA, respectively, t.s.;  $R$  is the reflux ratio;  $F_{SA}$  is the amount of SA, kmol/h;  $Q$  is the energy consumption in the column boilers, MW;  $t_D$  and  $t_W$  are the temperatures of the distillate and the bottom product, respectively, °C. The total energy consumption for separation (the duty of the column boilers) and the total number of theoretical stages in the distillation columns of the ED flowsheet, given in Table 7, show that the separation of the M–TBA–MTBE–W mixture can be carried out with a single agent—DMSO.

In general, based on the analysis of the SPED of four- and five-component systems and the assessment of the effect of SA on the relative volatility of the azeotropic components of the MCS, basic technological flowsheets for separating mixtures have been developed and static parameters of the apparatus operation have been determined (column efficiency,

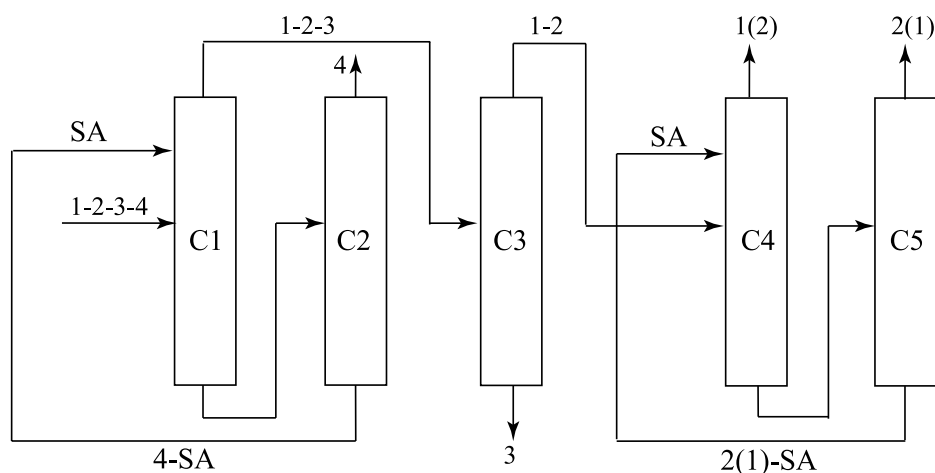


**Fig. 5.** Principal technological flowsheet for the M (1)–MTBE (2)–TBA (3)–W (4) mixture separation with dimethylsulfoxide or ethylene glycol as SA: C1 and C4 are the ED columns, C2 and C5 are the SA recovery columns, and C3 is the TBA isolation column.

Table 3. Column operation parameters and separation results for ED flowsheet with ethylene glycol

Col.	P, kPa	F <sub>SA</sub>	N	N <sub>F</sub> /N <sub>SA</sub>	R	Distillate composition, mol. fr.						Bottom composition, mol. fr.						Q, MW	t <sub>p</sub> , °C	t <sub>w</sub> , °C
						M	W	MTBE	TBA	SA	M	W	MTBE	TBA	SA	M	W			
1	101.32	375	50	41/4	1.35	0.50	0.0005	0.25	0.2495	-	-	0.05	-	0.0001	0.949	3.57	60.3	178.3		
2	101.32	-	20	-	2.8	-	0.998	-	0.002	-	0.0001	-	-	-	0.9999	1.20	97.6	-		
3	101.32	-	40	-	4	0.666	0.002	0.33	0.002	-	0.0025	0.0005	-	0.997	-	2.79	53.15	82.45		
4	101.32	350	52	29/4	4.9	0.9967	-	0.0033	-	-	-	-	0.054	-	0.946	4.28	64.3	170.2		
5	101.32	-	20	-	5	0.0046	0.0018	0.993	0.0006	-	-	0.0001	-	-	0.9999	1.27	54.7	197.1		

Table 4. Column operation parameters and separation results for ED flowsheet with dimethylsulfoxide

Col.	P, kPa	F <sub>SA</sub>	N	N <sub>F</sub> /N <sub>SA</sub>	R	Distillate composition, mol. fr.						Bottom composition, mol. fr.						Q, MW	t <sub>p</sub> , °C	t <sub>w</sub> , °C
						M	W	MTBE	TBA	SA	M	W	MTBE	TBA	SA	M	W			
1	101.32	50	49	31/4	1.15	0.5	-	0.25	0.25	-	следы traces	0.286	-	-	0.714	1.24	60.35	148.6		
2	80	-	15	-	3	0.0004	0.9996	-	-	-	-	-	-	-	0.9999	0.99	93.4	151.8		
3	101.32	-	40	-	4	0.6664	0.0001	0.333	0.0005	-	0.0015	-	-	0.9985	-	2.79	53.15	82.8		
4	101.32	130	37	28/3	4.4	0.006	-	0.994	-	-	0.0002	0.0001	0.0537	-	0.946	1.33	54.8	123.3		
5	80	-	14	-	1	0.0043	0.0018	0.993	0.0009	-	0.0001	-	-	-	0.9999	1.13	58.4	181.8		

Table 5. Column operation parameters and separation results for ED flowsheet with ethylene glycol and dimethylsulfoxide

Col.	$P$ , kPa	$F_{SA}$	$N$	$N_F/N_{SA}$	$R$	Distillate composition, mol. fr.						Bottom composition, mol. fr.						$Q$ , MW	$t_b$ , °C	$t_w$ , °C
						M	W	MTBE	TBA	SA	M	W	MTBE	TBA	SA	M	W			
1	101.32	375	50	41/4	1.35	0.5	0.0005	0.25	0.2495	–	–	0.05	0	0.001	0.949	3.57	60.3	178.3		
2	101.32	–	20	–	2.8	–	0.998	–	0.002	–	–	–	–	–	0.9999	1.20	97.6	197.1		
3	101.32	–	40	–	4	0.666	0.0006	0.3332	0.0002	–	0.0025	0.0001	–	0.997	–	2.79	53.15	82.45		
4	101.32	130	37	28/3	4.4	0.006	–	0.994	–	–	0.234	–	0.0007	0.0002	0.7651	1.33	54.8	123.3		
5	80	–	14	–	1	0.996	0.0001	0.0032	0.0007	–	0.0001	–	–	–	0.9999	1.13	58.4	151.8		

Table 6. Column operation parameters and separation results for ED flowsheet with dimethylsulfoxide and ethylene glycol

Col.	$P$ , kPa	$F_{SA}$	$N$	$N_F/N_{SA}$	$R$	Distillate composition, mol. fr.						Bottom composition, mol. fr.						$Q$ , MW	$t_b$ , °C	$t_w$ , °C
						M	W	MTBE	TBA	SA	M	W	MTBE	TBA	SA	M	W			
1	101.32	50	49	34/4	1.15	0.5	–	0.25	0.25	–	0.0001	0.2859	–	–	0.714	1.24	60.35	148.6		
2	80	–	15	–	3	0.0004	0.9996	–	–	–	–	–	–	0.0001	0.9999	0.99	93.4	151.8		
3	101.32	–	40	–	4	0.666	0.0001	0.333	0.0005	–	0.0010	–	–	0.9990	–	2.79	53.15	82.5		
4	101.32	350	52	29/4	4.9	0.9966	–	0.0034	–	–	0.0002	–	0.0537	–	0.946	4.28	64.3	170.2		
5	101.32	–	20	–	5	0.004	0.001	0.993	0.0015	–	0.0001	–	–	–	0.9999	1.27	54.7	197.1		

reflux ratios, feed level of the initial mixture and SA, and agent consumption), providing energy savings of up to 30% while ensuring the required product quality. Table 8 summarizes the studied systems and methods on which the separation flowsheet of mixtures of different compositions is based.

### CONCLUSIONS

The revealed features of the formation of phase equilibrium diagrams and the peculiarities of the distillation separation of different complexity mixtures are used to improve the methodology of synthesis of separation flowsheets and the choice of energy-efficient separation modes of multicomponent mixtures.

The main methodology provisions relate to the following issues:

- to define the boundaries of the system under study and to form an experimental base (collecting background information, conducting a full-scale experiment) necessary to solve the task;

- to justify a choice of a phase equilibrium model and to obtain a set of model parameters reproducing the properties of the system with a relative error not exceeding 3–5%. In some cases, this range can be changed: when studying a system containing components with similar properties, the description accuracy should be increased to 1.0–1.5%; when modeling a system with more than two liquid phases, the relative error values may be 6–7%;

- to study the composition space of the phase diagram (to analyze the boundary space of the second dimension with determination of the number of nodal points (stable and unstable), saddle points (with nonzero Poincare index), the number of distillation regions, closed contours forming one-dimensional boundaries of the separating manifold of dimension  $(n - 2)$ , and one-dimensional binodals; to determine the internal structure of the simplex (to predict the presence of an internal singular point, the structure of internal separatrix hyper (surfaces), and the structure of splitting areas);

- to assess the possibility of using at the first stage special modes of distillation (direct and indirect sequences) or the MCS fractionation due to sharp distillation with favorable ratios of the coefficients of distribution of components between phases (the first apparatus is a column) or due to splitting (the first apparatus is a decanter). The implementation of these techniques is possible in the absence of internal separatrix surfaces or a favorable mutual arrangement of binodal and separatrix manifolds;

- when it is impossible to implement one of the listed above techniques, the special methods based on the addition of SA should be used. It is necessary to choose the SA (individual or binary) and predict separation products based on new techniques developed by the authors [31];

- to synthesize and structural optimize the flowsheets representing a combination of various functional complexes, in particular, several ED complexes with one or different agents;

**Table 7.** Comparison of ED flowsheets with different sets of agents

ED mode	Separating agent, kmol/h		$\Sigma N$ , t.s.	$\Sigma Q_p$ , $i = 1-5$ , MW
	Column 1	Column 4		
Mode 1	375 EG	350 EG	182	13.11
Mode 2	50 DMSO	130 DMSO	155	7.47
Mode 3	50 DMSO	350 EG	176	10.58
Mode 4	375 EG	130 DMSO	161	10.01

Note: 100 kmol/h of M-TBA-MTBE-W mixture; DMSO is dimethyl sulfoxide, EG is ethylene glycol.

Table 8. Investigated multicomponent systems and methods of different composition mixtures separation

No.	System	Production	Separation flowsheet (method)	Lit.
1	Ethyl acetate–Benzene–Toluene–Butyl acetate	Mixture of solvents for biodegradable polymer production	Alternative variants (direct, indirect, sharp separation sequence)	[35, 37]
2	Acetone–Toluene–Butyl acetate–o-Xylene	Mixture of solvents for epoxy primer production	The advantage of sharp separation sequence in the first stage of separation	[35, 37]
3	Acetone–Methanol–Ethanol–Propanol-2	Model mixture		
4	Methanol–Methyl acetate–Acetic acid–Acetic anhydride	Reaction mixture for acetic anhydride production	[37, 38]	–
5	Methyl-2-hydroxybutyrate–Methoxypropyl acetate–Ethyl lactate–Ethylethoxypropionate	Mixture of solvents for liquid crystal display production		
6	Acetone–Chloroform–Ethanol–Water	Mixture of solvents for vitamin C production	Autoextractive-heteroazeotropic distillation, (SA – water)	[47]
7	Acetone–Chloroform–Propanol-2–Water			
8	Ethanol–Water–Toluene–Butyl acetate–Ethylellosol	Solvents in the flexography process	Extractive distillation using sulfolane, EG, DMSO	[33]
9	Acetone–Water–Isopropylbenzene–Alpha-methylstyrol–Phenol	Phenol production by cumulus method	Optimization of the extractive distillation block (SA – DEG)	–
10	1,2-Dichloroethane–Chloroform–cis-Dichloroethylene	Chloroform production		
11	Diethyl ether–Hexane–Ethyl acetate–Ethanol (Water)	Solvents for dihydroquercetin production	The composition of solvents is recommended (a mixture of organic substances in the absence of water)	[39]

Table 8. Continued

No.	System	Production	Separation flowsheet (method)	Lit.
12	Methanol–Ethanol–Acetonitrile–Water (SA – glycerin, DMSO)	Model mixture	Alternative variants of flowsheets containing two ED complexes with different SA	[40]
13	Methanol–Tetrahydrofuran–Acetonitrile–Water (SA – DMSO, glycerin)	Tetrahydrofuran production		–
14	Methanol– <i>tert</i> -Butanol–Methyltretbutyl ether–Water (SA – DMSO)	Methyltretbutyl ether production		–
15	Acetone–Methanol–Tetrahydrofuran–Chloroform (SA – DMSO, NMP, TBA)	Model mixture		[41]
16	Ethyl Acetate–Methyl ethyl ketone–Cyclohexane–Propanol-2 (SA – NMP)	Model mixture		–
				Alternative ED flowsheets of different structures

Note: EG is ethylene glycol, DMSO is dimethyl sulfoxide, NMP is *N*-methylpyrrolidone, TBA is tributylamine, DEG is diethylene glycol

– to conduct a local full-scale experiment in order to verify individual results (features of phase equilibrium, including in the presence of SA, and modes of operation of distillation columns).

The improving of the procedure for the synthesis of flowsheets for the distillation separation of multicomponent mixtures was based on original methods for studying the of the MCS phase diagram structures, the selection of additional substances (optimization at the level of the physicochemical subsystem of technology development), a variety of separation flowsheets structures (structural optimization of flowsheets): new results of a computational experiment obtained by varying the apparatus parameters, in particular, column efficiency, feed stages, and reflux ratios (parametric optimization); and new results of a full-scale experiment that allowed establishing the presence of previously unknown ternary, quaternary azeotropes, confirming the adequacy of mathematical modeling of liquid–vapor and liquid–liquid phase equilibria, and calculating the selectivity of SA in the MCS ED.

Various initial MCS fractionation methods were considered, which allow already at the first stage dividing the mixture into smaller constituents, the separation features of which are well known. Thus, it becomes possible to use well-known features and specific parameters of the separation flowsheets of binary and ternary mixtures, which are presented in the literature, including the article authors' works, and to solve the tasks set. It is shown that the reduction of energy consumption of flowsheets (up to 30% while ensuring the required quality of products) is associated with the implementation of a sharp distillation mode as an alternative to the limit modes (direct and indirect sequences), the use of the initial mixture pre-splitting, and the choice of SA in the processes of heteroazeotropic ED, including binary, showing in some cases the positive synergistic effect on increasing the SA selectivity.

#### Acknowledgments

The study was supported by the Russian Science Foundation (grant No. 19-19-00620).

#### Authors' contributions

**A.K. Frolkova** – development of approaches to the synthesis of energy-efficient flowsheets of multicomponent mixtures separation, and writing the paper;

**A.V. Frolkova** – calculation of phase equilibrium, development of separation flowsheets, and parametric optimization of flowsheets;

**V.M. Raeva** – calculation of phase equilibrium, development of separation flowsheets, and parametric optimization of flowsheets;

**V.I. Zhuchkov** – conducting experimental studies on the selection of extractive agents.

The authors declare no conflicts of interest.

## REFERENCES

1. Timofeyev V.S., Serafimov L.A., Timoshenko A.V. *Principy tehnologii osnovnogo organicheskogo i neftehimicheskogo sinteza (The principles of the technology of basic organic and petrochemical synthesis)*. Moscow: Vysshaya shkola; 2010. 408 p. (in Russ.). ISBN 978-5-06-006067-6
2. Serafimov L.A., Timofeev V.S., Frolkova A.K. Qualitative research of technological processes and industries as a stage of their intensification based on mathematical modeling with the help of a computer. *Intensifikatsiya tekhnologii: materialy, tekhnologii, oborudovanie = Intensification Technological Processes: Materials, Technologies, Equipment*. 2009;(6):9–32 (in Russ.).
3. Zharov V.T., Serafimov L.A. *Fiziko-himicheskie osnovy distillatsii i rektifikatsii (Physico-chemical principles of distillation and rectification)*. Leningrad: Khimiya; 1975. 240 p. (in Russ.).
4. Frolkova A.V., Maevskii M.A., Frolkova A.K., Pletnev D.B. Developing Energy-Efficient Technologies for Obtaining Organic Substances Based on a Comprehensive Study of the Reaction and Separation Constituents. *Theor. Found. Chem. Eng.* 2020;54(6):1215–1222. <https://doi.org/10.1134/S0040579520060159>
5. Frolkova A.K. *Razdelenie azeotropnykh smesei. Fiziko-khimicheskie osnovy i tekhnologicheskie priemy (Separation of azeotropic mixtures. Physico-chemical fundamentals and technological methods)*. Moscow: VLADOS; 2010. 192 p. (in Russ.). ISBN 978-5-691-01743-8
6. Frolkova A.V., Akishina A.A., Maevskii M.A., Ablizin M.A. Flowsheets of multicomponent multiphase systems separation and material balance calculation features. *Theor. Found. Chem. Eng.* 2017;51(3):313–319. <https://doi.org/10.1134/S0040579517030034>
7. Frolkova A.K., Sebyakin A.Yu., Serafimov L.A. Peculiarities of distillation separation of multicomponent separating mixtures. In: *Teoreticheskie i prakticheskie aspekty razrabotki innovatsionnykh resursosberegayushchikh tekhnologii razdeleniya zhidkikh smesei: Materialy vserossiiskoi nauchno-prakticheskoi konferentsii (Theoretical and practical aspects of the development of innovative resource-saving technologies for the separation of liquid mixtures: Proceedings of the All-Russian Scientific and Practical Conference)*. Barnaul. 2016. P. 28–31 in Russ.).
8. Lei Z., Xi X., Dai C., Zhu J., Chen B. Extractive Distillation with the Mixture of Ionic Liquid and Solid Inorganic Salt as Entrainers. *AIChE J.* 2014;60(8):2994–3004. <https://doi.org/10.1002/aic.14478>
9. You X.Q., Rodriguez-Donis I., Gerbaud V. Improved design and efficiency of the extractive distillation process for acetone–methanol with water. *Ind. Eng. Chem. Res.* 2015;54(1):491–501. <https://doi.org/10.1021/ie503973a>
10. Wu Y., Chien I. Design and control of heterogeneous azeotropic column system for the separation of pyridine and water. *Ind. & Eng. Chem. Res.* 2009;48(23):10564–10576. <https://doi.org/10.1021/ie901231s>
11. Skiborowski M., Harwardt A., Marquardt W. Efficient optimization-based design for the separation of heterogeneous azeotropic mixtures. *Comp. & Chem. Eng.* 2015;72:34–51. <https://doi.org/10.1016/j.compchemeng.2014.03.012>

## СПИСОК ЛИТЕРАТУРЫ

1. Тимофеев В.С., Серафимов Л.А., Тимошенко А.В. *Принципы технологии основного органического и нефтехимического синтеза*. М.: Высшая школа; 2010. 408 с. ISBN 978-5-06-006067-6
2. Серафимов Л.А., Тимофеев В.С., Фролкина А.К. Качественные исследования технологических процессов и производства как этап их интенсификации на основе математического моделирования с помощью ЭВМ. *Интенсификация технологий: материалы, технологии, оборудование*. 2009;(6):9–32.
3. Жаров В.Т., Серафимов Л.А. *Физико-химические основы дистилляции и ректификации*. Л.: Химия, 1975. 240 с.
4. Frolkova A.V., Maevskii M.A., Frolkova A.K., Pletnev D.B. Developing Energy-Efficient Technologies for Obtaining Organic Substances Based on a Comprehensive Study of the Reaction and Separation Constituents. *Theor. Found. Chem. Eng.* 2020;54(6):1215–1222. <https://doi.org/10.1134/S0040579520060159>
5. Фролкина А.К. *Разделение азеотропных смесей. Физико-химические основы и технологические приемы*. М.: ВЛАДОС; 2010. 192 с. ISBN 978-5-691-01743-8
6. Frolkova A.V., Akishina A.A., Maevskii M.A., Ablizin M.A. Flowsheets of multicomponent multiphase systems separation and material balance calculation features. *Theor. Found. Chem. Eng.* 2017;51(3):313–319. <https://doi.org/10.1134/S0040579517030034>
7. Фролкина А.К., Себякин А.Ю., Серафимов Л.А. Особенности ректификационного разделения многокомпонентных расслаивающихся смесей. *Теоретические и практические аспекты разработки инновационных ресурсосберегающих технологий разделения жидких смесей: Материалы всероссийской научно-практической конференции*. Барнаул. 2016. С. 28–31.
8. Lei Z., Xi X., Dai C., Zhu J., Chen B. Extractive Distillation with the Mixture of Ionic Liquid and Solid Inorganic Salt as Entrainers. *AIChE J.* 2014;60(8):2994–3004. <https://doi.org/10.1002/aic.14478>
9. You X.Q., Rodriguez-Donis I., Gerbaud V. Improved design and efficiency of the extractive distillation process for acetone–methanol with water. *Ind. Eng. Chem. Res.* 2015;54(1):491–501. <https://doi.org/10.1021/ie503973a>
10. Wu Y., Chien I. Design and control of heterogeneous azeotropic column system for the separation of pyridine and water. *Ind. & Eng. Chem. Res.* 2009;48(23):10564–10576. <https://doi.org/10.1021/ie901231s>
11. Skiborowski M., Harwardt A., Marquardt W. Efficient optimization-based design for the separation of heterogeneous azeotropic mixtures. *Comp. & Chem. Eng.* 2015;72:34–51. <https://doi.org/10.1016/j.compchemeng.2014.03.012>
12. Denes F., Lang P., Joulia X. Generalized closed double-column system for batch heteroazeotropic distillation. *Sep. Purif. Technol.* 2012;89:297–308. <https://doi.org/10.1016/j.seppur.2012.01.042>
13. Hegely L., Gerbaud V., Lang P. Generalized model for heteroazeotropic batch distillation with variable decanter hold-up. *Sep. Purif. Technol.* 2013;115:9–19. <https://doi.org/10.1016/j.seppur.2013.04.031>
14. Modla G.P., Lang B.K., Molnar K. Batch heteroazeotropic rectification under continuous entrainer feeding: I. Feasibility studies. *Comp. Aided Chem. Eng.* 2003;15:974–977. [https://doi.org/10.1016/S1570-7946\(03\)80434-0](https://doi.org/10.1016/S1570-7946(03)80434-0)
15. Tóth A.J., Szanyi A., Haaze E., Mizsey P. Separation of process wastewater with extractive heterogeneously – azeotropic distillation. *Hungarian J. Ind. & Chem.* 2016;44(1):29–32. <https://doi.org/10.1515/hjic-2016-0003>

12. Denes F., Lang P., Joulia X. Generalized closed double-column system for batch heteroazeotropic distillation. *Sep. Purif. Technol.* 2012;89:297–308. <https://doi.org/10.1016/j.seppur.2012.01.042>
13. Hegely L., Gerbaud V., Lang P. Generalized model for heteroazeotropic batch distillation with variable decanter hold-up. *Sep. Purif. Technol.* 2013;115:9–19. <https://doi.org/10.1016/j.seppur.2013.04.031>
14. Modla G.P., Lang B.K., Molnar K. Batch heteroazeotropic rectification under continuous entrainer feeding: I. Feasibility studies. *Comp. Aided Chem. Eng.* 2003;15:974–977. [https://doi.org/10.1016/S1570-7946\(03\)80434-0](https://doi.org/10.1016/S1570-7946(03)80434-0)
15. Tóth A.J., Szanyi A., Haaze E., Mizsey P. Separation of process wastewater with extractive heterogeneous – azeotropic distillation. *Hungarian J. Ind. & Chem.* 2016;44(1):29–32. <https://doi.org/10.1515/hjic-2016-0003>
16. Szanyi A., Mizsey P., Fonyo Z. Novel hybrid separation processes for solvent recovery based on positioning the extractive heterogeneous azeotropic distillation. *Chem. Eng. Proc.* 2004;43(3):327–338. [https://doi.org/10.1016/s0255-2701\(03\)00132-6](https://doi.org/10.1016/s0255-2701(03)00132-6)
17. Benyounes H., Shen W., Gerbaud V. Entropy flow and energy efficiency analysis of extractive distillation with a heavy entrainer. *Ind. Eng. Chem. Res.* 2014;53(12):4778–4791. <https://doi.org/10.1021/ie402872n>
18. Kraemer K., Harwardt A., Skiborowski M., Mitra S., Marquardt W. Shortcut-based design of multicomponent heteroazeotropic distillation. *Chem. Eng. Res. & Design.* 2011;89(8):1168–1189. <https://doi.org/10.1016/j.cherd.2011.02.026>
19. Szanyi A., Mizsey P., Fonyó Z. Separation of highly non-ideal quaternary mixtures with extractive heterogeneous-azeotropic distillation. *Chem. Biochem. Eng. Q.* 2005;19(2):111–121.
20. Клейменова М.Н., Комарова Л.Ф., Лазуткина Ю.С. Создание ресурсосберегающих технологий в производстве кремнийорганических эмалей на основе ректификации. *Химия в интересах устойчивого развития.* 2013;21(2):211–218.
21. Yus D., Moonyong L. Distillation design and optimization of quaternary azeotropic mixtures for waste solvent recovery. *J. Ind. Eng. Chem.* 2018;67:255–265. <https://doi.org/10.1016/j.jiec.2018.06.036>
22. Gerbaud V., Rodríguez-Donis I. Distillation: Equipment and Processes. Charter 6. In: Gorak A., Oluji Z. (Eds.). *Extractive Distillation.* Academic Press; 2014. P. 201–245. <https://doi.org/10.1016/B978-0-12-386878-7.00006-1>
23. Huang H.-H., Ramaswamy S., Tschirner U.W., Ramarao B.V. A review of separation technologies in current and future biorefineries. *Sep. Purif. Technol.* 2008;62(1):1–21. <https://doi.org/10.1016/j.seppur.2007.12.011>
24. Zieborak K. On the quaternary azeotropes formed by paraffinic and naphthenic hydrocarbons with benzene, ethanol and water. *Rocz. Chem.* 1951;25(3):388–391.
25. Zieborak K., Galska A. A method for determining the composition of quaternary azeotropes and the position of heteroazeotropic lines. *Bull. Acad. Pol. Sci.* 1955;3(7):379.
26. Kominek-Szczepanik M. Four-component azeotropes. *Rocz. Chem.* 1959;33(2):553.
27. Imamura I., Kutsuwa Y., Matsuyama H. Reduction of the existing region of a quaternary azeotrope by use of a topological condition. *Kagaku Kogaku Ronbunshu.* 1992;18(4):535–538. <https://doi.org/10.1252/kakoronbunshu.18.535>
28. Wang Q., Yan X.-H., Chen G.-H., Han S.-J. Measurement and prediction of quaternary azeotropes for cyclohexane + 2-propanol + ethyl acetate + butanone system at elevated pressures. *J. Chem. Eng. Data.* 2003;48(1):66–70. <https://doi.org/10.1021/je020091a>
29. Galska-Krajewska A., Zieborak K. Quaternary positive-negative azeotrope. *Rocz. Chem.* 1962;36(1):119.
30. Zieborak K., Galska-Krajewska A. Quaternary positive-negative azeotrope. *Bull. Acad. Pol. Sci.* 1959;7(4):253.
31. Serafimov L.A., Frolkova A.K., Frolkova A.V. Poincaré integral invariants and separating manifolds of equilibrium open evaporation diagrams. *Theor. Found. Chem. Eng.* 2013;47(2):124–127. <https://doi.org/10.1134/S0040579512060218>
32. Охлопкова Е.А., Фролкова А.В., Фролкова А.К. Термодинамико-топологический анализ структуры фазовой диаграммы пятикомпонентной системы и синтез схемы разделения смеси органических продуктов. *Химия и технология органических веществ.* 2020;4(16):15–23. [https://doi.org/10.54468/25876724\\_2020\\_4\\_15](https://doi.org/10.54468/25876724_2020_4_15)

27. Imamura I., Kutsuwa Y., Matsuyama H. Reduction of the existing region of a quaternary azeotrope by use of a topological condition. *Kagaku Kogaku Ronbunshu*. 1992;18(4):535–538. <https://doi.org/10.1252/kakoronbunshu.18.535>
28. Wang Q., Yan X.-H., Chen G.-H., Han S.-J. Measurement and prediction of quaternary azeotropes for cyclohexane + 2-propanol + ethyl acetate + butanone system at elevated pressures. *J. Chem. Eng. Data*. 2003;48(1):66–70. <https://doi.org/10.1021/je020091a>
29. Galska-Krajewska A., Zieborak K. Quaternary positive-negative azeotrope. *Rocz. Chem.* 1962;36(1):119.
30. Zieborak K., Galska-Krajewska A. Quaternary positive-negative azeotrope. *Bull. Acad. Pol. Sci.* 1959;7(4):253.
31. Serafimov L.A., Frolkova A.K., Frolkova A.V. Poincaré integral invariants and separating manifolds of equilibrium open evaporation diagrams. *Theor. Found. Chem. Eng.* 2013;47(2):124–127. <https://doi.org/10.1134/S0040579512060218>
32. Okhlopko E.A., Frolkova A.V., Frolkova A.K. Thermodynamic-topological analysis of the of the phase diagram structure of a five-component system and separation scheme synthesis for a mixture of organic products. *Khimiya i tekhnologiya organicheskikh veshchestv = Chemistry and Technology of Organic Substances*. 2020;4(16):15–23 (in Russ.). [https://doi.org/10.54468/25876724\\_2020\\_4\\_15](https://doi.org/10.54468/25876724_2020_4_15)
33. Frolkova A.V., Makhnarilova E.G. Determination of separatrix manifold structure of five-component system phase diagram. In: *22nd International Conference on Chemical Thermodynamics in Russia (RCCT-2019)*: Book of Abstracts. Saint Petersburg, Russia, June 19-23; 2019. P. 250.
34. Frolkova A.V., Frolkova A.K., Ososkova T.E. Topological transformations of phase diagrams of quaternary systems through the boundary tangential azeotrope stage. *Russ. Chem. Bull.* 2020;69(11):2059–2066. <https://doi.org/10.1007/s11172-020-3000-7>
35. Пешехонцева М.Е., Маевский М.А., Гаганов И.С., Фролкина А.В. Области энергетического преимущества схем разделения смесей, содержащих компоненты с близкими летучестями. *Тонкие химические технологии*. 2020;15(3):7–20. <https://doi.org/10.32362/2410-6593-2020-15-3-7-20>
36. Фролкина А.В., Маевский М.А., Фролкина А.К., Плетнев Д.Б. Разработка энергоэффективных технологий получения органических веществ на основе комплексного исследования реакционной и разделительной составляющей. *Теор. основы хим. технологии*. 2020;54(6):706–713. <https://doi.org/10.31857/S0040357120060159>
37. Фролкина А.В., Пешехонцева М.С., Гаганов И.С. Промежуточное заданное разделение при ректификации четырехкомпонентных смесей. *Тонкие химические технологии*. 2018;13(3):41–48. <https://doi.org/10.32362/24106593-2018-13-3-41-48>
38. Frolkova A.V., Shashkova Y.I., Frolkova A.K., Mayevskiy M.A. Comparison of alternative methods for methyl acetate + methanol + acetic acid + acetic anhydride mixture separation. *Fine Chem. Technol.* 2019;14(5):51–60. <https://doi.org/10.32362/2410-6593-2019-14-5-51-60>
39. Frolkova A.V., Logachev, Ososkova T.E. Separation of diethyl ether + hexane + ethyl acetate + ethanol quaternary system via extractive distillation. *Izv. Vyssh. Uchebn. Zaved. Khim. Khim. Tekhnol.* 2020;63(10):59–63. <https://doi.org/10.6060/ivkkt.20206310.6228>
40. Рыжкин Д.А., Раева В.М. Анализ энергопотребления схем экстрактивной ректификации четырехкомпонентной смеси растворителей. *Изв. вузов. Химия и хим. технология*. 2021;64(6):47–55. <https://doi.org/10.6060/ivkkt.20216406.6326>
41. Raeva V.M., Stoyakina I.E. Selecting Extractive Agents on the Basis of Composition–Excess Gibbs Energy Data. *Russ. J. Phys. Chem. A*. 2021;95(9):1779–1790. <https://doi.org/10.1134/S003602442109020X>
42. Frolkova A.V., Mayevskiy M.A., Smirnov A.Yu. Phase Equilibrium of Systems Cyclohexene + Water + Cyclohexanone + N-Methyl-2-pyrrolidone (+Acetonitrile). *J. Chem. Eng. Data*. 2019;64(6):2888–2893. <https://doi.org/10.1021/acs.jced.9b00245>
43. Frolkova A.V., Mayevskiy M.A., Frolkova A.K. Analysis of Phase Equilibrium Diagrams of Cyclohexene + Water + Cyclohexanone + Solvent System. *J. Chem. Eng. Data*. 2018;63(3):679–683. <https://doi.org/10.1021/acs.jced.7b00870>
44. Serafimov L.A. Thermodynamical and topological analysis of liquid-vapor phase equilibrium diagrams and problems rectification of multicomponent mixtures. In: S.I. Kuchanov (Ed.). *Mathematical Method in Contemporary Chemistry*. Amsterdam: Gordon and Breach Publishers; 1996. Chapter 10. P. 557–605.
45. Frolkova A., Frolkova A., Gaganov I. The study of the extractive and auto-extractive distillation of azeotropic mixtures. *Chem. Eng. Technol.* 2021;44(2):1397–1402. <https://doi.org/10.1002/ceat.202100024>
46. Okhlopko E.A., Frolkova A.V. Comparative Analysis of Separation Schemes of Reaction Mixtures of Epichlorohydrin Production in the Presence of Various Solvents. *Theor. Found. Chem. Eng.* 2019;53(6):1028–1034. <https://doi.org/10.1134/S0040579519060101>

39. Frolkova A.V., Logachev, Ososkova T.E. Separation of diethyl ether + hexane + ethyl acetate + ethanol quaternary system via extractive distillation. *Izv. Vyssh. Uchebn. Zaved. Khim. Khim. Tekhnol.* 2020;63(10):59–63. <https://doi.org/10.6060/ivkkt.20206310.6228>
40. Ryzhkin D.A., Raeva V.M. Analysis of energy consumption of extractive distillation flowsheets of four-component solvent mixture. *Izv. Vyssh. Uchebn. Zaved. Khim. Khim. Tekhnol. = ChemChemTech.* 2021;64(6):47–55 (in Russ.). <https://doi.org/10.6060/ivkkt.20216406.6326>
41. Raeva V.M., Stoyakina I.E. Selecting Extractive Agents on the Basis of Composition–Excess Gibbs Energy Data. *Russ. J. Phys. Chem. A.* 2021;95(9):1779–1790. <https://doi.org/10.1134/S003602442109020X>
42. Frolkova A.V., Mayevskiy M.A., Smirnov A.Yu. Phase Equilibrium of Systems Cyclohexene + Water + Cyclohexanone + *N*-Methyl-2-pyrrolidone (+Acetonitrile). *J. Chem. Eng. Data.* 2019;64(6):2888–2893. <https://doi.org/10.1021/acs.jced.9b00245>
43. Frolkova A.V., Mayevskiy M.A., Frolkova A.K. Analysis of Phase Equilibrium Diagrams of Cyclohexene + Water + Cyclohexanone + Solvent System. *J. Chem. Eng. Data.* 2018;63(3):679–683. <https://doi.org/10.1021/acs.jced.7b00870>
44. Serafimov L.A. Thermodynamical and topological analysis of liquid-vapor phase equilibrium diagrams and problems rectification of multicomponent mixtures. In: S.I. Kuchanov (Ed.). *Mathematical Method in Contemporary Chemistry.* Amsterdam: Gordon and Breach Publishers; 1996. Chapter 10. P. 557–605.
45. Frolkova A., Frolkova A., Gaganov I. The study of the extractive and auto-extractive distillation of azeotropic mixtures. *Chem. Eng. Technol.* 2021;44(2):1397–1402. <https://doi.org/10.1002/ceat.202100024>
46. Okhlopova E.A., Frolkova A.V. Comparative Analysis of Separation Schemes of Reaction Mixtures of Epichlorohydrin Production in the Presence of Various Solvents. *Theor. Found. Chem. Eng.* 2019;53(6):1028–1034. <https://doi.org/10.1134/S0040579519060101>
47. Frolkova A.V., Ososkova T.E., Frolkova A.K. Thermodynamic and Topological Analysis of Phase Diagrams of Quaternary Systems with Internal Singular Points. *Theor. Found. Chem. Eng.* 2020;54(3):407–419. <https://doi.org/10.1134/S0040579520020049>  
[Original Russian Text: Frolkova A.V., Ososkova T.E., Frolkova A.K. Thermodynamic and topological analysis of phase diagrams of quaternary systems with internal singular points. *Teoreticheskie osnovy khimicheskoi tekhnologii.* 2020;54(3):286–298. <https://doi.org/10.31857/S0040357120020049>]
48. Raeva V.M., Sazonova A.Yu. Separation of ternary mixtures by extractive distillation with 1,2-ethandiol and glycerol. *Chem. Eng. Res. Des.* 2015;99:125–131. <https://doi.org/10.1016/j.cherd.2015.04.032>
49. Zhao L., Lyu X., Wang W., Shan J., Qiu T. Comparison of heterogeneous azeotropic distillation and extractive distillation methods for ternary azeotrope ethanol/toluene/water separation. *Comp. Chem. Engineering.* 2017;100:27–37. <https://doi.org/10.1016/j.compchemeng.2017.02.007>
50. Zhao Y., Jia H., Geng X., Wen G., Zhu Z., Wang Y. Comparison of Conventional Extractive Distillation and Heat Integrated Extractive Distillation for Separating Tetrahydrofuran/Ethanol/Water. *Chem. Eng. Transactions.* 2017;61:751–756. <https://doi.org/10.3303/CET1761123>
51. Yang A., Zou H., Chien I.L., Wang D., Shun'an W., Jingzheng R., Weifeng S. Optimal Design and Effective Control of Triple-Column Extractive Distillation for Separating Ethyl Acetate/Ethanol/Water with Multi-Azeotrope. *Ind. Eng. Chem. Res.* 2019;58(17):7265–7283. <https://doi.org/10.1021/acs.iecr.9b00466>
52. Shi X., Zhu X., Zhao X., Zhang Z. Performance evaluation of different extractive distillation processes for separating ethanol/tert-butanol/water mixture. *Process Safety and Environmental Protection.* 2020;137:246–260. <https://doi.org/10.1016/j.psep.2020.02.015>
53. Zhaoyuan M., Dong Y., Jiangang Z., Huiyuan L., Chen Zhengrun C., Peizhe C., Zhaoyou Z., Lei W., Yinglong W., Yixin M., Jun G. Efficient recovery of benzene and *n*-propanol from wastewater via vapor recompression assisted extractive distillation based on techno-economic and environmental analysis. *Process Safety and Environmental Protection.* 2021;148:462–472. <https://doi.org/10.1016/j.psep.2020.10.033>
47. Фролкива А.В., Ососкова Т.Е., Фролкива А.К. Термодинамико-топологический анализ фазовых диаграмм четырехкомпонентных систем с внутренними особыми точками. *Теор. основы хим. технологии.* 2020;54(3):286–298. <https://doi.org/10.31857/S0040357120020049>
48. Раева В.М., Сазонова А.Ю. Separation of ternary mixtures by extractive distillation with 1,2-ethandiol and glycerol. *Chem. Eng. Res. Des.* 2015;99:125–131. <https://doi.org/10.1016/j.cherd.2015.04.032>
49. Zhao L., Lyu X., Wang W., Shan J., Qiu T. Comparison of heterogeneous azeotropic distillation and extractive distillation methods for ternary azeotrope ethanol/toluene/water separation. *Comp. Chem. Engineering.* 2017;100:27–37. <https://doi.org/10.1016/j.compchemeng.2017.02.007>
50. Zhao Y., Jia H., Geng X., Wen G., Zhu Z., Wang Y. Comparison of Conventional Extractive Distillation and Heat Integrated Extractive Distillation for Separating Tetrahydrofuran/Ethanol/Water. *Chem. Eng. Transactions.* 2017;61:751–756. <https://doi.org/10.3303/CET1761123>

51. Yang A., Zou H., Chien I.L., Wang D., Shun'an W., Jingzheng R., Weifeng S. Optimal Design and Effective Control of Triple-Column Extractive Distillation for Separating Ethyl Acetate/Ethanol/Water with Multi-Azeotrope. *Ind. Eng. Chem. Res.* 2019;58(17):7265–7283. <https://doi.org/10.1021/acs.iecr.9b00466>

52. Shi X., Zhu X., Zhao X., Zhang Z. Performance evaluation of different extractive distillation processes for separating ethanol/tert-butanol/water mixture. *Process Safety and Environmental Protection.* 2020;137:246–260. <https://doi.org/10.1016/j.psep.2020.02.015>

53. Zhaoyuan M., Dong Y., Jiangang Z., Huiyuan L., Chen Zhengrun C., Peizhe C., Zhaoyou Z., Lei W., Yinglong W., Yixin M., Jun G. Efficient recovery of benzene and *n*-propanol from wastewater via vapor recompression assisted extractive distillation based on techno-economic and environmental analysis. *Process Safety and Environmental Protection.* 2021;148:462–472. <https://doi.org/10.1016/j.psep.2020.10.033>

#### About the authors:

**Alla K. Frolkova**, Dr. Sci. (Eng.), Professor, Head of the Department of Chemistry and Technology of Basic Organic Synthesis, M.V. Lomonosov Institute of Fine Chemical Technologies, MIREA – Russian Technological University (86, Vernadskogo pr., Moscow, 119571, Russia). E-mail: [frolkova@gmail.com](mailto:frolkova@gmail.com). Scopus Author ID 35617659200, ResearcherID G-7001-2018, <https://orcid.org/0000-0002-9763-4717>

**Anastasiya V. Frolkova**, Cand. Sci. (Eng.), Associate Professor, Department of Chemistry and Technology of Basic Organic Synthesis, M.V. Lomonosov Institute of Fine Chemical Technologies, MIREA – Russian Technological University (86, Vernadskogo pr., Moscow, 119571, Russia). E-mail: [frolkova\\_nastya@mail.ru](mailto:frolkova_nastya@mail.ru). Scopus Author ID 12782832700, ResearcherID N-4517-2014, <https://orcid.org/0000-0001-5675-5777>

**Valentina M. Raeva**, Cand. Sci. (Eng.), Associate Professor, Department of Chemistry and Technology of Basic Organic Synthesis, M.V. Lomonosov Institute of Fine Chemical Technologies, MIREA – Russian Technological University (86, Vernadskogo pr., Moscow, 119571, Russia). Email: [raevalentinal@gmail.com](mailto:raevalentinal@gmail.com). Scopus Author ID 6602836975, Researcher ID C-8812-2014, <https://orcid.org/0000-0002-5664-4409>

**Valery I. Zhuchkov**, Cand. Sci. (Eng.), Associate Professor, Department of Chemistry and Technology of Basic Organic Synthesis, M.V. Lomonosov Institute of Fine Chemical Technologies, MIREA – Russian Technological University (86, Vernadskogo pr., Moscow, 119571, Russia). E-mail: [v-zhuchkov@yandex.ru](mailto:v-zhuchkov@yandex.ru). Scopus Author ID 57198290642, Researcher ID AAA-3117-2020, <https://orcid.org/0000-0002-5729-3356>

#### Об авторах:

**Фролкива Алла Константиновна**, д.т.н., профессор, заведующий кафедрой химии и технологии основного органического синтеза Института тонких химических технологий им. М.В. Ломоносова ФГБОУ «МИРЭА – Российский технологический университет» (119571, Россия, Москва, пр-т Вернадского, д. 86). E-mail: [frolkova@gmail.com](mailto:frolkova@gmail.com). ResearcherID G-7001-2018, Scopus Author ID 35617659200, <https://orcid.org/0000-0002-9763-4717>

**Фролкива Анастасия Валериевна**, к.т.н., доцент, кафедра химии и технологии основного органического синтеза Института тонких химических технологий им. М.В. Ломоносова ФГБОУ «МИРЭА – Российский технологический университет» (119571, Россия, Москва, пр-т Вернадского, д. 86). E-mail: [frolkova\\_nastya@mail.ru](mailto:frolkova_nastya@mail.ru). Scopus Author ID 12782832700, ResearcherID N-4517-2014, <https://orcid.org/0000-0001-5675-5777>

**Раева Валентина Михайловна**, к.т.н., доцент кафедры химии и технологии основного органического синтеза Института тонких химических технологий им. М.В. Ломоносова ФГБОУ ВО «МИРЭА – Российский технологический университет» (119571, Россия, Москва, пр-т Вернадского, д. 86). Email: raevalentina1@gmail.com. Scopus Author ID 6602836975, Researcher ID C-8812-2014, <https://orcid.org/0000-0002-5664-4409>

**Жучков Валерий Иванович**, к.т.н., старший научный сотрудник, доцент кафедры химии и технологии основного органического синтеза Института тонких химических технологий им. М.В. Ломоносова ФГБОУ «МИРЭА – Российский технологический университет» (119571, Россия, Москва, пр-т Вернадского, д. 86). E-mail: v-zhuchkov@yandex.ru. Scopus Author ID 57198290642, Researcher ID AAA-3117-2020, <https://orcid.org/0000-0002-5729-3356>

*The article was submitted: 25.02.2022; approved after reviewing: 29.03.2022; accepted for publication: 11.04.2022.*

*Translated from Russian into English by N. Isaeva.*

*Edited for English language and spelling by Quinton Scribner, Awatera.*

**CHEMISTRY AND TECHNOLOGY OF MEDICINAL COMPOUNDS  
AND BIOLOGICALLY ACTIVE SUBSTANCES**

**ХИМИЯ И ТЕХНОЛОГИЯ ЛЕКАРСТВЕННЫХ ПРЕПАРАТОВ  
И БИОЛОГИЧЕСКИ АКТИВНЫХ СОЕДИНЕНИЙ**

ISSN 2686-7575 (Online)

<https://doi.org/10.32362/2410-6593-2022-17-2-107-130>



UDC 547.1

REVIEW ARTICLE

## Bifunctional gallium cation chelators

**Anna G. Polivanova**✉, **Inna N. Solovieva**, **Dmitrii O. Botev**, **Danil Y. Yuriev**,  
**Alyona N. Mylnikova**, **Maxim S. Oshchepkov**

*D.I. Mendeleev Russian University of Chemical Technology, Moscow, 125047 Russia*

✉ *Corresponding author, e-mail: zagchem@mail.ru*

### Abstract

**Objectives.** *The chemistry of  $^{67}\text{Ga}$  and  $^{68}\text{Ga}$  radionuclides plays a key role in nuclear medicine for applications in radiopharmaceuticals, in particular, in noninvasive in vivo molecular imaging techniques. The use of radiometals for labeling biomolecules typically requires the use of bifunctional chelators, which contain a functional group for covalent bonding with the targeting vector in addition to the polydentate fragment coordinating the metal. The aim of the present review article is to analyze the currently accumulated experimental material on the development and application of bifunctional chelators of gallium cations in medical research, as well as to identify the main requirements for the structure of the chelator and its complexes with  $^{68}\text{Ga}$ , which are used to create effective Ga-based pharmaceutical preparations.*

**Results.** *The review analyzed macrocyclic bifunctional chelators forming stable in vivo complexes with  $^{68}\text{Ga}$  and acyclic chelators, whose main advantage is faster complexation kinetics due to the short half-life of  $^{68}\text{Ga}$ . The advantages and disadvantages of both types of ligands were evaluated. In addition, a critical analysis of the binding constants and the conditions for the formation of complexes was presented. Examples of the influence of the geometry, lipophilicity, and total charge of the metal complex on the biodistribution of target radiopharmaceuticals were also given.*

**Conclusions.** *Despite the progress made in the considered areas of bifunctional chelators, the problem of correlating the chemical structure of a metal-based radiopharmaceutical with its behavior in vivo remains important. Comparative studies of drugs having an identical targeting vector but containing different bifunctional chelating agents could help further elucidate the effect*

of metal chelate moiety on pharmacokinetics. In order to create effective bifunctional chelating agents, it is necessary to take into account such factors as the stability and inertness of the chelator and its complexes under physiological conditions, lipophilicity, complexation kinetics, chelation selectivity, combinatoriality of the basic structure, along with economic aspects, e.g., the availability of raw materials and the complexity of the synthesis scheme.

**Keywords:** bifunctional chelator, ligand, gallium, radiopharmaceutical

**For citation:** Polivanova A.G., Solovieva I.N., Botev D.O., Yuriev D.Y., Mylnikova A.N., Oshchepkov M.S. Bifunctional gallium cation chelators. *Tonk. Khim. Tekhnol. = Fine Chem. Technol.* 2022;17(2):107–130 (Russ., Eng.). <https://doi.org/10.32362/2410-6593-2022-17-2-107-130>

## ОБЗОРНАЯ СТАТЬЯ

# Бифункциональные хелаторы к катиону галлия

**А.Г. Поливанова** ✉, **И.Н. Соловьёва**, **Д.О. Ботев**, **Д.Ю. Юрьев**, **А.Н. Мыльникова**, **М.С. Ощепков**

Российский химико-технологический университет им. Д.И. Менделеева, Москва, 125047 Россия

✉ Corresponding author, e-mail: zagchem@mail.ru

### Аннотация

**Цели.** Химия радионуклидов  $^{67}\text{Ga}$  и  $^{68}\text{Ga}$  играет одну из ключевых ролей в ядерной медицине для применения в радиофармпрепаратах, в частности, в неинвазивных методах молекулярной визуализации *in vivo*. Использование радиометаллов для мечения биомолекул обычно требует использования бифункциональных хелаторов, которые, кроме полидентатного фрагмента, координирующего металл, содержат функциональную группу для ковалентного связывания с вектором-мишенью. Цели данного обзора – проанализировать накопленный к настоящему времени экспериментальный материал, касающийся разработки и применения в медицинских исследованиях бифункциональных хелаторов к катиону галлия, а также выявить и проанализировать основные требования, предъявляемые к структуре хелатора и его комплексов с  $^{68}\text{Ga}$ , необходимые для создания эффективных фармакологических препаратов на его основе.

**Результаты.** Рассмотрены макроциклические бифункциональные хелаторы, образующие стабильные *in vivo* комплексы с  $^{68}\text{Ga}$ , а также ациклические хелаторы, преимущество которых заключается в более быстрой кинетике комплексообразования, что является ключевым фактором, учитывающим короткий период полураспада  $^{68}\text{Ga}$ . Проведена оценка достоинств и недостатков обоих типов лигандов. Кроме того, осуществлен критический анализ констант связывания и условий образования комплексов. Рассмотрены примеры влияния природы металлического комплекса (геометрия, липофильность, общий заряд) на биораспределение целевых радиофармацевтических препаратов.

**Выводы.** Несмотря на достигнутые успехи в рассмотренных направлениях создания бифункциональных хелаторов, по-прежнему важной остается проблема корреляции химической структуры радиофармпрепаратов на основе металлов с их поведением *in vivo*. В этом отношении сравнительные исследования препаратов, имеющих идентичный вектор нацеливания, но включающих разные бифункциональные хелатирующие агенты,

могут помочь в дальнейшем выявлении влияния металл-хелатного фрагмента на фармакокинетику. В целом можно отметить, что для создания эффективного бифункционального хелатирующего агента нужно принимать во внимание целую совокупность факторов, включающую стабильность и инертность хелатора и его комплексов в физиологических условиях, липофильность, кинетику комплексообразования, селективность хелатирования, комбинаторность базовой структуры, а также экономические аспекты: доступность сырья, сложность схемы синтеза.

**Ключевые слова:** бифункциональный хелатор, лиганд, галлий, радиофармпрепарат

**Для цитирования:** Поливанова А.Г., Соловьёва И.Н., Ботев Д.О., Юрьев Д.Ю., Мьльникова А.Н., Ощепков М.С. Бифункциональные хелаторы к катиону галлия. *Тонкие химические технологии*. 2022;17(2):107–130. <https://doi.org/10.32362/2410-6593-2022-17-2-107-130>

## INTRODUCTION

Unlike other methods such as X-rays, computed tomography (CT) and ultrasound, which predominantly provide anatomical information, non-invasive molecular imaging allows chemical and biological processes to be measured and visualized in living systems.

Nuclear medicine is a molecular imaging technique based around radioactive isotopes used as tracers. The two main imaging techniques used in nuclear medicine are single photon emission computed tomography (SPECT) and positron emission tomography (PET).

Although PET has certain advantages in comparison to SPECT, such as high resolution and sensitivity, as well as the ability to quantitative evaluation due to a standardized attenuation correction method, the use of PET is limited due to the short half-lives of the four traditional standard isotopes:  $^{11}\text{C}$  ( $t_{1/2} = 20$  min),  $^{13}\text{N}$  ( $t_{1/2} = 10$  min),  $^{15}\text{O}$  ( $t_{1/2} = 2$  min), and  $^{18}\text{F}$  ( $t_{1/2} = 110$  min). With the exception of  $^{18}\text{F}$ , the solution to this problem requires the maintenance of a cyclotron for isotope production in the immediate vicinity of the imaging apparatus. Despite high equipment maintenance costs, the rise in the use of PET imaging over the past decades has been largely driven by the successful use of [ $^{18}\text{F}$ ] fluorodeoxyglucose, helping PET to

become an indispensable tool for diagnosing various types of malignant neoplasms. Consequently, PET has evolved from a research tool to a practical, highly efficient clinical imaging technique, which has had a tremendous impact on clinical medicine and pharmaceutical development. This progress has also spurred the development of other imaging techniques such as PET–CT and PET–magnetic resonance imaging, as well as fluorescence imaging.

However, the use of traditional short-living isotopes hinders the study of long-term processes, limiting this method to the study of fast biological processes. For this reason, non-standard PET radioisotopes have been produced and investigated. The wider half-life ranges of such isotopes offer better compatibility with the biological half-lives of certain target vectors used for the development of new radiopharmaceuticals. In this context, radioactive metals such as zirconium, yttrium, indium, gallium, and copper were considered [1].

Gallium-68 ( $^{68}\text{Ga}$ ), which has a half-life of 1.13 h, decays with emission of positrons and capture of electrons (11%). The increased interest in  $^{68}\text{Ga}$  is based on its availability from the  $^{68}\text{Ge}/^{68}\text{Ga}$  generator system, which permits the cost-effective use of  $^{68}\text{Ga}$ -based radiopharmaceuticals in clinical centers lacking a local cyclotron. Although  $^{68}\text{Ge}/^{68}\text{Ga}$  generators were first introduced more than 50 years ago, the most important factor

in the recent growth in the number of  $^{68}\text{Ga}$ -based radiopharmaceuticals has been the progress in generators' design. A new generation of these systems is able to produce  $^{68}\text{Ga}$  as  $[^{68}\text{Ga}]\text{GaCl}_3$ , which solved critical impurity problems and made such generators commercially available. The decay of the  $^{68}\text{Ge}$  isotope to  $^{68}\text{Ga}$  with a half-life of 270.8 days allows its use to obtain long-living generator systems having an estimated period of 1–2 years for radiopharmaceutical applications.

The use of radiometals for labeling biomolecules usually requires the use of bifunctional chelators (BFC), which bind the metal at one end and contain a functional group for covalent bonding with the targeting vector at the other end (Table).

The choice of BFC is determined by the nature and oxidation state of the metal radionuclide. The optimal BFC should ideally meet the following requirements:

**Table.** Stability constants ( $\log \beta_1$ ) and synthesis conditions of  $^{67/68}\text{Ga}$  bifunctional chelating complexes

Chelating agent*	$\log \beta_1$	$^{67/68}\text{Ga}$ binding conditions	RCY** (%)	Reference
DOTA (1)	21.3	pH = 4.8, 5 min, 95°C	>90	[2]
NOTA (3)	30.7	pH = 3.5, 10 min, 95°C	>95	[3]
NODASA (3a)	–***	0.5 M $\text{CH}_3\text{COONH}_4$ , 25 min, 90°C	–	[4]
NODAGA (3b)	–	25 min, 95°C	95	[5]
<i>p</i> -SCN-Bn-NOTA (3c)	–	pH = 6.0, 10 min, 25°C	89	[5]
NODAPA-OH (3d)	–	pH = 2.8, 3 min, 85°C	85	[5]
NODAPA-NCS (3e)	–	pH = 2.8, 3 min, 75°C	85	[5]
NODAPA-(NCS) <sub>2</sub> (3f)	–	pH = 2.8, 3 min, 75°C	–	[5]
TRAP (3g)	26.24	pH = 3.0, 3 min, 40°C	95	[6]
NOPO (3h)	25.01	2.7 M HEPES, 5 min, 25°C	99	[7]
H <sub>5</sub> NOA2P (3i)	34.44	pH = 7.4, 30 min, 95°C	–	[8]
H <sub>3</sub> NOKA	–	pH = 6.0, 60 min, 25°C	35	[9]
DATA <sup>p</sup> (4a)	–	pH = 4.7, 1–10 min, 25°C	93	[10]
DATA <sup>m</sup> (4b)	21.7	pH = 4.7, 1 min, 25°C	97	[10]
PhDATA <sup>pph</sup> (4c)	–	pH = 4.7, 1–10 min, 25°C	93	[10]

Table. Continued

Chelating agent*	log $\beta_1$	$^{67/68}\text{Ga}$ binding conditions	RCY** (%)	Reference
DATA <sup>ph</sup> (4d)	–	pH = 4.7, 1–10 min, 25°C	84	[10]
NO <sub>2</sub> Bn-PCTA (5)	19.37	pH = 3–5, 25°C	96	[10]
Diamsar (6a)	–	0.1 M CH <sub>3</sub> COONa, 35 min, 85°C	98	[11]
DiamsarDGA (6b)	–	30 min, 85°C	98	[11]
H <sub>2</sub> dedpa (8)	28.11	0.1 M CH <sub>3</sub> COONa, 10 min, 25°C	97	[12]
HBED (7)	38.51	pH = 4.2, 4 min, 95°C	99	[13]
HBED-CC (7a)	–	pH = 4.2, 4 min, 25°C pH = 4.8, 10 min, 25°C	99 96	[14, 15]
KP46 (11)	36.79	pH < 2.0, 25°C	–	[16]
EHP	27.52	pH = 7.4, 15 min, 25°C	–	[17]
EHMP	29.55	pH = 7.4, 15 min, 25°C	–	[17]
CP256 (14a)	–	pH = 6.5, 5 min, 25°C	95	[18]
NTP(PrHP) <sub>3</sub> (14c)	33.34	pH = 7.4, 25°C	98	[19]
DFO (15)	28.6	pH = 4.5, 5 min, 25°C	96	[20]
Df-Bz-NCS (15a)	–	pH = 7.2, 5 min, 25°C	>90	[21]

\* All abbreviations are described below in the text of the article.

\*\* RCY is a radiochemical yield.

\*\*\*No data is available.

- Stability/inertness: BFC should form thermodynamically stable and kinetically inert complexes to prevent any ligand exchange or hydrolysis *in vivo*.
- Kinetics of rapid complexation: for biological targeting vectors, BFC radiolabeling should be effective and fast at low temperatures and low pH.
- Selectivity: BFC must selectively bind the metal of interest in order to avoid low specific activity during radioactive labeling, for example, due to the presence of other decay products.
- Universal chemistry of conjugation: the flexibility of conjugation of BFC with functional groups of target vectors allows optimizing pharmacokinetics by regulating the polarity of the entire conjugate.
- Affordability: BFC preparation should be simple, fast, cost-effective, and scalable for preparing several grams of product with the minimum possible number of reaction steps.

However, the success of BFC is not guaranteed even while meeting all of the requirements above. The two most important parameters of BFC that affect the properties of radiopharmaceuticals *in vivo* are the total charge and lipophilicity of the corresponding BFC metal complex. These parameters are determined by the geometry and set of BFC donors, as well as by the coordinated radiometal. For example, some peptide targeting vectors conjugated to identical BFC but labeled with different radiometals differ in binding to the receptor and behavior *in vivo* [22].

In recent years, various structural types of chelating agents with high stability and selectivity towards Ga(III) have been proposed for use in *in vivo* diagnostics.

### MACROCYCLIC GALLIUM CHELATING AGENTS

In recent years, the development of BFCs in general, as well as chelators to Ga(III), has mainly focused on polyaza macrocyclic ligands (Fig. 1). Such systems minimize transchelation or metal loss *in vivo*, which is beneficial for their use as radiopharmaceuticals.

In order to saturate all coordination sites on the six-coordinated Ga(III) cation, several multidentate derivatives of TACN (1,4,7-triazacyclononane) and cyclene (1,4,7,10-tetraazacyclododecane) with additional thiol-S, carboxylate-O and phosphonate-O donor groups were developed by introducing side branches on the secondary amines of the corresponding

macrocycle [23–29]. The most prominent representative of this category is the DOTA (1) ligand (1,4,7,10-tetraazacyclododecane-1,4,7,10-tetraacetic acid (Fig. 1). The thermodynamic constant of formation of the Ga-DOTA complex  $\log \beta_1 = 21.3$  is slightly higher than that of the Ga(III)-transferrin complex [2].

A donor set of  $N_4O_2$  of the cyclene fragment and two carboxylate groups encapsulate the metal center in the Ga-DOTA complex with cis-pseudo-octahedral geometry (Fig. 1) [30, 31]. Consequently, Ga-DOTA complexes have a negative overall charge under physiological conditions. Due to the kinetic inertness of the macrocycle, the complexation kinetics of DOTA are slow. Due to DOTA (1) radiolabeling requiring conventional or microwave heating to achieve adequate yields and specific activity, its application is limited to thermally stable target vectors [32–34].

Smith *et al.* investigated tunable  $^{68}\text{Ga}$ -labelled DO2A-like macrocycles for myocardial perfusion imaging (Fig. 2). By furnishing the DO2A (2) pendant arms, it was possible to influence the lipophilicity and charge while retaining a 6-coordination site for  $\text{Ga}^{3+}$  (Fig. 2). Radiolabelling was carried out at  $100^\circ\text{C}$  for 30 min with a pH of 4.93 in a NaOAc buffer [0.2 M, 0.5 mL]. The compounds with the highest lipophilicity [ $^{68}\text{Ga}$ ] GaDO2A-(xy-TXP)<sub>2</sub> ( $\log D_{7.4} = 0.28 \pm 0.01$ ) and [ $^{68}\text{Ga}$ ]GaDO2A-(xy)<sub>2</sub> ( $\log D_{7.4} = 0.31 \pm 0.01$ ) were assessed in an *ex vivo* Langendorff isolated perfused heart model. Uptake in compromised hearts was found to be significantly lower for both  $^{68}\text{Ga}$ -labelled complexes than in healthy hearts [35].

The NOTA (3) ligand (1,4,7-triazacyclononane-1,4,7-triacetic acid) (Fig. 1), which is rapidly and efficiently radiolabeled at room temperature, is highly stable *in vivo* [36–38]. Due to the smaller size of the corresponding cavity compared to DOTA, triazacyclononane ligands exhibit high conformational and size selectivity with respect to Ga(III). The NOTA (3) ligand and its derivatives bind Ga(III) in pseudo-octahedral coordination— $N_3O_3$  with low deformation, leading to complexes having a neutral total charge at physiological pH (Fig. 1) [39, 40].

The thermodynamic stability of the Ga-NOTA complex ( $\log \beta_1 = 30.7$ ) is about nine orders higher than that of Ga-DOTA [3]. This results from its excellent incorporation of a small Ga(III) cation into the NOTA (3) nine-membered triazamacrocyclic cavity. Regarding conjugation to targeting vectors, the use of one side functional group of the carboxylic acid DOTA (1) does not affect its ability to bind the metal, since only two of the four available carboxylic acid groups are involved in metal coordination. In the case of NOTA (3), conjugation

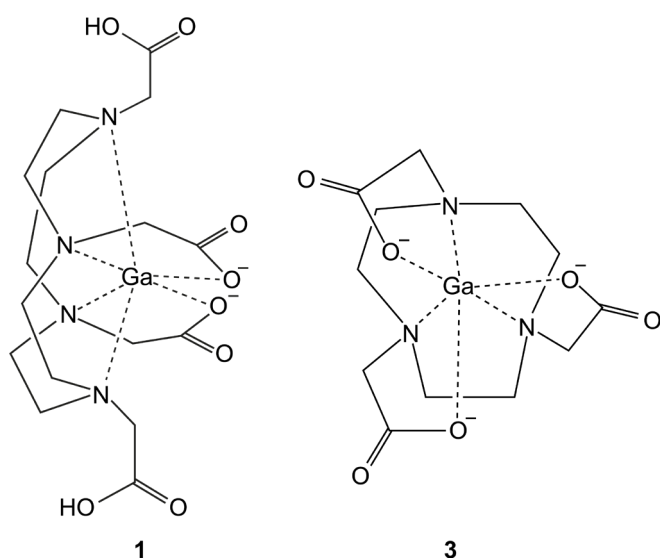


Fig. 1. DOTA (1) and NOTA (3) complexes with gallium.

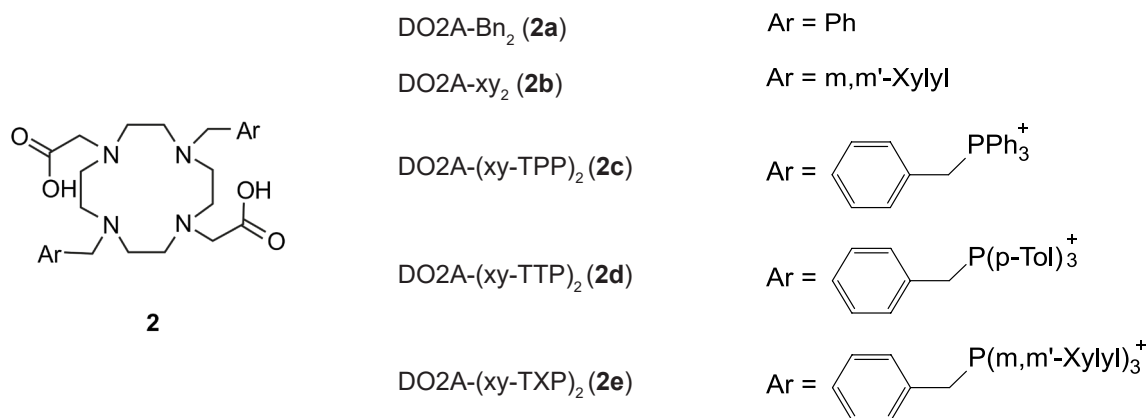


Fig. 2. DO2A (**2**) structural analogues.

can be achieved either using bifunctional derivatives of NOTA or using one of the three available carboxylic acid functional groups. However, if one of the carboxylic acid side groups is used for conjugation, the coordination properties of NOTA (**3**) are potentially impaired due to the impossibility of achieving the preferred stable octahedral coordination.

In order to preserve the hexadentate coordination of NOTA while ensuring covalent conjugation with the target vector, a range of derivatives have been developed: *p*-SCN-Bn-NOTA (**3c**) (S-2-(4-isothiocyanatobenzyl)-1,4,7-triazacyclononane-1,4,7-triacetic acid), NODASA (**3a**) (1,4,7-triazacyclononane-*N*-succinic acid-*N'*,*N''*-diacetic acid), and NODAGA (**3b**) (1,4,7-triazacyclononane-*N*-glutamic acid-*N'*,*N''*-diacetic acid) (Fig. 3). These compounds exhibit high labeling efficiency and stability *in vivo* [4, 39–42].

Other ligands NODAPA-OH (**3d**) and NODAPA-(NCS)<sub>*n*</sub> (**3e**, **3f**) (*n* = 1–2), which demonstrate radioactive labeling efficiency comparable to NOTA (**3**), are available due to an economical and cost-effective synthesis scheme. At pH 2.8, 85% of all tested ligands were

radiolabeled in 3 min at 45°C for NOTA (**3**) and NODAPA-OH (**3d**) and at 75°C for NODAPA-(NCS)<sub>*n*</sub> (**3e**, **3f**). The stability of the corresponding <sup>68</sup>Ga complexes was in the same range as the related NOTA, with less than 2% activity loss after 3 h in a rat plasma study. The possibility of using NODAPA-NCS (**3e**) was also demonstrated by conjugation with L-lysine and glucosamine with a yield of 65%–73% [5].

Another approach to the creation of multimeric TACN-based radiopharmaceuticals is *N,N,N'*-trisubstituted BFC PrP9(TRAP) (**3g**) (Fig. 4) (1,4,7-triazacyclononane-1,4,7-tris[methyl(2-carboxyethyl)phosphinic acid] using methyl(2-carboxyethyl)phosphinic acid [6].

In accordance with the crystal structure, the PrP9 (**3g**) ligand encapsulates the <sup>68</sup>Ga(III) cation with an N<sub>3</sub>O<sub>3</sub> donor distorted in an antiprismatic manner due to the amino groups of the macrocycle and side arms of the deprotonated phosphinic acid. Careful analysis of the Ga-PrP9 bond angles, which are close to a perfect octahedron, shows that the Ga-PrP9 complex is less constrained than its structurally related counterparts Ga-NOTA and Ga-NODASA, resulting in the cavity formed by

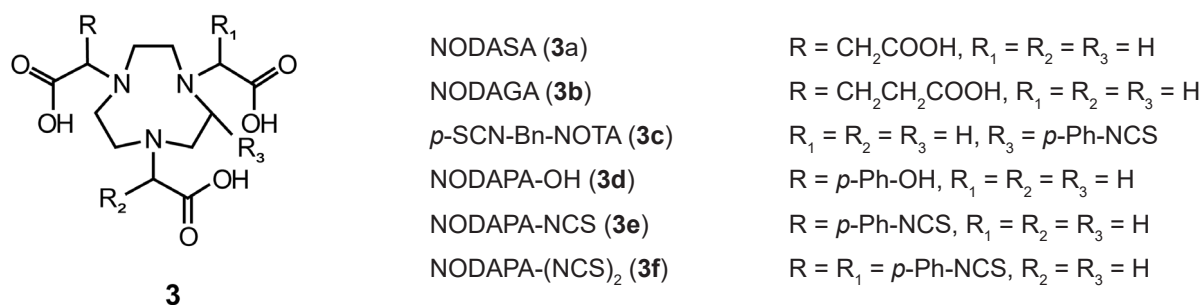


Fig. 3. Structural analogues of NOTA (**3**).

PrP9 (**3g**) being a good fit for Ga(III) coordination [32, 39]. Since adjacent carboxylic acid functional groups are not coordinated to the metal center, they can serve as connection points to targeting vectors. The thermodynamic stability constant ( $\log \beta_1$ ) of 26.24 is high enough for radiopharmaceutical applications. Ligand PrP9 (**3g**) additionally exhibits selectivity for small cations similar to that of NOTA (**3**), while the constants of formation of complexes with Cu(II) and Zn(II) are 10 orders of magnitude lower than those of the corresponding complex Ga(III). The  $^{68}\text{Ga}$  radiolabeling yields for PrP9 of over 95% were achieved within 5 min at 60°C in the pH range 1–5. The functionalization of carboxylic acid side chains did not significantly affect the labeling efficiency. A unique feature of PrP9 is the ability to give high labeling yields at very low pH.

Another phosphorylated analogue of NOTA, NOPO (Fig. 4a, **3h**) also exhibits exceptional selectivity to Ga(III), demonstrating a high proportion of gallium incorporation even in a medium containing a large quantity of other metal impurities [7]. In addition, this chelator is characterized by efficient complex formation even at room temperature and low concentrations (1–10  $\mu\text{M}$ ).

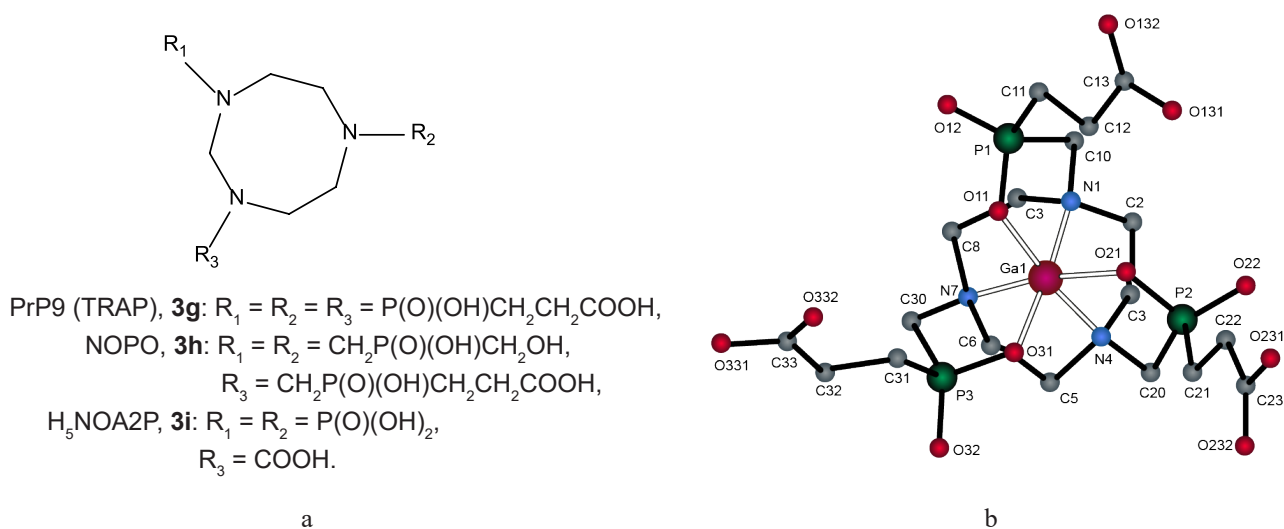
A derivative of phosphonic acid  $\text{H}_5\text{NOA2P}$  (**3i**) (1,4,7-triazacyclononane-*N,N'*-bis(methylene-phosphonic acid)-*N''*-methylene-carboxylic acid) (Fig. 4a) belongs to the class of triazacyclic ligands. Its high binding constant with  $^{69}\text{Ga}$   $\log \beta_1 = 34.44$  surpasses NOTA (**3**) and DOTA (**1**). However, the radiolabeling of such a structure occurs quite slowly at 95°C for 30 min. The stability of this complex

at pH 7.4 is somewhat higher than that of Ga(III) with transferrin. With regard to biological activity, it has been established that, despite the rather high stability of  $\text{H}_5\text{NOA2P}$  (**3i**) *in vivo*, it is quickly excreted from the body by the kidneys. Nevertheless, the possibility of more efficient binding to peptides or octreotide for similar structures containing two methylenephosphonic groups has been noted. This demonstrates the potential for a more detailed study of the bioconjugation of such complexes in living systems [8].

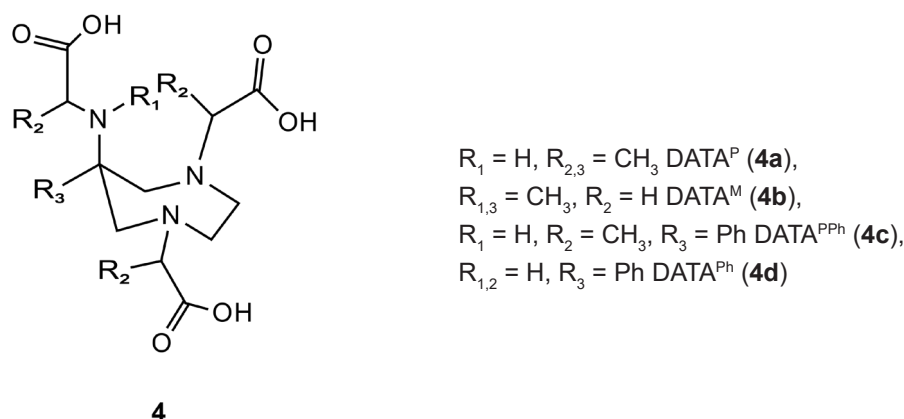
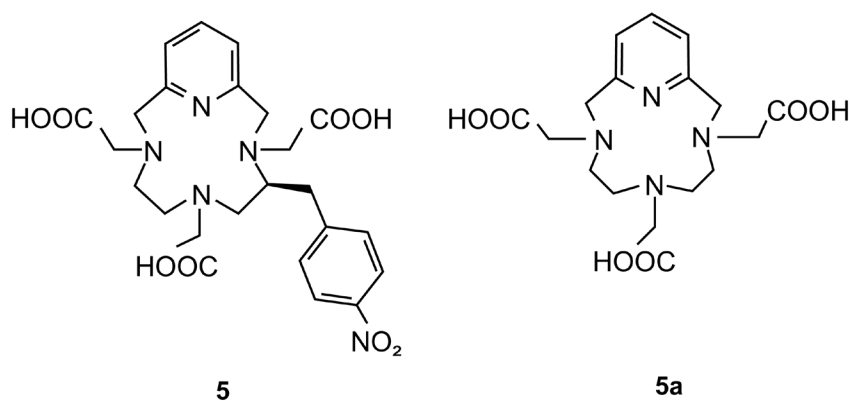
Hexadentate chelators based on 6-amino-1,4-diazepine triacetate (DATA, **4**) form octahedral complexes with Ga(III) (Fig. 5).

For all four chelators, the radiochemical yield was quite high for 10 min. For  $\text{DATA}^{\text{Ph}}$  (**4a**) and  $\text{DATA}^{\text{M}}$  (**4b**), they reached 97% and 93%; for  $\text{DATA}^{\text{Ph}}$  (**4c**) and  $\text{DATA}^{\text{Ph}}$  (**4d**), the yields were 93% and 84% after 1 and 10 min, respectively. The fact that such complexes exist across a wide range of temperatures and pH (4–7) makes them quite labile and widely applicable for various bioconjugates, especially if they are sensitive to the conditions of the biological environment. The fairly wide spread of lipophilicity for all four complexes is also of great importance for individual distribution *in vivo*, allowing a chelator for the vector to be more accurately selected [10, 43, 44].

A macrocyclic chelator based on a chelating agent, which was developed two decades ago, has recently been tested for radiopharmaceutical purposes [45]. Ligand *p*- $\text{NO}_2$ -Bn-PCTA (**5**) (PCTA (**5a**) = 3,6,9,15-tetraazabicyclo[9.3.1]pentadeca-1,11,13-triene-3,6,9-triacetic acid) (Fig. 6) is based



**Fig. 4.** (a) Structures of PrP9 TRAP (**3g**), NOPO (**3h**), and  $\text{H}_5\text{NOA2P}$  (**3i**); (b) crystal structure of PrP9 (TRAP) (**3g**) with gallium [6].

Fig. 5. DATA (**4**) and its analogues.Fig. 6. *p*-NO<sub>2</sub>-Bn-PCTA (**5**).

on a 12-membered tetraaza macrocycle containing a pyridine group with a *p*-nitrobenzyl substituent, which can be converted to an isocyanide for attachment to a targeting vector [46].

The lower thermodynamic stability ( $\log \beta_1 = 19.37$ ) of complexes of PCTA (**5a**) with metals can be attributed to their lower overall basicity as compared with the corresponding DOTA (**1**) complexes. As a consequence, the competition between protons and metal ions for PCTA (**5a**) is lower than for DOTA (**1**), making PCTA (**5a**) the best ligand over the entire pH range. In addition, PCTA was found to have a much faster complexation than DOTA (**1**) [46]. The *p*-NO<sub>2</sub>-Bn-PCTA ligand (**5**), which demonstrated higher labeling efficiency compared to *p*-NO<sub>2</sub>-Bn-DOTA (**1a**), achieved a radiochemical yield of over 96% at pH 3 to 5 and room temperature.

The <sup>67/68</sup>Ga-*p*-NO<sub>2</sub>-Bn-PCTA complexes were highly kinetically stable with little degradation or loss of <sup>67</sup>Ga following incubation for 24 h at pH 2. In the presence of excess apotransferrin at 37°C, <sup>68</sup>Ga-*p*-NO<sub>2</sub>-Bn-PCTA showed transchelation of approximately 10% to protein within 4 h.

Sarcophagin-type BFCs (sarcophagin = sar = 3,6,10,13,16,19-hexaazabicyclo[6.6.6]icosane) were originally developed for <sup>64</sup>Cu radiopharmaceuticals but have recently been evaluated for <sup>68</sup>Ga labeling (Fig. 7a).

Metal complexes of this chelator type are extremely stable due to the rigidity and encapsulating nature of the cell's amino ligand backbone. In the crystal structure of the Ga(III)-(1-NH<sub>3</sub>-8-NH<sub>2</sub>)-sar complex, the Ga(III) cation is six-coordinated with the N<sub>6</sub> donor in a trigonally distorted octahedral geometry [11].

For the conjugation of two cyclic RGD peptides to target the α<sub>v</sub>β<sub>3</sub> integrin receptor, a diamsar derivative with two glutamic acid residues conjugated to primary amino groups through amide bonds was studied [11]. In contrast to labeling with <sup>64</sup>Cu, which usually gives high yields at room temperature, for labeling the <sup>68</sup>Ga bioconjugate, the diamsar-RGD dimeric complex was heated at 85°C for 30 min. However, a quantitative labeling with a yield of more than 98% was achieved this way. The <sup>68</sup>Ga-labeled conjugate showed no transfer

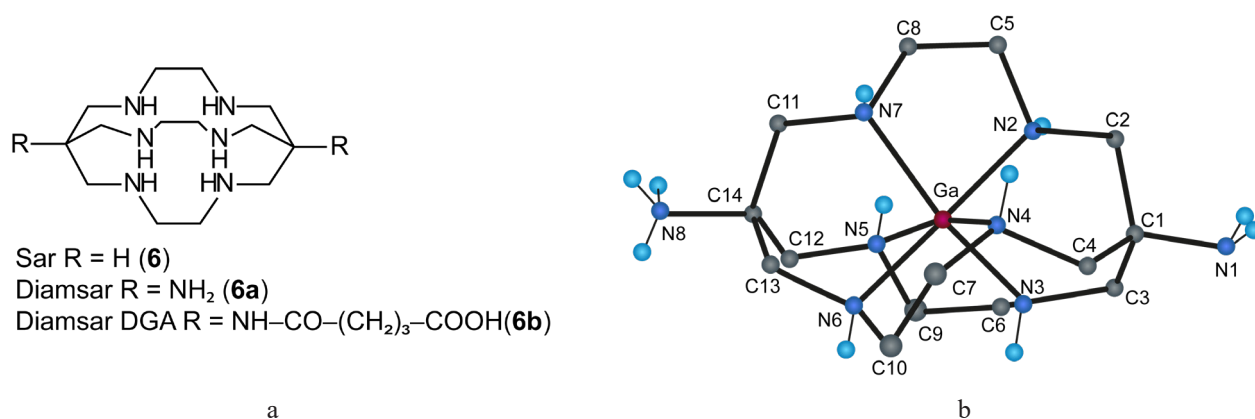


Fig. 7. (a) The sarcaphagin-type BFC structure, (b) X-ray diffraction analysis results of diamsar (**6a**) complex with gallium [11].

to apotransferrin for up to 2 h in an *in vitro* study, but showed specific binding to the receptor *in vitro* and demonstrated high selective tumor uptake with predominantly renal clearance in biodistribution and microPET imaging studies.

### ACYCLIC CHELATORS

The macrocyclic effect generally results in kinetically more inert and thermodynamically more stable metal complexes of macrocyclic chelators compared to acyclic ligands, making macrocycle-based BFCs more attractive for radiopharmaceutical applications. However, the fairly successful *in vivo* acyclic chelators are superior to their macrocyclic counterparts. A significant advantage of acyclic ligands is their faster metal binding, which leads to faster radioactive labeling, especially in the case of shorter-lived radiometals such as <sup>68</sup>Ga [47, 48].

A representative ligand of this class is the acyclic chelator HBED (*N,N'*-bis-(2-hydroxybenzyl)-ethylenediamine-*N,N'*-diacetic acid) (**7**). Based on an EDTA-type framework with two hanging phenolic branches, this ligand has recently attracted increased attention in the development of BFC for radiopharmaceutical applications (Fig. 8) [14, 49].

When this ligand was developed in the 1950s, it was observed to form highly stable complexes with Ga(III) ( $\log \beta_1 = 38.51$ ) [13]. The acyclic bifunctional ligand HBED-CC (*N,N'*-bis-[2-hydroxy-5-(carboxyethyl)-benzyl]ethylenediamine-*N,N'*-diacetic acid) (**7a**), which is characterized by rapid and efficient radioactive labeling at room temperature, has high *in vivo* stability; for this reason, it is used for labeling thermosensitive biomolecules [14, 15, 49]. An intact monoclonal antibody (mAb) used as a model protein with a recombinant diabody was consequentially linked to HBED-CC (**7a**) [49]. <sup>68</sup>Ga binding

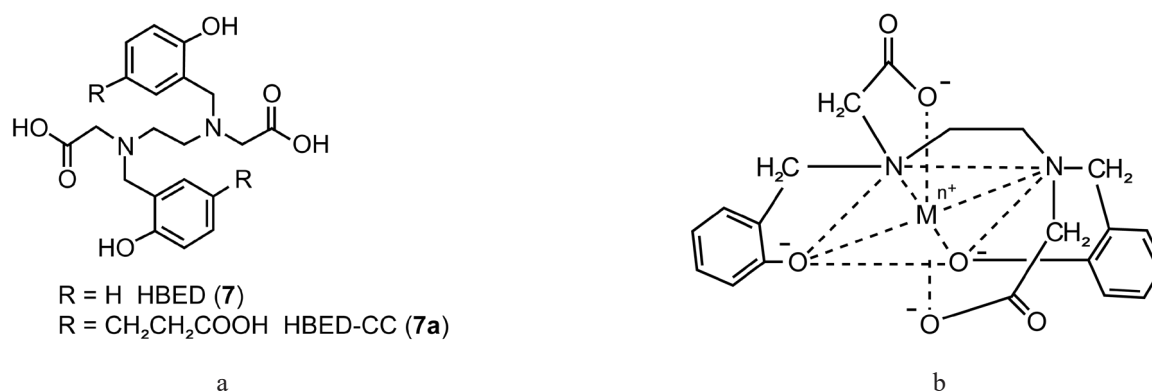


Fig. 8. (a) HBED (**7**) and HBED-CC (**7a**), (b) HBED complex (**7**) with gallium.

to the HBED-CC-mAb bioconjugate gave high radiochemical yields under mild conditions. Complexation at pH 4.1 for 5 min at 40°C produced a 89% yield of radiolabeled bioconjugate, as compared with diabody labeling, which achieved a slightly lower yield of 85% in a HEPES buffer at pH 4.5 and 40°C. Binding assays showed that labeled  $^{68}\text{Ga}$ -HBED-CC did not significantly affect the receptor binding of the antibody and the diabody. In addition, the acyclic BFC HBED-CC (**7a**) was evaluated in a second comparative study with NOTA (**7a**) [14]. HBED-CC (**7a**) was conjugated to protein via activated *N*-hydroxysuccinimide. The protein used in this study was single chain vascular endothelial growth factor (VEGF) expressed with a cysteine containing fusion tag (Cys-tag) for site-specific conjugation of PEGylated bifunctional chelating agents. The corresponding bioconjugates HBED-CC (**7a**) and NOTA (**3**) were labeled at pH 4.2 and room temperature. Under these conditions, the HBED-CC conjugate (**7a**) bound quantitatively (98.7%) within 4 min, while the binding to NOTA (**3**) was 50%. To achieve a comparable labeling result for NOTA (**3**), an incubation of more than 10 min was required.

The HBED-CC (**7a**) and NOTA (**3**) conjugates were highly stable, as it was demonstrated by a long-term radiochemical study of human serum, in which no decomplexation was observed after 72 h. In cell-to-cell binding studies with 293/KDR cells, both radiolabeled bioconjugates showed comparable binding with nearly identical  $K_D$  values (0.67 for HBED-CC (**7a**) vs. 0.59 for NOTA (**3**)), which are in excellent agreement with other radiolabeled scVEGF tracers. Biodistribution studies of both indicators using *ex vivo* imaging and PET

in mice with tumor showed a similar distribution pattern for both indicators, however, liver uptake of the HBED-CC conjugate (**7a**) was markedly lower than for the NOTA analogue (**3**). On the other hand, the renal uptake of NOTA (**3**) was lower compared to HBED-CC (**7a**).

A possible modification of HBED-CC (**7a**) at propionic acid residues led to the creation of mono- and bis-condensation products with 4-amino-*N*-(4-((3-bromophenyl)amino)quinazolin-6-yl)butanamide. MTT analysis of mono- and bis-condensed products and their corresponding complexes showed  $\text{IC}_{50}$  values below 70  $\mu\text{M}$  in the A431 cancer cell line, making them the first complexes of Ga(III) with quinazoline derivatives demonstrating antiproliferative activity in the micromolar range described in literature. Previous studies of quinazoline analogues coupled to the DOTA (**1**) chelator and labeled with  $^{67}\text{Ga}$  did not show any cytotoxicity even at higher concentrations [15].

Pyridine chelators are actively developed, one of the best examples being H<sub>2</sub>dedpa (**8**) (6,6'-(ethane-1,2-diylbis(azandiylbis(methylene) dipicolinic acid) (R = H) and its corresponding precursor (R = 1-methyl-4 nitrobenzene) (**8a**) (Fig. 9), which also belong to acyclic chelators [12].

The H<sub>2</sub>dedpa (**8**) ligand binds Ga(III) in a distorted octahedral manner with two carboxylate donor atoms, two pyridine ring nitrogens, and two secondary amine N-donor atoms both in solution and in the solid state, and forms Ga(III) complexes with a high thermodynamic stability ( $\log \beta_1 = 28.11$ ). The coupling of H<sub>2</sub>dedpa (**8**) and its  $^{68}\text{Ga}$  bioconjugate precursor gave quantitative yields within 10 min at room temperature. Once formed, the complex remains intact up to 97% for 2 h in an *in vitro* transferrin challenge experiment.

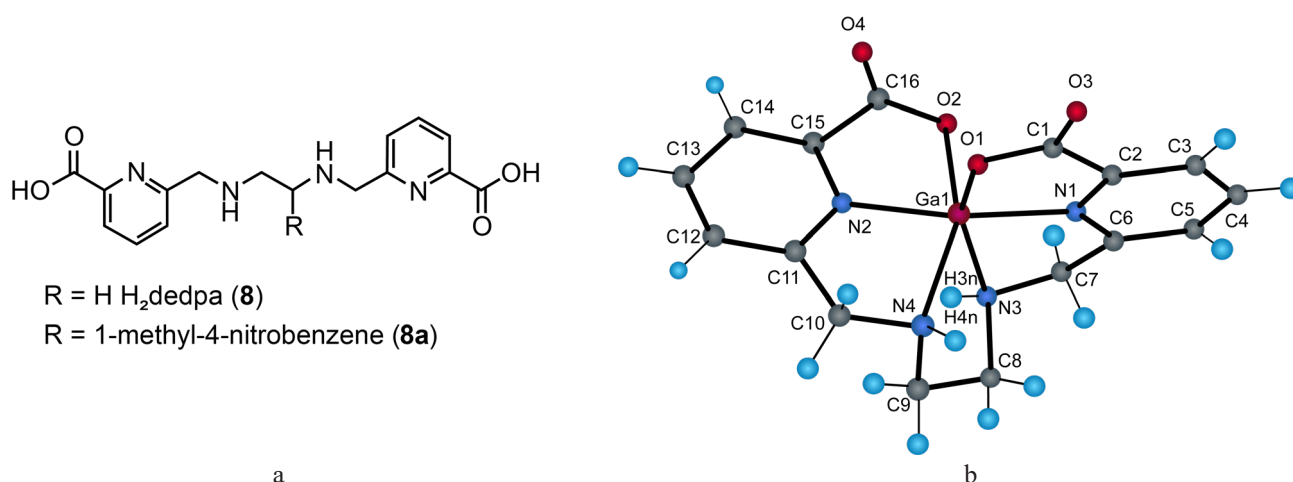


Fig. 9. (a) H<sub>2</sub>dedpa structure (**8**), (b) a crystal structure of H<sub>2</sub>dedpa with gallium [12].

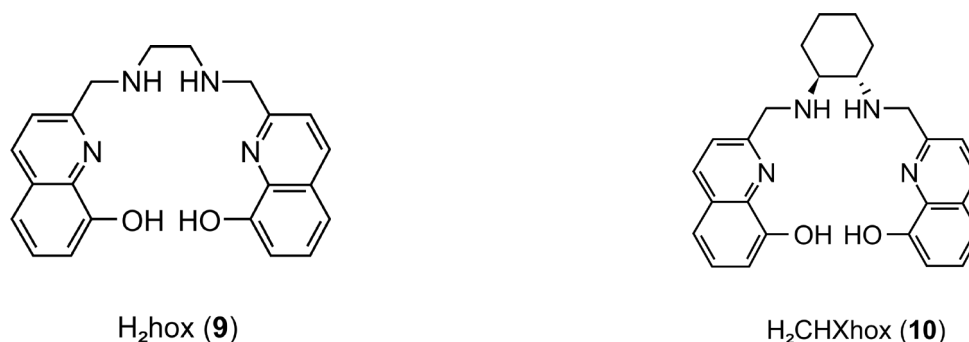


Fig. 10. Structural formulas of  $\text{H}_2\text{hox}$  (9) and  $\text{H}_2\text{CHXhox}$  (10).

Increasing the degree of preorganization by adding a *trans*-1,2-cyclohexanediamine backbone, such as in  $\text{H}_2\text{hox}$  (9) and  $\text{H}_2\text{CHXhox}$  (10), results in an increase in the kinetic inertness of the complex (Fig. 10). This modification also resulted in a higher thermodynamic stability of  $[\text{natGa}]\text{H}_2\text{CHXhox}$  compared to  $[\text{natGa}]\text{H}_2\text{hox}$ , and a superior stability of  $[\text{natGa}]\text{H}_2\text{CHXhox}$  at pH 1. Radiolabeling of both  $\text{H}_2\text{hox}$  (9) (5 min, 25°C,  $1 \cdot 10^{-7}$  M, pH 8.5), and  $\text{H}_2\text{CHXhox}$  (10) (~1 min,  $\Delta$ ,  $2.1 \cdot 10^{-5}$  M, pH 5) with  $^{68}\text{Ga}$  chloride proceeded in a short period of time and showed good *in vivo* stability along with limited toxicity *in vitro*. Due to milder radiolabeling conditions, these chelators are promising candidates as BFC for biological vectors [35].

Tris(8-quinolinolate) gallium(III) (KP46) (11) has been developed to provide high oral bioavailability of gallium during cancer treatment. In contrast to gallium(III) chloride, KP46 (11) shows higher cellular uptake in rat glioblastoma cells, causing a significant decrease in intracellular levels of deoxyribonucleoside triphosphate [16].

KP46 (11) is 10 times more active against A549 human lung malignant adenocarcinoma cells than gallium chloride, which exhibited dose- and time-dependent cytotoxicity, while KP46 (11) cytotoxic activity was dose-dependent only. These results suggested that the mechanisms of action of gallium chloride and KP46 (11) are different [50]. To evaluate the safety, toxicity profile and pharmacokinetics of the drug, a phase I trial of KP46 (11) was conducted in 2004. Seven patients with advanced malignant solid tumors located in the kidney, ovary, stomach, and parotid gland were treated with KP46 (11). Oral administration of KP46 (11) was effective in three out of four patients with renal cell carcinoma. Studies have shown that a long terminal half-life, high total clearance, and a large apparent volume of distribution characterize the pharmacokinetics of gallium [16, 51].

Its analogue, 5-chloro-8-quinolinol (12), can also form a tris-coordinated structure, where nitrogen and oxygen atoms coordinate the gallium atom (Fig. 11).

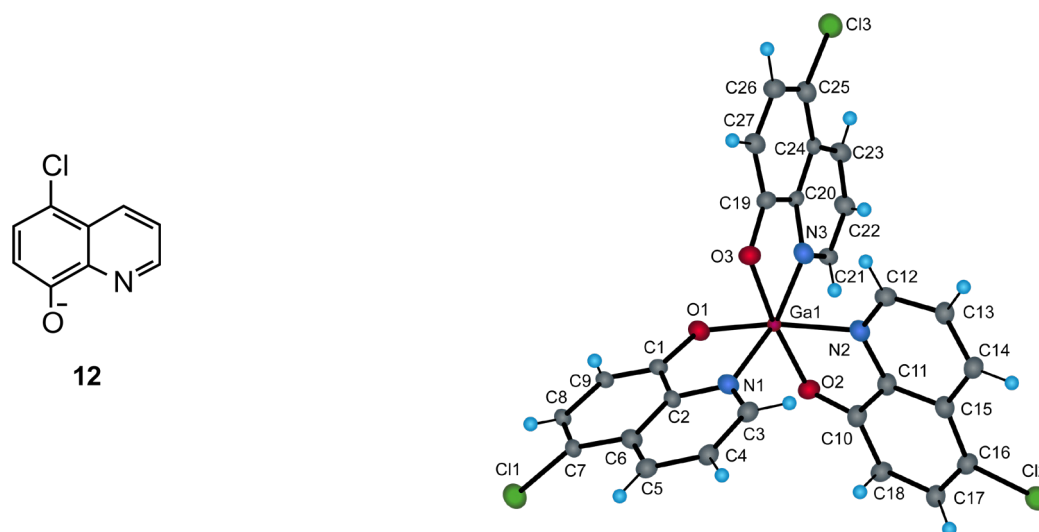


Fig. 11. (a) 5-Chloro-8-quinolinone (12), (b) its crystal structure with gallium [52].

This complex was tested for cytotoxicity against A2780 ovarian cancer cells, MDA-MB-231 breast carcinoma (derived from a metastasis site), HCT116 epithelial colorectal cancer cell line, and MRC5pd30 non-cancerous human lung tissue cells. The complex showed good activity against a whole panel of cancer cell lines with  $IC_{50}$  values in the low micromolar concentration range. It exhibited potency comparable to clinically used cisplatin in cisplatin-responsive A2780 cells, but was significantly more active in cisplatin-initially resistant colon and breast cancer cells, including the difficult-to-treat, highly metastatic MDA-MB-231 cell line. In addition, it showed a clear selectivity for malignant tumor cells compared to benign lung fibroblastoma (MRC5pd30) [52].

Dimethoxypyridine-3-carboxylic acid is also capable of complexing with  $Ga^{III}$ — $[Ga^{III}_2(\mu-DMP-kO:kO')]_2$  (**13**), forming a tetracoordinate structure with a distorted tetrahedral configuration, with two *tert*-butyl groups and two different oxygen atoms of two different metal-bound carboxylate ligands (Fig. 12).

The *in vitro* cytotoxicity of  $[Ga^{III}_2(\mu-DMP-kO:kO')]_2$  (**13**) against the HeLa human adenocarcinoma, Fem-x human malignant melanoma, K562 human myelogenous leukemia, and MDA-MB-361 human breast carcinoma showed a dose-dependent antiproliferative effect. The complex has a higher cytotoxic activity against K562 compared to other cell lines, indicating some preferential activity under these conditions [53].

In a series of ligands based on 3-hydroxy-4-pyridinone (GPO), the hexadentate chelator CP256

(R = acyl) (**14a**) and its bifunctional version YM103 (R = *N*-(3-amino-3-oxopropyl)-3-(2,5-dioxo-2,5-dihydro-1H-pyrrol-1-yl)propane) (**14b**) showed a very high labeling efficiency at room temperature with a radiochemical yield of more than 98% within 5 min at pH 6.5 (Fig. 13) [18].

In studies of the stability of the  $^{68}Ga$ -CP256 complex in human serum under control infection with apotransferrin, neither decomplexation nor transchelation was observed, which indicates its high stability and inertness. PET imaging studies using the C2Ac protein as a target vector, which is analogous to the phosphatidylserine-binding domain of synaptotagmin I, further confirmed stability *in vivo*.

Another chelator based on hexadentate GPO, NTP(PrHP)<sub>3</sub> (**14c**), is used as a metal-binding agent for chelation therapy and may be suitable for labeling  $^{68}Ga$  biomolecules (Fig. 14) [54, 55]. The NTP(PrHP)<sub>3</sub> ligand (**14c**) forms a hexacoordinate complex with Ga(III) with high thermodynamic stability ( $\log \beta_1 = 33.34$ ), however, it has been shown in titration experiments that at pH > 6 it changes to a water-insoluble form, what should be explicitly avoided in radiopharmaceutical applications. However, the therapeutic concentrations at which this drug can be used are an order of magnitude lower than the concentrations that have a significant effect on its solubility.

The radiochemical purity of the  $^{67}Ga$ -NTP(PrHP)<sub>3</sub> complex was more than 98%. Due to the ability of NTP(PrHP)<sub>3</sub> (**14c**) to coordinate  $^{67}Ga$  *in vivo*, its activity was investigated by co-administration

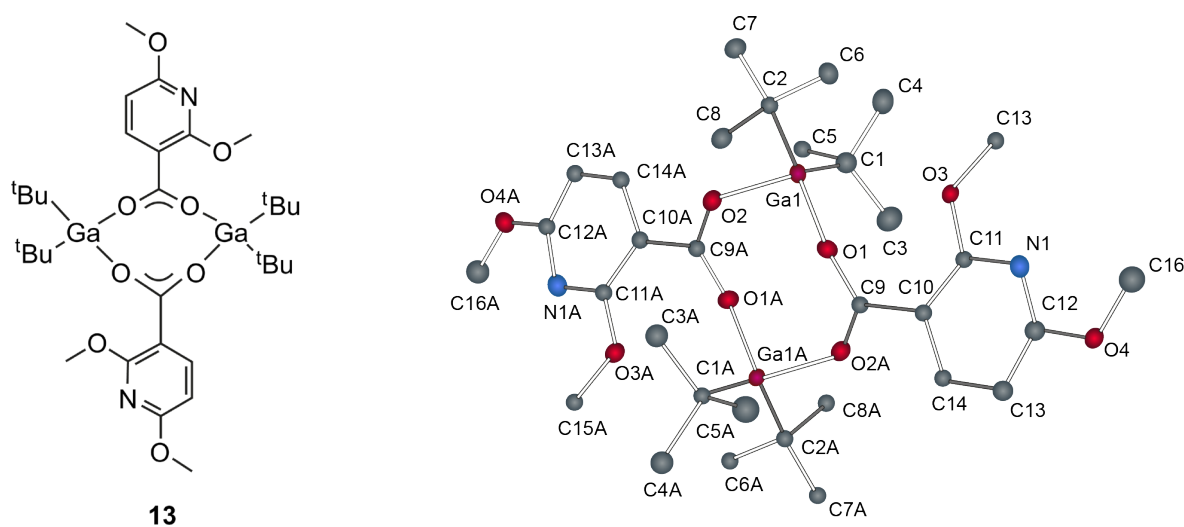
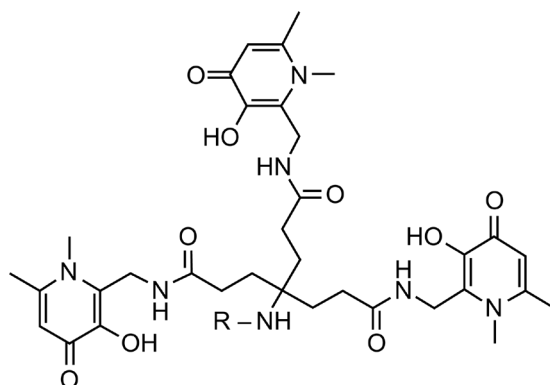


Fig. 12. (a)  $[Ga^{III}_2(\mu-DMP-kO:kO')]_2$  (**13**), (b) its crystal structure with  $Ga^{III}_2$  [53].



R = H DPO (**14**),

R = acyl CP256 (**14a**),

R = *N*-(3-amino-3-oxopropyl)-3-(2,5-dioxo-2,5-dihydro-1H-pyrrol-1-yl)propane YM103 (**14b**).

**Fig. 13.** DPO (**14**), CP256 (**14a**), and YM103 (**14b**).

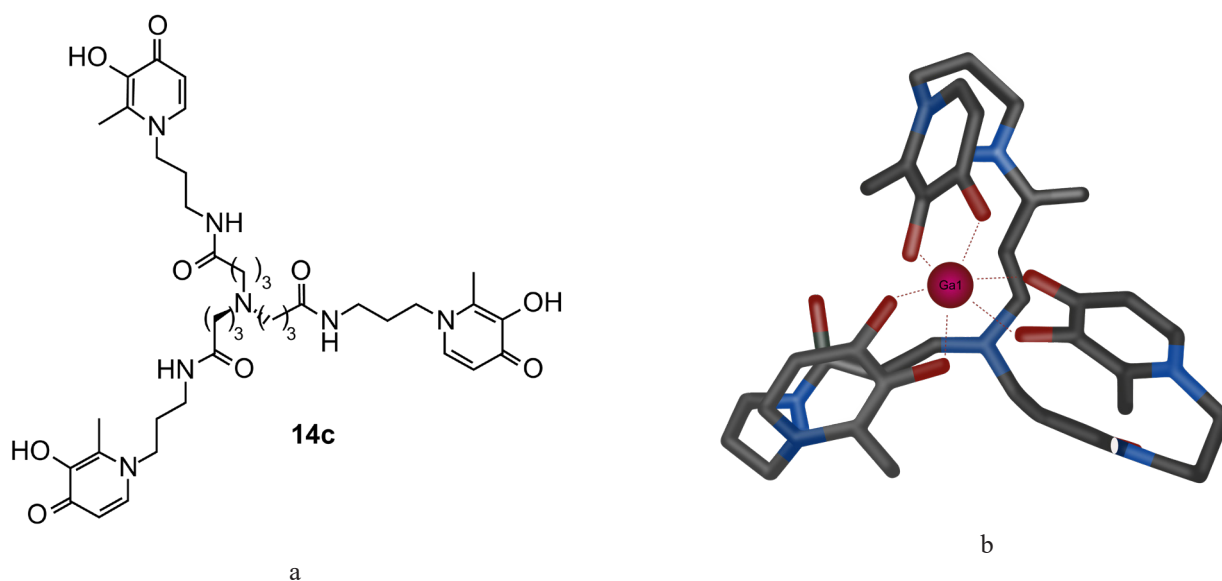


**Fig. 14.** (a) Structure of NTP(PrHP)<sub>3</sub> (**14c**), (b) XRD results of its complex with gallium [54].

of the ligand after injection of <sup>67</sup>Ga-citrate, which causes a rapid clearance of <sup>67</sup>Ga from blood, muscles, and bones. In an additional biodistribution study of the <sup>67</sup>Ga-NTP(PrHP)<sub>3</sub> complex, no significant differences in uptake and clearance were noted. A study of the <sup>67</sup>Ga-NTP(PrHP)<sub>3</sub> complex, carried out on Wistar rats, showed that it was mainly localized in the blood, kidneys, and liver after 30 and 60 min with little or no absorption by other organs. <sup>67</sup>Ga-NTP(PrHP)<sub>3</sub> was rapidly cleared from the blood and only 2% of the administered dose was present after 60 min. After 24 h, the complex was largely eliminated from all tissues, with the

exception of the kidneys, where about 10% of the original concentration was still present.

The deferoxamine (DFO) chelator (**15**) is well known for its use in iron chelation therapy (Fig. 15). The similarity of high-spin Fe(III) with Ga(III) determines the ability of DFO (**15**) to form complexes with Ga(III), which also have high thermodynamic stability. The possibility of its use as a BFC for gallium radioisotopes has been proven in combination with peptides and small molecules [20, 56, 57].

<sup>67</sup>Ga labeling was effective, but the complex was poorly retained in cells after antibody

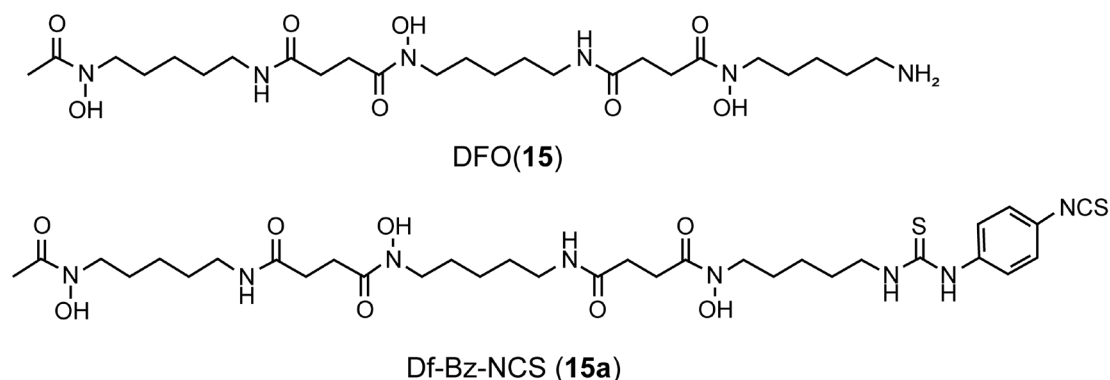


Fig. 15. DFO (15) and Df-Bz-NCS (15a).

internalization and, probably, after biotransformation. Van Dongen *et al.* have addressed this issue: he used BFC Df-Bz-NCS (*p*-isothiocyanatobenzyl-desferrioxamine) (15a), which was conjugated with the 7D12 nanobody against the epidermal growth factor receptor (EGFR) (Fig. 15) [21].  $^{68/67}\text{Ga}$  labeling was achieved by incubating the Df-bioconjugate at pH 7.2 for 5 min, followed by column purification. The  $^{68/67}\text{Ga}$ -Df-Bz-NCS-7D12 conjugate was stable in human serum with a radioactivity loss of less than 2% at 2 h and 7% at 24 h. In biodistribution studies,  $^{68}\text{Ga}$  labeled 7D12 nanobody showed high uptake in A431 tumors. There was no significant accumulation in other organs, with the exception of the kidneys. In PET imaging studies, the tumor was clearly visualized using  $^{68}\text{Ga}$ -Df-Bz-NCS-7D12.

Bispidines (compounds based on the core of 3,7-diazabicyclo[3.3.1]nonane) (16) are widely used chelators with a well-organized coordination site (Fig. 16). They have been used to form complexes with a range of metals, including radioactive ones such as copper-64, whose complexes

have proven to be extremely inert. However, the use of bispidines for the chelation of Ga(III) and, in particular,  $^{68}\text{Ga}$ , remained relatively unexplored until recently [58].

Bispidine ligand (16) was first used for complex formation with Ga(III) and was labeled with  $^{68}\text{Ga}$ . Despite its 5-coordinate nature, the resulting complex is stable in serum for more than 2 h, showing a ligand system well matched to the imaging window of  $^{68}\text{Ga}$  PET. To show the versatility of the bispidine ligand (16) and its potential use in PET, a bifunctional chelator was conjugated to a porphyrin. The resulting compound showed the same level of serum stability as the unconjugated  $^{68}\text{Ga}$  complex.

The complexation of Ga(III) with bispidine (16) was carried out at pH 4–4.5 and reflux. A radiochemical yield of 89% was achieved at a ligand concentration of 100  $\mu\text{M}$ , while at 200  $\mu\text{M}$  the yield was 94% (Fig. 17).

In terms of complexation kinetics and radiolabeling efficiency, bispidine (16) is not as effective as NOTA (3) and the phosphine analogue TRAP (3g), which can be labeled with a radioactive

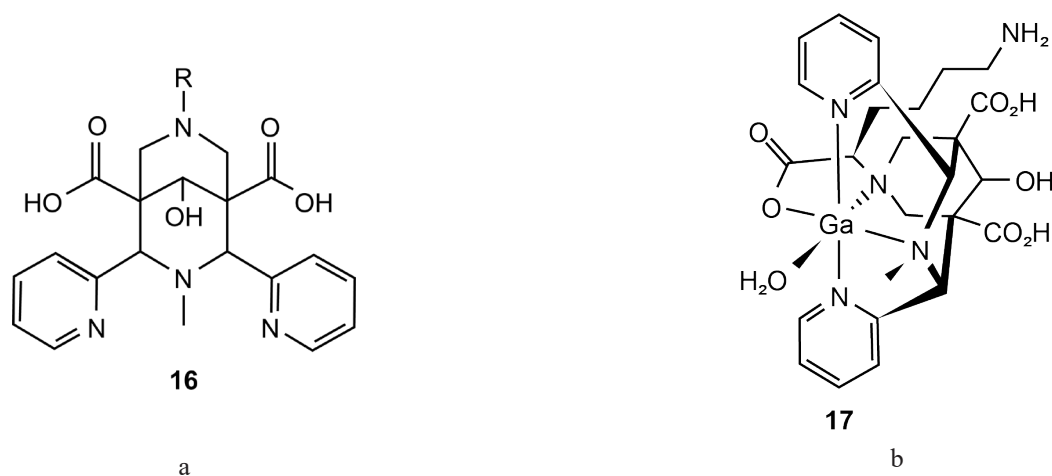


Fig. 16. (a) Bispidine (16), (b) complex of bispidine with gallium (17) [58].

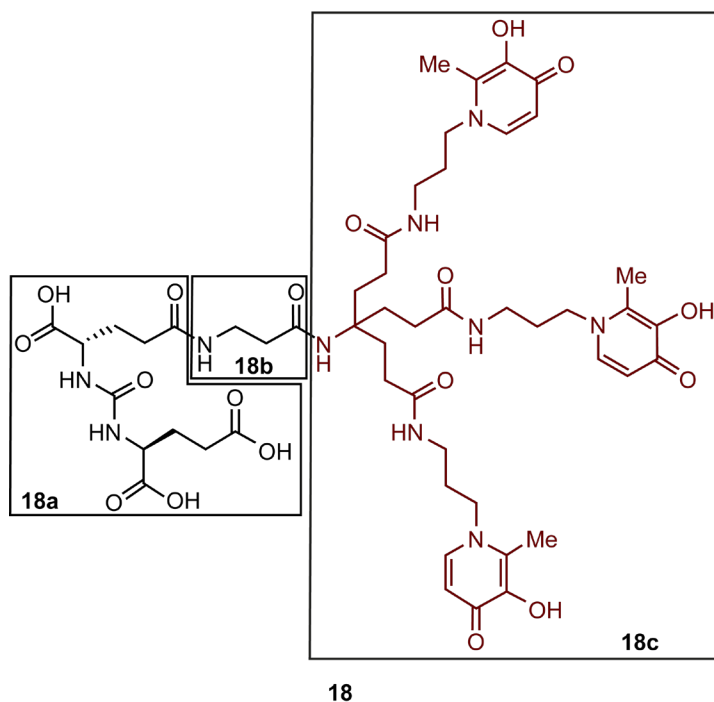


Fig. 17. DUPA- $\beta$ -Ala-KC18 (**18**).

isotope at much lower concentrations at 95°C or at room temperature using large excess of ligand. A similar trend is observed when compared with acyclic ligands such as H<sub>2</sub>dedpa (**8**) and H<sub>3</sub>dpa (**8b**). These differences are not surprising, since bispidine is a pentadentate ligand, which is not optimal for Ga(III) complexation in terms of kinetics, selectivity, and thermodynamic stability.

However, based on observations of the behavior of analogous <sup>64</sup>Cu compounds, one can expect positive results in terms of kinetic inertness when using a bispidine framework. When evaluating radiochemical stability, decomplexation was not observed for 2 h at 37°C, which proves the suitability of this ligand for <sup>68</sup>Ga-PET *in vivo*. In addition, it is contemplated that radiochemical yields and radiolabeling conditions can be further improved by using other bispidine derivatives, in particular those with a hexadentate coordination site [58].

A recently emerging class of chelators is based on tris-(hydroxypyridinone) (THP) (**17**). THP-peptide bioconjugates complex with <sup>68</sup>Ga rapidly and quantitatively at room temperature, neutral pH, and micromolar ligand concentrations, which makes them suitable for the synthesis of PET radiopharmaceuticals. A bifunctional chelator named THP-PSMA (**17a**) represents this class of compounds. In THPPSMA (**17a**) there are three groups of 1,6 dimethyl-3-hydroxy-4-pyridinone and glutamate-urea-lysine. In addition to the

aforementioned advantages, the chelation process with this <sup>68</sup>Ga ligand is not affected by the presence of other metal ions such as Fe<sup>3+</sup>. However, <sup>68</sup>Ga-THP-PSMA showed lower absolute tumor uptake compared to <sup>68</sup>Ga-PSMA-11 [59].

For this reason, a new conjugate was synthesized containing 3-hydroxypyridin-4-one (**17**) and a fragment of DUPA (**18a**) (2-[3-(1,3-dicarboxypropyl)-ureido]-pentanedioic acid), called DUPA- $\beta$ -Ala-KC18 (Fig. 17). In DUPA- $\beta$ -Ala-KC18 (**18**), DUPA (**18a**) acts as a PSMA (prostate specific membrane antigen) targeting moiety and KC18 (**18c**) acts as a Ga(III) chelating moiety;  $\beta$ -Ala (**18b**) was used as a linker to separate the segments. The performed studies have found that DUPA- $\beta$ -Ala-KC18 (**18**) can quickly form a stable complex with <sup>nat</sup>Ga<sup>3+</sup>, which implies that DUPA- $\beta$ -Ala-KC18 (**18**) can be efficiently labeled with <sup>68</sup>Ga [60].

Another promising class of ligands for gallium are thiosemicarbazone derivatives, which have potentially high antitumor activity. It was shown that thiosemicarbazones in complex with Ga(III) inhibit the activity of ribonucleoside diphosphate reductase (RDR) and have antiproliferative properties. Due to its similarity to Fe(III), Ga(III) affects the availability of intracellular iron, but also interacts directly with RDR by competing with iron for its binding site in the R2 subunit of the enzyme. The combination of the central metal and ligand, which are directed to the same molecular target using different mechanisms of action, can constitute a strategy for obtaining potent RDR inhibitors in which the two structural components exhibit a synergistic effect [61].

The reaction of 2-acetylpyridine *N*-dimethylthiosemicarbazone with GaCl<sub>3</sub> leads to the formation of the complex [GaL<sub>2</sub>][GaCl<sub>4</sub>] (KP1089) (Fig. 18). The gallium atom in this compound is coordinated with two nearly planar tridentate ligands. The coordination polyhedron approaches an octahedron, where two ligands are bonded to the gallium atom through the nitrogen atom of the pyridine ring, the nitrogen atom, and the sulfur atom of thiosemicarbazide [62]. The complex was tested for cytotoxicity against human tumor cell lines SW480 (colon adenoma), SK-BR-3 (breast adenocarcinoma), and 41M (ovarian carcinoma) [62].

[GaL<sub>2</sub>][GaCl<sub>4</sub>] had a strong antiproliferative effect at nanomolar concentrations in 41M, SK-BR-3, and SW480 cells, and the cytotoxicity of the complex was slightly higher against 41M cells than for free thiosemicarbazone. Similar results were obtained with SK-BR-3 and SW480 cells.

Alkylthiosemicarbazones (**20a-d**) (Fig. 19a) modified at the N4 position and their complexes with metals also exhibit significant anticancer

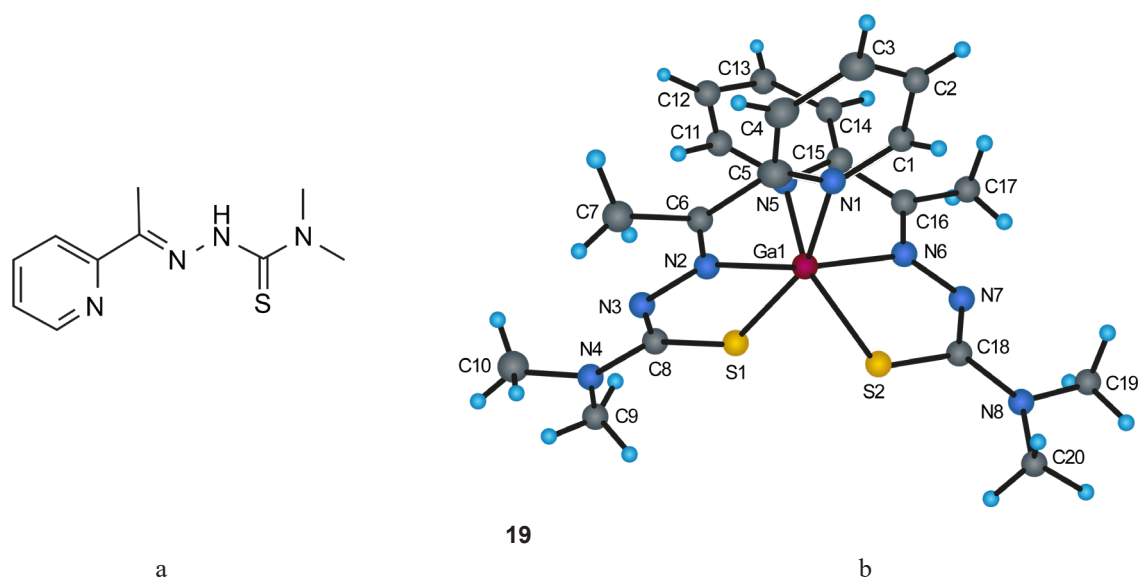


**Fig. 18.** (a) 2-acetylpyridine <sup>4</sup>*N*-dimethylthiosemicarbazone (**19**) structure, (b) crystal structure of [GaL<sub>2</sub>][GaCl<sub>4</sub>] [62].

activity. Upon modification of the methyl, phenyl, and pyridyl groups at the R<sub>1</sub> position of  $\alpha$ -*N*-heterocyclic piperidylthiosemicarbazones, the activity increases consistently. For  $\alpha$ -*N*-heterocyclic piperidylthiosemicarbazones (**21a-c**) (Fig. 19b), a decrease in activity is observed upon modification of the R<sub>2</sub> substituent in the H  $\rightarrow$  methyl  $\rightarrow$  ethyl series at the position of the pyrazine fragment.

It is also important to note that  $\alpha$ -*N*-heterocyclic piperidylthiosemicarbazones (**21a-c**) and their complexes with gallium exhibit low toxicity (IC<sub>50</sub> > 30  $\mu$ m) towards normal cells (MRC-5).

The results of a study of cellular Ga uptake performed on the MCF-7 cell line showed that complexes of thiosemicarbazone ligands with gallium are easily absorbed by cells and thus have a potentially high bioavailability. Regarding the mechanism of anticancer activity, it was found that these complexes have the ability to increase the expression of the transferrin-1 receptor (TfR1) and at the same time to suppress the expression of ferritin, which leads, on the one hand, to an increase in the intracellular concentration of iron and, on the other hand, to a decrease in the possibility of its deposition and causes toxic effects. In addition, complexes of thiosemicarbazone ligands with gallium showed a rather high ability to activate apoptosis by acting simultaneously on several proteins involved in the mechanism of its intracellular activation. It was shown that both the parent thiosemicarbazone ligands and, to a greater extent, their complexes with gallium, are able to increase the expression of caspases-3, -7 and -9, along with

an increase in the expression of cytochrome c (cyt-c) and apoptotic protease activating factor-1 (apaf-1), which together cause irreversible cell apoptosis. These experimental results indicate a great potential for using Ga(III) complexes with thiosemicarbazone ligands as effective anticancer drugs [63, 64].

2-Acetylpyridine- and 2-pyridiniformamidiso nicotinoylhydrazones HAPIH (**22**) and HPAmIH (**23**) form a complex with Ga(III) in the form of a zwitterion (Fig. 20). The hexadentate structure is formed due to the coordination of Ga(III) with the nitrogens of the pyridinium rings, free hydroxyls and nitrogens of the enamine fragment, thereby forming a zwitterionic structure.

HAPIH (**22**) and HPAmIH (**23**) were tested against HL-60 (leukemia), MCF-7 (breast cancer), HCT-116 (colorectal cancer), PC3 (prostate cancer) and HEK-293 (non-malignant human embryonic kidney cells). HAPIH (**22**) was most cytotoxic against colorectal cancer cells IC<sub>50</sub> = 1.6  $\mu$ M. Also, for HEK-293, both ligands turned out to be 25 times less toxic compared to other cells of malignant neoplasms [65].

The 2-acetylpyridine-7-isoquinoline thiosemicarbazone analogue (**24**) (Fig. 21) proved to be quite effective in complex with Ga(III) as an antimalarial drug against *P. falciparum*.

In addition, this complex was thirty-one times more active against HCT-116 cells (carcinoma), four times more effective against Caco-2 (adenocarcinoma) and two and a half times more effective against HT-29 (adenocarcinoma) by comparison with etoposide after 72 h. The complex was found

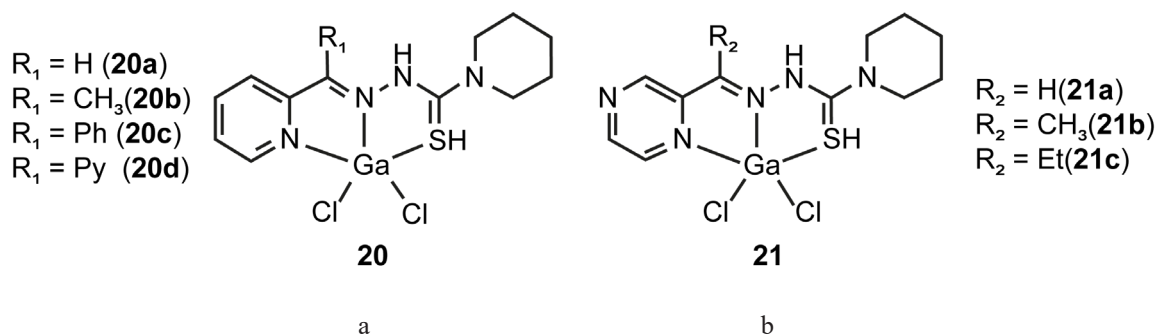


**Fig. 19.** (a) Structures of complexes of alkylthiosemicarbazones (**20**),  
 (b) structures of complexes of piperidylthiosemicarbazones with gallium chloride (**21**).

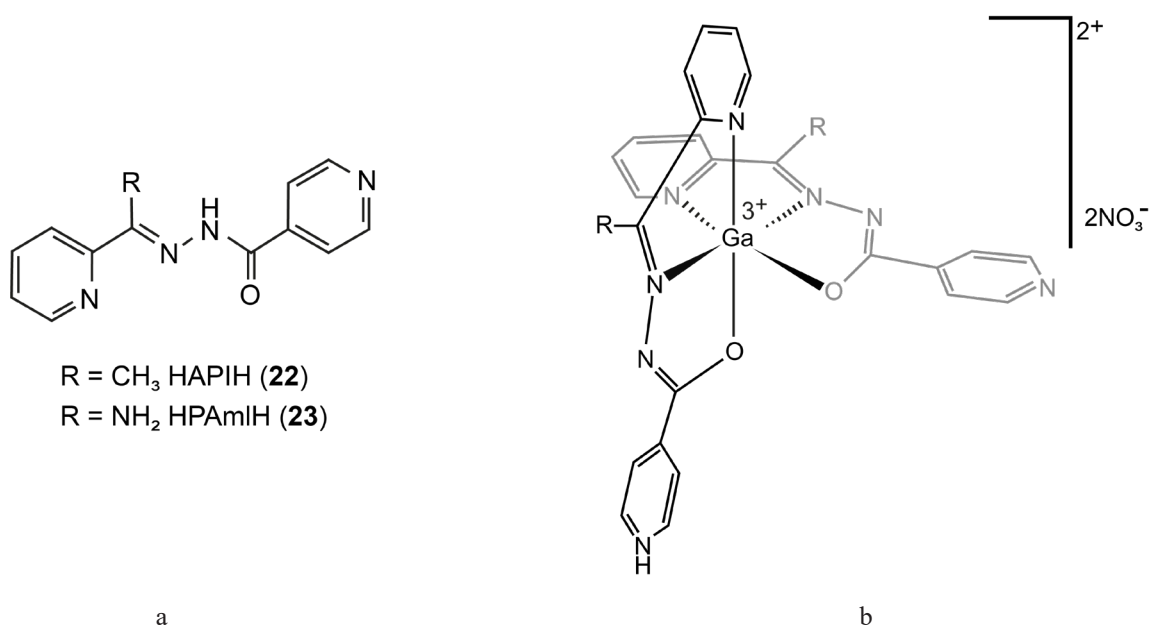


**Fig. 20.** (a) Structure of HAPIH (**22**) and HPAmIH (**23**), (b) their complexes with gallium nitrate [65].

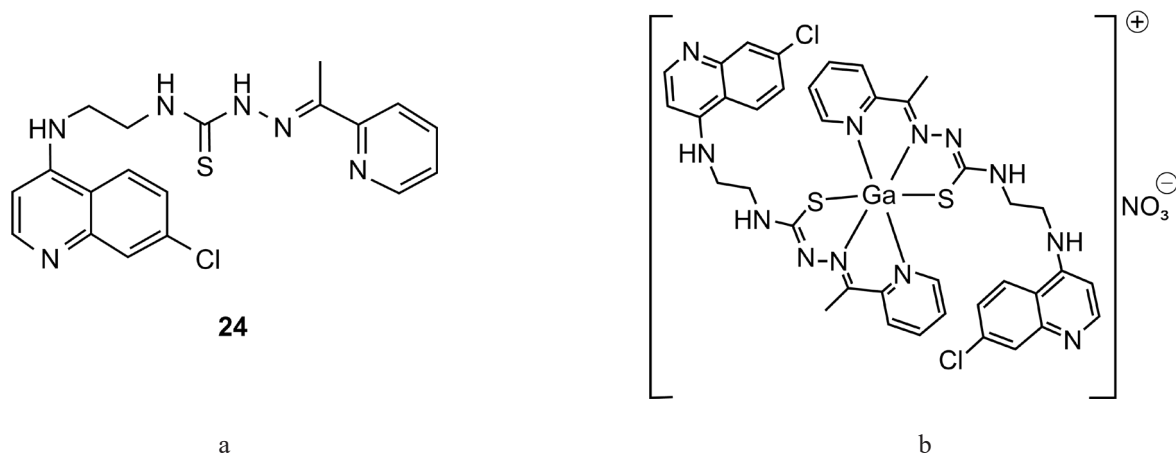


**Fig. 21.** (a) *N*-(2-((7-chloroquinolin-4-yl)amino)ethyl)-2-(1-(pyridin-2-yl)ethylidene) hydrazinecarbothioamide (**24**),  
 (b) its complex with gallium nitrate.

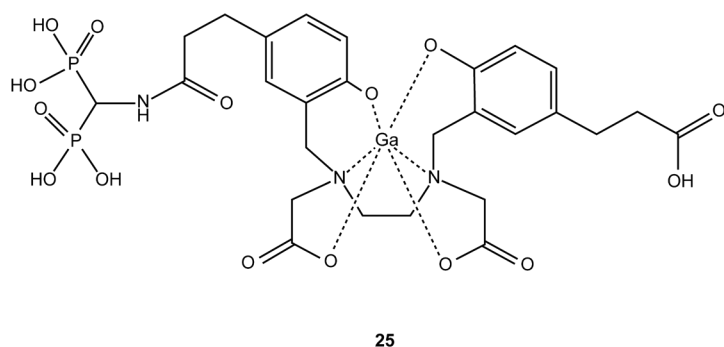


**Fig. 22.** Chemical structure of methylene diphosphate [ $^{68}\text{Ga}$ ]Ga-P15-041 (**25**).

to be non-cytotoxic compared to the benign colonic fibroblast cell line (CCD-18Co), showing  $\text{IC}_{50} = 11.81 \pm 1.42$  mM after 72 h [66].

In one of the latest studies of BFC to gallium, metastatic foci of prostate cancer were successfully visualized using [ $^{68}\text{Ga}$ ]Ga-P15-041 (**25**) (Fig. 22), with the absorption in the lesion constantly exceeding the background.

Dynamic image analysis of [ $^{68}\text{Ga}$ ]Ga-P15-041 uptake shows signal improvement relative to constant background over time for tumors with the highest uptake, but signal-to-noise ratio analysis shows that imaging is optimal between 60 and 90 min post-injection. Dynamic and dosimetric analyses show that [ $^{68}\text{Ga}$ ]Ga-P15-041-PET imaging of prostate bone metastases in humans is possible, but further studies are needed to refine the initial results [67].

## CONCLUSIONS

Over the past decades, tremendous progress has been made in the development of metal-based radiopharmaceuticals for PET, facilitating their use in the early detection of diseases. Significant progress has also been made in the development of bifunctional  $^{68}\text{Ga}$  chelators that reliably bind the corresponding metal center *in vivo*. However, new BFCs should be developed with caution, as increased stringency can reduce labeling kinetics; therefore, higher temperatures and longer reaction times are required to achieve sufficient labeling yields. In addition to macrocyclic BFC, *in vivo* stable  $^{68}\text{Ga}$  complexes formed with acyclic chelators have the advantage of faster labeling kinetics, which is a key factor given the short half-life of  $^{68}\text{Ga}$ . Despite the

significant progress, the problem of correlating the chemical structure of metal-based radiopharmaceuticals with their behavior *in vivo* remains to be solved. In this respect, comparative studies of drugs that have an identical targeting vector but include different BFCs may help further reveal the effect of the metal chelate moiety on pharmacokinetics. At the same time, the choice of the BFC's chelating fragment depends on the nature and degree of oxidation of the radiometal. There are many examples in literature showing that the nature of the BFC metal complex (geometry, lipophilicity, and total charge) plays a key role in determining the biodistribution of target radiopharmaceuticals.

Today, the main goal in the development of metal-based radiopharmaceuticals is the selection of effective bifunctional chelating agents, whose system forms a radiometal chelate with high thermodynamic stability and kinetic inertness to maintain the label on the targeting vector. The accumulation of radiometal in non-target tissues should not only be minimized in order to enhance image contrast, but also to minimize patients' exposure to radiation, which is particularly important in the case of radiotherapy applications.

Efficient and quantitative radioactive labeling eases the introduction of new indicators into clinical practice, allowing the preparation of radiopharmaceuticals without the need for additional purification.

Another important step for clinical translation is the selection of BFC to adjust the polarity and charge of the entire conjugate as a means of optimizing the clearance pathway and pharmacokinetics. For example, the clearance of a radiopharmaceutical from the blood should be slow enough to ensure optimal delivery to the target site, but at the same time rapid enough to avoid unnecessary radiation exposure. Thus, in order to create a BFC with high stability, efficient radioactive labeling kinetics and favorable pharmacokinetics is required along with a deep understanding of the radiometal coordination chemistry.

## Acknowledgments

The presented work was supported by the Ministry of Science and Higher Education of the Russian Federation within the framework of the state task (project FSSM-2020-0004) "Development of the basics for obtaining and studying the interaction with the body of new multifunctional nanosized macromolecular systems for the targeted delivery of drugs, diagnostics and radiopharmaceuticals to combat the main socially significant diseases, including theranostics."

**Authors' contributions**

**A.G. Polivanova** – review of publications on the topic of the article, writing the text of the article, scientific editing;

**I.N. Solovieva** – review of publications on the topic of the article, writing the text of the article, analysis and systematization of the material;

**D.O. Botev** – review of publications on the topic of the article, writing the text, technical editing;

**D.Y. Yuriev** – review of publications on the topic of the article, technical editing, bibliography design;

**A.N. Mylnikova** – review of publications on the topic of the article, writing the text;

**M.S. Oshchepkov** – scientific editing, critical revision with valuable intellectual content.

*The authors declare no conflicts of interest.*

**REFERENCES**

1. Bartholomä M. Recent developments in the design of bifunctional chelators for metal-based radiopharmaceuticals used in Positron Emission Tomography. *Inorganica Chim. Acta.* 2012;389:36–51. <https://doi.org/10.1016/j.ica.2012.01.061>

2. Clarke E.T., Martell A.E. Stabilities of trivalent metal ion complexes of the tetraacetate derivatives of 12-, 13- and 14-membered tetraazamacrocycles. *Inorganica Chim. Acta.* 1991;190(1):37–46. [https://doi.org/10.1016/S0020-1693\(00\)80229-7](https://doi.org/10.1016/S0020-1693(00)80229-7)

3. Clarke E.T., Martell A.E. Stabilities of the Fe(III), Ga(III) and In(III) chelates of *N,N',N''*-triazacyclononanetriacetic acid. *Inorganica Chim. Acta.* 1991;181(2):273–280. [https://doi.org/10.1016/S0020-1693\(00\)86821-8](https://doi.org/10.1016/S0020-1693(00)86821-8)

4. Velikyan I., Beyer G.J., Bergstrom-Pettermann E. The importance of high specific radioactivity in the performance of <sup>68</sup>Ga-labeled peptide. *Nucl. Med. Biol.* 2008;35(5):529–536. <https://doi.org/10.1016/j.nucmedbio.2008.03.002>

5. Riss P.J., *et al.* NODAPA-OH and NODAPA-(NCS)<sub>n</sub>: Synthesis, <sup>68</sup>Ga-radiolabelling and *in vitro* characterisation of novel versatile bifunctional chelators for molecular imaging. *Bioorg. Med. Chem. Lett.* 2008;18(2):5364–5367. <https://doi.org/10.1016/j.bmcl.2008.09.054>

6. Notni J., Hermann P., Havlíčková J., *et al.* A Triazacyclononane-Based Bifunctional Phosphinate Ligand for the Preparation of Multimeric <sup>68</sup>Ga Tracers for Positron Emission Tomography. *Chem. Eur. J.* 2010;16(24):7174–7185. <https://doi.org/10.1002/chem.200903281>

7. Simeček J., *et al.* A monoreactive bifunctional triazacyclononane phosphinate chelator with high selectivity for gallium-68. *ChemMedChem.* 2012;8(7):1375–1378. <https://doi.org/10.1002/cmde.201200261>

8. Prata M.I.M., *et al.* Gallium(III) chelates of mixed phosphonate-carboxylate triazamacrocyclic ligands relevant to nuclear medicine: Structural, stability and *in vivo* studies. *J. Inorg. Biochem.* 2017;177:8–16. <https://doi.org/10.1016/j.jinorgbio.2017.08.015>

9. Yang C.-T., Sreerama S.G., Hsieh W.-Y. Synthesis and Characterization of a Novel Macrocyclic Chelator with 3-Hydroxy-4-Pyrone Chelating Arms and Its Complexes with Medicinally Important Metals. *Inorg. Chem.* 2008;47(7):2719–2727. <https://doi.org/10.1021/ic7022506>

10. Seemann J., Waldron B.P., Roesch F. Approaching 'Kit-Type' Labelling with <sup>68</sup>Ga: The DATA Chelators. *ChemMedChem.* 2015;10(6):1019–1026. <https://doi.org/10.1002/cmde.201500092>

11. Ma M.T., Neels O.C., Denoyer D., Roselt P., *et al.* Gallium-68 Complex of a Macrobicyclic Cage Amine Chelator Tethered to Two Integrin-Targeting Peptides for Diagnostic Tumor Imaging. *Bioconjugate Chem.* 2011;22(10):2093–2103. <https://doi.org/10.1021/bc200319q>

12. Boros E., *et al.* Acyclic chelate with ideal properties for <sup>68</sup>Ga PET imaging agent elaboration. *J. Am. Chem. Soc.* 2010;132(44):15726–15733. <https://doi.org/10.1021/ja106399h>

13. Sun Y., *et al.* Idum(III) and gallium(III) complexes of bis(aminoethanethiol) ligands with different denticities: stabilities, molecular modeling, and *in vivo* behavior. *J. Med. Chem.* 1996;39(2):458–470. <https://doi.org/10.1021/jm9505977>

14. Eder M., Krivoshein A.V., Backer M., Backer J.M. ScVEGF-PEG-HBED-CC and scVEGF-PEG-NOTA conjugates: comparison of easy-to-label recombinant proteins for [<sup>68</sup>Ga]PET imaging of VEGF receptors in angiogenic vasculature. *Nucl. Med. Biol.* 2010;37(4):405–412. <https://doi.org/10.1016/j.nucmedbio.2010.02.001>

15. Liolios C., et al. Synthesis, characterization and evaluation of  $^{68}\text{Ga}$  labelled monomeric and dimeric quinazoline derivatives of the HBED-CC chelator targeting the epidermal growth factor receptor. *Bioorg. Chem.* 2020;100:103855. <https://doi.org/10.1016/j.bioorg.2020.103855>
16. Timerbaev A.R. Advances in developing tris(8-quinolinolato)gallium(III) as an anticancer drug: critical appraisal and prospects. *Metallomics.* 2009;1(3):193–198. <https://doi.org/10.1039/b902861g>
17. Enyedy É.A., Mészáros J.P., Spengler G., Hanif M. Comparative solution studies and cytotoxicity of gallium(III) and iron(III) complexes of 3-hydroxy-2(1H)-pyridinones. *Polyhedron.* 2019;172:141–147. <https://doi.org/10.1016/j.poly.2019.04.010>
18. Berry D.J., Ma Y., Ballinger J.R., Tavaré R. Efficient bifunctional gallium-68 chelators for positron emission tomography: tris(hydroxypyridinone) ligands. *ChemComm.* 2011;47(25):7068. <https://doi.org/10.1039/C1CC12123E>
19. Chaves S., Marques S.M., Matos A.M.F., Nunes A. New Tris(hydroxypyridinones) as Iron and Aluminium Sequestering Agents: Synthesis, Complexation and *In Vivo* Studies. *Chem. Eur. J.* 201;16(34):10535–10545. <https://doi.org/10.1002/chem.201001335>
20. Mathias C.J., Lewis M.R., Richert D.E., Laforest R., et al. Preparation of  $^{66}\text{Ga}$  and  $^{68}\text{Ga}$ -labeled Ga(III)-deferoxaminefolate as potential folate-receptor-targeted PET radiopharmaceuticals. *Nucl. Med. Biol.* 2003;30(7):725–731. [https://doi.org/10.1016/s0969-8051\(03\)00080-5](https://doi.org/10.1016/s0969-8051(03)00080-5)
21. Vosjan M.J.W.D., Perk L.R., Roovers R.C., Visser G.W.M., et al. Facile labelling of an anti-epidermal growth factor receptor Nanobody with  $^{68}\text{Ga}$  via a novel bifunctional desferal chelate for immuno-PET. *Eur. J. Nucl. Med. Mol. Imaging.* 2011;38(4):753–763. <https://doi.org/10.1007/s00259-010-1700-1>
22. Fani M., et al. PET of somatostatin receptor-positive tumors using  $^{64}\text{Cu}$ - and  $^{68}\text{Ga}$ -somatostatin antagonists: the chelate makes the difference. *J. Nucl. Med.* 2011;52(7):1110–1118. <https://doi.org/10.2967/jnumed.111.087999>
23. Martell A.E., Motekaitis R.J., Clarke E.T., Delgado R., et al. Stability constants of metal complexes of macrocyclic ligands with pendant donor groups. *Supramol. Chem.* 1996;6(3–4):353–363. <https://doi.org/10.1080/10610279608032555>
24. Ma R., Welch M.J., Reibenspies J. Stability of metal ion complexes of 1,4,7-tris(2-mercaptoethyl)-1,4,7-triazacyclonane (TACN-TM) and molecular structure of  $\text{In}(\text{C}_{12}\text{H}_{24}\text{N}_3\text{S}_3)$ . *Inorg. Chim. Acta.* 1995;236(1–2):75–82. [https://doi.org/10.1016/0020-1693\(95\)04617-1](https://doi.org/10.1016/0020-1693(95)04617-1)
25. Craig A.S., Parker D., Adams H. Stability,  $^{71}\text{Ga}$ NMR, and crystal structure of a neutral gallium(III) complex of 1,4,7-triazacyclononatriacetate: a potential radiopharmaceutical? *J. Chem. Soc., Chem. Commun.* 1989;(23):1793–1794. <https://doi.org/10.1039/C39890001793>
26. Broan C.J., Cox J.P.L., Craig A.S., Katakly R., et al. Structure and solution stability of indium and gallium complexes of 1,4,7-triazacyclononatriacetate and of yttrium complexes of 1,4,7,10-tetraazacyclododecane-tetraacetate and related ligands: kinetically stable complexes for use in imaging and radioimmunotherapy. X-Ray molecular structure of the indium and gallium complexes of 1,4,7-triazacyclononane-1,4,7-triacetic acid. *J. Chem. Soc., Perkin Trans. 2.* 1991;2(1):87–99. <https://doi.org/10.1039/P29910000087>
27. Kruper W.J., Rudolf P.R., Langhoff C.A. Unexpected selectivity in the alkylation of polyazamacrocycles. *J. Org. Chem.* 1993;58(15):3869–3876. <https://doi.org/10.1021/jo00067a018>
28. Chappell L.L., Rogers B.E., Khzaeli M.B., Mayo M.S. Improved synthesis of the bifunctional chelating agent 1,4,7,10-tetraaza-*N*-(1-carboxy-3-(4-nitrophenyl)propyl)-*N',N'',N'''*-tris(acetic acid)cyclododecane (PA-DOTA). *Bioorg. Med. Chem.* 1999;7(11):2313–2320. [https://doi.org/10.1016/s0968-0896\(99\)00171-6](https://doi.org/10.1016/s0968-0896(99)00171-6)
29. Prata M.I.M., Santos A.C., Geraldes C.F.G.C. Characterisation of  $^{67}\text{Ga}^{3+}$  complexes of triaza macrocyclic ligands: biodistribution and clearance studies. *Nucl. Med. Biol.* 1999;26(6):707–710. [https://doi.org/10.1016/s0969-8051\(99\)00041-4](https://doi.org/10.1016/s0969-8051(99)00041-4)
30. Heppeler A., Froidevaux S., Mäcke H.R., Jermann E., et al. Radiometal-Labelled Macrocyclic Chelator-Derivatised Somatostatin Analogue with Superb Tumour-Targeting Properties and Potential for Receptor-Mediated Internal Radiotherapy. *Chem. Eur. J.* 1999;5(7):1974–1981. [https://doi.org/10.1002/\(SICI\)1521-3765\(19990702\)5:7%3C1974::AID-CHEM1974%3E3.0.CO;2-X](https://doi.org/10.1002/(SICI)1521-3765(19990702)5:7%3C1974::AID-CHEM1974%3E3.0.CO;2-X)
31. Viola N.A., Rarig R.S., Ouellette W., Doyle R.P. Synthesis, structure and thermal analysis of the gallium complex of 1,4,7,10-tetraazacyclo-dodecane-*N,N',N'',N'''*-tetraacetic acid (DOTA). *Polyhedron.* 2006;25(18):3457–3462. <https://doi.org/10.1016/j.poly.2006.06.039>
32. Velikyan I., Beyer G.J., Långström B. Microwave-Supported Preparation of  $^{68}\text{Ga}$  Bioconjugates with High Specific Radioactivity. *Bioconjugate Chem.* 2004;15(3):554–560. <https://doi.org/10.1021/bc030078f>
33. Decristoforo C., Hernandez Gonzalez I., Carlsen J., Rupprich M., et al.  $^{68}\text{Ga}$ - and  $^{111}\text{In}$ -labelled DOTA-RGD peptides for imaging of  $\alpha\beta 3$  integrin expression. *Eur. J. Nucl. Med. Mol. Imaging.* 2008;35(8):1507–1515. <https://doi.org/10.1007/s00259-008-0757-6>
34. Griffiths G.L., et al. Reagents and methods for PET using bispecific antibody pretargeting and  $^{68}\text{Ga}$ -radiolabeled bivalent haptan-peptide-chelate conjugates. *J. Nucl. Med.* 2004;45(1):30–39.
35. Sneddon D., Cornelissen B. Emerging chelators for nuclear imaging. *Curr. Opin. Chem. Biol.* 2021;63:152–162. <https://doi.org/10.1016/j.cbpa.2021.03.001>
36. Al-Nahhas A., et al. Gallium-68 PET: a new frontier in receptor cancer imaging. *Anticancer Res.* 2007;27(6B):4087–4094.
37. Al-Nahhas A., Win Z., Szyszko T., Singh A. What can gallium-68 PET add to receptor and molecular imaging? *Eur. J. Nucl. Med. Mol. Imaging.* 2007;34(12):1897–1901. <https://doi.org/10.1007/s00259-007-0568-1>
38. Velikyan I., Maecke H., Langstrom B. Convenient preparation of  $^{68}\text{Ga}$ -based PET-radiopharmaceuticals at room temperature. *Bioconjugate Chem.* 2008;19(2):569–573. <https://doi.org/10.1021/bc700341x>
39. André J. P., Maecke H. R., Zehnder M., Macko L. 1,4,7-Triazacyclononane-1-succinic acid-4,7-diacetic acid (NODASA): a new bifunctional chelator for radio gallium-labelling of biomolecules. *Chem. Commun.* 1998;(12):1301–1302. <https://doi.org/10.1039/A801294F>
40. André J.P., Mäcke H., Kaspar A., Künnecke B. *In vivo* and *in vitro*  $^{27}\text{Al}$  NMR studies of aluminum(III) chelates of triazacyclononane polycarboxylate ligands. *J. Inorg. Biochem.* 2002;88(1):1–6. [https://doi.org/10.1016/s0162-0134\(01\)00340-3](https://doi.org/10.1016/s0162-0134(01)00340-3)

41. Eisenwiener K.-P., *et al.* NODAGATOC, a new chelator-coupled somatostatin analogue labeled with [ $^{67/68}\text{Ga}$ ] and [ $^{111}\text{In}$ ] for SPECT, PET, and targeted therapeutic applications of somatostatin receptor (hsst2) expressing tumors. *Bioconjugate Chem.* 2002;13(3):530–541. <https://doi.org/10.1021/bc010074f>
42. Jeong J.M., *et al.* Preparation of a promising angiogenesis PET imaging agent:  $^{68}\text{Ga}$ -labeled c(RGDyK)-isothiocyanatobenzyl-1,4,7-triazacyclononane-1,4,7-triacetic acid and feasibility studies in mice. *J. Nucl. Med.* 2008;49(5):830–836. <https://doi.org/10.2967/jnumed.107.047423>
43. Waldron B.P., Parker D., Burchardt C., Yufit D.S. Structure and stability of hexadentate complexes of ligands based on AAZTA for efficient PET labelling with gallium-68. *Chem. Commun.* 2017;49(6):579–581. <https://doi.org/10.1039/C2CC37544C>
44. Parker D., Waldron B.P. Conformational analysis and synthetic approaches to polydentate perhydro-diazepine ligands for the complexation of gallium(III). *Org. Biomol. Chem.* 2013;11(17):2827. <https://doi.org/10.1039/C3OB40287H>
45. Costa J., Delgado R. Metal complexes of macrocyclic ligands containing pyridine. *Inorg. Chem.* 1993;32(23):5257–5265. <https://doi.org/10.1021/ic00075a052>
46. Ferreira C.L., Lamsa E., Woods M., Duan Y. Evaluation of Bifunctional Chelates for the Development of Gallium-Based Radiopharmaceuticals. *Bioconjugate Chem.* 2010;21(3):531–536. <https://doi.org/10.1021/bc900443a>
47. Liu S., Edwards D.S. Bifunctional chelators for therapeutic lanthanide radiopharmaceuticals. *Bioconjugate Chem.* 2001;12(1):7–34. <https://doi.org/10.1021/bc000070v>
48. Moreau J., Guillon E., Pierrard J.-C., Rimbault J. Complexing Mechanism of the Lanthanide Cations  $\text{Eu}^{3+}$ ,  $\text{Gd}^{3+}$ , and  $\text{Tb}^{3+}$  with 1,4,7,10-Tetrakis(carboxymethyl)-1,4,7,10-tetraazacyclododecane (dota)—Characterization of Three Successive Complexing Phases: Study of the Thermodynamic and Structural Properties of the Complexes by Potentiometry, Luminescence Spectroscopy, and EXAFS. *Chem. Eur. J.* 2004;10(20):5218–5232. <https://doi.org/10.1002/chem.200400006>
49. Eder M., *et al.* Tetrafluorophenolate of HBED-CC: a versatile conjugation agent for  $^{68}\text{Ga}$ -labeled small recombinant antibodies. *Eur. J. Nucl. Med. Mol. Imaging.* 2008;35(10):1878–1886. <https://doi.org/10.1007/s00259-008-0816-z>
50. Collery P., Lechenault F., Cazabat A. Juvin E., *et al.* Inhibitory effects of gallium chloride and tris (8-quinolinolato) gallium(III) on A549 human malignant cell line. *Anticancer Res.* 2000;20(2A):955–8.
51. Lessa J.A., Parrilha G.L., Beraldo H. Gallium complexes as new promising metallodrug candidates. *Inorg. Chim. Acta.* 2012;393:53–63. <https://doi.org/10.1016/j.ica.2012.06.003>
52. Litecká M., Hreusová M., Kašpárková J., Gyepes R., *et al.* Low-dimensional compounds containing bioactive ligands. Part XIV: High selective antiproliferative activity of tris(5-chloro-8-quinolinolato)-gallium(III) complex against human cancer cell lines. *Bioorg. Med. Chem. Lett.* 2020;30(13):127206. <https://doi.org/10.1016/j.bmcl.2020.127206>
53. Gómez-Ruiz S., Ceballos-Torres J., Prashar S., Fajardo M. One ligand different metal complexes: Biological studies of titanium(IV), tin(IV) and gallium(III) derivatives with the 2,6-dimethoxy-pyridine-3-carboxylato-ligand. *J. Organometallic Chem.* 2011;696(20):3206–3213. <https://doi.org/10.1016/j.jorganchem.2011.06.036>
54. Chaves S., Marques S.M., Matos A.M.F., Nunes A., *et al.* New Tris(hydroxypyridinones) as Iron and Aluminium Sequestering Agents: Synthesis, Complexation and *in Vivo* Studies. *Chem. Eur. J.* 2010;16(34):10535–10545. <https://doi.org/10.1002/chem.201001335>
55. Chaves S., Mendonça A.C., Marques S.M., Prata M.I. A gallium complex with a new tripodal tris-hydroxypyridinone for potential nuclear diagnostic imaging: solution and *in vivo* studies of  $^{67}\text{Ga}$ -labeled species. *J. Inorg. Biochem.* 2011;105(1):31–38. <https://doi.org/10.1016/j.jinorgbio.2010.09.012>
56. Smith-Jones P.M., Stolz B., Bruns C., *et al.* Gallium-67/gallium-68-[DFO]-octreotide—a potential radiopharmaceutical for PET imaging of somatostatin receptor positive tumors: synthesis and radiolabeling *in vitro* and preliminary *in vivo* studies. *J. Nucl. Med.* 1994;35(2):317–325.
57. Mathias C.J., *et al.* Receptor-mediated targeting of  $^{67}\text{Ga}$ -deferoxamine-folate to folate-receptor-positive human KB tumor xenografts. *Nucl. Med. Biol.* 1999;26(1):23–25. [https://doi.org/10.1016/S0969-8051\(98\)00076-6](https://doi.org/10.1016/S0969-8051(98)00076-6)
58. Price T.W., *et al.* Evaluation of a bispidine-based chelator for gallium-68 and of the porphyrin conjugate as PET/PDT theranostic agent. *Chem. Eur. J.* 2020;26(34):7602–7608. <https://doi.org/10.1002/chem.201905776>
59. Imberti C., *et al.* Manipulating the *in Vivo* Behaviour of  $^{68}\text{Ga}$  with Tris(Hydroxypyridinone) Chelators: Pretargeting and Blood Clearance. *Int. J. Mol. Sci.* 2020;21(4):1496. <https://doi.org/10.3390/ijms21041496>
60. Zhou X., *et al.* Design and synthesis of a new conjugate of a tris(3-hydroxy-4-pyridinone) chelator (KC18) for potential use as gallium-68-labeled prostate-specific membrane antigen (PSMA) radiopharmaceutical. *Results in Chemistry.* 2021;3:100240. <https://doi.org/10.1016/j.rechem.2021.100240>
61. Kowol C.R., Berger R., Eichinger R., Roller A., *et al.* Gallium(III) and Iron(III) Complexes of  $\alpha$ -N-Heterocyclic Thiosemicarbazones: Synthesis, Characterization, Cytotoxicity, and Interaction with Ribonucleotide Reductase. *J. Med. Chem.* 2007;50(6):1254–1265. <https://doi.org/10.1021/jm0612618>
62. Arion V.B., *et al.* Synthesis, structure, spectroscopic and *in vitro* antitumour studies of a novel gallium(III) complex with 2-acetylpyridine (4)*N*-dimethylthiosemicarbazone. *J. Inorg. Biochem.* 2002;91(1):298–305. [https://doi.org/10.1016/S0162-0134\(02\)00419-1](https://doi.org/10.1016/S0162-0134(02)00419-1)
63. Qi J., Yao Q., Qian K., Tian L., *et al.* Gallium(III) complexes of  $\alpha$ -N-heterocyclic piperidyl-thiosemicarbazones: Synthesis, structure-activity relationship, cellular uptake and activation of caspases-3/7/9. *J. Inorg. Biochem.* 2018;186:42–50. <https://doi.org/10.1016/j.jinorgbio.2018.05.005>
64. Qi J., *et al.* Synthesis, antiproliferative activity and mechanism of gallium(III)-thiosemicarbazone complexes as potential anti-breast cancer agents. *Eur. J. Med. Chem.* 2018;154:91–100. <https://doi.org/10.1016/j.ejmech.2018.05.016>

65. Firmino G. dos S.S., André S.C., Hastenreiter Z., Campos V.K., et al. *In vitro* assessment of the cytotoxicity of Gallium(III) complexes with Isoniazid-Derived Hydrazones: Effects on clonogenic survival of HCT-116 cells. *Inorganica Chim. Acta.* 2019;497:119079. <https://doi.org/10.1016/j.ica.2019.119079>

66. Kumar K., et al. Highly potent anti-proliferative effects of a gallium(III) complex with 7-chloroquinoline thiosemicarbazone as a ligand: synthesis, cytotoxic and antimalarial evaluation. *Eur. J. Med. Chem.* 2014;86:81–86. <https://doi.org/10.1016/j.ejmech.2014.08.054>

67. Doot R.K., Young A.J., Daube-Witherspoon M.E., Alexoff D., Labban K.J., Lee H., Wu Z., Zha Z., Choi S.R., Ploessl K.H. Biodistribution, dosimetry, and temporal signal-to-noise ratio analyses of normal and cancer uptake of [<sup>68</sup>Ga] Ga-P15-041, a gallium-68 labeled bisphosphonate, from first-in-human studies. *Nucl. Med. Biol.* 2020;86:1–8. <https://doi.org/10.1016/j.nucmedbio.2020.04.002>

#### About the authors:

**Anna G. Polivanova**, Cand. Sci. (Chem.), Associate Professor, Department of Chemistry and Technology of Biomedical Preparations, Mendeleev University of Chemical Technology of Russia (9, Miusskaya pl., Moscow, 125047, Russia). E-mail: zagchem@mail.ru. <https://orcid.org/0000-0003-4502-0745>

**Inna N. Solovieva**, Cand. Sci. (Chem.), Associate Professor, Department of Chemistry and Technology of Biomedical Preparations, Mendeleev University of Chemical Technology of Russia (9, Miusskaya pl., Moscow, 125047, Russia). E-mail: solandsol@yandex.ru. <https://orcid.org/0000-0002-0079-6710>

**Dmitrii O. Botev**, Master Student, Department of Chemistry and Technology of Biomedical Preparations, Mendeleev University of Chemical Technology of Russia (9, Miusskaya pl., Moscow, 125047, Russia). E-mail: botev.dm@gmail.com. <https://orcid.org/0000-0003-4954-6779>

**Danil Yu. Yuriev**, Master Student, Leading Engineer, Department of Chemistry and Technology of Biomedical Preparations, Mendeleev University of Chemical Technology of Russia (9, Miusskaya pl., Moscow, 125047, Russia). E-mail: danilyuriev35@yandex.ru. <https://orcid.org/0000-0002-5906-4020>

**Alyona N. Mylnikova**, Leading Engineer, Assistant, Department of Chemistry and Technology of Biomedical Preparations, Mendeleev University of Chemical Technology of Russia (9, Miusskaya pl., Moscow, 125047, Russia). E-mail: pobeg\_is\_raya@mail.ru. <https://orcid.org/0000-0002-8297-8322>

**Maxim S. Oshchepkov**, Dr. Sci. (Chem.), Head of the Department of Chemistry and Technology of Biomedical Preparations, Mendeleev University of Chemical Technology of Russia (9, Miusskaya pl., Moscow, 125047, Russia). E-mail: maxim.os@mail.ru. Scopus Author ID 50262866400, ResearcherID AAA-6443-2022, <https://orcid.org/0000-0002-2892-4884>

#### Об авторах:

**Поливанова Анна Геннадьевна**, к.х.н., доцент кафедры химии и технологии биомедицинских препаратов Российского химико-технологического университета им. Д.И. Менделеева (125047, Россия, Москва, Миусская площадь, д. 9). E-mail: zagchem@mail.ru. <https://orcid.org/0000-0003-4502-0745>

**Соловьёва Инна Николаевна**, к.х.н., доцент кафедры химии и технологии биомедицинских препаратов Российского химико-технологического университета им. Д.И. Менделеева (125047, Россия, Москва, Миусская площадь, д. 9). E-mail: solandsol@yandex.ru. <https://orcid.org/0000-0002-0079-6710>

**Ботев Дмитрий Олегович**, магистрант, кафедра химии и технологии биомедицинских препаратов Российского химико-технологического университета им. Д.И. Менделеева (125047, Россия, Москва, Миусская площадь, д. 9). E-mail: botev.dm@gmail.com. <https://orcid.org/0000-0003-4954-6779>

**Юрьев Данил Юрьевич**, магистрант, ведущий инженер, кафедра химии и технологии биомедицинских препаратов Российского химико-технологического университета им. Д.И. Менделеева (125047, Россия, Москва, Миусская площадь, д. 9). E-mail: danilyuriev35@yandex.ru. <https://orcid.org/0000-0002-5906-4020>

**Мьльникова Алёна Николаевна**, ведущий инженер, ассистент, кафедра химии и технологии биомедицинских препаратов Российского химико-технологического университета им. Д.И. Менделеева (125047, Россия, Москва, Миусская площадь, д. 9). E-mail: pobeg\_is\_raya@mail.ru. <https://orcid.org/0000-0002-8297-8322>

**Оценков Максим Сергеевич**, д.х.н., заведующий кафедрой химии и технологии биомедицинских препаратов Российского химико-технологического университета им. Д.И. Менделеева (125047, Россия, Москва, Миусская площадь, д. 9). E-mail: maxim.os@mail.ru. Scopus Author ID 50262866400, ResearcherID AAA-6443-2022, <https://orcid.org/0000-0002-2892-4884>

*The article was submitted: March 22, 2022; approved after reviewing: April 18, 2022; accepted for publication: April 22, 2022.*

*The text was submitted by the authors in English.*

*Edited for English language and spelling by Thomas Beavitt.*

**CHEMISTRY AND TECHNOLOGY OF MEDICINAL COMPOUNDS  
AND BIOLOGICALLY ACTIVE SUBSTANCES**

**ХИМИЯ И ТЕХНОЛОГИЯ ЛЕКАРСТВЕННЫХ ПРЕПАРАТОВ  
И БИОЛОГИЧЕСКИ АКТИВНЫХ СОЕДИНЕНИЙ**

ISSN 2686-7575 (Online)

<https://doi.org/10.32362/2410-6593-2022-17-2-131-139>



UDC 615.28

RESEARCH ARTICLE

**Screening medicinal plant extracts for xanthine  
oxidase inhibitory activity**

**Anh C. Ha<sup>1,2,✉</sup>, Chinh D.P. Nguyen<sup>1,2</sup>, Tan M. Le<sup>1,2</sup>**

<sup>1</sup>Faculty of Chemical Engineering, Ho Chi Minh City University of Technology (HCMUT), 268 Ly Thuong Kiet Street, Ho Chi Minh City, Vietnam

<sup>2</sup>Vietnam National University Ho Chi Minh City (VNU-HCM), Linh Trung Ward, Thu Duc District, Ho Chi Minh City, Vietnam

✉ Corresponding author, e-mail: [hcanh@hcmut.edu.vn](mailto:hcanh@hcmut.edu.vn)

**Abstract**

**Objectives.** The study aimed to test the ethanol extracts of ten medicinal plants for xanthine oxidase inhibitory activity.

**Methods.** The degree of xanthine oxidase inhibitory activity was determined by measuring the absorbance spectrophotometrically at 290 nm, which is associated with uric acid formation. The selected medicinal plants included Piper lolot C.DC. (Piperaceae), Pandanus amaryllifolius R.(Pandanaeae), Brassica juncea L. (Brassicaceae), Piper betle L. (Piperaceae), Perilla frutescens L. (Lamiaceae), Anacardium occidentale L. (Anacardiaceae), Polygonum barbatum L. (Polygonaceae), Artocarpus Altilis P. (Moraceae), Vitex negundo L. (Verbenaceae), Annona squamosal L. (Annonaceae), which were selected based on folk medicine.

**Results.** The results showed that the Piper betle L. has a strong ability to inhibit xanthine oxidase with an IC<sub>50</sub> value of up to 1.18 µg/mL, compared to allopurinol 1.57 µg/mL. Different parts of Piper betle L. were compared and the leaves of Piper betle L. showed the best value for xanthine oxidase inhibitory and antioxidant activity.

**Conclusions.** Piper betle L. showed the best potential for inhibition of xanthine oxidase among ten medicinal plants. Piper betle L. leaf extract showed strong xanthine oxidase inhibitory and antioxidant activity, compared to the whole plant, and the stem extract, which promises to be applied in the treatment of gout.

**Keywords:** anti-gout, xanthine oxidase inhibitors, medicinal plants

**For citation:** Ha A.C., Nguyen Ch.D.P., Le T.M. Screening medicinal plant extracts for xanthine oxidase inhibitory activity. *Tonk. Khim. Tekhnol. = Fine Chem. Technol.* 2022;17(2):131–139. <https://doi.org/10.32362/2410-6593-2022-17-2-131-139>

## НАУЧНАЯ СТАТЬЯ

# Скрининг экстрактов лекарственных растений на ингибирующую активность ксантиноксидазы

А.К. Ха<sup>1,2,✉</sup>, Ч.Д.П. Нгуен<sup>1,2</sup>, Т.М. Ле<sup>1,2</sup>

<sup>1</sup>Химико-технологический факультет, Технологический университет Хошимина, 268 Ли Тхьонг Кьет ул., г. Хошимин, Вьетнам

<sup>2</sup>Вьетнамский национальный университет, Район Тхёк, г. Хошимин, Вьетнам

✉ Автор для переписки, e-mail: hcanh@hcmut.edu.vn

## Аннотация

**Цели.** Исследование было направлено на проверку этанольных экстрактов десяти лекарственных растений на ингибиторную активность ксантиноксидазы.

**Методы.** Степень ингибирующей активности ксантиноксидазы определяли путем спектрофотометрического измерения поглощения при 290 нм, вызываемого образованием мочевой кислоты. В состав отобранных лекарственных растений вошли перец-лолот (*Piperaceae*), пандан (*Pandanaceae*), горчица сарептская (*Brassicaceae*), бетель (*Piperaceae*), перилла обыкновенная (*Lamiaceae*), кешью (*Anacardiaceae*), конопля (*Polygonaceae*), хлебное дерево (*Moraceae*), прутняк китайский (*Verbenaceae*), сахарное яблоко (*Annonaceae*), отобранные на основе их применения в народной медицине.

**Результаты.** Результаты показали, что бетель обладает сильной способностью ингибировать ксантиноксидазу со значением  $IC_{50}$  до 1.18 мкг/мл по сравнению с аллопуринолом 1.57 мкг/мл. Были проведены сравнения различных частей бетеля, и листья бетеля показали наилучшие показатели ингибирования ксантиноксидазы и антиоксидантной активности.

**Выводы.** Бетель показал лучший потенциал ингибирования ксантиноксидазы среди десяти лекарственных растений. Экстракт листьев бетеля показал сильное подавление ксантиноксидазы и антиоксидантную активность по сравнению с целым растением и экстрактом стебля, которые применяются при лечении подагры.

**Ключевые слова:** антиподагра, ингибиторы ксантиноксидазы, лекарственные растения

**Для цитирования:** Ха А.С., Nguyen Ch.D.P., Le T.M. Screening medicinal plant extracts for xanthine oxidase inhibitory activity. *Tonk. Khim. Tekhnol. = Fine Chem. Technol.* 2022;17(2):131–139. <https://doi.org/10.32362/2410-6593-2022-17-2-131-139>

## INTRODUCTION

Gout is the most common inflammatory arthritis characterized by hyperuricemia, arthritis, tophaceous deposits, and renal calculi associated with a high serum uric acid level [1]. The prevalence and incidence of gout disease have increased annually due to changes in diet and lifestyle, such as fast food, lack of exercise, etc. [2]. Globally, the reported prevalence of gout ranges from 0.1% to approximately 10%, and

the incidence from 0.3 to 6 cases per 1000 people per year [3]. Xanthine oxidase (XO) inhibitors are the mainstay of the therapy to reduce serum urate levels in patients with gout [4]. XO is an enzyme involved in the purine metabolism of purine which catalyzes the oxidation of hypoxanthine to xanthine and of xanthine to the uric acid [5]. Inhibition of XO helps to increase uric acid excretion and reduce uric acid production, which reduces the risk of gout [6]. Allopurinol, a clinically available drug is widely

used for the management of hyperuricemia in patients with gout, was proved to have some adverse effects consisting of hypersensitivity reactions, skin rash, and gastrointestinal distress [7, 8]. For these reasons, the search for alternative therapeutic strategies, particularly those that involve the use of natural products with low side effects, is gaining interest. There is an increase in research, which investigate medicinal plants that contain chemical constituents with potential biological activity for the treatment of diseases, including gout treatment [9].

Vietnam is home of about 12000 species of greatly appreciated plants and about 36% of which have medicinal properties [10]. Some plants and their phytochemicals are worth investigating as possible inhibitors, of XO inhibition as they have been used as food or food supplements for many years and found to be safe for human bodies [11]. Many medicinal plants have traditionally been used in folk medicine to treat a variety of complications such as gout. In fact, several plants have been reported in pharmacopeia as antigout products, and most of them have demonstrated this activity experimentally. However, these plants are underutilized and require additional research to confirm this effect. Therefore, this work aimed to identify medical plants with antigout potential of *Piper lolot* C.DC., *Pandanus amaryllifolius* R., *Brassica juncea* L., *Piper betle* L., *Perilla frutescens* L., *Anacardium occidentale* L., *Polygonum barbatum* L., *Artocarpus Altilis* P., *Vitex negundo* L., *Annona squamosal* L. by evaluation of the *in vitro* XO inhibitory activity of them. The total phenolic and flavonoid content of the tested extracts was also determined, identifying the importance of these compounds as XO inhibitors.

## MATERIALS AND METHODS

### Materials and Chemicals

The leaves or whole plants samples of ten plants (Table 1) were collected in An Giang province, Vietnam, in February 2020, during dry season which is appropriated for harvesting these plants. They were washed for removing residue of some plant and dust, then dried under natural air flow in shadow until the moisture content diminished to 12% and then grounded and stored in a sealed bag for further use. The plants were authenticated by the Department of Ecology and Evolutionary Biology, Faculty of Biology and Biotechnology, Ho Chi Minh City University of Science, Vietnam National University.

Absolute ethanol (C<sub>2</sub>H<sub>5</sub>OH), methanol (CH<sub>3</sub>OH), sodium nitrite (NaNO<sub>2</sub>), sodium carbonate (Na<sub>2</sub>CO<sub>3</sub>), sodium hydroxide (NaOH), aluminum chloride (AlCl<sub>3</sub>), dimethyl sulfoxide (DMSO), ferric chloride (AlCl<sub>3</sub>), diclofenac sodium and other reagents of analytical

grade were obtained from Merck (Darmstadt, FR, Germany). Folin-Ciocalteu's reagent, quercetin, xanthine oxidase (XO) (4.5 U/mL, from bovine milk), xanthine, ascorbic acid, allopurinol, 1,1-Diphenyl-2-picrylhydrazyl (DPPH), and gallic acid (GA) were provided by Sigma-Aldrich (Singapore).

### Preparation of plant extract

The dried plant powder (20 g) was extracted at 45°C in absolute ethanol for 45 min with the 10:1 mL/g solvent-to-sample ratio. Subsequently, the extract was filtered by vacuum filtration, and the filtrate was concentrated by a vacuum rotary evaporator (BUCHI, USA) to remove excess solvent.

### Qualitative phytochemical screening

Phytochemical screening of the of medicinal plant extracts was used to determine the presence of bioactive compounds: polyphenols, flavonoids, alkaloids, and tannins [12–14].

### Determination of total polyphenol content

The polyphenol concentration in the extracts was determined by the Folin–Ciocalteu's assay with slight modification [15]. In summary, 40 µL of the diluted extract at different concentrations was thoroughly mixed with 200 µL of Folin–Ciocalteu's reagent. The mixture was kept for reaction for 5 min at 25°C, followed by the addition of 600 µL of Na<sub>2</sub>CO<sub>3</sub> 20 w/v % and 3160 µL of distilled water. The mixture absorbance was measured at the 760 nm wavelength using a Genesys 10S UV-vis Spectrophotometer (Thermo Fisher Scientific, USA). Total polyphenol content was determined in milligram of gallic acid equivalent per gram of sample (mg GAE/g). The calibration curve for gallic acid was created to calculate the phenolic content as the following equation:  $y = 0.0013x - 0.0262$  ( $R^2 = 0.994$ ) where  $y$  is the absorbance and  $x$  is the concentration as gallic acid equivalents (mg GAE/mL).

### Determination of total flavonoid content

The concentration of polyphenols in the extracts was quantified using the aluminium chloride colorimetric assay method [16]. Briefly, 0.5 mL of the extract dissolved in methanol was mixed with 2 mL of distilled water and then 0.15 mL of NaNO<sub>2</sub> 5%. The mixture was incubated for reaction in 5 min, followed by the addition of 0.15 mL of 10% AlCl<sub>3</sub>. Then, 1.0 mL of NaOH 1M and 1.2 mL of distilled water were added. The absorbance of the mixture was measured at the 425 nm wavelength. The number of total flavonoids was shown as milligrams of Quercetin equivalents per gram of sample (mg QUE/g), using quercetin to perform the calibration curve:  $y = 0.001x - 0.0048$  ( $R^2 = 0.9986$ ) where  $y$  is the absorbance and  $x$  is concentration as quercetin equivalents (µg/mL).

Table 1. Phytochemical screening results from leaf extract of ten plants

Medicinal plants	Plant part used	Bioactive compounds			
		Polyphenols	Flavonoids	Alkaloids	Tannins
<i>Piper lolot</i> C.DC.	Whole plant	+	+	–	+
<i>Pandanus amaryllifolius</i> R.	Leaves	+	+	++	+
<i>Brassica juncea</i> L.	Whole plant	+	+	+	+
<i>Piper betle</i> L.	Whole plant	++	+	–	++
<i>Perilla frutescens</i> L.	Leaves	++	+	+	++
<i>Anacardium occidentale</i> L.	Leaves	++	++	–	++
<i>Polygonum barbatum</i> L.	Leaves	++	++	–	++
<i>Artocarpus altilis</i> P.	Leaves	++	++	+	++
<i>Vitex negundo</i> L.	Leaves	+	+	+	+
<i>Annona squamosa</i> L.	Leaves	++	++	++	++

– Not detected, + Slightly positive reaction, and ++ Strong positive reaction

#### In vitro XO inhibitory activity assay

XO enzyme catalyzes the conversion of hypoxanthine and xanthine into uric acid, a direct cause of gout [5]. XO inhibitory activity assay is widely used to determine the anti-gout activity of the plant extracts [17]. In this study, XO inhibitory activity of the extract was determined using an *in vitro* assay with slight modification to the Abd El-Rahman and Abd-ELHak method [18].

The assay was carried out on a 48-well plate. The reaction mixture included 250 µL extract in DMSO, 5% 175 µL sodium phosphate buffer (pH 7.5) and 150 µL enzyme (0.2 units/mL of XO in phosphate buffer). The mixture was incubated for 15 min at 37°C. Afterward, 300 µL of xanthine (mM) and incubated for 30 min at 37°C. The reaction was stopped with the addition of 125 µL HCl 1M. The absorbance was measured at 290 nm by Genesys 10S UV-Vis Spectrophotometer (Thermo Fisher Scientific, USA). Allopurinol was used as a positive control. The assay mixture without a sample was used as a negative control. XO inhibitory activity was expressed as the percentage inhibition of XO and calculated by Eq. 1:

$$\text{XO inhibition} = \frac{A_{\text{blank}} - A_{\text{sample}}}{A_{\text{blank}}} \times 100\% \quad (1)$$

with  $A_{\text{blank}}$  is the absorbance at 290 nm of blank,  $A_{\text{sample}}$  is the absorbance at 290 nm of the sample.

#### DPPH radical scavenging activity

The free radical scavenging activity of the extracts was determined using the DPPH radical in methanol. The assay was carried out with a slight modification to the Sharma and Bhat method [19]. In the methanol solution, DPPH had a purple color that gradually changed to a yellow color in reaction with antioxidants. Briefly, 180 µL of DPPH in methanol was mixed with 120 µL of sample in the methanol at different concentrations. The reaction mixture was homogenized thoroughly by a vortex machine and kept in the dark at 25°C for 30 min. Ascorbic acid (Vitamin C) and methanol were used as the positive control and negative control, respectively. The absorbance of the mixture was measured at 517 nm using a Genesys 10S UV-Vis Spectrophotometer (Thermo Fisher Scientific, USA) to calculate the percentage of inhibition as follows:

$$\begin{aligned} \text{DPPH radical scavenging activity} &= \\ &= \frac{A_{\text{control}} - A_{\text{sample}}}{A_{\text{control}}} \times 100\% \quad (2) \end{aligned}$$

where  $A_{\text{control}}$  is the absorbance of the negative control, and  $A_{\text{sample}}$  is the absorbance of the test solution.

#### Statistical analysis

All experiments were carried out in triplicate and the data were expressed as mean ± standard deviation (SD).

## RESULTS AND DISCUSSION

## Phytochemical screening of medicinal plant extracts

Many natural compounds have shown the anti-XO enzyme ability such as polyphenols, flavonoids, alkaloids, tannins, etc [20]. The phytochemical screening of ten plants was carried out to identify the bioactive compounds, and the result is shown in Table 1. All extracts have the presence of flavonoids, polyphenols, and tannins with different quantities. All plants have the presence of alkaloids except *Piper lolot* C.DC., *Piper betle* L., *Anacardium occidentale* L., and *Polygonum barbatum* L. The presence of these diverse bioactive compounds indicated the potential for various biological activities. Polyphenols, which are secondary metabolites produced by higher plants, have a variety of biological effects, including antioxidant, anti-inflammatory, anti-carcinogenic, and anti-gout [21]. Flavonoids have the inhibitory activity of various enzymes, such as XO, peroxidase, and nitric oxide synthase, which are involved in the production of free radicals, resulting in less oxidative damage to macromolecules [22]. Tannins, water-soluble polyphenols, have a variety of *in vitro* bioactivities, the most well studied of which are antimicrobial and antioxidant properties [23]. Alkaloids show strong biological effects on human organisms, especially anti-inflammatory while inflammatory is the most popular gout symptom [24]. Preliminary phytochemical screening shows the potential of medicinal plants for gout treatment.

## Total polyphenol content, total flavonoid content, and XO inhibitory activity of plant extracts

Polyphenols and flavonoids are considered the main bioactive chemical constituents and are found ubiquitously in plants [25]. Therefore, the total polyphenol content (TPC) and total flavonoid content (TFC) of the extracts were determined and the results are described in Table 2. The TPC of the three sample extracts ranged from 32.13 to 427.89 mg GAE/g, while the TFC ranged from 50.34 to 605.81 mg QUE/g. The *Piper betle* L. had the highest value of both TPC (427.89 mg GAE/g) and TFC (605.81 mg QUE/g). The significant value of TPC, and TFC which higher around 13–19 times than the lowest values. Therefore, *Piper betle* L. was predicted to show high potential in inhibiting XO inhibition because XO inhibition of plant extract may be related to TPC, TFC, and the chemical structures of individual phenolic.

The XO inhibitory activity of ten plants was also presented by their IC<sub>50</sub> values, shown in Table 2. Most medicinal plants have XO inhibitory activity, ranging from 1.18 µg/mL to 280 µg/mL. As expected, *Piper betle* L. with the highest TPC and TFC showed the best inhibitory activity of the XO inhibitory activity with the lowest value of IC<sub>50</sub> (1.18 µg/mL) which was lower than allopurinol (1.57 µg/mL). The results agree with one study reported on the XO that the IC<sub>50</sub> value of *Piper betle* L. was 16.5 µg/mL compared to the value of allopurinol, 6.16 µg/mL [26]. *Artocarpus Altilis* P. showed a value of IC<sub>50</sub> of 32.31 µg/mL which

Table 2. TPC, TFC, and XO inhibitory activity of ten plants

Medicinal plants	TPC (mg GAE/g)	TFC (mg QUE/g)	IC <sub>50</sub> (µg/mL)
<i>Piper lolot</i> C.DC.	73.56 ± 3.98	69.59 ± 1.82	<10% × 300 µM <sup>a</sup>
<i>Pandanus amaryllifolius</i> R.	41.15 ± 0.54	50.34 ± 0.63	<50% × 300 µM <sup>a</sup>
<i>Brassica juncea</i> L.	32.13 ± 0.49	78.68 ± 2.10	<20% × 300 µM <sup>a</sup>
<i>Piper betle</i> L.	427.89 ± 3.52	605.81 ± 11.60	1.18 ± 0.02
<i>Perilla frutescens</i> L.	104.62 ± 0.20	137.75 ± 3.01	88.04 ± 2.83
<i>Anacardium occidentale</i> L.	122.78 ± 0.89	150.52 ± 3.99	81.21 ± 1.55
<i>Polygonum barbatum</i> L.	70.45 ± 0.71	85.52 ± 2.93	113.94 ± 7.99
<i>Artocarpus altilis</i> P.	140.60 ± 0.42	309.53 ± 1.58	32.31 ± 1.08
<i>Vitex negundo</i> L.	75.80 ± 0.62	82.11 ± 2.90	280.00 ± 10.78
<i>Annona squamosa</i> L.	100.20 ± 0.94	223.06 ± 4.75	72.03 ± 1.58
<i>Allopurinol</i>	–	–	1.57 ± 0.01

<sup>a</sup>Inhibitory activity (%) at the highest tested concentration

was about 30 times higher than *Piper betle* L. one when the TPC and TFC values were approximately 2.7 and 1.7 times, respectively, lower than those of the *Piper betle* L. In addition, *Annona squamosal* L., *Perilla frutescens* L., *Anacardium occidentale* L., had  $IC_{50}$  values ranging from 72.03 to 88.04  $\mu\text{g/mL}$ . *Polygonum Barbatum* L. and *Vitex negundo* L. had a value of  $IC_{50}$  greater than 100  $\mu\text{g/mL}$ , which was in accordance with their low TPC and TFC (<100 mg/g). *Piper lolot* C.DC., *Pandanus amaryllifolius* R., and *Brassica juncea* L. showed no inhibitory activity with the inhibition percentage lower than 50% at 0.3 mg/mL. The strong inhibitory activity of *Piper betle* L. XO was predicted to be related to hydroxychavicol, which was a phenolic compound identified in *Piper betle* L. and found to be a more potent XO inhibitor than allopurinol [27]. Out of ten plants, *Piper betle* L. was selected as the most promising medicinal plant in XO inhibitory activity, and the different parts of *Piper betle* L. were surveyed for more details.

#### Study on the *Piper betle* L. different parts

In this study, the TPC, TFC, XO inhibitory activity, and antioxidant activity of different parts (stem, leaves, and whole plant) of the *Piper betle* L.

were determined to provide the basis for further investigation of this plant (see Figure). The TPC and TFC of leaf extract were the highest values of 437.12 mg GAE/g and 668.18 mg QUE/g, respectively, and the stem extract had the lowest values of TPC and TFC. Thus, the leaf extract showed the best ability to inhibit XO with an  $IC_{50}$  value of 0.82  $\mu\text{g/mL}$  when compared to the value of the stem extract and the whole plant extract, 2.62  $\mu\text{g/mL}$  and 1.18  $\mu\text{g/mL}$ , respectively, and compared to allopurinol (1.57  $\mu\text{g/mL}$ ). Moreover, the leaf extract also showed the most potent antioxidant activity with the lowest value of  $IC_{50}$  of 4.21  $\mu\text{g/mL}$ , which is lower than that of ascorbic acid (5.92  $\mu\text{g/mL}$ ). In addition, several studies showed similar results that the total amounts of polyphenols and flavonoids of leaf extract were higher than those of stem extract, and the antioxidant activity of leaf extract was also better [28, 29]. Clinical evidence suggests that hyperuricemia could be a significant risk factor for diabetes in gout patients and therefore the pathogenesis of both acute and chronic pancreatitis can be related to oxidative stress [30, 31]. From these results, the leaf extract of *Piper betle* L. promises to be a potential anti-gout agent and used for the treatment of gout and its complications.

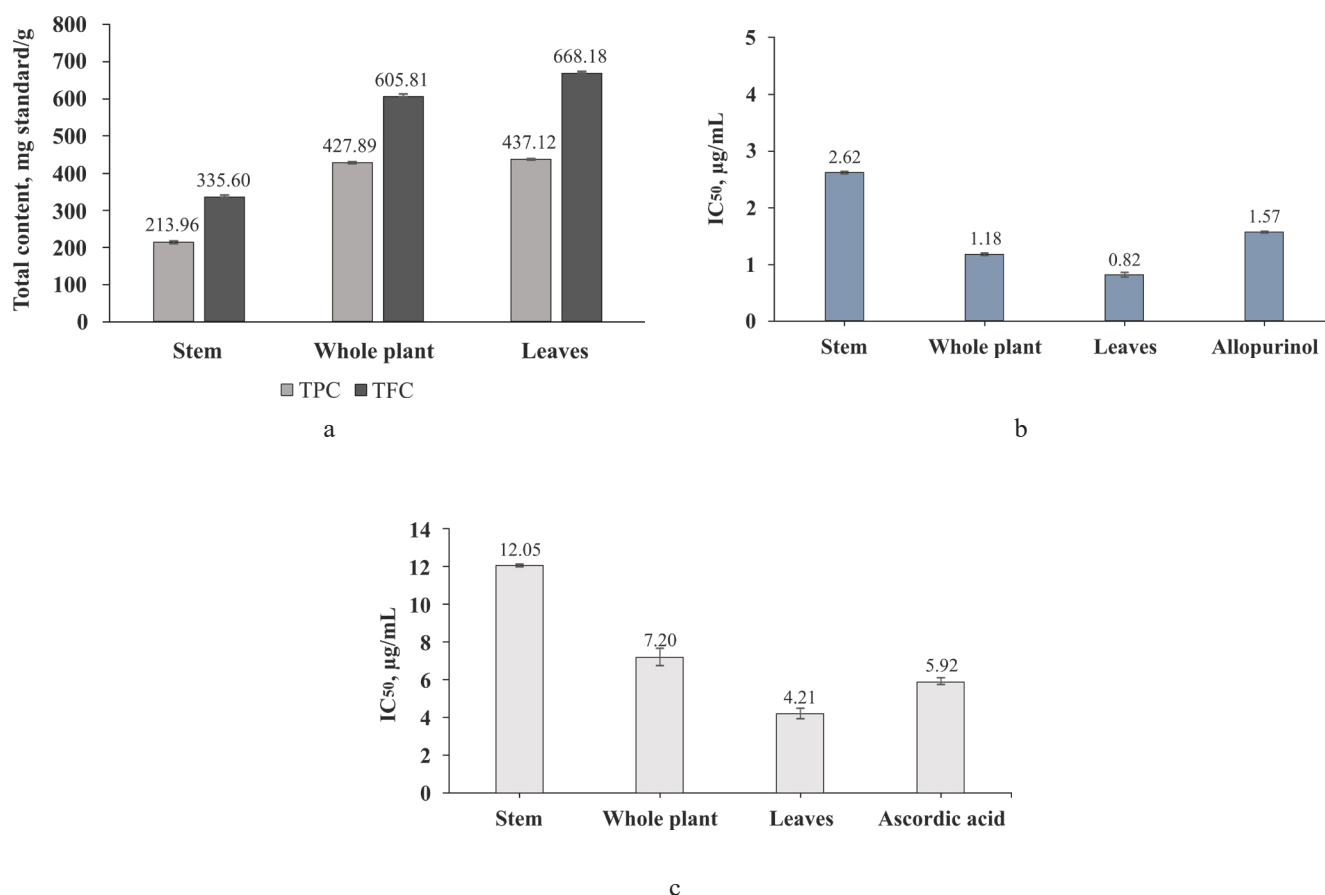


Figure. (a) TPC and TFC, (b) XO inhibitory activity, and (c) antioxidant activity of different parts of *Piper betle* L.

## CONCLUSIONS

The present work evaluated and screened medicinal plants for XO inhibitory activity. The extract of *Piper betle* L. showed strong XO inhibitory activity with an  $IC_{50}$  value lower than allopurinol (1.57  $\mu\text{g}/\text{mL}$ ) with high TPC and TFC. The *Piper betle* L. leaf was the part of the *Piper betle* L. that showed the best inhibitory activity and also antioxidant activity with an  $IC_{50}$  value of 0.82  $\mu\text{g}/\text{mL}$  and 4.21  $\mu\text{g}/\text{mL}$ , respectively. In summary, *Piper betle* L. leaf could be a good candidate for future studies of this plant on the treatment of gout and its complications.

## Acknowledgments

We acknowledge the support of time and facilities from Ho Chi Minh City University of Technology (HCMUT), VNU-HCM, for this study.

## Author's contributions

**Anh C. Ha** – developing the concept and methodology of the study, supervising, writing and editing the text of the article.

**Chinh D.P. Nguyen** – conducting research, writing the literature review, and editing the text of the article;

**Tan M. Le** – developing the concept, formal analysis, conducting research, and writing the text of the article;

*The authors declare no conflicts of interest.*

## REFERENCES

- Ragab G., Elshahaly M., Bardin T. Gout: An old disease in new perspective—A review. *J. Adv. Res.* 2017;8(5):495–511. <https://doi.org/10.1016/j.jare.2017.04.008>
- Safiri S., Kolahi A.A., Cross M., Carson-Chahhoud K., Hoy D., Almasi-Hashiani A., *et al.* Prevalence, incidence, and years lived with disability due to gout and its attributable risk factors for 195 countries and territories 1990–2017: A systematic analysis of the global burden of disease study 2017. *Arthritis & Rheumatology.* 2020;72(11):1916–27. <https://doi.org/10.1002/art.41404>
- Kuo C.-F., Grainge M.J., Zhang W., Doherty M. Global epidemiology of gout: prevalence, incidence and risk factors. *Nat. Rev. Rheumatol.* 2015;11(11):649–662. <https://doi.org/10.1038/nrrheum.2015.91>
- Borges F., Fernandes E., Roleira F. Progress towards the discovery of xanthine oxidase inhibitors. *Curr. Med. Chem.* 2002;9(2):195–217. <https://doi.org/10.2174/0929867023371229>
- Kostić D.A., Dimitrijević D.S., Stojanović G.S., Palić I.R., Đorđević A.S., Ickovski J.D. Xanthine oxidase: isolation, assays of activity, and inhibition. *J. Chem.* 2015;2015:294858. <https://doi.org/10.1155/2015/294858>
- Theoduloz C., Franco L., Ferro E., Rarschmann G.S. Xanthine oxidase inhibitory activity of Paraguayan Myrtaceae. *J. Ethnopharmacol.* 1988;24(2-3):179–183. [https://doi.org/10.1016/0378-8741\(88\)90149-3](https://doi.org/10.1016/0378-8741(88)90149-3)
- McKendrick M., Geddes A. Allopurinol hypersensitivity. *British Medical J.* 1979;1(6169):988. <https://doi.org/10.1136/bmj.1.6169.988>
- Pacher P., Nivorozhkin A., Szabó C. Therapeutic effects of xanthine oxidase inhibitors: renaissance half a century after the discovery of allopurinol. *Pharmacolog. Rev.* 2006;58(1):87–114. <https://doi.org/10.1124/pr.58.1.6>
- Salmerón-Manzano E., Garrido-Cardenas J.A., Manzano-Agugliaro F. Worldwide research trends on medicinal plants. *Int. J. Environ. Res. Public Health.* 2020;17(10):3376. <https://doi.org/10.3390/ijerph17103376>
- Duong-Trung N., Quach L.-D., Nguyen C.-N. Learning deep transferability for several agricultural classification problems. *Int. J. Adv. Comput. Sci. Appl.* 2019;10(1). <http://doi.org/10.14569/IJACSA.2019.0100107>
- Azmi S., Jamal P., Amid A. Xanthine oxidase inhibitory activity from potential Malaysian medicinal plant as remedies for gout. *Int. Food Res. J.* 2012;19(1):159–165.

12. De Silva G.O., Abeysundara A.T., Aponso M.M.W. Extraction methods, qualitative and quantitative techniques for screening of phytochemicals from plants. *Am. J. Essent. Oils Nat. Prod.* 2017;5(2):29–32.
13. Kerroui S., Lrhorfi L., Amal S., Ouafae E., abdellahi Lella O., Bahia B., *et al.* Qualitative study of bioactive components of dill (*Anethum graveolens* L.) from Northern Morocco. *Eur. Sci. J.* 2016;12(27). <https://doi.org/10.19044/esj.2016.v12n27p335>
14. Nagalingam S., Sasikumar C.S., Cherian K.M. Extraction and preliminary phytochemical screening of active compounds in Morinda citrifolia fruit. *Asian J. Pharm. Clin. Res.* 2012;5(2):179–81.
15. Sánchez-Rangel J.C., Benavides J., Heredia J.B., Cisneros-Zevallos L., Jacobo-Velázquez D.A. The Folin–Ciocalteu assay revisited: improvement of its specificity for total phenolic content determination. *Anal. Methods.* 2013;5(21):5990–5999. <https://doi.org/10.1039/C3AY41125G>
16. Baba S.A., Malik S.A. Determination of total phenolic and flavonoid content, antimicrobial and antioxidant activity of a root extract of *Arisaema jacquemontii* Blume. *Journal of Taibah University for Science (JTUSCI)*. 2015;9(4):449–454. <https://doi.org/10.1016/j.jtusci.2014.11.001>
17. Do N.H., Le T.M., Nguyen C.D., Ha A.C. Optimization of total flavonoid content of ethanolic extract of *Persicaria pulchra* (Bl.) Soják for the inhibition of  $\alpha$ -glucosidase enzyme. *Fine Chem. Technol.* 2020;15(4):39–50. <https://doi.org/10.32362/2410-6593-2020-15-4-39-50>
18. Abd El-Rahman H.S., Abd-ELHak N.A. Xanthine oxidase inhibitory activity and antigout of celery leek parsley and molokhia. *Adv. Biochem.* 2015;3(4):40–50. <https://doi.org/10.11648/j.ab.20150304.11>
19. Sharma O.P., Bhat T.K. DPPH antioxidant assay revisited. *Food Chem.* 2009;113(4):1202–1205. <https://doi.org/10.1016/j.foodchem.2008.08.008>
20. Mehmood A., Ishaq M., Zhao L., Safdar B., Rehman Au., Munir M., *et al.* Natural compounds with xanthine oxidase inhibitory activity: A review. *Chem. Biol. Drug Des.* 2019;93(4):387–418. <https://doi.org/10.1111/cbdd.13437>
21. Han X., Shen T., Lou H. Dietary polyphenols and their biological significance. *Int. J. Mol. Sci.* 2007;8(9):950–988. <https://doi.org/10.3390/i8090950>
22. Rashid M., Fareed M., Rashid H., Aziz H., Ehsan N., Khalid S., *et al.* Flavonoids and their biological secrets. In: Ozturk M., Hakeem K. (Eds.). *Plant and Human Health*. 2019;2:579–605. [https://doi.org/10.1007/978-3-030-03344-6\\_24](https://doi.org/10.1007/978-3-030-03344-6_24)
23. Sieniawska E., Baj T. Tannins. In: *Pharmacognosy*: Elsevier; 2017. P. 199–232. <https://doi.org/10.1016/B978-0-12-802104-0.00010-X>
24. Barbosa-Filho J.M., Piuvezam M.R., Moura M.D., Silva M.S., Lima K.V.B., da-Cunha E.V.L., *et al.* Anti-inflammatory activity of alkaloids: A twenty-century review. *Rev. Bras. Farmacogn.* 2006;16(1):109–139. <https://doi.org/10.1590/S0102-695X2006000100020>
25. Zulkifli S.A., Abd Gani S.S., Zaidan U.H., Halmi M.I.E. Optimization of total phenolic and flavonoid contents of defatted pitaya (*Hylocereus polyrhizus*) seed extract and its antioxidant properties. *Molecules.* 2020;25(4):787. <https://doi.org/10.3390/molecules25040787>
26. Vikrama Chakravarthi P., Murugesan S., Arivuchelvan A., Sukumar K., Arulmozhi A., Jagadeeswaran A. *In vitro* xanthine oxidase inhibitory activity of *Piper betle* and *Phyllanthus niruri*. *J. Pharmacogn. Phytochem.* 2018;7(5):959–961.
27. Murata K., Nakao K., Hirata N., Namba K., Nomi T., Kitamura Y., *et al.* Hydroxychavicol: a potent xanthine oxidase inhibitor obtained from the leaves of betel, *Piper betle*. *J. Nat. Med.* 2009;63(3):355–359. <https://doi.org/10.1007/s11418-009-0331-y>
28. Ghasemzadeh A., Jaafar H.Z., Rahmat A. Antioxidant activities, total phenolics and flavonoids content in two varieties of Malaysia young ginger (*Zingiber officinale* Roscoe). *Molecules.* 2010;15(6):4324–4333. <https://doi.org/10.3390/molecules15064324>
29. Pyo Y.-H., Lee T.-C., Logendra L., Rosen R.T. Antioxidant activity and phenolic compounds of Swiss chard (*Beta vulgaris* subspecies *cycla*) extracts. *Food Chem.* 2004;85(1):19–26. [https://doi.org/10.1016/S0308-8146\(03\)00294-2](https://doi.org/10.1016/S0308-8146(03)00294-2)
30. Krishnan E., Akhras K., Sharma H., Marynchenko M., Wu E., Tawk R., *et al.* Relative and attributable diabetes risk associated with hyperuricemia in US veterans with gout. *QJM: An International Journal of Medicine.* 2013;106(8):721–729. <https://doi.org/10.1093/qjmed/hct093>
31. Monfared S.S.M.S., Vahidi H., Abdolghaffari A.H., Nikfar S., Abdollahi M. Antioxidant therapy in the management of acute, chronic and post-ERCP pancreatitis: a systematic review. *World J. Gastroenterol: WJG.* 2009;15(36):4481–4490. <https://doi.org/10.3748/wjg.15.4481>

#### About the authors:

**Anh C. Ha**, PhD., Doctor of Medicinal Chemistry, Faculty of Chemical Engineering, Ho Chi Minh City University of Technology (268 Ly Thuong Kiet Street, District 10, Ho Chi Minh City, Vietnam); Vietnam National University Ho Chi Minh City (Linh Trung Ward, Thu Duc District, Ho Chi Minh City, Vietnam). E-mail: hcanh@hcmut.edu.vn. <https://orcid.org/0000-0001-7919-4028>

**Chinh D.P. Nguyen**, BEng., Postgraduate Student, Faculty of Chemical Engineering, Ho Chi Minh City University of Technology (268 Ly Thuong Kiet Street, District 10, Ho Chi Minh City, Vietnam); Vietnam National University Ho Chi Minh City (Linh Trung Ward, Thu Duc District, Ho Chi Minh City, Vietnam). Email: npdchinh.sdh19@hcmut.edu.vn. <https://orcid.org/0000-0002-2820-3913>

**Tan M. Le**, MSc., Master of Chemical Engineering, Faculty of Chemical Engineering, Ho Chi Minh City University of Technology (268 Ly Thuong Kiet Street, District 10, Ho Chi Minh City, Vietnam); Vietnam National University Ho Chi Minh City (Linh Trung Ward, Thu Duc District, Ho Chi Minh City, Vietnam). Email: lmtan.sdh20@hcmut.edu.vn. <https://orcid.org/0000-0002-7956-1067>

**Об авторах:**

**Ань К. Ха**, PhD, к.м.н., Химико-технологический факультет, Технологический университет Хошимина (268 Ли Тхыонг Кьет ул., Район 10, г. Хошимин, Вьетнам); Вьетнамский национальный университет Хошимина (Линь Чунг Уорд, Район Тхёк, г. Хошимин, Вьетнам). E-mail: hcanh@hcmut.edu.vn. <https://orcid.org/0000-0001-7919-4028>

**Чин Д.П. Нгуен**, аспирант, Химико-технологический факультет, Технологический университет Хошимина (268 Ли Тхыонг Кьет ул., Район 10, г. Хошимин, Вьетнам); Вьетнамский национальный университет Хошимина (Линь Чунг Уорд, Район Тхёк, г. Хошимин, Вьетнам). E-mail: npdchinh.sdh19@hcmut.edu.vn. <https://orcid.org/0000-0002-2820-3913>

**Тан М. Ле**, аспирант, Химико-технологический факультет, Технологический университет Хошимина (268 Ли Тхыонг Кьет ул., Район 10, г. Хошимин, Вьетнам); Вьетнамский национальный университет Хошимина (Линь Чунг Уорд, Район Тхёк, г. Хошимин, Вьетнам). E-mail: lmtan.sdh20@hcmut.edu.vn. <https://orcid.org/0000-0002-7956-1067>

*The article was submitted: October 29, 2021; approved after reviewing: December 15, 2021; accepted for publication: April 14, 2022.*

*The text was submitted by the authors in English.*

*Edited for English language and spelling by Quinton Scribner, Awatera.*

**BIOCHEMISTRY AND BIOTECHNOLOGY**

**БИОХИМИЯ И БИОТЕХНОЛОГИЯ**

ISSN 2686-7575 (Online)

<https://doi.org/10.32362/2410-6593-2022-17-2-140-151>



UDC 615.275.2

RESEARCH ARTICLE

**Investigation of the anti-influenza activity of siRNA complexes against the cellular genes *FLT4*, *Nup98*, and *Nup205* *in vitro***

**Evgeny A. Pashkov<sup>1,2,✉</sup>, Maria O. Korotysheva<sup>1</sup>, Anastasia V. Pak<sup>1</sup>, Evgeny B. Faizuloev<sup>2</sup>, Alexander V. Sidorov<sup>2</sup>, Alexander V. Poddubikov<sup>2</sup>, Elizaveta P. Bystritskaya<sup>2</sup>, Yuliya E. Dronina<sup>1,3</sup>, Viktoriia K. Solntseva<sup>1</sup>, Tatiana A. Zaiceva<sup>1</sup>, Evgeny P. Pashkov<sup>1</sup>, Anatoly S. Bykov<sup>1</sup>, Oxana A. Svitich<sup>1,2</sup>, Vitaliy V. Zverev<sup>1,2</sup>**

<sup>1</sup>I.M. Sechenov First Moscow State Medical University (Sechenov University), Moscow, 119991 Russia

<sup>2</sup>I. Mechnikov Research Institute of Vaccines and Sera, Moscow, 105064 Russia

<sup>3</sup>N.F. Gamaleya National Research Center for Epidemiology and Microbiology, Moscow, 123098 Russia

✉ Corresponding author, e-mail: pashckov.j@yandex.ru

**Abstract**

**Objectives.** Evaluation of changes in the viral activity of influenza A/WSN/33 after complex knockdown of combinations of cellular genes *FLT4*, *Nup98* and *Nup205* in human lung cell culture A549.

**Methods.** The work was carried out using the equipment of the Center for Collective Use of the I. Mechnikov Research Institute of Vaccines and Sera, Russia. The authors performed transfection of combinations of small interfering ribonucleic acid (siRNA) complexes that cause simultaneous disruption of the expression of cellular genes *FLT4*, *Nup98*, and *Nup205*. Within three days from the moment of transfection and infection, the supernatant fluid and cell lysate were taken for subsequent viral reproduction intensity determination using the titration method for cytopathic action. The dynamics of changes in the concentration of viral ribonucleic acid (vRNA) was determined by real-time reverse transcription polymerase chain reaction (real-time RT-PCR). The nonparametric Mann–Whitney test was used to calculate statistically significant differences between groups.

**Results.** Using all of the combinations of siRNA complexes, cell viability did not decrease below the threshold level of 70%. In cells treated with complex *FLT4.2* + *Nup98.1* + *Nup205* at the multiplicity of infection (MOI) equal to 0.1, a significant decrease in viral reproduction by 1.5 lg was noted on the first day in relation to nonspecific and viral controls. The use of siRNA complexes at MOI 0.01 resulted in a more pronounced antiviral effect. The viral titer in cells treated with siRNA

complexes *FLT4.2 + Nup98.1* and *Nup98.1 + Nup205* decreased by 1.5 lg on the first day. In cells treated with complexes *FLT4.2 + Nup205* and *FLT4.2 + Nup98.1 + Nup205*, it decreased by 1.8 and 2.0 lg on the first day and by 1.8 and 2.5 lg on the second day, respectively, in relation to nonspecific and viral controls. When conducting real-time RT-PCR, a significant decrease in the concentration of vRNA was noted. At MOI 0.1, a 295, 55, and 63-fold decrease in the viral load was observed with the use of siRNA complexes *FLT4.2 + Nup98.1*, *Nup98.1 + Nup205*, and *FLT4.2 + Nup98.1 + Nup205*, respectively. On the second day, a decrease in vRNA was also observed in cells treated with complex A. A 415-fold decrease in vRNA on the third day was noted in cells treated with complex *FLT4.2 + Nup205*. At MOI 0.01, the concentration of vRNA decreased 9.5 times when using complex B relative to nonspecific and viral control.

**Conclusions.** The study showed a pronounced antiviral effect of siRNA combinations while simultaneously suppressing the activity of cellular genes (*FLT4*, *Nup98*, and *Nup205*), whose expression products are playing important role in the viral reproduction process, and obtained original designs of siRNA complexes. The results obtained are of great importance for the creation of emergence prophylactic and therapeutic drugs, whose action is based on the mechanism of RNA interference.

**Keywords:** RNA interference, influenza A virus, gene expression, mRNA, small interfering RNA, viral RNA

**For citation:** Pashkov E.A., Korotysheva M.O., Pak A.V., Faizuloev E.B., Sidorov A.V., Poddubikov A.V., Bystritskaya E.P., Dronina Yu.E., Solntseva V.K., Zaiceva T.A., Pashkov E.P., Bykov A.S., Svitich O.A., Zverev V.V. Investigation of the anti-influenza activity of siRNA complexes against the cellular genes *FLT4*, *Nup98*, and *Nup205* *in vitro*. *Tonk. Khim. Tekhnol.* = *Fine Chem. Technol.* 2022;17(2):140–151 (Russ., Eng.). <https://doi.org/10.32362/2410-6593-2022-17-2-140-151>

## НАУЧНАЯ СТАТЬЯ

# Исследование противогриппозной активности комплексов миРНК против клеточных генов *FLT4*, *Nup98* и *Nup205* на модели *in vitro*

Е.А. Пашков<sup>1,2,✉</sup>, М.О. Коротышева<sup>1</sup>, А.В. Пак<sup>1</sup>, Е.Б. Файзулов<sup>2</sup>,  
А.В. Сидоров<sup>2</sup>, А.В. Поддубиков<sup>2</sup>, Е.П. Быстрицкая<sup>2</sup>, Ю.Е. Дронина<sup>1,3</sup>,  
В.К. Солнцева<sup>1</sup>, Т.А. Зайцева<sup>1</sup>, Е.П. Пашков<sup>1</sup>, А.С. Быков<sup>1</sup>,  
О.А. Свитич<sup>1,2</sup>, В.В. Зверев<sup>1,2</sup>

<sup>1</sup>Первый Московский государственный медицинский университет им. И.М. Сеченова Минздрава России (Сеченовский Университет), Москва, 119991 Россия

<sup>2</sup>Научно-исследовательский институт вакцин и сывороток им. И.И. Мечникова Минздрава России, Москва, 105064 Россия

<sup>3</sup>Национальный исследовательский центр эпидемиологии и микробиологии им. почетного академика Н.Ф. Гамалеи Минздрава России, Москва, 123098 Россия

✉ Автор для переписки, e-mail: [pashkov.j@yandex.ru](mailto:pashkov.j@yandex.ru)

## Аннотация

**Цели.** Оценка изменения вирусной активности гриппа A/WSN/33 после комплексного нокдауна комбинаций клеточных генов *FLT4*, *Nup98* и *Nup205* в культуре легочных клеток человека A549.

**Методы.** Работа выполнена с использованием оборудования центра коллективного пользования Научно-исследовательского института вакцин и сывороток им И.И. Мечникова (Россия). Авторами выполнялась трансфекция комбинаций комплексов миРНК, вызывающих одновременное нарушение экспрессии клеточных генов *FLT4*, *Nip98* и *Nip205*. В течение трех дней с момента трансфекции и заражения проводился отбор надосадочной жидкости и клеточного лизата для последующего определения интенсивности вирусной репродукции по методу титрования по цитопатическому действию. Динамику изменения концентрации вирусной рибонуклеиновой кислоты (вРНК) определяли методом обратной транскрипции и полимеразной цепной реакции в режиме реального времени (ОТ-ПЦР-РВ). Для вычисления статистически значимых различий между группами использовали непараметрический критерий Манна-Уитни.

**Результаты.** При использовании всех комбинаций комплексов малых интерферирующих РНК (миРНК) жизнеспособность клеток не снижалась ниже порогового уровня в 70%. В клетках, обработанных комплексом *FLT4.2* + *Nip98.1* + *Nip205* при множественности заражения (*Multiplicity of infection, MOI*) 0.1 достоверное снижение вирусной репродукции на 1.5 lg отмечалось на первые сутки по отношению к неспецифическому и вирусному контролю. Использование комплексов миРНК при *MOI* 0.01 приводило к более выраженному противовирусному эффекту. Вирусный титр в клетках, обработанных комплексами миРНК *FLT4.2* + *Nip98.1* и *Nip98.1* + *Nip205* снижался на первые сутки на 1.5 lg. В клетках, обработанных комплексами *FLT4.2* + *Nip205* и *FLT4.2* + *Nip98.1* + *Nip205* снижался на 1.8 и 2 lg на первые сутки и на 1.8 и 2.5 lg на вторые сутки соответственно по отношению к неспецифическому и вирусному контролю. При проведении ОТ-ПЦР-РВ отмечено достоверное снижение концентрации вирусной РНК. При *MOI* 0.1 снижение вирусной в 295, 55 и 63 раза отмечалось при использовании комплексов миРНК *FLT4.2* + *Nip98.1*, *Nip98.1* + *Nip205* и *FLT4.2* + *Nip98.1* + *Nip205* соответственно. На вторые сутки снижение вирусной РНК также отмечалось в клетках, обработанных комплексом *FLT4.2* + *Nip98.1*. Снижение вРНК на третьи сутки в 415 раз отмечалось в клетках, обработанных комплексом *FLT4.2* + *Nip205*. При *MOI* 0.01 концентрация вРНК снизилась в 9.5 раз при использовании комплекса *Nip98.1* + *Nip205* относительно неспецифического и вирусного контроля.

**Выводы.** В ходе исследования был показан выраженный противовирусный эффект комбинаций миРНК при одновременном подавлении активности клеточных генов (*FLT4*, *Nip98* и *Nip205*), чьи продукты экспрессии играют важное участие в процессе вирусной репродукции, а также получены оригинальные конструкции комплексов миРНК. Полученные результаты имеют важное значение для создания препаратов для экстренной профилактики и терапии, чье действие основано на механизме РНК-интерференции.

**Ключевые слова:** РНК-интерференция, вирус гриппа А, экспрессия генов, матричная РНК, малые интерферирующие РНК, вирусная РНК

**Для цитирования:** Пашков Е.А., Коротышева М.О., Пак А.В., Файзулоев Е.Б., Сидоров А.В., Поддубиков А.В., Быстрицкая Е.П., Дронина Ю.Е., Солнцева В.К., Зайцева Т.А., Пашков Е.П., Быков А.С., Свитич О.А., Зверев В.В. Исследование противогриппозной активности комплексов миРНК против клеточных генов *FLT4*, *Nip98* и *Nip205* на модели *in vitro*. *Тонкие химические технологии*. 2022;17(2):140–151. <https://doi.org/10.32362/2410-6593-2022-17-2-140-151>

## INTRODUCTION

The influenza virus is the cause of the most common anthroponotic infections affecting the upper respiratory tract. According to the World Health Organization, in 2021, up to 1.2 billion of new cases of influenza infection, up to 5 million cases of severe illness, and up to 650000 deaths were

observed worldwide<sup>1</sup>. Influenza A virus, which has high clinical significance and significant pandemic potential, poses an increased threat to global health [1]. Additionally, influenza complications can affect organ systems such as the central nervous,

<sup>1</sup> <https://www.euro.who.int/ru/media-centre/events/events/2021/10/flu-awareness-campaign-2021>

genitourinary, and cardiovascular systems. The risk of developing bacterial and fungal post-influenza complications is also no exception [2–5].

The continued threat of new epidemics and pandemics demonstrates that the progress made in the development of health infrastructure, even in the most developed countries, does not guarantee the protection of the population from newly emerging infections [6]. It is known that during outbreaks of bacterial infections, the answer to such challenges is sought in the development of new variants of antibacterial drugs. In the case of viral infections, today there are practically no approaches for the emergency development and creation of drugs. Some examples of the successful solution of this problem (human immunodeficiency virus protease inhibitor *Lopinavir* for the treatment of human immunodeficiency virus (HIV) infection; inhibitors of non-structural protein 5B—*Sofosbuvir*, *Dasabuvir*—for the treatment of infection caused by the virus hepatitis C) show that the development of emergency targeted antiviral drugs takes a long time, and the high cost of development makes them inaccessible for widespread use [7–9].

In parallel with this, the use of many anti-influenza drugs aimed at the therapy and prevention of this infection does not bring the desired result due to the fact that new viral strains resistant to these drugs are detected annually [10]. Modern vaccines also do not guarantee complete disease protection, since they do not always cause a sufficient immune response, against which the acquired immunity lasts only 6 months [11]. It should be borne in mind that influenza vaccines must be recycled every year, since new influenza virus strains appear every year, which reduces the effectiveness of previously created vaccines. In addition, vaccination is difficult for people who are allergic to egg white, as well as for people with immunodeficiency [12–15]. In summary, the creation of a universal platform for the rapid development of cost-effective and safe therapies for viral infections is of obvious relevance for ensuring human safety since this will allow creating approaches to control the circulation of influenza viruses pathogenic to humans.

Ribonucleic acid (RNA) interference (RNAi, RNAi) is a sequence of regulatory reactions in eukaryotic cells caused by a foreign double-stranded RNA molecule. The mechanism of RNA interference is the separation of exogenous double-stranded RNA into small sequences by *Dicer* endonuclease, which are small interfering RNAs (siRNAs). After that, siRNA binds to the RNA-induced gene shutdown complex (RNA-induced silencing complex or *RISC*),

which includes three proteins: Argonaut-2 (*Ago2*), the cellular protein activator of protein kinase R or protein activator of the interferon-induced protein kinase (*PACT*), and the transactivation response element RNA-binding protein (*TRBP*). The resulting complex degrades the target matrix RNA (mRNA) [16, 17].

To date, there is a trend towards the creation of drugs based on the RNA interference mechanism. *Patisiran* and *Givosiran*, which are used in the treatment of genetically determined diseases—amyloid polyneuropathy and acute hepatic porphyria—have already received approval for clinical use [18, 19]. There are also a number of antiviral drugs in various stages of clinical trials for the treatment of hepatitis C, respiratory syncytial virus (RSV) infection, and HIV infection [20, 22].

It should be kept in mind that one of the main factors that reduces the antiviral activity of RNA interference is the ability to “escape” from siRNAs specific to viral genes [23]. In view of this, the most important feature of the applied approach based on RNA interference inducers, which makes it possible to avoid the emergence of resistance of the virus to therapy, is the simultaneity of the therapeutic effect and the multiple targets of the destructive effect of synthetic oligonucleotides on the host cell transcripts, which are vital for the reproduction of the virus.

Since the antiviral effect of a single knockdown of cellular genes using siRNA was previously shown [24, 25], the purpose of this study is to experimentally substantiate and evaluate the effectiveness of the simultaneous knockdown of two or more cellular genes (*FLT4*, *Nup98*, and *Nup205*) in order to reduce the reproduction of the influenza A/WSN/33 virus (H1N1) in A549 cell culture.

## MATERIALS AND METHODS

### siRNA

The selection of siRNAs was carried out using the siDirect 2.0 resource. Oligoribonucleotides (*Syntol*, Russia) were diluted with water to a concentration of 100 pmol/μL. Next, complementary oligonucleotides (*Syntol*, Russia) were mixed, incubated in a thermostat at 60°C for 1 min, then cooled to room temperature. The prepared RNA duplexes were stored at –80°C. All work with finished duplexes was carried out using a cold tripod. The sequences of the siRNAs used are presented in Table 1. As a nonspecific control, *siL2* siRNA was used, which is specific to the firefly luciferase gene and does not affect the life cycle of A549 cells.

**Table 1.** siRNA sequences used in the work

siRNA	Sequence
<i>FLT4.2</i>	UGAAGUUCUGUUGAAAAAGdAdC CUUUUACAACAGAACUUCAdCdA
<i>Nup98.1</i>	AGUCUUUGUUUCAGAAAGCdGdC GCUUUCUGAAACAAAGACUdCdA
<i>Nup205</i>	UCAAAAUCUUUAUCAAGAAGdGdT CUUCUUGAUUAGAUUUUGAdAdG
<i>siL2</i> (nonspecific siRNA)	UUUCCGUCAUCGUCUUUCCdTdT GGAAAGACGAUGACGGAAAdTdT

### Virus

Influenza A/WSN/33 (H1N1) virus (*St. Jude's Children's Research Hospital*, USA) was used in the work. Cultivation and determination of the virus titer was carried out on a cell culture Madin-Darby Canine Kidney (MDCK).

### Cell culture

Cocker spaniel kidney cells MDCK (*Institut Pasteur*, France) and human lung adenocarcinoma cells A549 (*ATCC*, USA) were used in the work. MDCK cells were grown in MEM medium (*PanEco*, Russia) containing 5% Gibco fetal bovine serum (ESC) (*Fisher Scientific*, New Zealand), 40 µg/mL gentamicin (*PanEco*, Russia), and 300 µg/mL L-glutamine (*PanEco*, Russia) at 37°C in a CO<sub>2</sub> incubator. A549 cells were grown in DMEM medium (*PanEco*, Russia) containing 5% ESC, gentamicin 40 µg/mL, and L-glutamine 300 µg/mL at 37°C in a CO<sub>2</sub> incubator.

### MTT test

The survival of A549 cells treated with siRNA complexes was assessed using the methylthiazolyltetrazolium bromide (MTT) test. On days 1, 2, and 3 after transfection, 20 µL of MTT solution at a concentration of 5 mg/mL (*PanEco*, Russia) was added to the wells with cells of a 96-well plate and incubated at 37°C in an atmosphere of 5% CO<sub>2</sub> for 2 h. Next, the culture liquid was taken and added to the wells, 100 µL of isopropanol (*Sigma-Aldrich*, USA) in each well. Using a plate spectrophotometer (*Varioscan*, *Thermo Fisher Scientific*, USA), the optical density of each well was determined at 530 nm, considering the background values at 620 nm.

### Transfection of siRNA cells followed by infection

For transfection of siRNA complexes, A549 cells were seeded in 24-well plates at a seeding concentration of 1:3. After the formation of 80% cell monolayer, the cells were washed with phosphate-buffered saline and serum-free Opti-MEM medium (*Thermo Fisher Scientific*). Next, a mixture of Lipofectamin 2000 (*Thermo Fisher Scientific*) and Opti-MEM was added to the siRNA solution in Opti-MEM medium and incubated at room temperature for 20 min. The total concentration of each of the four siRNA complexes required for gene knockdown was 20 pmol/µL per well. The compositions of siRNA complexes and their sequences are listed in Tables 1, 2, and 3, respectively. After incubation, the complexes were added to the cells. *siL2* siRNA was used as a nonspecific control. The cells were then incubated at 37°C in a CO<sub>2</sub> incubator. After 4 h, the culture medium was removed from all wells, except for the negative control. Then, 0.5 mL of virus-containing liquid with a multiplicity of infection (MOI) of 0.1 and 0.01, consisting of DMEM medium, 0.001% tosyl phenylalanyl chloromethyl ketone (TPCK) (*Sigma-Aldrich*, Germany), and 40 µg/mL gentamicin was added. After that, the cells were again placed in a CO<sub>2</sub> incubator. Over the next three days, supernatant samples were taken for subsequent titration and a cell lysate was taken to assess the viral RNA (vRNA) concentration dynamics by real-time reverse transcription polymerase chain reaction (real-time RT-PCR).

### vRNA detection

vRNA was isolated from the cell lysate using a Ribosorb kit (*Helicon*, Russia). The OT-1 reagent kit (*Syntol*, Russia) was used to set up the reverse transcription reaction. Changes in the concentration

**Table 2.** Complex siRNA used in the work

Complex siRNA	Composition of complex siRNA
Complex A	<i>FLT4.2 + Nup98.1</i>
Complex B	<i>Nup98.1 + Nup205</i>
Complex C	<i>FLT4.2 + Nup205</i>
Complex D	<i>FLT4.2 + Nup98.1 + Nup205</i>

**Table 3.** Primers for real-time RT-PCR of the influenza A virus (IAV) M-gene

Primer	Sequence
IAV M F:	GGAATGGCTAAAGACAAGACCAAT
IAV M R:	GGGCATTTTGGACAAAGCGTCTAC
IAV M Pr: FAM	AGTCCTCGCTCACTGGGCACGGTG-BHQ1

of vRNA were monitored by quantitative real-time RT-PCR with a set of primers and probes for the M gene of the influenza A virus (IAV) [26]. Real-time polymerase chain reaction (PCR) was performed using a set of reagents for real-time PCR in the presence of EVA Green dye and ROX reference dye (*Syntol*, Russia). The working concentration of primers and probes was 10 pmol/ $\mu$ L and 5 pmol/ $\mu$ L, respectively. The real-time PCR reaction was carried out in a DT-96 amplifier (*DNA technology*, Russia). The temperature-time regime was 95°C—5 min (1 cycle); 62°C—40 s, 95°C—15 s (40 cycles). Primers and probes (*Synthol*, Russia) are presented in Table 3.

#### Virus titration at the endpoint of the cytopathic effect

The viral titer was determined by the extreme point of the visual manifestation of the cytopathic effect in the MDCK cell culture. MDCK cells were seeded into 96-well plates at an inoculum concentration of  $1 \cdot 10^4/\text{cm}^2$ . Two days later, the nutrient medium was removed from the wells, 10-fold serial dilutions of the viral material were added in a maintenance medium without trypsin, and incubated for four days in a CO<sub>2</sub> incubator at 37°C. On the fourth day, the titration results were visually recorded under a microscope for the presence of a specific cytopathic effect for the influenza virus (change, deformation, detachment of dead cells from the bottom of the well). Viral titer was calculated from [27] and expressed as the decimal logarithm of 50% tissue cytopathic doses in mL (lgTCD<sub>50/mL</sub>).

#### Statistical data processing

The statistical significance of the results obtained was determined using the Mann–Whitney test. The difference was considered significant at  $p \leq 0.01$  and  $p \leq 0.05$ .

## RESULTS

#### Effect of siRNA complexes on the survival of transfected cells

The survival rate of A549 cells transfected with siRNA was assessed for three days. By analogy with [28], the survival threshold was set at 70%. After 24 h, the viability of cells treated with complexes C and D decreased by 15%–17%. On the second day, the survival rate of cells treated with the same complexes did not practically change, however, the toxicity of complexes A and B for cells was 24% and 21%, respectively. On the third day, cell survival rates practically did not change. The survival rate of nontransfected cells was taken as 100%. Survival values were normalized to the mean absorbance of nontransfected cells at each respective time interval after transfection. The data obtained is presented in Table 4.

#### Effect of siRNA complexes on virus titer

In order to assess the viral activity dynamics, titration of the virus-containing liquid was carried out on MDCK cells, which was taken within three days from the moment the siRNA complexes were

introduced into the A549 cell cultures. The data shown in Fig. 1 indicates the ability of siRNA complexes to reduce the reproduction of the influenza virus *in vitro*. Figure 1a shows the decrease in viral titer at MOI = 0.1. It was found that at this MOI value, the use of the siRNA complex directed to the *FLT4*, *Nup98*, and *Nup205* genes led to a significant decrease in viral reproduction by 1.5 lgTCD<sub>50/mL</sub> on the first day compared to *siL2* siRNA. In nontransfected cell culture, virus titers increased over time, reaching peak values at 48 and 72 h. The same was noted in cells transfected with nonspecific *siL2* siRNA. Figure 1b shows that at MOI = 0.01, the viral titer in cells treated with the A and B complexes significantly decreased on the first day by 1.5 lgTCD<sub>50/mL</sub> relative to control ( $p < 0.05$ ). The use of the C and D complexes led to a significant decrease in viral titer by 1.8 and 2.0 lgTCD<sub>50/mL</sub> on the first day and by 1.8 and 2.5 lgTCD<sub>50/mL</sub> on the second day ( $p < 0.05$ ), respectively, according to the controls compared.

#### Influence of siRNAs on the vRNA concentration

Figure 2 shows the effect of siRNA on vRNA concentration *in vitro*. To assess the change in the concentration of vRNA, real-time RT-PCR was performed. Figure 2a shows that at MOI = 0.1, the use of the A, B, and D complexes led to a significant decrease in vRNA on the first day compared to *siL2* siRNA at 295, 55 and 63 times, respectively ( $p < 0.05$ ). On the second day, a 205-fold decrease in vRNA was observed in cells transfected with the A complex ( $p < 0.05$ ). When using the C complex,

a 415-fold decrease in vRNA was noted on the third day ( $p < 0.05$ ). Figure 2b shows that the concentration of vRNA in cells with MOI = 0.01 decreased by 9.5 times on the first day when using the B complex ( $p < 0.05$ ) compared with nonspecific control.

## DISCUSSION

This work is a continuation of studies on the evaluation of the antiviral activity of single knockdowns of the above cellular genes by means of siRNA, carried out by the authors earlier [21, 22]. A series of experiments was carried out to evaluate the efficiency of simultaneous knockdown of several cellular genes using siRNA complexes directed to the *FLT4*, *Nup98*, and *Nup205* genes. A pronounced antiviral effect of siRNAs directed simultaneously to several mRNAs of these genes was shown, and data were obtained indicating a correlation between a decrease in cellular gene expression and a decrease in viral reproduction. To assess the effectiveness of siRNA complexes, two methodological approaches were used: virus titration by the cytopathic effect and real-time RT-PCR, which were consistent with each other. In addition to the effective gene expression reduction, an important criterion for the use of siRNAs or their complexes is their low effect on the vital activity of cells as a result of knockdown of one or more target genes.

It was found that siRNA compositions directed simultaneously to the *FLT4*, *Nup98*, and *Nup205* genes did not reduce cell viability below the

**Table 4.** Cell survival after siRNA transfection in %

siRNA complex	1 <sup>st</sup> day	2 <sup>nd</sup> day	3 <sup>rd</sup> day
Complex A	98	76	75
Complex B	97	79	73
Complex C	85	84	86
Complex D	83	78	81
<i>siL2</i> (nonspecific)	98	84	95
K-(nontransfect.)	100	100	100

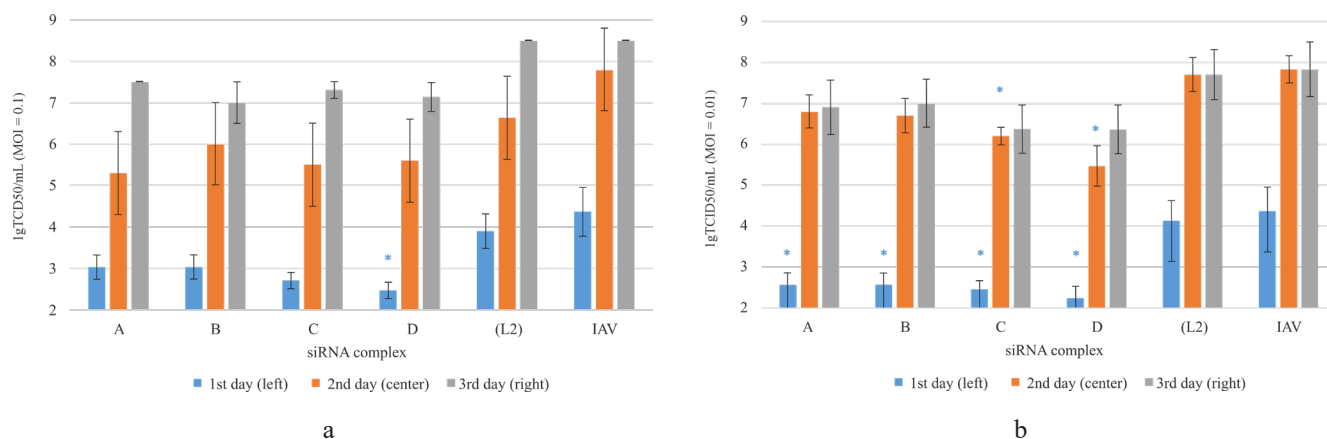


**Fig. 1.** (a) Multiplicity of infection (MOI) = 0.1; (b) MOI = 0.01. Influence of siRNAs complexes (A – *FLT4.2 + Nup98.1*; B – *Nup98.1 + Nup205*; C – *FLT4.2 + Nup205*; D – *FLT4.1 + Nup98.1 + Nup205*) directed to the *FLT4*, *Nup98*, and *Nup205* genes on the reproduction of the influenza virus (on the graph, the data are given in  $\log_{10}$ ).

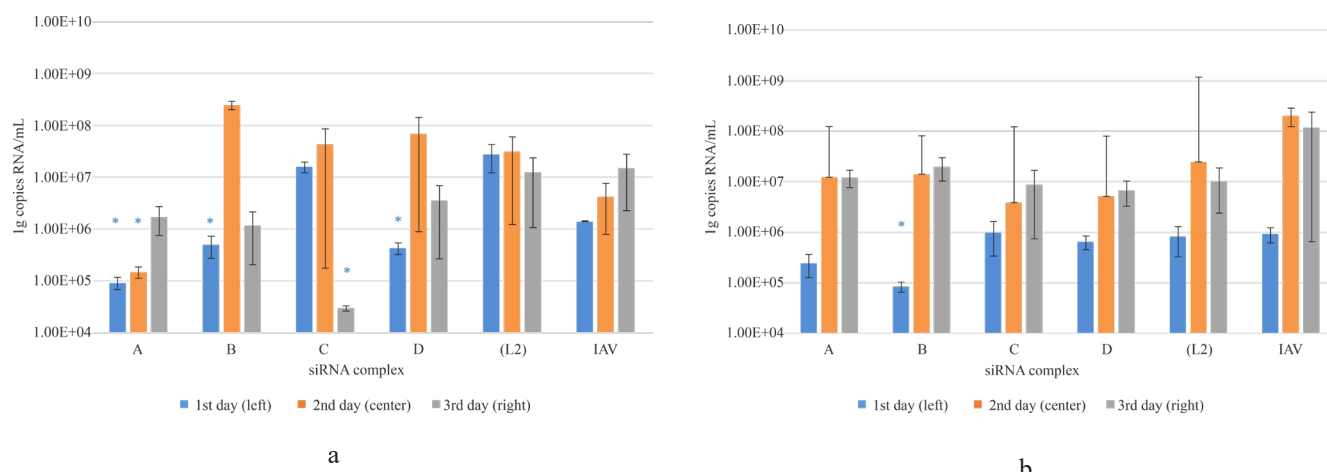


**Fig. 2.** (a) Multiplicity of infection (MOI) = 0.1; (b) MOI = 0.01. The effect of siRNA complexes (A, B, C, and D) on the concentration of vRNA (on the graph, the data are given in  $\log_{10}$ ).

threshold level of 70%, similarly to [28]. When titrating the virus by the cytopathic effect, the following decrease in viral activity was noted. At MOI = 0.1, a significant decrease in viral reproduction by 1.5  $\text{lgTCD}_{50/\text{mL}}$  was noted only when the D complex was used on the first day with respect to nonspecific *siL2* siRNA. The best result was noted at a multiplicity of infection of 0.01. Table 2 shows that at MOI = 0.01, the viral titer in cells treated with the A and B complexes significantly decreased on the first day by 1.5  $\text{lgTCD}_{50/\text{mL}}$  relative to the control ( $p < 0.05$ ). The use of the C and D complexes led to the significant decrease in viral titer by 1.8 and 2.0  $\text{lgTCD}_{50/\text{mL}}$  on the first day and by 1.8 and 2.5  $\text{lgTCD}_{50/\text{mL}}$  on the second day ( $p < 0.05$ ), respectively, compared with controls. According to the results of real-time RT-PCR, there was a decrease in the amount of vRNA in the cells treated with

complexes compared to controls. At MOI = 0.1, the use of the A, B, and D complexes led to a significant decrease in vRNA on the first day compared to *siL2* siRNA by factors of 295, 55, and 63, respectively ( $p < 0.05$ ). On the second day, a similar effect was noted in cells treated with the A complex. When using the B complex, a 415-fold decrease in vRNA was noted on the third day. Table 4 shows that the concentration of vRNA in cells with MOI = 0.01 decreased on the first day by 9.5 times when the B complex was used ( $p < 0.05$ ) compared with the nonspecific control. It should be noted that the accumulation of vRNA is apparently associated with the fact that a partial synthesis of vRNA was carried out, but there was no assembly of the virion. Against this background, the accumulation of vRNA occurred *in vitro*. Similar results were shown in the paper [29].

## CONCLUSIONS

Today, the issue of creating safe and effective drugs for the treatment and prevention of influenza and its complications is of great importance. In the present study, the data were obtained that the simultaneous knockdown of several cellular genes that play important roles in the process of viral endocytosis and nuclear import/export of vRNA using the siRNA complexes significantly and effectively reduced the reproduction of the influenza virus *in vitro*. Effective suppression of viral reproduction was noted when using the siRNA complex directed to all three genes at once. This indicates that the violation of viral reproduction simultaneously at different stages leads to the great effect and, as a result, to a decrease in viral activity. The results obtained make it possible to recommend siRNAs directed to cellular genes for research as potential drugs for emergency prevention and treatment of influenza in an animal model of infection. In parallel, the results obtained contribute to the development of principles for the rapid design and development

of specific and effective antiviral siRNAs that can be used to develop protection means against viruses belonging to different taxonomic groups. This technology should become highly universal and, in the future, can enter the system of rapid response to the emergence of new pathogenic viruses, pandemics, and biological terrorism.

### Acknowledgments

The authors are grateful to the Center for Collective Use of the I.I. Mechnikov Research Institute of Vaccines and Sera. The study was not sponsored.

### Authors' contributions

**E.A. Pashkov, M.O. Korotysheva, A.V. Pak,** and **Zaiceva T.A.** – conducting the experiments;

**E.A. Pashkov, E.P. Bystrikskaya, Yu.E. Dronina,** and **V.K. Solntseva** – writing the text of the article and the analysis of the obtained results;

**E.B. Fayzuloev, A.V. Poddubikov,** and **A.V. Sidorov** – scientific editing;

**E.P. Pashkov, A.S. Bykov, O.A. Svitich,** and **V.V. Zverev** – idea of the study, summary, and general management.

The authors declare no conflicts of interest.

## REFERENCES

- Peteranderl C., Herold S., Schmoldt C. Human Influenza Virus Infections. *Semin. Respir. Crit. Care Med.* 2016;37(4):487–500. <https://doi.org/10.1055/s-0036-1584801>
- Sellers S.A., Hagan R.S., Hayden F.G., Fischer W.A. 2nd. The hidden burden of influenza: A review of the extrapulmonary complications of influenza infection. *Influenza Other Respir. Viruses.* 2017;11(5):372–393. <https://doi.org/10.1111/irv.12470>
- Koehler P., Bassetti M., Kochanek M., Shimabukuro-Vornhagen A., Cornely O.A. Intensive care management of influenza-associated pulmonary aspergillosis. *Clin. Microbiol. Infect.* 2019;25(12):1501–1509. <https://doi.org/10.1016/j.cmi.2019.04.031>
- Radzišauskienė D., Vitkauskaitė M., Žvinytė K., Mameniškienė R. Neurological complications of pandemic A(H1N1)2009pdm, postpandemic A(H1N1)v, and seasonal influenza A. *Brain Behav.* 2021;11(1):e01916. <https://doi.org/10.1002/brb3.1916>
- Kalil A.C., Thomas P.G. Influenza virus-related critical illness: pathophysiology and epidemiology. *Crit. Care.* 2019;23(1):258. <https://doi.org/10.1186/s13054-019-2539-x>
- Webby R.J., Webster R.G. Emergence of influenza A viruses. *Philos. Trans. R. Soc. Lond. B Biol. Sci.* 2001;356(1416):1817–1828. <https://doi.org/10.1098/rstb.2001.0997>
- Kirby B.J., Symonds W.T., Kearney B.P., Mathias A.A. Pharmacokinetic, Pharmacodynamic, and Drug-Interaction Profile of the Hepatitis C Virus NS5B Polymerase Inhibitor Sofosbuvir. *Clin. Pharmacokinet.* 2015;54(7):677–690. <https://doi.org/10.1007/s40262-015-0261-7>
- Gentile I., Buonomo A.R., Borgia G. Dasabuvir: A Non-Nucleoside Inhibitor of NS5B for the Treatment of Hepatitis C Virus Infection. *Rev. Recent Clin. Trials.* 2014;9(2):115–123. <https://doi.org/10.2174/1574887109666140529222602>
- Magro P., Zanella I., Pescarolo M., Castelli F., Quiros-Roldan E. Lopinavir/ritonavir: Repurposing an old drug for HIV infection in COVID-19 treatment. *Biomed. J.* 2021;44(1):43–53. <https://doi.org/10.1016/j.bj.2020.11.005>
- Han J., Perez J., Schafer A., Cheng H., Peet N., Rong L., Manicassamy B. Influenza Virus: Small Molecule Therapeutics and Mechanisms of Antiviral Resistance. *Curr. Med. Chem.* 2018;25(38):5115–5127. <https://doi.org/10.2174/0929867324666170920165926>
- Castle S.C. Clinical relevance of age-related immune dysfunction. *Clin. Infect. Dis.* 2000;31(2):578–585. <https://doi.org/10.1086/313947>
- Looi Q.H., Foo J.B., Lim M.T., Le C.F., Show P.L. How far have we reached in development of effective influenza vaccine? *Int. Rev. Immunol.* 2018;37(5):266–276. <https://doi.org/10.1080/08830185.2018.1500570>
- Pleguezuelos O., James E., Fernandez A., Lopes V., Rosas L.A., Cervantes-Medina A., Cleath J., Edwards K., Neitzey D., Gu W., Hunsberger S., Taubenberger J.K., Stoloff G., Memoli M.J. Efficacy of FLU-v, a broad-spectrum influenza vaccine, in a randomized phase IIb human influenza challenge study. *npj Vaccines.* 2020;5(1):22. <https://doi.org/10.1038/s41541-020-0174-9>
- Wang F., Chen G., Zhao Y. Biomimetic nanoparticles as universal influenza vaccine. *Smart Mater. Med.* 2020;1:21–23. <https://doi.org/10.1016/j.smim.2020.03.001>

15. Smith M. Vaccine safety: medical contraindications, myths, and risk communication. *Pediatr. Rev.* 2015;36(6):227–238. <https://doi.org/10.1542/pir.36.6.227>
16. McManus M.T., Sharp P.A. Gene silencing in mammals by small interfering RNAs. *Nat. Rev. Genet.* 2002;3(10):737–747. <https://doi.org/10.1038/nrg908>
17. Pashkov E.A., Faizuloev E.B., Svitich O.A., Sergeev O.V., Zverev V.V. The potential of synthetic small interfering RNA-based antiviral drugs for influenza treatment. *Voprosy Virusologii = Problems of Virology.* 2020;65(4):182–190 (in Russ.). <https://doi.org/10.36233/0507-4088-2020-65-4-182-190>
18. Adams D., Suhr O.B. Patisiran, an investigational RNAi therapeutic for patients with hereditary transthyretin-mediated (hATTR) amyloidosis: Results from the phase 3 APOLLO study. *Revue Neurologique.* 2018;174(S1):S37. <https://doi.org/10.1016/j.neuro.2018.01.085>
19. Zhao L., Wang X., Zhang X., Liu X., Zhang Y., Zhang S. Therapeutic strategies for acute intermittent porphyria. *Intractable & Rare Diseases Research.* 2020;9(4):205–216. <https://doi.org/10.5582/irdr.2020.03089>
20. Van der Ree M.H., et al. Miravirsin dosing in chronic hepatitis C patients results in decreased microRNA-122 levels without affecting other microRNAs in plasma. *Alimentary Pharmacology & Therapeutics.* 2015;43(1):102–113. <https://doi.org/10.1111/apt.13432>
21. DeVincenzo J., et al. A randomized, double-blind, placebo-controlled study of an RNAi-based therapy directed against respiratory syncytial virus. *Proceedings of the National Academy of Sciences (PNAS).* 2010;107(19):8800–8805. <https://doi.org/10.1073/pnas.0912186107>
22. Qureshi A., Tantray V.G., Kirmani A.R., Ahangar A.G. A review on current status of antiviral siRNA. *Rev. Med. Virol.* 2018;28(4):1976. <https://doi.org/10.1002/rmv.1976>
23. Lesch M., Luckner M., Meyer M., Weege F., Gravenstein I., Raftery M., Sieben C., Martin-Sancho L., Imai-Matsushima A., Welke R.W., Frise R., Barclay W., Schönrich G., Herrmann A., Meyer T.F., Karlas A. RNAi-based small molecule repositioning reveals clinically approved urea-based kinase inhibitors as broadly active antivirals. *PLoS Pathog.* 2019;15(3):e1007601. <https://doi.org/10.1371/journal.ppat.1007601>
24. Pashkov E.A., Faizuloev E.B., Korchevaya E.R., Rtishchev A.A., Cherepovich B.S., Sidorov A.V., Poddubikov A.V., Bystritskaya E.P., Dronina Yu.E., Bykov A.S., Svitich O.A., Zverev V.V. Knockdown of *FLT4*, *Nup98*, and *Nup205* cellular genes as a suppressor for the viral activity of Influenza A/WSN/33 (H1N1) in A549 cell culture. *Tonk. Khim. Tekhnol. = Fine Chem. Technol.* 2021;16(6):476–489 (in Russ.). <https://doi.org/10.32362/2410-6593-2021-16-6-476-489>
25. Pashkov E.A., Korchevaya E.R., Faizuloev E.B., Pashkov E.P., Zvereva T.A., Rtishchev A.A., Poddubikov A.V., Svitich O.A., Zverev V.V. Creation of model for studying the antiviral effect of small interfering RNAs *in vitro*. *Sanitarnyi vrach.* 2022;1 (in Russ.). <https://doi.org/10.33920/med-08-2201-07>
26. Lee H.K., Loh T.P., Lee C.K., Tang J.W., Chiu L., Koay E.S. A universal influenza A and B duplex real-time RT-PCR assay. *J. Med. Virol.* 2012;84(10):1646–1651. <https://doi.org/10.1002/jmv.23375>
27. Ramakrishnan M.A. Determination of 50% endpoint titer using a simple formula. *World J. Virol.* 2016;5(2):85–86. <https://doi.org/10.5501/wjv.v5.i2.85>
28. Estrin M.A., Hussein I.T.M., Puryear W.B., Kuan A.C., Artim S.C., Runstadler J.A. Host-directed combinatorial RNAi improves inhibition of diverse strains of influenza A virus in human respiratory epithelial cells. *PLoS One.* 2018;13(5):e0197246. <https://doi.org/10.1371/journal.pone.0197246>
29. Piasecka J., Lenartowicz E., Soszynska-Jozwiak M., Szutkowska B., Kierzek R., Kierzek E. RNA Secondary Structure Motifs of the Influenza A Virus as Targets for siRNA-Mediated RNA Interference. *Mol. Ther. Nucleic Acids.* 2020;19:627–642. <https://doi.org/10.1016/j.omtn.2019.12.018>

#### About the authors:

**Evgeny A. Pashkov**, Postgraduate Student, Department of Microbiology, Virology and Immunology, I.M. Sechenov First Moscow State Medical University (Sechenov University) (8, Trubetskaya ul., Moscow, 119991, Russia); Junior Researcher, Laboratory of Molecular Immunology, Federal State Budgetary Scientific Institution “I. Mechnikov Research Institute of Vaccines and Sera” (5A, Malyy Kazennyi pereulok, Moscow, 105064, Russia). E-mail: pashckov.j@yandex.ru. <https://orcid.org/0000-0002-5682-4581>

**Maria O. Korotysheva**, Student, International School “Medicine of the Future,” I.M. Sechenov First Moscow State Medical University (Sechenov University) (8, Trubetskaya ul., Moscow, 119991, Russia). E-mail: trans.mutation@mail.ru. <https://orcid.org/0000-0001-7216-1266>

**Anastasia V. Pak**, Student, Institute of Clinical Medicine, I.M. Sechenov First Moscow State Medical University (Sechenov University) (8, Trubetskaya ul., Moscow, 119991, Russia). E-mail: dcnnpk@gmail.com. <https://orcid.org/0000-0003-4295-7858>

**Evgeny B. Faizuloev**, Cand. Sci. (Biol.), Head of the Laboratory of Molecular Virology, Federal State Budgetary Scientific Institution “I. Mechnikov Research Institute of Vaccines and Sera” (5A, Malyy Kazennyi pereulok, Moscow, 105064, Russia). E-mail: faizuloev@mail.ru. <https://orcid.org/0000-0001-7385-5083>

**Alexander V. Sidorov**, Cand. Sci. (Biol.), Head of the Laboratory of DNA viruses, Federal State Budgetary Scientific Institution "I. Mechnikov Research Institute of Vaccines and Sera" (5A, Malyi Kazennyi pereulok, Moscow, 105064, Russia). E-mail: sashasidorov@yandex.ru. <https://orcid.org/0000-0002-3561-8295>

**Alexander A. Poddubikov**, Cand. Sci. (Biol.), Head of the Laboratory of Microbiology of Opportunistic Pathogenic Bacteria, Federal State Budgetary Scientific Institution "I. Mechnikov Research Institute of Vaccines and Sera" (5A, Malyi Kazennyi pereulok, Moscow, 105064, Russia). E-mail: poddubikov@yandex.ru. <https://orcid.org/0000-0001-8962-4765>

**Elizaveta P. Bystritskaya**, Junior Researcher, Laboratory of Molecular Immunology, Federal State Budgetary Scientific Institution "I. Mechnikov Research Institute of Vaccines and Sera" (5A, Malyi Kazennyi pereulok, Moscow, 105064, Russia). E-mail: lisabystritskaya@gmail.com. <https://orcid.org/0000-0001-8430-1975>

**Yuliya E. Dronina**, Cand. Sci. (Med.), Associate Professor, Department of Microbiology, Virology and Immunology, I.M. Sechenov First Moscow State Medical University (Sechenov University) (8, Trubetskaya ul., Moscow, 119991, Russia); Senior Researcher, Laboratory of Legionellosis, N.F. Gamaleya National Research Center for Epidemiology and Microbiology (The Gamaleya National Center) (18, Gamaleya ul., Moscow, 123098, Russia). E-mail: droninayu@mail.ru. <https://orcid.org/0000-0002-6269-2108>

**Viktorii K. Solntseva**, Cand. Sci. (Med.), Senior Lecturer, A.A. Vorobiev Department of Microbiology, Virology and Immunology, I.M. Sechenov First Moscow State Medical University (Sechenov University) (8, Trubetskaya ul., Moscow, 119991, Russia). E-mail: speak\_to\_vika@mail.ru. <https://orcid.org/0000-0003-3783-9232>

**Tatyana A. Zaiceva**, Cand. Sci. (Med.), Senior Lecturer, A.A. Vorobiev Department of Microbiology, Virology and Immunology, I.M. Sechenov First Moscow State Medical University (Sechenov University) (8, Trubetskaya ul., Moscow, 119991, Russia). E-mail: zat25@yandex.ru. <https://orcid.org/0000-0001-9205-322X>

**Evgeny P. Pashkov**, Dr. Sci. (Med.), Professor, A.A. Vorobiev Department of Microbiology, Virology and Immunology, I.M. Sechenov First Moscow State Medical University (Sechenov University) (8, Trubetskaya ul., Moscow, 119991, Russia). E-mail: 9153183256@mail.ru. <https://orcid.org/0000-0002-4963-5053>

**Anatoly S. Bykov**, Dr. Sci. (Med.), Professor, Department of Virology and Immunology, I.M. Sechenov First Moscow State Medical University (Sechenov University) (8, Trubetskaya ul., Moscow, 119991, Russia). E-mail: bykov@mail.ru. <https://orcid.org/0000-0002-8099-6201>

**Oxana A. Svitich**, Corresponding Member of the Russian Academy of Sciences, Dr. Sci. (Med.), Head of the Federal State Budgetary Scientific Institution "I. Mechnikov Research Institute of Vaccines and Sera," Head of the Laboratory of Molecular Immunology, Federal State Budgetary Scientific Institution "I. Mechnikov Research Institute of Vaccines and Sera" (5A, Malyi Kazennyi pereulok, Moscow, 105064, Russia); Professor, Department of Microbiology, Virology and Immunology, I.M. Sechenov First Moscow State Medical University (Sechenov University) (8, Trubetskaya ul., Moscow, 119991, Russia). E-mail: svitichoa@yandex.ru. <https://orcid.org/0000-0003-1757-8389>

**Vitaliy V. Zverev**, Full Member of the Russian Academy of Sciences, Dr. Sci. (Biol.), Scientific Director of the Federal State Budgetary Scientific Institution "I. Mechnikov Research Institute of Vaccines and Sera" (5A, Malyi Kazennyi pereulok, Moscow, 105064, Russia); Head of the Department of Microbiology, Virology and Immunology, I.M. Sechenov First Moscow State Medical University (Sechenov University) (8, Trubetskaya ul., Moscow, 119991, Russia). E-mail: vitalyzverev@outlook.com. <https://orcid.org/0000-0002-0017-1892>

#### Об авторах:

**Пашков Евгений Алексеевич**, аспирант, кафедра микробиологии, вирусологии и иммунологии, Первый Московский государственный медицинский университет им. И.М. Сеченова Минздрава России (Сеченовский Университет), (119991, Россия, Москва, ул. Трубецкая, д. 8, с. 2); младший научный сотрудник, лаборатория молекулярной иммунологии, Научно-исследовательский институт вакцин и сывороток им. И.И. Мечникова (105064, Россия, Москва, Малый Казенный переулок, д. 5А). E-mail: pashkov.j@yandex.ru. <https://orcid.org/0000-0002-5682-4581>

**Коротышева Мария Олеговна**, студент, Международная школа «Медицина Будущего», Первый Московский государственный медицинский университет им. И.М. Сеченова Минздрава России (Сеченовский Университет) (119991, Россия, Москва, ул. Трубецкая, д. 8, с. 2). E-mail: trans.mutation@mail.ru. <https://orcid.org/0000-0001-7216-1266>

**Пак Анастасия Витальевна**, студент, Институт клинической медицины им. Н.В. Склифосовского, Первый Московский государственный медицинский университет им. И.М. Сеченова Минздрава России (Сеченовский Университет) (119991, Россия, Москва, ул. Трубецкая, д. 8, с. 2). E-mail: dcnpk@gmail.com. <https://orcid.org/0000-0003-4295-7858>

**Файзулов Евгений Бахтиёрович**, к.б.н., заведующий лабораторией молекулярной вирусологии, Научно-исследовательский институт вакцин и сывороток им. И.И. Мечникова (105064, Россия, Москва, Малый Казенный переулок, д. 5А). E-mail: faizulov@mail.ru. <https://orcid.org/0000-0001-7385-5083>

**Сидоров Александр Викторович**, к.б.н., заведующий лабораторией ДНК-содержащих вирусов, Научно-исследовательский институт вакцин и сывороток им. И.И. Мечникова (105064, Россия, Москва, Малый Казенный переулок, д. 5А). E-mail: sashasidorov@yandex.ru. <https://orcid.org/0000-0002-3561-8295>

**Поддубиков Александр Владимирович**, к.б.н., заведующий лабораторией микробиологии условно-патогенных бактерий, Научно-исследовательский институт вакцин и сывороток им. И.И. Мечникова (105064, Россия, Москва, Малый Казенный переулок, д. 5А). E-mail: poddubikov@yandex.ru. <https://orcid.org/0000-0001-8962-4765>

**Быстрицкая Елизавета Петровна**, младший научный сотрудник, лаборатория молекулярной вирусологии, Научно-исследовательский институт вакцин и сывороток им. И.И. Мечникова (105064, Россия, Москва, Малый Казенный переулок, д. 5А). E-mail: lisabystritskaya@gmail.com. <https://orcid.org/0000-0001-8430-1975>

**Дронина Юлия Евгеньевна**, к.м.н., доцент кафедры микробиологии, вирусологии и иммунологии, Первый Московский государственный медицинский университет им. И.М. Сеченова Минздрава России (Сеченовский Университет), (119991, Россия, Москва, ул. Трубецкая, д. 8, с. 2); старший научный сотрудник, лаборатория легионеллеза, Национальный исследовательский центр эпидемиологии и микробиологии им. почетного академика Н.Ф. Гамалеи (123098, Россия, Москва, ул. Гамалеи, д. 18). E-mail: droninayu@mail.ru. <https://orcid.org/0000-0002-6269-2108>

**Солнцева Виктория Константиновна**, к.м.н., старший преподаватель кафедры микробиологии, вирусологии и иммунологии им. академика А.А. Воробьева, Первый Московский государственный медицинский университет им. И.М. Сеченова Минздрава России (Сеченовский Университет) (119991, Россия, Москва, ул. Трубецкая, д. 8, с. 2). E-mail: speak\_to\_vika@mail.ru. <https://orcid.org/0000-0003-3783-9232>

**Зайцева Татьяна Александровна**, к.м.н., старший преподаватель кафедры микробиологии, вирусологии и иммунологии им. академика А.А. Воробьева, Первый Московский государственный медицинский университет им. И.М. Сеченова Минздрава России (Сеченовский Университет) (119991, Россия, Москва, ул. Трубецкая, д. 8, с. 2). E-mail: zat25@yandex.ru. <https://orcid.org/0000-0001-9205-322X>

**Пашков Евгений Петрович**, д.м.н., профессор кафедры микробиологии, вирусологии и иммунологии им. академика А.А. Воробьева, Первый Московский государственный медицинский университет им. И.М. Сеченова Минздрава России (Сеченовский Университет) (119991, Россия, Москва, ул. Трубецкая, д. 8, с. 2). E-mail: 9153183256@mail.ru. <https://orcid.org/0000-0002-4963-5053>

**Быков Анатолий Сергеевич**, д.м.н., профессор кафедры микробиологии, вирусологии и иммунологии, Первый Московский государственный медицинский университет им. И.М. Сеченова Минздрава России (Сеченовский Университет), (119991, Россия, Москва, ул. Трубецкая, д. 8, с. 2). E-mail: bykov@mail.ru. <https://orcid.org/0000-0002-8099-6201>

**Свитич Оксана Анатольевна**, чл.-корр. РАН, д.м.н., директор, заведующий лабораторией молекулярной иммунологии, Научно-исследовательский институт вакцин и сывороток им. И.И. Мечникова (105064, Россия, Москва, Малый Казенный переулок, д. 5А); профессор кафедры микробиологии, вирусологии и иммунологии, Первый Московский государственный медицинский университет им. И.М. Сеченова Минздрава России (Сеченовский Университет), (119991, Россия, Москва, ул. Трубецкая, д. 8, с. 2). E-mail: svitichoa@yandex.ru. <https://orcid.org/0000-0003-1757-8389>

**Зверев Виталий Васильевич**, академик РАН, д.б.н., научный руководитель Научно-исследовательского института вакцин и сывороток им. И.И. Мечникова (105064, Россия, Москва, Малый Казенный переулок, д. 5А); заведующий кафедрой микробиологии, вирусологии и иммунологии, Первый Московский государственный медицинский университет им. И.М. Сеченова Минздрава России (Сеченовский Университет), (119991, Россия, Москва, ул. Трубецкая, д. 8, с. 2). E-mail: vitalyzverev@outlook.com. <https://orcid.org/0000-0002-0017-1892>

*The article was submitted: March 15, 2022; approved after reviewing: March 30, 2022; accepted for publication: April 20, 2022.*

*Translated from Russian into English by H. Moshkov.*

*Edited for English language and spelling by Quinton Scribner, Awatera.*

---

**SYNTHESIS AND PROCESSING OF POLYMERS  
AND POLYMERIC COMPOSITES**

---

**СИНТЕЗ И ПЕРЕРАБОТКА ПОЛИМЕРОВ  
И КОМПОЗИТОВ НА ИХ ОСНОВЕ**

---

ISSN 2686-7575 (Online)

<https://doi.org/10.32362/2410-6593-2022-17-2-152-163>

UDC 532.696:678.07.074



RESEARCH ARTICLE

## **Influence of various factors on surface properties of elastomeric materials based on nitrile butadiene rubbers**

**Olga A. Dulina**✉, **Evgeniya V. Eskova**, **Alina D. Tarasenko**, **Svetlana V. Kotova**

MIREA – Russian Technological University (M.V. Lomonosov Institute of Fine Chemical Technologies), Moscow, 119571 Russia

✉ Corresponding author, e-mail: [doa1503991@yandex.ru](mailto:doa1503991@yandex.ru)

### **Abstract**

**Objectives.** The influence of the technological additive content and accelerated aging conditions on the surface energy and elastic-strength properties of nitrile butadiene rubbers with an average acrylic acid nitrile content and rubbers based on them were studied in the paper.

**Methods.** The free surface energy of the samples was determined under the standard conditions and in the accelerated aging conditions with the use of the Owens, Wendt, Rabel, and Kaelble method.

**Results.** It was shown that the elastomeric materials surface energy is influenced by surfactants such as rosin and stearic acid, which are typical ingredients of rubber compounds. It was also found that the thermal aging effect on the physical and mechanical properties of rubbers based on nitrile butadiene rubbers depends on the method of rubber isolation from latex and on the nature of the surfactant components in the samples.

**Conclusions.** The analysis of the results obtained shows that the change in the vulcanizates physical and mechanical properties, depending on the technological additive content and the temperature effect, occurs along with a change in the critical surface tension.

**Keywords:** nitrile butadiene rubber, free surface energy, surface tension, surfactant, surface properties, physical and mechanical properties of polymers, thermal aging

**For citation:** Dulina O.A., Eskova E.V., Tarasenko A.D., Kotova S.V. Influence of various factors on surface properties of elastomeric materials based on nitrile butadiene rubbers. *Tonk. Khim. Tekhnol. = Fine Chem. Technol.* 2022;17(2):152–163 (Russ., Eng.). <https://doi.org/10.32362/2410-6593-2022-17-2-152-163>

## НАУЧНАЯ СТАТЬЯ

# Влияние различных факторов на поверхностные свойства эластомерных материалов на основе бутадиен-нитрильных каучуков

О.А. Дулина<sup>✉</sup>, Е.В. Еськова, А.Д. Тарасенко, С.В. Котова

МИРЭА – Российский технологический университет (Институт тонких химических технологий им. М.В. Ломоносова), Москва, 119571 Россия

<sup>✉</sup> Автор для переписки, e-mail: [doa1503991@yandex.ru](mailto:doa1503991@yandex.ru)

### Аннотация

**Цели.** Изучение влияния содержания технологических добавок и условий ускоренного старения на поверхностную энергию, упруго-прочностные и адгезионные характеристики резин на основе бутадиен-нитрильных каучуков со средним содержанием нитрила акриловой кислоты.

**Методы.** С помощью метода Оуэнса–Вендта–Рабеля–Каелбле была определена свободная поверхностная энергия образцов в стандартных условиях и условиях ускоренного старения.

**Результаты.** Было показано, что на поверхностную энергию эластомерных материалов оказывают влияние поверхностно-активные вещества, такие как канифоль и стеариновая кислота, являющиеся типичными ингредиентами резиновых смесей, а также было установлено, что влияние условий ускоренного старения на физико-механические свойства резин на основе бутадиен-нитрильных каучуков зависит от способа выделения каучука из латекса и природы поверхностно-активных компонентов, входящих в состав образцов. Предполагается, что это происходит за счет миграции на поверхность образцов низкомолекулярных компонентов и поверхностно-активных веществ.

**Выводы.** Анализ полученных результатов показывает, что изменение физико-механических свойств вулканизатов в зависимости от содержания технологической добавки и воздействия температуры происходит наряду с изменением критического поверхностного натяжения.

**Ключевые слова:** бутадиен-нитрильный каучук, свободная поверхностная энергия, поверхностное натяжение, поверхностно-активное вещество, поверхностные свойства, физико-механические свойства полимеров, термостарение

**Для цитирования:** Дулина О.А., Еськова Е.В., Тарасенко А.Д., Котова С.В. Влияние различных факторов на поверхностные свойства эластомерных материалов на основе бутадиен-нитрильных каучуков. *Тонкие химические технологии.* 2022;17(2):152–163. <https://doi.org/10.32362/2410-6593-2022-17-2-152-163>

## INTRODUCTION

Nitrile-butadiene rubbers (NBR) are widely used in the production of rubber products operating, inter alia, in aggressive environments and at the elevated temperatures. They are used in almost all industries [1].

Rubber is the multicomponent composite material with a multiphase structure, in which the polymer is in a highly elastic state with high segmental mobility. Therefore, the surface properties of rubber-based products are determined by the nature of polymers, the conditions for their preparation and surface formation, as well as by the composition of the polymer material containing a considerable amount of powdered dispersed fillers and various low molecular weight additives that can migrate into the surface layers and affect the surface free energy (SFE) [1–3]. All this, together with aggressive factors that have a significant impact on the state of product material and of its surface, entails a change in the surface properties and, as a result, in the product operational characteristics.

In connection with the foregoing, it is advisable to find a way of assessing the state of the surface subjected to aggressive action in order to identify changes in its properties during operation.

In the works of Tarasenko and Dulina [4, 5], the effect of low molecular weight rubber compound additives on the surface properties was studied. It was found that the elastomer compositions surface properties significantly depend on the rubber compound ingredients solubility and on their adsorption properties. It was found that the effect of surfactants on the surface energy of rubber compounds is different and depends on their nature. Sulfur, as a partially soluble component, does not affect the samples surface energy in small amounts, and if it is present in the system in amounts greater than the solubility limit, it significantly reduces the SFE.

The aim of this work was to study the stearic acid and rosin content effect on the surface energy and elastic-strength properties of rubber samples based on NBRs, with an average content of acrylic acid nitrile, among other things, under the accelerated aging conditions of rubbers.

## EXPERIMENTAL

The objects of study were NBR samples with an average acrylic acid nitrile content. The samples were obtained by two different methods of isolation from latex [6]. Besides, rubbers based on them were studied.

SKN-26 SM rubber (*Voronezh branch of Scientific-Research Institute of Synthetic Rubber, Voronezh, Russia*) was obtained using an alkyl sulfonate emulsifier. The latter is almost completely washed out in the process of isolation from the latex. BNKS-28 AMN rubber (*Krasnoyarsk Synthetic Rubber plant, SIBUR Holding, Krasnoyarsk, Russia*) was obtained using fatty acids, followed by neutralization at the phase boundary to obtain the emulsifier—the potassium or sodium salt of the fatty acid. The rubber was isolated from the latex with the calcium or magnesium chloride solution. As a result, the emulsifier and coagulator interaction products remained in the polymer—slightly soluble salts of fatty acids.

Rubber samples were obtained using the following formulation: for 100 mass fractions of the unvulcanized rubber, zinc oxide (*Empils-Zink, Rostov-on-Don, Russia*)—5 mass fractions, sulfur (*Rosneft, Moscow, Russia*)—2 mass fractions, carbon black P-514 (*Omsktekhuglerod, Omsk, Russia*)—50 mass fractions, and accelerator CBS (*VitaHim, Dzerzhinsk, Russia*)—1.2 mass fractions. The vulcanization time corresponded to the optimum vulcanization for this type of rubber compound.

To determine the critical surface tension, which is a criterion for estimating the SFE of rubber samples, the Owens, Wendt, Rabel, and Kaelble (OWRK) method was chosen. It is based on determining the contact angles of material surface wetting by liquids with different surface tension [7–9]. The OWRK method is more preferable, because the Zisman method, which is widely used to assess the surface state, does not take into account the surface energy polar component contribution. Studies [10] have shown that the surface energy values obtained by the Zisman method practically reproduce the SFE dispersion component values calculated by the OWRK method.

The obtained contact angles values are used to calculate the SFE using a mathematical model, according to which the SFE is the sum of the dispersion and polar components [11–14].

For determining the SFE, unvulcanized rubber samples were obtained by pressing between fluoroplast films. Rubber samples were pressed plates.

Since this work considers the SFE as the comparative characteristic for the series of samples under study, standard requirements were imposed on wetting liquids: physicochemical characteristics stability during storage and high surface tension and its dispersion and polar components values. These values should provide sufficiently large and reliably measured contact angles. As a result, water

and nonvolatile alcohols—propylene glycol, ethylene glycol, and glycerin—were chosen as wetting liquids.

The contact angles were determined by the sessile drop method using an LK-1 goniometer (*OpenScience*, Russia). The device makes it possible to obtain an image of a drop lying on a substrate using a digital video camera, export the image to a computer, and determine the contact angle by the tangent method.

The elastomeric material surface was cleaned with an inert solvent, ethanol. After that, a drop was applied to the cleaned surface of the sample using a microsyringe. The contact angles were measured after an hour of rest of the samples. This was necessary for the formation of an equilibrium surface layer after surface treatment with the cleaning solvent [15].

The main physical and mechanical properties of the studied rubbers were determined in accordance with the current state standards (GOST 263-75<sup>1</sup>, GOST 27110-86<sup>2</sup>, GOST 270-75<sup>3</sup>, GOST 262-93<sup>4</sup>, GOST 6768-75<sup>5</sup>).

## RESULTS AND DISCUSSION

In order to study the influence on the NBRs surface properties of non-rubber components, the content and nature of which is determined by the rubber obtaining method, the critical surface tension was determined by the OWRK method. The results presented in Table 1 indicate that the rubbers production characteristics affect their surface properties.

**Table 1.** Surface properties of nitrile butadiene rubbers obtained by different methods of isolation from latex

Rubber brand	SFE*, mJ/m <sup>2</sup>
SKN-26 SM	28
BNKS-28 AMN	22.4

\*Surface free energy determined by the OWRK method.

SKN-26 SM rubber obtained with the use of an alkyl sulfonate emulsifier, which is almost completely washed out in the process of isolation from the latex, has a more polar surface. BNKS-28 AMN rubber has a lower SFE. This rubber contains a residual emulsifier—sparingly soluble salts of fatty acids capable of migrating to the surface and reducing the samples surface tension.

The critical surface tension of samples obtained based on unvulcanized rubbers was determined at certain time intervals (0, 1, 3, and 24 h) after cleaning the surface. As can be seen from Table 2, the dependence obtained for the unvulcanized rubbers is also preserved for the rubber samples based on them. The surfaces of the rubber samples based on “pure” SKN-26 SM unvulcanized rubber have higher polarity. An increase in the time elapsed after surface cleaning slightly decreases the critical surface tension of all the types of samples. This is explained by the system tendency to a minimum of SFE, mainly due to the release of its lowering components to the surface.

Similar studies were carried out for rubber samples, in which the content of anionic surfactants—stearic acid and rosin—was varied (Table 2).

An analysis of the presented results makes it possible to conclude that in case of rubber based on “pure” SKN-26 SM unvulcanized rubber, an increase in the stearic acid and rosin content decreases the SFE, probably, due to surfactant migration to the samples surface, and the stearic acid effect being more significant.

In case of rubbers based on BNKS-28 AMN, the introduction of surfactants also decreases the SFE, but a greater effect is manifested upon the introduction of rosin. It is possible that resin acids that are part of rosin interact with divalent metal salts remaining in the system after coagulation, thus forming divalent metals salts of the resin acids with more pronounced surface-active properties.

In all the cases, these tendencies in the corresponding samples are preserved for 24 h after the moment of purification. However, the effect from the introduced surfactants becomes less significant.

To expand the understanding of the stearic acid and rosin role in the NBR-based elastomeric

<sup>1</sup> GOST 263-75. USSR State Standard. Rubber. Method for determination of Shore A hardness. Moscow: Izd. Standartov; 1989 (in Russ.).

<sup>2</sup> GOST 27110-86. USSR State Standard. Rubber. Method for determination of rebound elasticity on the Shob type machine. Moscow: Izd. Standartov; 1987 (in Russ.).

<sup>3</sup> GOST 270-75. Interstate Standard. Rubber. Method of the determination elastic and tensile stress-strain properties. Moscow: Standartinform; 2008 (in Russ.).

<sup>4</sup> GOST 262-93. Interstate Standard. Rubber, vulcanized. Determination of tear strength (trouser, angle and crescent test pieces). Moscow: IPK Izd. Standartov; 2002 (in Russ.).

<sup>5</sup> GOST 6768-75. USSR State Standard. Rubber and rubberized fabric. Method for determination of bond strength at ply separation. Moscow: Izd. Standartov; 1998 (in Russ.).

**Table 2.** Surface free energy of rubber samples based on nitrile butadiene rubber containing surfactants in accelerated aging conditions

Samples composition	SFE,* mJ/m <sup>2</sup>				Temperature duration, h
	Time after surface cleaning, h				
	0	1	3	24	
SKN-26 SM	38.4	37.0	36.3	34.8	0
	34.3	31.1	30.5	30.0	6
	36.7	34.0	33.8	33.3	12
	43.4	41.5	40.9	40.1	18
SKN-26 SM + 1 mass fract. of rosin	33.8	31.1	30.8	28.2	0
	36.5	35.8	34.1	33.4	6
	34.6	31.7	30.8	27.3	12
	38.6	33.7	32.1	29.6	18
SKN-26 SM + 2 mass fract. of rosin	32.3	29.9	29.1	28.3	0
	31.1	28.8	27.3	27.1	6
	32.3	27.2	26.8	26.6	12
	31.8	25.3	24.6	23.2	18
SKN-26 SM + 1 mass fract. of stearic acid	31.3	30.5	28.2	25.1	0
	29.5	27.6	25.6	23.1	6
	29.2	26.3	25.2	23.3	12
	27.4	25.8	24.7	22.9	18
SKN-26 SM + 2 mass fract. of stearic acid	27.3	26.2	24.7	21.4	0
	22.1	21.9	21.0	18.0	6
	20.4	20.6	20.1	17.2	12
	21.1	19.5	19.1	17.0	18
BNKS-28 AMN	34.4	33.9	32.4	30.2	0
	28.5	25.1	24.8	23.5	6
	34.7	34.1	32.8	30.4	12
	34.5	34.2	32.4	29.9	18
BNKS-28 AMN + 1 mass fract. of rosin	30.2	29.3	28.5	26.9	0
	32.0	31.2	29.8	27.6	6
	35.6	34.0	32.4	29.4	12
	36.8	35.1	33.3	32.1	18

Table 2. Continued

Samples composition	SFE,* mJ/m <sup>2</sup>				Temperature duration, h
	Time after surface cleaning, h				
	0	1	3	24	
BNKS-28 AMN + 2 mass fract. of rosin	31.9	30.2	27.8	24.4	0
	32.4	31.5	30.9	30.5	6
	34.8	33.2	31.6	29.7	12
	40.9	40.3	39.4	38.4	18
BNKS-28 AMN + 1 mass fract. of stearic acid	31.8	31.0	30.6	30.4	0
	25.5	25.0	24.5	23.9	6
	29.8	29.7	29.5	28.0	12
	28.1	27.6	25.9	24.6	18
BNKS-28 AMN + 2 mass fract. of stearic acid	31.5	31.3	30.8	29.4	0
	25.0	24.6	23.9	23.5	6
	31.5	30.9	30.2	29.6	12
	30.3	28.6	27.1	24.4	18

\*Surface free energy determined by the OWRK method.

materials properties formation, we studied the accelerated aging conditions effect on the surface energy of NBR-based rubber samples without surfactants and containing 1 or 2 mass fractions of rosin or stearic acid. The samples were subjected to accelerated aging<sup>6</sup> at 100°C for 6, 12, and 18 h (Table 2).

In case of all the rubber samples, the dependence of the critical surface tension is nonlinear and passes through an extremum. This trend is basically preserved 24 h after cleaning the surface.

An analysis of the critical surface tension dependence on the thermal aging time for rubber samples based on SKN-26 SM indicates that in case of samples containing surfactants (rosin or stearic acid), the increase of the thermal aging time slightly decreases the SFE, while for a sample without a surfactant, SFE grows.

<sup>6</sup> GOST ISO 188-2013. Interstate Standard. Vulcanized rubber and thermoplastics. Accelerated ageing and heat resistance tests. Moscow: Standartinform; 2014 (in Russ.).

For rubber samples based on BNKS-28 AMN, the effect of thermal aging on surface properties is the least pronounced in most cases.

These results can be explained by the complex physicochemical processes occurring in the elastomeric material under the action of elevated temperature. Under such conditions, oxidation actively takes place. It is accompanied by the formation of polar groups, free radicals, and intermediate products, in particular, oxidation inhibitors. When heated, rubbers can form substances incompatible with unvulcanized rubber, and these substances can migrate to the surface. The complex of changes occurring in the polymer upon heating results in the change in the structure of the polymer matrix and significantly affects the surface properties. Just like for samples not exposed to temperature, the critical surface tension decreases as a result of the system tendency to the equilibrium state as the time elapsed after cleaning increases.

The above research results show that NBRs differing in the methods of production and in the technological additives content have various

surface properties. So, it was logical to assume that the factors affecting the surface properties also affect the physical and mechanical properties of vulcanizates.

As the analysis of the literature data [6, 7, 11, 17] shows, the emulsifier–coagulating agent systems used in the NBR synthesis affect the complex of rubber compounds and rubbers properties. In this work, a comparative assessment for the effect of rosin and stearic acid content on the physicomechanical, technical, and adhesive properties of elastomeric materials was carried out. Tables 3 and 4 present test results for vulcanizates based on two NBR grades: BNKS-28 AMN and SKN-26 SM. They have similar molecular weights and differ in the concentration of nonrubber impurities remaining in the rubbers commercially produced by emulsion polymerization. Considering that NBR-based rubbers are recommended for rubber products operating at elevated temperatures, vulcanizates subjected to the procedure of accelerated thermal-oxidative aging were studied (Table 4). In addition, the accelerated aging conditions have a significant effect on the polymer material structure, as a result of which both its surface and bulk properties change.

The data presented in Table 3 indicate that as the content of rosin and stearic acid increases to

2 mass fractions (per 100 mass fractions of rubber), the strength indicators level comparable to the base composition is preserved. In case of vulcanizates based on BNKS-28 AMN, an increase in their concentration resulted in the most significant changes in terms of relative and residual elongation and tear resistance; in case of rubbers based on SKN-26 SM—in terms of relative elongation. This is consistent with the data of [16]. An analysis of the indicators of vulcanizates subjected to the accelerated aging procedure demonstrates the preservation of the trends in changes in the elastic-strength properties identified for the original rubbers upon the introduction of rosin and stearic acid. At the same time, after aging, an increase in the relative tensile strength and hardness of the vulcanizates is observed. In this case, the relative and permanent elongation, elasticity and tear resistance decrease, which indicates the predominance of structuring processes in elastomeric materials under the action of elevated temperatures in the air.

The adhesive properties of rubbers were evaluated by the adhesive joints delamination method, in which the substrates—vulcanizates based on BNKS-28 AMN and SKN-26 SM—were glued together using a cold curing adhesive composition based on chloroprene rubber. According to the data obtained (Table 3),

**Table 3.** Influence of the kind and content of technological additives on the physical, mechanical, and operational characteristics of rubbers based on nitrile butadiene rubber

Indicators	Additives content				
	Without additives	Rosin		Stearic acid	
		1	2	1	2
<b>BNKS-28 AMN</b>					
Tensile strength, MPa	19.2 ± 2.1	18.3 ± 2.1	18.9 ± 1.9	18.6 ± 1.6	18.1 ± 1.8
Elongation at break, %	335 ± 30	345 ± 30	410 ± 38	315 ± 25	310 ± 24
Residual elongation, %	8.0 ± 0.9	9.0 ± 1.0	14.0 ± 1.5	9.0 ± 0.8	12.0 ± 1.1
Tear resistance, kN/m	23.0 ± 2.2	28.0 ± 2.9	30.0 ± 3.1	31.0 ± 2.7	24.0 ± 2.4
Rebound elasticity, %	19.0 ± 2.0	20.0 ± 2.0	21.0 ± 2.2	19.0 ± 1.8	19.0 ± 1.8
Shore hardness, A	62.0 ± 5.0	59.0 ± 5.0	60.0 ± 5.2	61.0 ± 5.1	60.0 ± 5.0
Adhesion strength, kN/m	2.0 ± 0.22	2.5 ± 0.23	2.8 ± 0.25	1.8 ± 0.16	1.7 ± 0.20

Table 3. Continued

Indicators	Additives content				
	Without additives	Rosin		Stearic acid	
		1	2	1	2
<b>SKN-26 SM</b>					
Tensile strength, MPa	19.4 ± 2.4	19.4 ± 2.4	20.0 ± 2.7	18.9 ± 2.7	18.7 ± 2.7
Elongation at break, %	300 ± 28	340 ± 33	380 ± 36	275 ± 25	285 ± 21
Residual elongation, %	8.0 ± 0.9	8.0 ± 1.0	8.0 ± 1.1	8.0 ± 0.7	8.0 ± 0.7
Tear resistance, kN/m	25.0 ± 2.8	23.0 ± 2.8	24.0 ± 2.9	23.0 ± 3.2	23.0 ± 3.0
Rebound elasticity, %	15.0 ± 1.4	14.0 ± 1.4	14.0 ± 1.4	17.0 ± 2.0	16.0 ± 1.8
Shore hardness, A	63.0 ± 4.4	62 ± 5.0	61.0 ± 5.1	62 ± 5.0	64 ± 5.8
Adhesion strength, kN/m	2.5 ± 0.20	3.2 ± 0.26	3.1 ± 0.29	2.2 ± 0.20	2.2 ± 0.21

Table 4. Influence of the kind and content of technological additives on the physical, mechanical and operational characteristics of rubbers based on nitrile butadiene rubber subjected to accelerated aging

Indicators	Additives content				
	Without additive	Rosin		Stearic acid	
		1	2	1	2
<b>BNKS-28 AMN</b>					
Tensile strength, MPa	21.1 ± 2.0	18.9 ± 1.8	19.5 ± 1.9	20.7 ± 1.9	20.1 ± 2.0
Elongation at break, %	320 ± 33	330 ± 33	390 ± 38	300 ± 31	290 ± 30
Residual elongation, %	7.0 ± 0.7	8.0 ± 0.8	12.0 ± 1.3	8.0 ± 0.7	10.0 ± 0.9
Tear resistance, MPa	21.0 ± 2.2	25.0 ± 2.7	27.0 ± 2.8	28.0 ± 2.6	22.0 ± 2.0
Rebound elasticity, %	17.0 ± 1.7	18.0 ± 1.9	19.0 ± 1.9	17.0 ± 1.7	18.0 ± 1.7
Shore hardness, A	64.0 ± 6.5	60.0 ± 6.2	61.0 ± 6.2	64.0 ± 6.3	63.0 ± 6.0

Table 4. Continued

Indicators	Additives content				
	Without additive	Rosin		Stearic acid	
		1	2	1	2
<b>SKN-26 SM</b>					
Tensile strength, MPa	21.8 ± 1.7	20.0 ± 1.9	20.6 ± 1.9	21.0 ± 1.9	20.8 ± 1.8
Relative extension, %	290 ± 23	320 ± 29	360 ± 31	260 ± 23	270 ± 25
Elongation at break, %	7.0 ± 0.6	8.0 ± 0.7	8.0 ± 0.7	7.0 ± 0.6	7.0 ± 0.6
Tear resistance, MPa	24.0 ± 1.9	21.0 ± 1.9	22.0 ± 2.0	21.0 ± 1.5	21.0 ± 1.6
Rebound elasticity, %	14.0 ± 1.1	13.0 ± 1.1	13.0 ± 1.2	16.0 ± 1.5	15.0 ± 1.3
Shore hardness, A	66.0 ± 5.3	63.0 ± 5.5	62.0 ± 5.4	65.0 ± 4.8	67.0 ± 4.9

vulcanizates based on paraffin rubber demonstrated a lower level of adhesive properties in the entire range of rosin and stearic acid content. The positive effect of rosin on the delamination resistance index of samples of adhesive joints was predictable, given the ability of rosin to increase the elastomeric materials adhesiveness and gummosity [2]. At the same time, the introduction of stearic acid deteriorated a little the adhesive properties of the studied rubbers. The noted regularities in the change in adhesive strength upon increasing the concentration of technological additives and depending on the grade of NBR used in the elastomeric substrates can be explained by the migration of these components to the rubber surface and by the effects of intermolecular interaction of the nitrile groups of rubber with molecules of the introduced acid and fatty acid salts already contained in NBR. This decreases the share of “free” nitrile groups and the polarity of the substrate surface (Table 1), and, consequentially, this decreases the intensity of physicochemical interactions at the polychloroprene–NBR rubber interface of the adhesive film.

Traditionally, higher carboxylic acids and their derivatives having a biphilic nature are used in the composition of elastomeric compositions as ingredients of polyfunctional action. Fatty acids and their salts acting as dispersants and mollifiers/plasticizers improve the compositions

processability and the distribution quality of rubber compound ingredients, positively affecting the vulcanizates properties complex [2]. Being activators of diene rubbers vulcanization with sulfur-containing vulcanizing systems, they affect the vulcanization kinetics and the vulcanization network structure, and they have a significant effect on the complex of technical properties of rubbers [2, 3, 5]. However, it is known [17] that the activators action mechanisms of the sulfur-containing vulcanizing system in NBRs fundamentally differ from those known for unsaturated nonpolar rubbers. Analysis of the data (Tables 3 and 4) indicates a significant role of nonrubber impurities—fatty acid salts in NBRs—in the formation of a set of properties of elastomeric materials. This role is determined by the conditions of their industrial synthesis. This analysis requires additional deeper study using modern physicochemical research methods.

## CONCLUSIONS

The method for evaluating the surface properties of elastomeric materials based on NBRs makes it possible to purposefully control the strength and adhesion properties of vulcanizates, their resistance to aging by introducing technologically active additives. Comparison of the obtained results showed that the change in the physical and

mechanical properties of vulcanizates, depending on the content of technological additives and the effect of temperature, is accompanied by a change in the critical surface tension. This, as expected, is caused by migration of the low molecular weight additive to the surface, which leads to a cumulative change in both surface and bulk properties of elastomeric materials. During operation, especially under the temperature influence, the migration of components increases and changes the surface state. This can be monitored by the change in the surface energy. The accumulation of the certain amount of statistical data concerning the effect of accelerated aging on the properties of vulcanizates based on various rubbers and concerning the change in critical surface tension will make it possible to judge not only the change

in surface properties, but also the rubber product physical and mechanical characteristics and, thus, to control its condition under operation.

### Authors' contributions

**O.A. Dulina** – development of the research concept, formulation and discussion of the experiment results;

**E.V. Eskova** – analysis and processing the data obtained, discussion of the experiment results;

**A.D. Tarasenko** – study of surface properties of the samples, data collection and processing, and formatting the text of the article;

**S.V. Kotova** – study of the physical and mechanical properties of samples, discussion of the experiment results.

*The authors declare no conflicts of interest.*

## REFERENCES

1. Dick J.S. *Tekhnologiya reziny: Retsepturostroenie i ispytaniya (Rubber Technology: Compounding and Testing for Performance)*: Shershnev. V.A. (Ed.). transl. from Engl. St. Petersburg: Nauchnye osnovy i tekhnologii; 2010. 617 p. (in Russ.). ISBN 978-5-91703-015-9  
[Dick J.S. *Rubber Technology: Compounding and Testing for Performance*. Hanser; 2009. 567 p. ISBN 978-3-44642-1554.]
2. Mark J.E., Erman B., Elrich F.R. (Eds.). *Kauchuk i rezina. Nauka i tekhnologiya (Science and Technology of Rubber)*: transl. from Engl. Dolgoprudnyi: Intellekt; 2011. 768 p. (in Russ.). ISBN 978-5-91559-018-1  
[Mark J.E., Erman B., Elrich F.R. (Eds.). *Science and Technology of Rubber*. Elsevier Academic Press; 2005. 743 p. ISBN 978-0-12464-7862.]
3. Grishin B.S. *Rastvorimost' i diffuziya nizkomolekulyarnykh veshchestv v kauchukakh i elastomernykh kompozitakh (Solubility and diffusion of low-molecular substances in rubbers and elastomeric composites)*. Kazan': KNITU; 2012. 142 p. (in Russ.). ISBN 978-5-7882-1371-2
4. Tarasenko A.D., Dulina O.A., Bukanov A.M. The effect of non-polymeric components of a rubber mixture on surface properties of elastomer compositions. *Tonk. Khim. Tekhnol. = Fine Chem. Technol.* 2018;3(5):67–72 (in Russ.). <https://doi.org/10.32362/2410-6593-2018-13-5-67-72>
5. Dulina O.A., Tarasenko A.D., Bukanov A.M., Ilyin A.A. The influence of the method of rubber isolation from latex on the properties of elastomeric materials based on butadiene-nitrile rubbers. *Tonk. Khim. Tekhnol. = Fine Chem. Technol.* 2017;12(4):85–90 (in Russ.). <https://doi.org/10.32362/2410-6593-2017-12-4-85-90>

## СПИСОК ЛИТЕРАТУРЫ

1. Дик Дж.С. Технология резины: рецептуростроение и испытания: пер. с англ.; под ред. В.А. Шершнева. СПб.: Научные основы и технологии; 2010. 617 с. ISBN 978-5-91703-015-9
2. Каучук и резина. Наука и технология: пер. с англ.; под ред. Дж. Марка, Б. Эрмана, Ф. Эйрича. Долгопрудный: Интеллект; 2011. 768 с. ISBN 978-5-91559-018-1
3. Гришин Б.С. Растворимость и диффузия низкомолекулярных веществ в каучуках и эластомерных композитах. Казань: Изд-во КНИТУ; 2012. 142 с. ISBN 978-5-7882-1371-2
4. Тарасенко А.Д., Дулина О.А., Буканов А.М. Влияние неполимерных компонентов резиновой смеси на поверхностные свойства эластомерных композиций. *Тонкие химические технологии*. 2018;13(5):67–72. <https://doi.org/10.32362/2410-6593-2018-13-5-67-72>
5. Дулина О.А., Тарасенко А.Д., Буканов А.М., Ильин А.А. Влияние способа выделения каучука из латекса на свойства эластомерных материалов на основе бутадиен-нитрильных каучуков. *Тонкие химические технологии*. 2017;12(4):85–90. <https://doi.org/10.32362/2410-6593-2017-12-4-85-90>
6. Папков В.Н., Гусев Ю.К., Блинов Е.В., Юрьев А.Н., Гадебский Г.А., Щелушкина Н.И., Чеботарева М.В., Решетникова Е.А. Разработка экологически чистых способов выделения бутадиен-нитрильных каучуков из латексов. *Промышленное производство и использование эластомеров*. 2010;(3):10–13.
7. Żenkiewicz M. Methods for the calculation of surface free energy of solids. *J. Achiev. Mater. Manufact. Eng.* 2007;24(1):37–145.

6. Papkov V.N., Gusev Ju.K., Blinov E.V., Jur'ev A.N., Gadebskii G.A., Shhelushkina N.I., Chebotareva M.V., Reshetnikova E.A. Development of environment friendly butadiene-nitrile rubbers (NBR) separation from latex. *Promyshlennoe proizvodstvo i ispol'zovanie elastomerov = Industrial Production and Use Elastomers*. 2010;(3):10–13 (in Russ.).
7. Żenkiewicz M. Methods for the calculation of surface free energy of solids. *J. Achiev. Mater. Manufact. Eng.* 2007;24(1):37–145.
8. Mironyuk A.V., Pridatko A.V., Sivolapov P.V., Sviderskii V.A. Aspects of polymer surfaces wetting. *Vostochno-Evropeiskii zhurnal peredovykh tekhnologii = Eastern European Journal of Enterprise Technologies*. 2014;1(6):23–26 (in Russ.). <https://doi.org/10.15587/1729-4061.2014.20797>
9. Rudawska A., Jacniacka E. Analysis for determining surface free energy uncertainly by the Owens–Wendt method. *Int. J. Adhes. Adhes.* 2009;29(4):451–457. <https://doi.org/10.1016/j.ijadhadh.2008.09.008>
10. Dulina O.A., Abramova A.D., Sitnikova D.V., Bukanov A.M. The effect of stearic acid on surface properties of elastomeric compositions based on butadienestyrene rubber. *Tonk. Khim. Tekhnol. = Fine Chem. Technol.* 2014;9(3):71–73 (in Russ.).
11. Frolova M.A., Tutygin A.S., Aizenshtadt A.M., Lesovik V.S., Makhova T.A., Pospelova T.A. Evaluation criteria of energy properties of surface of nanomaterials. *Nanosistemy: fizika. khimiya. matematika = Nanosystems: Phys. Chem. Math.* 2011;2(4):20–125 (in Russ.).
12. Starostina I.A., Stoyanov O.V. Development of methods for assessing the surface acid-base properties of polymer materials. *Vestnik Kazanskogo tekhnologicheskogo universiteta = Herald of Kazan Technological University*. 2010;(4):58–69 (in Russ.).
13. Domińczuk J., Krawczuk A. Comparison of surface free energy calculation methods. *Appl. Mech. Mater.* 2015;791:259–265. <https://doi.org/10.4028/www.scientific.net/AMM.791.259>
14. Kłonica M., Kuczmaszewski J. Determining the value of surface free energy on the basis of the contact angle. *Adv. Sci. Technol. Res. J.* 2017;11(1):66–74. <https://doi.org/10.12913/22998624/68800>
15. Dulina O.A., Sviridov E.I., Bukanov A.M. Some especially moisten rubbers of water. *Tonk. Khim. Tekhnol. = Fine Chem. Technol.* 2009;4(5):85–86 (in Russ.).
16. Evdokimov A.O., Bukanov A.M., Lyusova L.R., Petrogradsky A.V. The influence of residue emulsifier amounts on properties of nitrile rubbers and elastomeric materials based on them. *Fine Chemical Technologies*. 2018;13(5):58–66 (in Russ.). <https://doi.org/10.32362/2410-6593-2018-13-5-58-66>
17. Zakharov N.D., Kostrykina G.I. Some features of vulcanization of butadienenitrile rubbers. *Polymer Science U.S.S.A.* 1968;10(1):125–132. [https://doi.org/10.1016/0032-3950\(68\)90142-1](https://doi.org/10.1016/0032-3950(68)90142-1)
8. Миронюк А.В., Придатко А.В., Сиволапов П.В., Сvidersкий В.А. Особенности оценки смачивания полимерных поверхностей. *Восточно-Европейский журнал передовых технологий*. 2014;1(6):23–26. <https://doi.org/10.15587/1729-4061.2014.20797>
9. Rudawska A., Jacniacka E. Analysis for determining surface free energy uncertainly by the Owens–Wendt method. *Int. J. Adhes. Adhes.* 2009;29(4):451–457. <https://doi.org/10.1016/j.ijadhadh.2008.09.008>
10. Дулина О.А., Абрамова А.Д., Ситникова Д.В., Буканов А.М. Влияние стеариновой кислоты на поверхностные свойства эластомерных композитов на основе бутадиен-стирольных каучуков. *Вестник МИТХТ (Тонкие химические технологии)*. 2014;9(3):1–73.
11. Фролова М.А., Тутьгин А.С., Айзенштадт А.М., Лесовик В.С., Махова Т.А., Пospelova Т.А. Критерий оценки энергетических свойств поверхности. *Наносистемы: физика. химия. математика*. 2011;2(4):120–125.
12. Старостина И.А., Стоянов О.В. Развитие методов оценки поверхностных кислотно-основных свойств полимерных материалов. *Вестник Казанского технологического университета*. 2010;(4):58–69.
13. Domińczuk J., Krawczuk A. Comparison of surface free energy calculation methods. *Appl. Mech. Mater.* 2015;791:259–265. <https://doi.org/10.4028/www.scientific.net/AMM.791.259>
14. Kłonica M., Kuczmaszewski J. Determining the value of surface free energy on the basis of the contact angle. *Adv. Sci. Technol. Res. J.* 2017;11(1):66–74. <https://doi.org/10.12913/22998624/68800>
15. Дулина О.А., Свиридова Е.А., Буканов А.М. Некоторые особенности смачивания резин водой. *Вестник МИТХТ (Тонкие химические технологии)*. 2009;4(5):85–86.
16. Евдокимов А.О., Буканов А.М., Люсова Л.Р., Петроградский А.В. Влияние остаточных количеств эмульгатора в бутадиен-нитрильных каучуках на свойства эластомерных материалов. *Тонкие химические технологии*. 2018;13(5):58–66. <https://doi.org/10.32362/2410-6593-2018-13-5-58-66>
17. Захаров Н.Д., Кострыкина Г.И. Некоторые особенности вулканизации бутадиен-нитрильных каучуков. *Высокомолекулярные соединения. Серия А*. 1968;10(1):107–113.

#### About the authors:

**Olga A. Dulina**, Cand. Sci. (Chem.), Associate Professor, Department of Nanoscale Systems and Surface Phenomena, M.V. Lomonosov Institute of Fine Chemical Technologies, MIREA – Russian Technological University (86, Vernadskogo pr., Moscow, 119571, Russia). E-mail: [doa1503991@yandex.ru](mailto:doa1503991@yandex.ru). <https://orcid.org/0000-0002-2990-4447>

**Evgeniya V. Eskova**, Senior Lecturer, Department of Nanoscale Systems and Surface Phenomena, M.V. Lomonosov Institute of Fine Chemical Technologies, MIREA – Russian Technological University (86, Vernadskogo pr., Moscow, 119571, Russia). E-mail: eskovae@rambler.ru. <https://orcid.org/0000-0003-2536-1884>

**Alina D. Tarasenko**, Assistant, Department of Nanoscale Systems and Surface Phenomena, M.V. Lomonosov Institute of Fine Chemical Technologies, MIREA – Russian Technological University (86, Vernadskogo pr., Moscow, 119571, Russia). E-mail: ad\_abramova@mail.ru. <https://orcid.org/0000-0002-5457-0506>

**Svetlana V. Kotova**, Cand. Sci. (Eng.), Associate Professor, F.F. Koshelev Department of Chemistry and Technology of Elastomers Processing, M.V. Lomonosov Institute of Fine Chemical Technologies, MIREA - Russian Technological University (86, Vernadskogo pr., Moscow 119571, Russia). E-mail: s.v.kotova@mail.ru. <https://orcid.org/0000-0002-7076-4669>

**Об авторах:**

**Дулина Ольга Анатольевна**, к.х.н., доцент кафедры наноразмерных систем и поверхностных явлений им. С.С. Воюцкого Института тонких химических технологий им. М.В. Ломоносова ФГБОУ ВО «МИРЭА – Российский технологический университет» (119571, Россия, Москва, пр-т Вернадского, д. 86). E-mail: doa1503991@yandex.ru. <https://orcid.org/0000-0002-2990-4447>

**Еськова Евгения Владимировна**, старший преподаватель кафедры наноразмерных систем и поверхностных явлений им. С.С. Воюцкого Института тонких химических технологий им. М.В. Ломоносова ФГБОУ ВО «МИРЭА – Российский технологический университет» (119571, Россия, Москва, пр-т Вернадского, д. 86). E-mail: eskovae@rambler.ru. <https://orcid.org/0000-0003-2536-1884>

**Тарасенко Алина Дмитриевна**, ассистент кафедры наноразмерных систем и поверхностных явлений им. С.С. Воюцкого Института тонких химических технологий им. М.В. Ломоносова ФГБОУ ВО «МИРЭА – Российский технологический университет» (119571, Россия, Москва, пр-т Вернадского, д. 86). E-mail: ad\_abramova@mail.ru. <https://orcid.org/0000-0002-5457-0506>

**Котова Светлана Владимировна**, к.т.н., доцент кафедры Химии и технологии переработки эластомеров им. Ф.Ф. Кошелева Института тонких химических технологий им. М.В. Ломоносова ФГБОУ ВО «МИРЭА – Российский технологический университет» (119571, Россия, Москва, пр-т Вернадского, д. 86). E-mail: s.v.kotova@mail.ru. <https://orcid.org/0000-0002-7076-4669>

*The article was submitted: July 29, 2021; approved after reviewing: October 28, 2021; accepted for publication: April 08, 2022.*

*Translated from Russian into English by M. Povorin.*

*Edited for English language and spelling by Quinton Scribner, Awatera.*

**SYNTHESIS AND PROCESSING OF POLYMERS  
AND POLYMERIC COMPOSITES**

**СИНТЕЗ И ПЕРЕРАБОТКА ПОЛИМЕРОВ  
И КОМПОЗИТОВ НА ИХ ОСНОВЕ**

ISSN 2686-7575 (Online)

<https://doi.org/10.32362/2410-6593-2022-17-2-164-171>



UDC 678.6

RESEARCH ARTICLE

## Obtaining phthalate substituted post-consumer polyethylene terephthalate and its isothermal crystallization

**Kirill A. Kirshanov**<sup>✉</sup>, **Alexander Yu. Gervald**, **Roman V. Toms**,  
**Andrey N. Lobanov**

MIREA – Russian Technological University (M.V. Lomonosov Institute of Fine Chemical Technologies),  
Moscow, 119571 Russia

<sup>✉</sup>Corresponding author, e-mail: kirill\_kirshanov@mail.ru

### Abstract

**Objects.** Due to the polymer waste accumulation, the search for new directions for their utilization is urgent. Chemical recycling methods are of considerable interest, which allow one to obtain the original monomers or change the compositions of the copolymers. From the point of view of building a circular economy, a promising material is polyethylene terephthalate (PET), on the basis of which amorphous copolyesters can be obtained. The study aimed to analyze the simultaneous glycolysis and interchain exchange reactions of PET in the presence of the oligoethylene phthalate modifier with hydroxyl end groups and the study of isothermal crystallization of poly(ethylene phthalate-co-terephthalates) with different phthalate contents obtained in this way.

**Methods.** Oligoethylene phthalate is synthesized by polycondensation. Poly(ethylene phthalate-co-terephthalates) were obtained by the interaction of post-consumer PET with oligoethylene phthalate. The composition of the oligomer and copolymers was confirmed using Fourier-transform infrared spectroscopy, thermal characteristics and crystallization half-times were determined by differential scanning calorimetry.

**Results.** In this work, the use of the post-consumer PET chemical recycling process, aimed at obtaining copolyesters under the influence of small modifier amounts was proposed. The process consisted in carrying out the combined interchain exchange and degradation with a complex oligoester different from PET. Poly(ethylene phthalate-co-terephthalate) copolymers were obtained

via reaction of post-consumer poly(ethylene terephthalate) flakes and synthesized oligoethylene phthalate resin in the melt phase in the absence of catalyst. The effect of phthalate concentration in polymer on the isothermal crystallization of phthalate substituted poly(ethylene terephthalate) was estimated.

**Conclusions.** The hypothesis about the possibility of using an oligoester modifier to obtain the PET-based copolymer at the high rate and without reducing the molecular weight to values characteristic of a monomer or oligomer has been confirmed. The process can be used to obtain random copolyesters based on post-consumer PET. The phthalate unit concentration increase is followed by decrease in the glass transition temperature, temperature and heat of fusion, and increase in crystallization half-times. Phthalate has a better ability to retard PET crystallization than 2-methyl-1,3-propanediol or furandicarboxylic acid, but is inferior to some of the other modifiers known.

**Keywords:** polyethylene terephthalate, PET, copolyester, chemical recycling of PET, glycolysis, degradation, interchain exchange, isothermal crystallization

**For citation:** Kirshanov K.A., Gervald A.Yu., Toms R.V., Lobanov A.N. Obtaining phthalate substituted post-consumer polyethylene terephthalate and its isothermal crystallization. *Tonk. Khim. Tekhnol. = Fine Chem. Technol.* 2022;17(2):164–171 (Russ., Eng.). <https://doi.org/10.32362/2410-6593-2022-17-2-164-171>

## НАУЧНАЯ СТАТЬЯ

# Получение фталатзамещенного вторичного полиэтилентерефталата и изучение его изотермической кристаллизации

К.А. Киршанов✉, А.Ю. Гервальд, Р.В. Томс, А.Н. Лобанов

МИРЭА – Российский технологический университет (Институт тонких химических технологий им. М.В. Ломоносова), Москва, 119571 Россия

✉ Автор для переписки, e-mail: kirill\_kirshanov@mail.ru

### Аннотация

**Цели.** Накопление полимерных отходов в последнее время обуславливает поиск новых подходов к их утилизации. Значительный интерес представляют химические способы вторичной переработки, которые позволяют получить исходные мономеры или изменить составы сополимеров. С точки зрения построения экономики замкнутого цикла перспективным материалом является полиэтилентерефталат (ПЭТ), из которого в процессе химического рециклинга получают аморфные сополиэфир. Работа посвящена исследованию одновременного протекания реакций гликолиза и межцепного обмена ПЭТ в присутствии модификатора олигоэтиленфталата с гидроксильными концевыми группами и изучению изотермической кристаллизации поли(этилен фталат-со-терефталатов) с разным содержанием фталата, полученных таким способом.

**Методы.** Олигоэтиленфталат синтезирован поликонденсацией. Поли(этилен фталат-со-терефталаты) получены взаимодействием вторичного ПЭТ с олигоэтиленфталатом. Состав олигомера и сополимеров был подтвержден с использованием ИК-Фурье спектроскопии, термические характеристики и полупериоды кристаллизации определяли методом дифференциальной сканирующей калориметрии.

**Результаты.** Разработан процесс получения сополиэфиров, основанный на химическом рециклинге вторичного ПЭТ под действием малых количеств модификатора. Отличительной особенностью процесса является одновременное протекание реакций межцепного обмена и деструкции сложным олигоэфиром, отличным по природе от ПЭТ. Реакцией в расплаве вторичного ПЭТ и синтезированного олигоэтиленфталата в отсутствие катализатора были получены поли(этилен фталат-со-терефталаты). Изучено влияние концентрации фталата в полимере на температуру стеклования, температуру и теплоту плавления, изотермическую кристаллизацию фталатзамещенного ПЭТ.

**Выводы.** Подтверждена гипотеза о возможности использования олигоэфирного модификатора для получения сополимера на основе ПЭТ с высокой скоростью и без снижения молекулярной массы до значений, характерных для мономера или олигомера. Процесс может быть использован для получения статистических сополиэфиров на основе вторичного ПЭТ. С увеличением концентрации звеньев фталата происходит снижение температуры стеклования, температуры и теплоты плавления, увеличение полупериодов кристаллизации. Фталат обладает лучшей способностью замедлять кристаллизацию ПЭТ, чем 2-метил-1,3-пропандиол или фурандикарбоновая кислота, но уступает некоторым другим известным модификаторам.

**Ключевые слова:** полиэтилентерефталат, ПЭТ, ПЭТФ, сополиэфир, химический рециклинг ПЭТ, гликолиз, деструкция, межцепной обмен, изотермическая кристаллизация

**Для цитирования:** Киршанов К.А., Гервальд А.Ю., Томс Р.В., Лобанов А.Н. Получение фталатзамещенного вторичного полиэтилентерефталата и изучение его изотермической кристаллизации. *Тонкие химические технологии.* 2022;17(2):164–171. <https://doi.org/10.32362/2410-6593-2022-17-2-164-171>

## INTRODUCTION

Currently, an urgent problem is the processing of polymer waste, a significant part of which is a large-tonnage polyester—polyethylene terephthalate (PET) [1].

The most promising are PET processing methods based on chemical reactions, while the most studied are degradation reactions: glycolysis, hydrolysis, alcoholysis, acidolysis, and others [2–4].

Among them, PET glycolysis is of considerable interest. Heterogeneous glycolysis is the most widespread; however, examples of the process under homogeneous conditions both in solution [5–7] and in melt [8–10] are also known. The degradation of PET by oligoesters is of particular interest. The possibility of PET glycolysis with oligoethylene terephthalates of various molecular weights was described in [7]. A similar process was also studied

in [10], however, in this case, glycolysis is carried out with large amounts of a modifier (an oligoester, which is different in nature from PET), which leads to a low molecular weight product. At the same time, it is known that to obtain a higher molecular weight product, it is necessary to use low concentrations of the glycolysis agent [6]. Since the authors obtained a random copolymer in their work, in their study glycolysis was combined with another chemical processing method—interchain exchange.

Today, the interchain exchange reaction for the modification of PET macromolecules in industry is less significant than glycolysis [11–14]. Although the polymeric materials produced in this way may be contaminated with additives from the original PET composition or degradation products, the interchain exchange makes it possible to obtain copolyesters in a single step and at a relatively low energy cost. The interchain exchange reaction

rate depends on the concentration of end groups in the reaction space [12, 14], the content of which will be higher if the same amount of modifier is used, but with a low molecular weight.

Most often, the purpose of such a modification is to obtain amorphous polymers [1] with lower crystallinity and longer crystallization half-time. For example, to obtain an amorphous copolymer, a number of units, such as units of 1,4-cyclohexanedimethanol (CHDM) [15–19], CHDM and isophthalate [20], only isophthalate [21], 2,5-furandicarboxylic acid as an alternative to isophthalate [22], 1,3-propanediol [23], 2-methyl-1,3-propanediol [24], and tricyclodecane dimethanol [25] are introduced into the PET chain. Amorphous terephthalate-based polymers, as well as CHDM and isosorbide [26], CHDM, 1,4-butanediol, and oligo-l-lactide [27] are also known. One of the poorly studied comonomers is inexpensive phthalate [28, 29]. The products of glycolysis, methanolysis, and hydrolysis of such a copolymer are easily separated.

The aim of this work is to study the simultaneous reactions of glycolysis and interchain exchange of PET in the presence of small amounts of oligoethylene phthalate (OEP-1) modifier with hydroxyl end groups, as well as to study the isothermal crystallization of poly(ethylene phthalate-co-terephthalates) (PEPT) with different content of phthalate obtained in this way. The use of a low molecular weight modifier in the interchain exchange reaction should make it possible to achieve a high process rate [12, 14] and avoid thermal degradation, and at the studied phthalate concentrations, a decrease in molecular weight will have almost no effect on the hard-chain PEPT properties.

## EXPERIMENTAL

As the main raw material, transparent PET flakes were used, which are industrial products of crushing PET containers [7]. To calculate the degree of polycondensation, we used the data of [8], which indicated the average molecular weight equal to 26000 g/mol. The PET molecular weight value corresponds to the degree of polycondensation equal to 135.

Phthalic anhydride, chemically pure (*Sigma-Aldrich*, USA) was used without preliminary purification. Ethylene glycol, chemically pure (*Sigma-Aldrich*, USA) was pre-purified by vacuum distillation prior to use.

OEP-1 was obtained by the phthalic anhydride and ethylene glycol polycondensation. Ethylene glycol in a molar ratio of 1.25:1 was added to molten phthalic anhydride at 140°C in a 250 mL flask equipped with

a Liebig condenser. The mixture was kept for 1.5 h. The temperature was maintained using a heating mantle. After that, the temperature was raised to 190°C for 3 h, then the mixture was kept under a vacuum of 40 mbar until the end of the evolution of the water formed in the reaction.

PEPT of various compositions was obtained by the interchain exchange reaction in the melt in the absence of a catalyst. Pre-prepared PET flakes and synthesized OEP-1 were co-melted in a flask. The melt was stirred at a temperature of 280°C in an inert nitrogen gas stream until a constant viscosity was reached. The time to reach the melt constant viscosity was no more than 1.5 h for all samples.

Differential scanning calorimetry (DSC) curves were obtained on a DSC 204 F1 Phoenix calorimeter (*NETZSCH Gerätebau GmbH*, Germany) in an inert medium (argon) at the 10 deg/min scanning rate, as well as in an isothermal mode.

The composition of the products was confirmed by Fourier transform infrared spectroscopy (FTIR) on a Spectrum 65 FT-IR spectrometer (*Perkin Elmer*, USA) with a resolution of 1 cm<sup>-1</sup> in the range from 500 to 4000 cm<sup>-1</sup> at a temperature of 25°C. The oligomer average molecular weight value was determined from the infrared spectrum according to the procedure [6, 30].

## RESULTS AND DISCUSSION

The resulting oligoethylene terephthalate was examined by DSC. The absence of crystallization, melting, and the heat capacity increase peaks on the DSC curve indicates the formation of the completely amorphous oligomer. The oligomer average molecular weight value determined from the FTIR spectrum (Fig. 1) was 800 g/mol. The oligomer degree of polycondensation is approximately 4.

Thermal properties and isothermal crystallization were studied by DSC. The thermal characteristics of the obtained copolymers are given in the table.

In certain scientific literature, one can find disagreements in the thermal characteristics values of such copolymers [28, 29]. This may be due to both the difference in molecular weight and the composition of the original PET. Despite this, the obtained thermal characteristics correlate well with the known data both on the glass transition temperatures [28] and on the decrease in heat levels [28] and melting temperatures [29]. With the sample phthalate to terephthalate ratio increase from 0 (sample PET-1) to 15 (sample PEPT-15:85), the decrease in the melting point from 250 to 221°C and the heat of fusion from 71 to 45 J/g

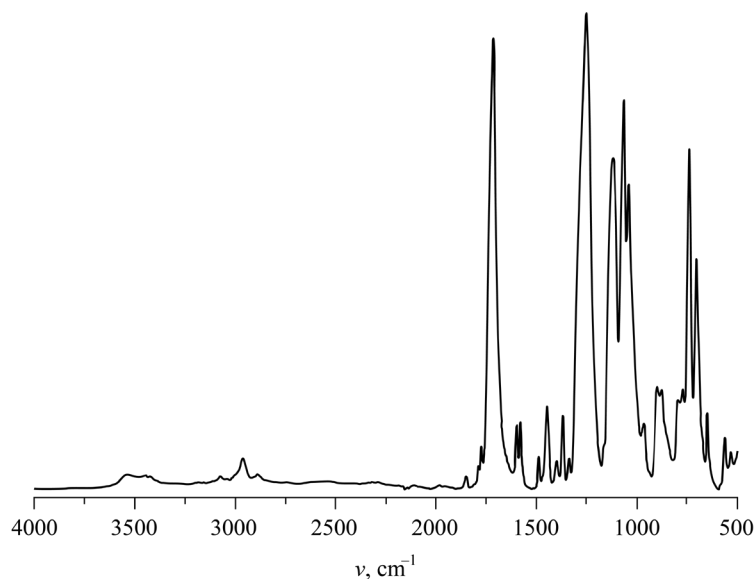


**Fig. 1.** Fourier-transform infrared (FTIR) spectrum of the OEP-1 sample (oligoethylene phthalate).

**Table.** Composition, polycondensation degree and thermal characteristics of copolymers

Polymer	Terephthalate to phthalate ratio	Degree of polycondensation	Glass transition temperature, °C	Melting point, °C	Heat of fusion, J/g
PET-1	100:0	135	78.4	250.4	71.2
PEPT-5:95	95:5	53	75.3	242.4	61.1
PEPT-10:90	90:10	33	72.2	233.3	53.6
PEPT-15:85	85:15	24	69.5	220.8	45.4

confirms the crystal structure violation at the chain regularity changing. There is also a decrease in the glass transition temperature from 78 to 70°C with the same increase in the phthalate concentration in the polymer.

The obtained PEPT composition was confirmed by the FTIR spectroscopy. The position and intensity of the peaks in the spectra of the samples (Fig. 2) corresponds to the theoretical data [6, 29].

The crystallization half-times were calculated from the isothermal DSC curves of the copolymers. The half-times of crystallization of copolymers at different temperatures are shown in Fig. 3.

Crystallization half-times with increasing comonomer concentration show the growth typical of PET-based copolymers.

In terms of crystallinity reduction, phthalic anhydride as a modifier is inferior to CHDM [15] and isosorbide [31], but is superior to 2-methyl-1,3-propanediol [24] and furandicarboxylic acid [32].

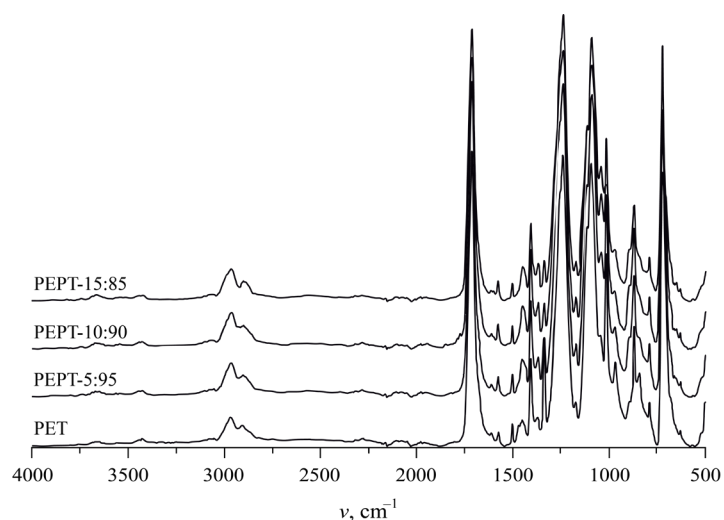


**Fig. 2.** FTIR spectra of PET, PEPT-5:95, PEPT-10:90, and PEPT-15:85 samples.

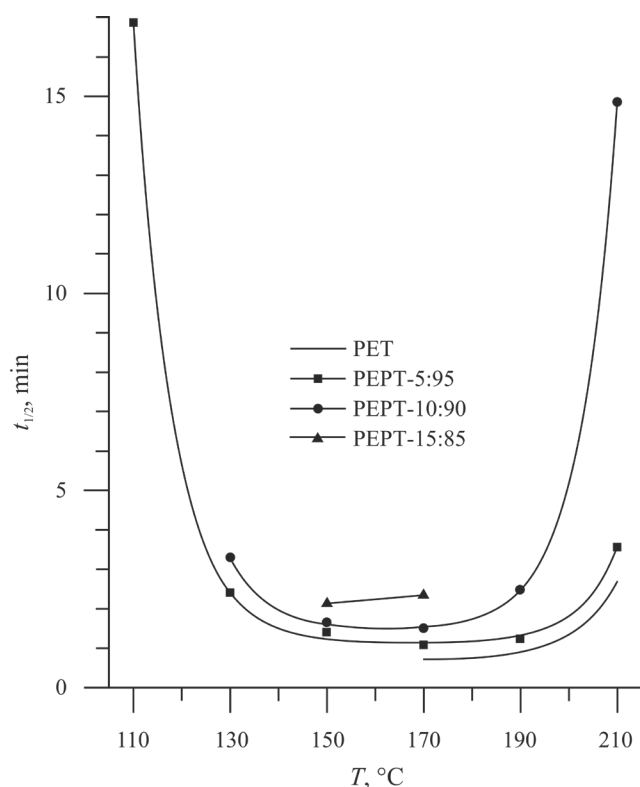


**Fig. 3.** Isothermal crystallization half-times  $t_{1/2}$ , min, of PET samples [32], PEPT-5:95, PEPT-10:90, and PEPT-15:85 at different temperatures  $T$ , °C.

## CONCLUSIONS

The simultaneous glycolysis and interchain exchange reactions can be used as a method for obtaining amorphous copolyesters based on recycled PET. The hypothesis about the possibility of using

a small amount of an oligoester modifier to obtain a PET-based copolymer at the high rate and without reducing the molecular weight to the values characteristic of the monomer or oligomer was confirmed.

The introduction of phthalate into PET macromolecules makes it possible to reduce the glass transition temperature, and temperature and fusion heat of the copolymer. It is also possible to observe a slowdown in crystallization with an increase in the concentration of phthalate, as evidenced by the crystallization half-time. Comparison of the PEPT crystallization isotherms with crystallization isotherms of other copolyesters leads to the conclusion that phthalate has a good ability to slow down crystallization.

### Authors' contributions

**K.A. Kirshanov** – planning and conducting research, collecting and analyzing experimental materials, writing the manuscript;

**A.Yu. Gervald** – management and scientific consulting;

**R.V. Toms** – scientific consulting and assistance in processing the results obtained;

**A.N. Lobanov** – management and preparation of material for publication.

*The authors declare no conflicts of interest.*

## REFERENCES

- Scheirs J., Long T.E. Modern Polyesters: Chemistry and Technology of Polyesters and Copolyesters. London: John Wiley & Sons, Ltd; 2003. 750 p. <https://doi.org/10.1002/0470090685>
- George N., Kurian T. Recent Developments in the Chemical Recycling of Postconsumer Poly(ethylene terephthalate) Waste. *Ind. Eng. Chem. Res.* 2014;53(37):14185–14198. <https://doi.org/10.1021/ie501995m>
- Khoonkari M., Haghghi A.H., Sefidbakht Y., Shekoohi K., Ghaderian A. Chemical Recycling of PET Wastes with Different Catalysts. *Int. J. Polym. Sci.* 2015;1–11. <https://doi.org/10.1155/2015/124524>
- Raheem A.B., Noor Z.Z., Hassan A., Hamid M.K.A., Samsudin S.A., Sabeen A.H. Current developments in chemical recycling of post-consumer polyethylene terephthalate wastes for new materials production: A review. *J. Clean. Prod.* 2019;225:1052–1064. <https://doi.org/10.1016/j.jclepro.2019.04.019>
- Liu B., Lu X., Ju Z., Sun P., Xin J., Yao X., Zhou Q., Zhang S. Ultrafast homogeneous glycolysis of waste polyethylene terephthalate via a dissolution-degradation strategy. *Ind. Eng. Chem. Res.* 2018;57(48):16239–16245. <https://doi.org/10.1021/acs.iecr.8b03854>
- Kirshanov K.A., Gervald A.Yu., Toms R.V. Obtaining oligoesters by directed glycolytic destruction of polyethylene terephthalate waste. *Plasticheskie massy.* 2020;1(11–12):51–53 (in Russ.). <https://doi.org/10.35164/0554-2901-2020-11-12-51-53>
- Kirshanov K.A., Toms R.V. Study of polyethylene terephthalate glycolysis with a mixture of bis(2-hydroxyethyl) terephthalate and its oligomers. *Plasticheskie massy.* 2021;1(3–4):50–52 (in Russ.). <https://doi.org/10.35164/0554-2901-2021-3-4-50-52>
- El Mejjatti A., Harit T., Riahi A., Khiari R., Bouabdallah I., Malek F. Chemical recycling of poly(ethylene terephthalate). Application to the synthesis of multiblock copolyesters. *eXPRESS Polymer Letters.* 2014;8(8):544–553. <https://doi.org/10.3144/expresspolymlett.2014.58>

9. Borisov V.A. Some ways of recycling the secondary polyethylene terephthalate. *Izvestiya Kabardino-Balkarskogo Gosudarstvennogo Universiteta = Proceeding of the Kabardino-Balkarian State University*. 2013;3(5):18–23 (in Russ.).
10. Colomines G., Robin J.-J., Tersac G. Study of the glycolysis of PET by oligoesters. *Polymer*. 2005;46(10):3230–3247. <https://doi.org/10.1016/j.polymer.2005.02.047>
11. Litmanovich A.D., Plate N.A., Kudryavtsev Y.V. Reactions in polymer blends: interchain effects and theoretical problems. *Progress in Polymer Science*. 2002;27:915–970. [https://doi.org/10.1016/S0079-6700\(02\)00003-5](https://doi.org/10.1016/S0079-6700(02)00003-5)
12. Krentsel' L.B., Makarova V.V., Kudryavtsev Ya.V., Govorun E.N., Litmanovich A.D., Markova G.D., Vasnev V.A., Kulichikhin V.G. Interchain exchange and interdiffusion in blends of poly(ethylene terephthalate) and poly(ethylene naphthalate). *Polym. Sci. Ser. A*. 2009;51(11–12):1241–1248. <https://doi.org/10.1134/S0965545X09110091>
13. Heidarzadeh N., Rafizadeh M., Taromi F.A., del Valle L.J., Franco L., Puiggali J. Biodegradability and biocompatibility of copoly(butylene sebacate-co-terephthalate)s. *Polym. Degrad. Stab.* 2017;135:18–30. <https://doi.org/10.1016/j.polymdegradstab.2016.11.013>
14. Collins S., Peace S.K., Richards R.W., MacDonald W.A., Mills P., King S.M. Transesterification in poly(ethylene terephthalate). Molecular weight and end group effects. *Macromolecules*. 2000;33(8):2981–2988. <https://doi.org/10.1021/ma991637>
15. Turner S.R. Development of amorphous copolyesters based on 1,4-cyclohexanedimethanol. *J. Polym. Sci.: A: Polym. Chem.* 2004;42(23):5847–5852. <https://doi.org/10.1002/pola.20460>
16. Shirali H., Rafizadeh M., Taromi F.A. Synthesis and characterization of amorphous and impermeable poly(ethylene-co-1,4-cyclohexylenedimethylene terephthalate)/organoclay nanocomposite via *in situ* polymerization. *J. Compos. Mater.* 2014;48(3):301–315. <https://doi.org/10.1177/0021998312471566>
17. Granado A., Iturriza L., Eguiazabal J.I. Structure and mechanical properties of blends of an amorphous polyamide and an amorphous copolyester. *J. Appl. Polym. Sci.* 2014;131(18):40785. <https://doi.org/10.1002/app.40785>
18. Tingting C., Guodong J., Jun Z. Isothermal crystallization behavior and crystal structure of poly(ethylene-terephthalate-co-1,4-cyclohexylenedimethyleneterephthalate) (PET/CT) copolyesters. *Cryst. Res. Technol.* 2014;49(4):232–243. <https://doi.org/10.1002/crat.201300369>
19. Tingting C., Guodong J., Jun Z. Alkali resistance of poly(ethylene terephthalate) (PET) and poly(ethylene glycol-co-1,4-cyclohexanedimethanol terephthalate) (PETG) copolyesters: the role of composition. *Polym. Degrad. Stab.* 2015;120:232–243. <https://doi.org/10.1016/j.polymdegradstab.2015.07.008>
20. Seung W.H., Hee S.M., Jong S.B., Eui S.Y., Seung S.I. Synthesis and crystallization behaviors of modified PET copolymers. *Fibers Polym.* 2012;1(2):76–82. <https://doi.org/10.1007/BF02875189>
21. Nagahata R., Sugiyama J., Velmathi S., Nakao Y., Goto M., Takeuchi K. Synthesis of poly(ethylene terephthalate-co-isophthalate) by copolymerization of ethylene isophthalate cyclic dimer and bis(2-hydroxyethyl) terephthalate. *Polym. J.* 2004;36(6):483–488. <https://doi.org/10.1295/polymj.36.483>
22. Liyuan S., Yajie Z., Jinggang W., Fei L., Zhen J., Xiaoqing L., Jin Z. 2,5-Furandicarboxylic acid as a sustainable alternative to isophthalic acid for synthesis of amorphous poly(ethylene terephthalate) copolyester with enhanced performance. *J. Appl. Polym. Sci.* 2018;47186. <https://doi.org/10.1002/app.47186>
23. Kim J.H., Lee S.Y., Park J.H., Lyoo W.S., Noh S.K. Kinetics of polycondensation and copolycondensation of bis(3-hydroxypropyl terephthalate) and bis(2-hydroxyethyl terephthalate). *J. Appl. Polym. Sci.* 2000;77(3):693–698. [https://doi.org/10.1002/\(SICI\)1097-4628\(20000718\)77:3<693::AID-APP24>3.0.CO;2-Q](https://doi.org/10.1002/(SICI)1097-4628(20000718)77:3<693::AID-APP24>3.0.CO;2-Q)
24. Lewis C.L., Spruiell J.E. Crystallization of 2-methyl-1,3-propanediol substituted poly(ethylene terephthalate). I. Thermal behavior and isothermal crystallization. *J. Appl. Polym. Sci.* 2006;100(4):2592–2603. <https://doi.org/10.1002/app.22786>
25. Tsai Y., Fan C-H., Wu J-H. Synthesis, microstructures and properties of amorphous poly(ethylene terephthalate-co-tricyclodecanedimethylene terephthalate). *J. Polym. Res.* 2016;23(3):23–42. <https://doi.org/10.1007/s10965-016-0933-5>
26. Legrand S., Jacquelin N., Amedro H., Saint-Loup R., Pascault J.-P., Rousseau A., Fenouillot F. Synthesis and properties of poly(1,4-cyclohexanedimethylene-co-isosorbide terephthalate), a biobased copolyester with high performances. *Eur. Polym. J.* 2019;115:22–29. <https://doi.org/10.1016/j.eurpolymj.2019.03.018>
27. Wang B., Zhang Y., Song P., Guo Z., Cheng J., Fang Z. Synthesis, characterization, and properties of degradable poly(l-lactic acid)/poly(butylene terephthalate) copolyesters containing 1,4-cyclohexanedimethanol. *J. Appl. Polym. Sci.* 2011;120(5):2985–2995. <https://doi.org/10.1002/app.33373>
28. Lee B., Lee J.W., Lee S.W., Yoon J., Ree M. Synthesis and non-isothermal crystallization behavior of poly(ethylene phthalate-co-terephthalate)s. *Polym. Eng. Sci.* 2004;44(9):1682–1691. <https://doi.org/10.1002/pen.20168>
29. Connor D.M., Allen S.D., Collard D.M., Liotta C.L., Schiraldi D.A. Effect of comonomers on the rate of crystallization of pet: U-turn comonomers. *J. Appl. Polym. Sci.* 2001;81(7):1675–1682. <https://doi.org/10.1002/app.1599>
30. Du B., Yang R., Xie X. Investigation of hydrolysis in poly(ethylene terephthalate) by FTIR-ATR. *Chin. J. Polym. Sci.* 2014;32(2):230–235. <https://doi.org/10.1007/s10118-014-1372-6>
31. Descamps N., Fernandez F., Heijboer P., Saint-Loup R., Jacquelin N. Isothermal crystallization kinetics of poly(ethylene terephthalate) copolymerized with various amounts of isosorbide. *Appl. Sci.* 2020;10(3):1046. <https://doi.org/10.3390/app10031046>
32. Terzopoulou Z., Papadopoulos L., Zamboulis A., Papageorgiou D.G., Papageorgiou G.Z., Bikiaris D.N. Tuning the properties of furandicarboxylic acid-based polyesters with copolymerization: a review. *Polymers*. 2020;12(6):1209. <https://doi.org/10.3390/polym12061209>

**About the authors:**

**Kirill A. Kirshanov**, Postgraduate Student, Engineer, S.S. Medvedev Department of Chemistry and Technology of Macromolecular Compounds, M.V. Lomonosov Institute of Fine Chemical Technologies, MIREA – Russian Technological University (86, Vernadskogo pr., Moscow, 119571, Russia). E-mail: kirill\_kirshanov@mail.ru. <https://orcid.org/0000-0002-2611-2217>

**Alexander Yu. Gervald**, Cand. Sci. (Chem.), Associate Professor, S.S. Medvedev Department of Chemistry and Technology of Macromolecular Compounds, M.V. Lomonosov Institute of Fine Chemical Technologies, MIREA – Russian Technological University (86, Vernadskogo pr., Moscow, 119571, Russia). E-mail: gervald@bk.ru. <https://orcid.org/0000-0003-0843-7082>

**Roman V. Toms**, Cand. Sci. (Chem.), Associate Professor, S.S. Medvedev Department of Chemistry and Technology of Macromolecular Compounds, M.V. Lomonosov Institute of Fine Chemical Technologies, MIREA – Russian Technological University (86, Vernadskogo pr., Moscow, 119571, Russia). E-mail: toms.roman@gmail.com. <https://orcid.org/0000-0002-6911-1636>

**Andrey N. Lobanov**, Cand. Sci. (Chem.), Associate Professor, S.S. Medvedev Department of Chemistry and Technology of Macromolecular Compounds, M.V. Lomonosov Institute of Fine Chemical Technologies, MIREA – Russian Technological University (86, Vernadskogo pr., Moscow, 119571, Russia). E-mail: anlobanov@yandex.ru. <https://orcid.org/0000-0001-6435-4965>

**Об авторах:**

**Киришанов Кирилл Андреевич**, аспирант, инженер кафедры химии и технологии высокомолекулярных соединений им. С.С. Медведева Института тонких химических технологий им. М.В. Ломоносова ФГБОУ ВО «МИРЭА – Российский технологический университет» (119571, Россия, Москва, пр-т Вернадского, д. 86). E-mail: kirill\_kirshanov@mail.ru. <https://orcid.org/0000-0002-2611-2217>

**Гервальд Александр Юрьевич**, к.х.н., доцент кафедры химии и технологии высокомолекулярных соединений им. С.С. Медведева Института тонких химических технологий им. М.В. Ломоносова ФГБОУ ВО «МИРЭА – Российский технологический университет» (119571, Россия, Москва, пр-т Вернадского, д. 86). E-mail: gervald@bk.ru. <https://orcid.org/0000-0003-0843-7082>

**Томс Роман Владимирович**, к.х.н., доцент кафедры химии и технологии высокомолекулярных соединений им. С.С. Медведева Института тонких химических технологий им. М.В. Ломоносова ФГБОУ ВО «МИРЭА – Российский технологический университет» (119571, Россия, Москва, пр-т Вернадского, д. 86). E-mail: toms.roman@gmail.com. <https://orcid.org/0000-0002-6911-1636>

**Лобанов Андрей Николаевич**, к.х.н., доцент кафедры химии и технологии высокомолекулярных соединений им. С.С. Медведева Института тонких химических технологий им. М.В. Ломоносова ФГБОУ ВО «МИРЭА – Российский технологический университет» (119571, Россия, Москва, пр-т Вернадского, д. 86). E-mail: anlobanov@yandex.ru. <https://orcid.org/0000-0001-6435-4965>

*The article was submitted: November 30, 2021; approved after reviewing: January 10, 2022; accepted for publication: April 08, 2022.*

*Translated from Russian into English by H. Moshkov.*

*Edited for English language and spelling by Quinton Scribner, Awatera.*

ISSN 2686-7575 (Online)

<https://doi.org/10.32362/2410-6593-2022-17-2-172-181>



UDC 546.15 + 546.65

RESEARCH ARTICLE

## Comparison of the rare earth complexes iodides and polyiodides with biuret

Aleksandr D. Kornilov<sup>1</sup>, Mikhail S. Grigoriev<sup>2</sup>, Elena V. Savinkina<sup>1,✉</sup>

<sup>1</sup>MIREA – Russian Technological University (M.V. Lomonosov Institute of Fine Chemical Technologies), Moscow, 119571 Russia

<sup>2</sup>Frumkin Institute of Physical Chemistry and Electrochemistry, Russian Academy of Sciences, Moscow, 119071 Russia

✉ Corresponding author, e-mail: savinkina@mirea.ru

### Abstract

**Objectives.** Currently, several hundred polyiodide compounds have been synthesized and structurally characterized, but so far, no formation patterns for certain polyiodide ions have been revealed. The purpose of this work is to continue the search for formation regularities of polyiodides, including polyiodides of lanthanide complexes.

**Methods.** Iodide and polyiodide of samarium complexes with biuret (BU),  $[\text{Sm}(\text{BU})_4]\text{I}_3 \cdot \text{BU} \cdot 2\text{H}_2\text{O}$  and  $[\text{Sm}(\text{BU})_4][\text{I}_5][\text{I}]_2$ , were first synthesized and characterized by X-ray diffraction analysis and infrared spectroscopy, respectively.

**Results.** The obtained compounds complement the row of isostructural lanthanide (La–Gd) complexes. Structures of corresponding iodides and polyiodides were compared in detail. Both types of the compounds contain complex cations of the same composition; however, their structures differ significantly. The central atom coordination polyhedron can be described as a distorted square antiprism and a distorted dodecahedron, respectively. Even greater differences are observed in the outer sphere of complex compounds. The iodide compound crystals contain uncoordinated iodide ions, a biuret molecule and two water molecules. In the polyiodide compound, cations together with isolated  $\text{I}^-$  ions form a three-dimensional framework with the channels, in which linear  $\text{I}_5^-$  ions are united in infinite linear chains by weak interactions.

**Conclusions.** The replacement of an iodide ion with a polyiodide ion in complex compounds of lanthanides with BU leads to changes in both the inner sphere and the outer sphere of the cation complex, including the supramolecular level. The presence of iodine infinite linear chains in polyiodides allows expecting the presence of anisotropic electrical conductivity along this direction.

**Keywords:** lanthanides, samarium, iodide, polyiodide, crystal structure, anisotropy

**For citation:** Kornilov A.D., Grigoriev M.S., Savinkina E.V. Comparison of the rare earth complexes iodides and polyiodides with biuret. *Tonk. Khim. Tekhnol. = Fine Chem. Technol.* 2022;17(2):172–181 (Russ., Eng.). <https://doi.org/10.32362/2410-6593-2022-17-2-172-181>

## НАУЧНАЯ СТАТЬЯ

# Сравнение иодидов и полииодидов комплексов редкоземельных элементов с биуретом

А.Д. Корнилов<sup>1</sup>, М.С. Григорьев<sup>2</sup>, Е.В. Савинкина<sup>1,✉</sup>

<sup>1</sup>МИРЭА – Российский технологический университет (Институт тонких химических технологий им. М.В. Ломоносова), Москва, 119571 Россия

<sup>2</sup>Институт физической химии и электрохимии им. А.Н. Фрумкина Российской академии наук, Москва, 119071 Россия

✉ Автор для переписки, e-mail: savinkina@mirea.ru

### Аннотация

**Цели.** В настоящее время синтезировано и структурно охарактеризовано несколько сотен полииодидных соединений, однако до сих пор не выявлено закономерностей образования тех или иных полииодид-ионов. Целью настоящей работы является продолжение поиска закономерностей образования полииодидов, в том числе полииодидов комплексов лантанидов.

**Методы.** Впервые синтезированы и охарактеризованы методами рентгеноструктурного анализа и инфракрасной спектроскопии, соответственно, иодид и полииодид комплексов самария с биуретом (BU) состава  $[Sm(BU)_4]I_3 \cdot BU \cdot 2H_2O$  и  $[Sm(BU)_4][I_3][I]_2$ .

**Результаты.** Полученные соединения пополняют ряд изоструктурных комплексов лантанидов от La до Gd. Проведено детальное сравнение структур иодидных и полииодидных соединений. Установлено, что оба типа соединений содержат комплексный катион одного состава, однако его строение существенно различается в иодидных и полииодидных соединениях. Координационный полиэдр центрального атома можно описать как искаженную квадратную антипризму и искаженный додекаэдр, соответственно. Еще большие различия наблюдаются во внешней сфере комплексных соединений. Кристаллы иодидного соединения содержат некоординированные иодид-ионы, молекулу BU и две молекулы воды. В полииодидном соединении катионы вместе с одиночными ионами  $I^-$  образуют трехмерный каркас, в каналах которого находятся линейные ионы  $I_3^-$ , объединенные слабыми взаимодействиями в бесконечные линейные цепи.

**Выводы.** Замена иодид-иона на полииодид-ион в комплексных соединениях редкоземельных элементов с ВU приводит к изменению как внутренней сферы катионного комплекса, так и внешней сферы, включая супрамолекулярный уровень. Присутствие бесконечных линейных цепей из атомов иода в структуре полииодидов комплексов лантанидов с ВU позволяет ожидать наличие анизотропной электропроводности вдоль этого направления.

**Ключевые слова:** лантаниды, самарий, иодид, полииодид, кристаллическая структура, анизотропия

**Для цитирования:** Корнилов А.Д., Григорьев М.С., Савинкина Е.В. Сравнение иодидов и полииодидов комплексов редкоземельных элементов с биуретом. *Тонкие химические технологии*. 2022;17(2):172–181. <https://doi.org/10.32362/2410-6593-2022-17-2-172-181>

## INTRODUCTION

One of the iodine features is its tendency to catenation, which results in the existence of numerous polyiodide ions [1]. At present, several hundred such compounds have been synthesized and structurally characterized, but so far, no regularities in the formation of certain polyiodide ions have been revealed. Even in the relatively simple  $\text{NMe}_4\text{I}-\text{I}_2$  system, several unusual compounds have recently been discovered [2]. It is believed that large polyiodide anions should be stabilized by large cations, including complex ones. These include complexes of rare earth elements (REE). Several such compounds have been prepared, with only the polyiodides of REE complexes with urea (Ur) being systematically studied.  $[\text{Ln}(\text{Ur})_8][\text{I}_5][\text{I}_3][\text{I}_2]$  ( $\text{Ln} = \text{La}-\text{Nd}, \text{Sm}-\text{Dy}$ ),  $[\text{Ln}(\text{Ur})_7][\text{I}_3]$  ( $\text{Ln} = \text{Ho}, \text{Er}$ ),  $[\text{Tm}(\text{Ur})_7][\text{I}_3] \cdot 2\text{I}_2$ , and  $[\text{Ln}(\text{Ur})_6][\text{I}_3]$  ( $\text{Ln} = \text{Yb}, \text{Lu}, \text{Sc}$ ) were isolated and structurally characterized [3–7]. It is noteworthy that the interaction of iodides of the above REEs (except Sc) with Ur produces isostructural compounds  $[\text{Ln}(\text{Ur})_4(\text{H}_2\text{O})_4]\text{I}_3$  [8]. The interaction of REE iodides with biuret ( $\text{NH}_2\text{CONHCONH}_2$ , BU) and iodine resulted in formation of isostructural compounds  $[\text{Ln}(\text{BU})_4][\text{I}_5][\text{I}_2]$  ( $\text{Ln} = \text{La}, \text{Nd}, \text{Gd}$ ) [9]. Regarding the corresponding iodide compounds, only two examples have been found in the literature.

In the  $\text{ErI}_3-\text{BU}-\text{H}_2\text{O}$  system, an incongruently soluble compound of the composition  $\text{ErI}_3 \cdot 4\text{BU}$ , characterized by infrared (IR) spectroscopy [10], was found, and the crystal structure of  $[\text{Gd}(\text{BU})_4]\text{I}_3 \cdot \text{BU} \cdot 2\text{H}_2\text{O}$  was studied [11].

The study aimed to synthesize and characterize iodide and polyiodide of a samarium complex with biuret and compare the obtained results with data on similar compounds of other REEs.

## EXPERIMENTAL

Reagents produced in Russia were used.

**Synthesis of  $[\text{Sm}(\text{BU})_4]\text{I}_3 \cdot \text{BU} \cdot 2\text{H}_2\text{O}$  (1).** Samarium oxide (reagent grade, 2.45 g) was treated with hydroiodic acid (anal. grade), previously purified by distillation in the presence of hypophosphorous acid; the resulting solution was evaporated until crystallization began, then cooled. The resulting crystals of samarium iodide hydrate were mixed with biuret (pur., 1.45 g), at that, crystallization water was released. To homogenize the reaction mixture, a few more distilled water drops were added and the mixture was left for a month for crystallization. The resulting light-yellow prismatic crystals were separated and dried.

**Synthesis of  $[\text{Sm}(\text{BU})_4][\text{I}_5][\text{I}]_2$  (2).** Synthesis was carried out similarly, but in the presence of iodine (reagent grade, 5.36 g). The reaction product is black opaque crystals of the elongated prism form.

IR absorption spectra were recorded with an EQUINOX 55 FT-IR spectrometer (Bruker, Germany). Samples were prepared as KBr pellets for the range of 50–4000  $\text{cm}^{-1}$  and as suspensions in Nujol placed on high density polyethylene (HDPE) windows for the range of 50–600  $\text{cm}^{-1}$ .

The crystal structure of **1** was studied with a KAPPA APEX II autodiffractometer (Bruker, Germany)<sup>1</sup>, MoK $\alpha$  radiation (0.71073 Å) at 100 K. The unit cell parameters were refined over the entire data set along with data processing.<sup>2</sup> Absorption corrections were introduced into the experimental reflection intensities.<sup>3</sup> The structure was solved by the direct method [12] and refined by the Least Squares method in the anisotropic approximation for all nonhydrogen atoms [13]. The H atoms of organic ligands are placed in geometrically calculated positions with isotropic temperature factors equal to 1.2 of equivalent isotropic factor of the N atom with

which they are bonded. The H atoms of crystallization water molecules were localized on the difference Fourier synthesis of electron density and refined with limited O–H distances and H–O–H angles and with  $U_{iso} = 1.5U_{eq}(\text{O})$ . The atomic coordinates and thermal parameters for the crystal structure **1** were deposited at the Cambridge Crystallographic Data Center<sup>4</sup> under the CCDC 2120579 number. The main experimental parameters and crystallographic characteristics of compound **1** are given in Table 1.

## RESULTS AND DISCUSSION

In the interaction of REE iodides with BU, polyiodides form more easily than the corresponding iodide complexes. Even if iodine is not added during the synthesis, the formation of not iodide, but polyiodide compounds often occur; in this case, the iodine necessary for the reaction form by the oxidation of  $\text{I}^-$  with atmospheric oxygen. In the case of samarium Sm, both compounds were obtained:  $[\text{Sm}(\text{BU})_4]\text{I}_3 \cdot \text{BU} \cdot 2\text{H}_2\text{O}$  (**1**) and  $[\text{Sm}(\text{BU})_4][\text{I}_5][\text{I}]_2$  (**2**).

**Table 1.** Crystal data, data collection, and refinement parameters for structure **1**

Characteristic	Value
Empirical formula	$\text{C}_{10}\text{H}_{29}\text{I}_3\text{N}_{15}\text{O}_{12}\text{Sm}$
$M$	1082.53
Crystal system	Triclinic
Space group	$P-1$
$a$ , Å	10.3152(3)
$b$ , Å	12.7034(4)
$c$ , Å	13.8461(4)
$\alpha$ , °	98.439(2)
$\beta$ , °	103.658(2)
$\gamma$ , °	112.284(1)
$V$ , Å <sup>3</sup>	1574.04(8)
$Z$	2
$T$ , K	100(2)
$D_{\text{calc}}$ , $\text{g cm}^{-3}$	2.284
$\mu(\text{K}\alpha)$ , $\text{mm}^{-1}$	4.880
Scan range, °	2.84–29.96
Index ranges	$-14 \leq h \leq 14; -17 \leq k \leq 17; -19 \leq l \leq 19$
Crystal dimensions, mm	$0.240 \times 0.300 \times 0.320$
Reflections collected	33839
Independent reflections	9075
Number of parameters refined	382
Goodness of fit	1.093
Final $R/wR$ [ $I \geq 2\sigma(I)$ ]	0.0323/0.0704

<sup>1</sup> APEX2, Bruker AXS Inc., Madison, Wisconsin, USA, 2006

<sup>2</sup> SAINT-Plus (Version 7.68), Bruker AXS Inc., Madison, Wisconsin, USA, 2007

<sup>3</sup> Sheldrick G. M. SADABS. Madison, Wisconsin (USA): Bruker AXS, 2008

<sup>4</sup> Cambridge Crystallographic Data Center, <http://www.ccdc.cam.ac.uk/conts/retrieving.html>

X-ray diffraction analysis of compound **1** was performed. The crystals contain: the  $[\text{Sm}(\text{BU})_4]^{3+}$  cation, coordination number is 8; uncoordinated iodide ions; a biuret molecule and two water molecules (Fig. 1). Structure **1** is isostructural to the analogous Gd compound [11]. However, the unit cell parameters determined in [11] differ from those given in Table 1. Parameters  $a$ ,  $b$ , and  $c$  are close for both structures; however, for structure **1**, all angles are greater than  $90^\circ$ , while for the Gd compound, they are smaller. This difference is due to the rules for choosing a standard cell, which require that the diagonals of the cell faces are not shorter than its edges. When the edge  $b$  is replaced in the standard elementary cell of the Gd compound ( $a = 10.374(4) \text{ \AA}$ ,  $b = 12.897(5) \text{ \AA}$ ,  $c = 13.854(5) \text{ \AA}$ ,  $\alpha = 71.46(3)^\circ$ ,  $\beta = 76.06(2)^\circ$ ,  $\gamma = 66.87(2)^\circ$ ) with the diagonal of the face  $ab$ , the parameters of the nonstandard cell ( $a = 10.374 \text{ \AA}$ ,  $b = 12.994 \text{ \AA}$ ,  $c = 13.854 \text{ \AA}$ ,  $\alpha = 97.08^\circ$ ,  $\beta = 103.94^\circ$ ,  $\gamma = 114.11^\circ$ ) are close to those given in Table 1 for the Sm compound.

It should be noted that in other previously studied Sm complex compounds with BU,  $[\text{Sm}(\text{BU})_4](\text{ClO}_4)_3$  [14] and  $[\text{Sm}(\text{BU})_4](\text{NO}_3)_3$  [15], outer-sphere BU molecules are absent.

Each BU molecule is coordinated through two oxygen atoms. The shape of the coordination polyhedron, as for the Gd compound, is a distorted square antiprism. The Sm–O bond lengths are 2.358(3)–2.442(3)  $\text{\AA}$ . It can be noted that the inner-sphere BU molecules are in the cis configuration,

while the outer-sphere molecules are in the trans configuration stabilized by an intramolecular H bond. In this case, the inner-sphere BU molecules are not planar, in contrast to the outer-sphere one: the angles between the OCN planes of two fragments of BU molecules are  $5.82^\circ$ – $15.41^\circ$  and  $2.02^\circ$ , respectively. In addition, for three ligands, a noticeable rotation of the Sm–O bonds about the mean plane of the ligand is observed, the torsion angles Sm–O–O–C are  $147^\circ$ – $157^\circ$  (for the fourth molecule, about  $176^\circ$ ). The outlet of the Sm atom from the planes of BU molecules is almost 1  $\text{\AA}$ . It should be noted that the single planar Sm–Bu fragment does not form H bonds with the outer-sphere BU molecules and water (it participates only in H bonds with the neighboring complex cation). Apparently, this favors the greater electron density delocalization along the chelate cycle [16, 17].

In structure **1**, the outer-sphere BU molecules are located among the complex cations and are united with them, as well as with crystallization water molecules and iodide ions, by H bonds. In this case, layers of complex cations and outer-sphere BU molecules can be seen in the structure; these layers are interconnected by water molecules (Fig. 2). The formation of hydrogen bonds of the N–H...O and O–H...O types leads to the formation of a three-dimensional framework, which is very characteristic of N,O-containing compounds [18–20].

For compound **2**, it was not possible to grow crystals suitable for X-ray diffraction analysis,

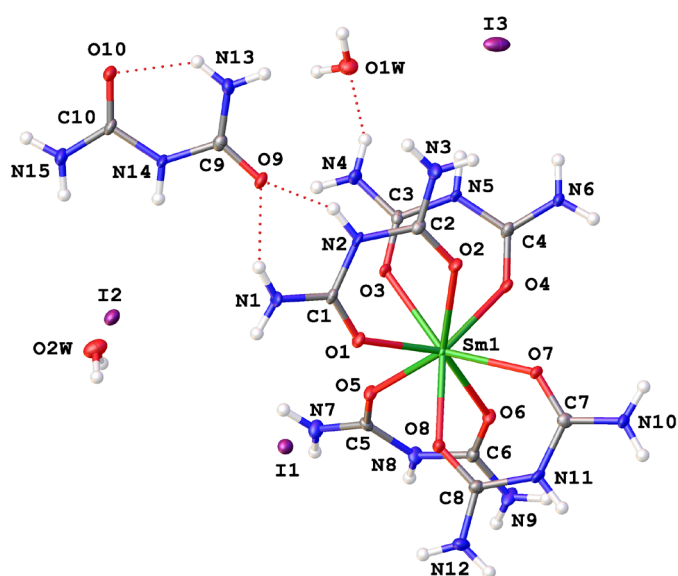


Fig. 1. Molecular structure of  $[\text{Sm}(\text{BU})_4]\text{I}_3 \cdot \text{BU} \cdot 2\text{H}_2\text{O}$  (**1**); ellipsoids 50%. H-bonds are shown with dotted lines.

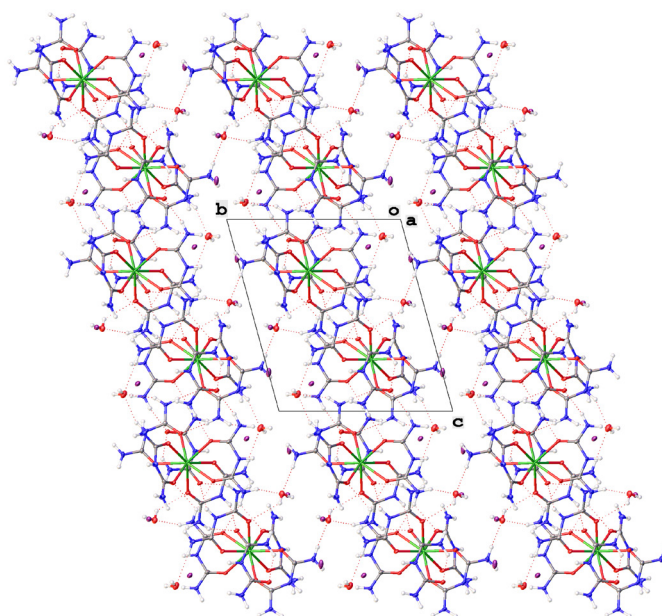


Fig. 2. Crystal packing of  $[\text{Sm}(\text{BU})_4]\text{I}_3 \cdot \text{BU} \cdot 2\text{H}_2\text{O}$  (**1**).

as well as to obtain high-quality powder diffraction patterns. Therefore, it was studied by IR spectroscopy in the region from 40 to 4000  $\text{cm}^{-1}$ . The main bands and their assignment for **2** and similar La, Nd, and Gd compounds are given in Table 2.

The  $\nu(\text{CO})$  frequency shifts towards lower values and  $\delta(\text{NH}_2)$  towards higher values indicates that BU is coordinated to Sm via O atoms. The bands at 71 and 95  $\text{cm}^{-1}$  in the compound **2** spectrum are assigned to  $\delta(\text{I-I-I})$ , and at 144  $\text{cm}^{-1}$ —to  $\nu(\text{I-I})$

**Table 2.** IR spectra of  $[\text{Ln}(\text{BU})_4][\text{I}_3][\text{I}]_2$

Biuret [17]	Ln				Assignment
	La [9]	Nd [9]	2 [this work]	Gd [9]	
	73 95	67 95	71 95	70 94	$\delta(\text{I-I-I})$
	144	144	143	143	$\nu(\text{I-I})$
	200 213	198 218	197 215	195 215	$\delta(\text{OMO}) + \nu_s(\text{MO})$
	–	242	241	250	$\delta(\text{OMO})$
	302	295 309	294	282 300	$\delta(\text{OMO}) + \nu_{\text{as}}(\text{MO})$
	399 421 444	395 442 457	397 417 445	398 415 446	$\nu_{\text{as}}(\text{MO})$
	496 522	482	490 522	487	$\pi(\text{MOC}) + \rho_r(\text{NH}_2)$
	591	582	582	582	$\pi(\text{NH}) + \delta(\text{MOC})$
710	643	648	647	650	$\delta(\text{C=O})$
770	770	769	769	770	$\delta(\text{C-NH}_2)$
946	945	944	944	948	$\nu(\text{CN}) + \nu(\text{C-NH}_2)$
1323	1330	1327	1326	1332	$\delta(\text{NH})$
1423 1499	1481	1480	1480	1487	$\nu(\text{CN}) + \nu(\text{C-NH}_2)$
1585	1608	1605	1607	1610	$\delta(\text{NH}_2)$
1719	1698	1688	1696	1700	$\nu(\text{CO})$
3254	3209 3259	3238 3272	3208 3269	3211 3264	$\nu_s(\text{NH}_2)$
3415	3405	3408	3388	3407	$\nu_{\text{as}}(\text{NH}_2)$

of polyiodide chains [21]. It should be noted that the compound **2** IR spectrum almost completely coincides with the spectra of previously studied Ln, Nd, and Gd polyiodides [9], especially in the long-wavelength region, where the characteristic vibrations of polyiodide particles are located.

Based on the isostructurality of  $[\text{Ln}(\text{BU})_4][\text{I}_5][\text{I}]_2$  (Ln = La, Nd, Gd) [9] and analysis of IR spectra (especially in the long wavelength region, which is extremely sensitive to the structure of the polyiodide anion), it can be assumed that the Sm compound also belongs to this isostructural series.

Polyiodide compounds, like iodide compounds, contain the complex cation  $[\text{Ln}(\text{BU})_4]^{3+}$ , but its structure differs from that of the cation in iodide compounds. Pairs of BU molecules and Ln atoms in  $[\text{Ln}(\text{BU})_4][\text{I}_5][\text{I}]_2$  are located in two almost perpendicular planes. The outlet of Ln atoms from the planes of BU molecules does not exceed 0.1 Å. The Ln coordination polyhedron can be described as a distorted dodecahedron.

The absence of water can be explained by the fact that poorly hydrated polyiodide ions are displaced from the aqueous medium into the solid phase, preventing water molecules from being fixed in the crystal lattice. This phenomenon can be used for further synthesis of anhydrous REE compounds, which are widely used [22].

Stabilization of polyiodide anions can be realized in two ways: polyiodide ions can be included in a supramolecular framework built by cations, or they themselves can form a framework, and cations will be located in its cavities [23]. In the previously studied polyiodides of amide complexes, the second variant was observed. However, in the case of BU compounds, it is the cations (together with single  $\text{I}^-$  ions) that form a three-dimensional framework, in the channels of which there are linear  $\text{I}_5^-$  ions, united by weak interactions into infinite linear chains, which should cause the presence of anisotropic electrical conductivity along this direction [9].

## REFERENCES

1. Svensson P.H., Kloo L. Synthesis, structure, and bonding in polyiodide and metal iodide–iodine systems. *Chem. Rev.* 2003;103(5):1649–1684. <https://doi.org/10.1021/cr0204101>
2. Petrov A.A., Fateev S.A., Zubavichus Y.V., Dorovatovskii P.V., Khrustalev V.N., Zvereva I.A., Petrov A.V., Goodilin E.A., Tarasov A.B. Methylammonium polyiodides: remarkable phase diversity of the simplest and low-melting alkylammonium polyiodide system. *J. Phys. Chem. Lett.* 2019;10(19):5776–5780. <https://doi.org/10.1021/acs.jpcllett.9b02360>

## CONCLUSIONS

An analysis of the iodides and polyiodides structure of REE complexes with BU showed that they contain  $[\text{Ln}(\text{BU})_4]^{3+}$  cationic complexes of the same composition but different structures. The complexes differ significantly in the mutual arrangement of the BU ligands and in the coordination polyhedra. Even greater differences can be noted in the outer-sphere of complex compounds. Iodide ions, water molecules, and uncoordinated BU, combined with complex cations by hydrogen bonds are in the outer-sphere of iodide compounds. In the outer-sphere of polyiodides, there are iodide ions, which together with complex cations form a three-dimensional framework, and pentaiodide ions, united by weak contacts into infinite linear chains. At the same time, there are no noticeable interactions between the polyiodide chains and the rest of the complex compound.

Thus, the replacement of the iodide ion by the polyiodide ion in REE–BU complex compounds leads to the change in both the inner-sphere and the outer-sphere of the cationic complex, including the supramolecular level.

## Acknowledgments

The study was performed using the equipment of the Centers for Collective Use of the MIREA–Russian Technological University and Frumkin Institute of Physical Chemistry and Electrochemistry, Russian Academy of Sciences, with the support of the Ministry of Science and Higher Education of the Russian Federation.

## Authors' contributions

**A.D. Kornilov** – synthesis and analysis of compounds, IR spectroscopy;

**M.S. Grigoriev** – X-ray diffraction analysis;

**E.V. Savinkina** – overall supervision, literature review, analysis of results, and writing the text of the article.

*The authors declare no conflicts of interest.*

## СПИСОК ЛИТЕРАТУРЫ

1. Svensson P.H., Kloo L. Synthesis, structure, and bonding in polyiodide and metal iodide–iodine systems. *Chem. Rev.* 2003;103(5):1649–1684. <https://doi.org/10.1021/cr0204101>
2. Petrov A.A., Fateev S.A., Zubavichus Y.V., Dorovatovskii P.V., Khrustalev V.N., Zvereva I.A., Petrov A.V., Goodilin E.A., Tarasov A.B. Methylammonium polyiodides: remarkable phase diversity of the simplest and low-melting alkylammonium polyiodide system. *J. Phys. Chem. Lett.* 2019;10(19):5776–5780. <https://doi.org/10.1021/acs.jpcllett.9b02360>

3. Alikberova L.Y., Mishin N.N., Mytareva A.I., Rukk N.S. Synthesis and structure of lanthanides iodide complexes with iodine and carbamide. *Tonk. Khim. Tekhnol. = Fine Chem. Technol.* 2008;3(3):61–64 (in Russ.).
4. Savinkina E.V., Golubev D.V., Grigoriev M.S. Synthesis and structural characterization of polyiodides of rare-earth urea complexes: Crystal structures of  $[\text{Ho}(\text{Ur})_7][\text{I}_3]_3$  and  $[\text{Pr}(\text{Ur})_8][\text{I}_5][\text{I}_3]_2[\text{I}_2]$ . *J. Coord. Chem.* 2015;68(23):4119–4129. <https://doi.org/10.1080/00958972.2015.1102230>
5. Savinkina E.V., Golubev D.V., Grigoriev M.S., Albov D.V. Iodine networks in polyiodides of M(III) urea complexes: Crystal structures of  $[\text{V}(\text{Ur})_6][\text{I}_3]_3$  and  $[\text{Dy}(\text{Ur})_8][\text{I}_5][\text{I}_3]_2[\text{I}_2]$ . *Polyhedron.* 2013;54(4):140–146. <https://doi.org/10.1016/j.poly.2013.02.026>
6. Alikberova L.Yu., Lyssenko K.A., Rukk N.S., Mytareva A.I. Carbamide-containing complexes of lanthanides: competition of hydrogen bonding and polyiodide ion formation. *Mendeleev Commun.* 2011;21(4):204–205. <https://doi.org/10.1016/j.mencom.2011.07.011>
7. Savinkina E.V., Golubev D.V., Grigoriev M.S. Synthesis, characterization, and crystal structures of iodides and polyiodides of scandium complexes with urea and acetamide. *J. Coord. Chem.* 2019;72(2):347–357. <https://doi.org/10.1080/00958972.2018.1555328>
8. Savinkina E.V., Golubev D.V., Podgornov K.V., Albov D.V., Grigoriev M.S., Davydova M.N. Different types of coordinated urea molecules in its complexes with rare-earth iodides and perchlorates. *Z. Anorg. Allgem. Chem.* 2013;639(1):53–58. <https://doi.org/10.1002/zaac.201200267>
9. Savinkina E.V., Golubev D.V., Grigoriev M.S., Komilov A. Synthesis and crystal structure of rare-earth biuret complexes with linear pentaiodide ions: Infinite polyiodide chains in a cationic framework. *J. Mol. Struct.* 2021;1227(5):129526. <https://doi.org/10.1016/j.molstruc.2020.129526>
10. Rukk N.S., Zaitseva M.G., Alikberova L.Y., Stepin B.D. Interaction of erbium iodide with biuret in an aqueous medium at 25°C. *Z. Neorgan. Khim. = Russ. J. Inorg. Chem.* 1989;34(10):2610–2612 (in Russ.).
11. Alikberova L.Y., Antonenko T.A., Albov D.V. Biuret complexes of lanthanum bromide and gadolinium iodide. *Tonk. Khim. Tekhnol. = Fine Chem. Technol.* 2015;10(1):66–71 (in Russ.).
12. Sheldrick G.M. A short history of SHELX. *Acta Crystallogr. Sect. A.* 2008;64(1):112–122. <https://doi.org/10.1107/S0108767307043930>
13. Sheldrick G.M. Crystal structure refinement with SHELXL. *Acta Crystallogr. Sect. C.* 2015;71(1):3–8. <https://doi.org/10.1107/S2053229614024218>
14. Haddad S.F. Structure of tetrakis(biuret)samarium(III) perchlorate. *Acta Crystallogr. Sect. C.* 1988;44(5):815–818. <https://doi.org/10.1107/S010827018800054X>
15. Haddad S.F. Structure of tetrakis(biuret)samarium(III) nitrate,  $[\text{Sm}(\text{NH}_2\text{CONHCONH}_2)_4](\text{NO}_3)_3$ . *Acta Crystallogr. Sect. C.* 1987;43(10):1882–1885. <https://doi.org/10.1107/S0108270187089753>
16. Adane L., Bharatam P.V. Tautomeric preferences and electron delocalization in biurets, thiobiurets, and dithiobiurets: An *ab initio* study. *Int. J. Quant. Chem.* 2008;108(7):1277–1286. <https://doi.org/10.1002/qua.21629>
17. Wang M.L., Zhong G.Q., Chen L. Synthesis, Optical Characterization, and Thermal Decomposition of Complexes Based on Biuret Ligand. *Int. J. Optics.* 2016;2016:5471818. <https://doi.org/10.1155/2016/5471818>
18. Hansen P.E. A spectroscopic overview of intramolecular hydrogen bonds of NH...O,S,N type. *Molecules.* 2021;26(9):2409. <https://doi.org/10.3390/molecules26092409>
3. Alikberova L.Y., Mishin N.N., Mytareva A.I., Rukk N.S. Synthesis and structure of lanthanides iodide complexes with iodine and carbamide. *Tonk. Khim. Tekhnol. = Fine Chem. Technol.* 2008;3(3):61–64 (in Russ.).
4. Savinkina E.V., Golubev D.V., Grigoriev M.S. Synthesis and structural characterization of polyiodides of rare-earth urea complexes: Crystal structures of  $[\text{Ho}(\text{Ur})_7][\text{I}_3]_3$  and  $[\text{Pr}(\text{Ur})_8][\text{I}_5][\text{I}_3]_2[\text{I}_2]$ . *J. Coord. Chem.* 2015;68(23):4119–4129. <https://doi.org/10.1080/00958972.2015.1102230>
5. Savinkina E.V., Golubev D.V., Grigoriev M.S., Albov D.V. Iodine networks in polyiodides of M(III) urea complexes: Crystal structures of  $[\text{V}(\text{Ur})_6][\text{I}_3]_3$  and  $[\text{Dy}(\text{Ur})_8][\text{I}_5][\text{I}_3]_2[\text{I}_2]$ . *Polyhedron.* 2013;54(4):140–146. <https://doi.org/10.1016/j.poly.2013.02.026>
6. Alikberova L.Yu., Lyssenko K.A., Rukk N.S., Mytareva A.I. Carbamide-containing complexes of lanthanides: competition of hydrogen bonding and polyiodide ion formation. *Mendeleev Commun.* 2011;21(4):204–205. <https://doi.org/10.1016/j.mencom.2011.07.011>
7. Savinkina E.V., Golubev D.V., Grigoriev M.S. Synthesis, characterization, and crystal structures of iodides and polyiodides of scandium complexes with urea and acetamide. *J. Coord. Chem.* 2019;72(2):347–357. <https://doi.org/10.1080/00958972.2018.1555328>
8. Savinkina E.V., Golubev D.V., Podgornov K.V., Albov D.V., Grigoriev M.S., Davydova M.N. Different types of coordinated urea molecules in its complexes with rare-earth iodides and perchlorates. *Z. Anorg. Allgem. Chem.* 2013;639(1):53–58. <https://doi.org/10.1002/zaac.201200267>
9. Savinkina E.V., Golubev D.V., Grigoriev M.S., Komilov A. Synthesis and crystal structure of rare-earth biuret complexes with linear pentaiodide ions: Infinite polyiodide chains in a cationic framework. *J. Mol. Struct.* 2021;1227(5):129526. <https://doi.org/10.1016/j.molstruc.2020.129526>
10. Rukk N.S., Zaitseva M.G., Alikberova L.Y., Stepin B.D. Interaction of erbium iodide with biuret in an aqueous medium at 25°C. *Z. Neorgan. Khim. = Russ. J. Inorg. Chem.* 1989;34(10):2610–2612 (in Russ.).
11. Alikberova L.Y., Antonenko T.A., Albov D.V. Biuret complexes of lanthanum bromide and gadolinium iodide. *Tonk. Khim. Tekhnol. = Fine Chem. Technol.* 2015;10(1):66–71 (in Russ.).
12. Sheldrick G.M. A short history of SHELX. *Acta Crystallogr. Sect. A.* 2008;64(1):112–122. <https://doi.org/10.1107/S0108767307043930>
13. Sheldrick G.M. Crystal structure refinement with SHELXL. *Acta Crystallogr. Sect. C.* 2015;71(1):3–8. <https://doi.org/10.1107/S2053229614024218>
14. Haddad S.F. Structure of tetrakis(biuret)samarium(III) perchlorate. *Acta Crystallogr. Sect. C.* 1988;44(5):815–818. <https://doi.org/10.1107/S010827018800054X>
15. Haddad S.F. Structure of tetrakis(biuret)samarium(III) nitrate,  $[\text{Sm}(\text{NH}_2\text{CONHCONH}_2)_4](\text{NO}_3)_3$ . *Acta Crystallogr. Sect. C.* 1987;43(10):1882–1885. <https://doi.org/10.1107/S0108270187089753>
16. Adane L., Bharatam P.V. Tautomeric preferences and electron delocalization in biurets, thiobiurets, and dithiobiurets: An *ab initio* study. *Int. J. Quant. Chem.* 2008;108(7):1277–1286. <https://doi.org/10.1002/qua.21629>
17. Wang M.L., Zhong G.Q., Chen L. Synthesis, Optical Characterization, and Thermal Decomposition of Complexes Based on Biuret Ligand. *Int. J. Optics.* 2016;2016:5471818. <https://doi.org/10.1155/2016/5471818>
18. Hansen P.E. A spectroscopic overview of intramolecular hydrogen bonds of NH...O,S,N type. *Molecules.* 2021;26(9):2409. <https://doi.org/10.3390/molecules26092409>

19. Shi X., Bao W. Hydrogen-bonded conjugated materials and their application in organic field-effect transistors. *Front. Chem.* 2021;9:723718. <https://doi.org/10.3389/fchem.2021.723718>

20. Galantsev A.V., Drobot D.V., Dorovatovsky P.V., Khrustalev V.N. Lanthanum complex with neridronic acid: synthesis and properties. *Tonk. Khim. Tekhnol. = Fine Chem. Technol.* 2019;14(2):70–77. <https://doi.org/10.32362/2410-6593-2019-14-2-70-77> (in Russ.).

21. Nour E.M., Chen L.H., Laane J. Far-infrared and Raman spectroscopic studies of polyiodides. *J. Phys. Chem.* 1986;90(13):2841–2846. <https://doi.org/10.1021/j100404a014>

22. Mishra S. Anhydrous scandium, yttrium, lanthanide and actinide halide complexes with neutral oxygen and nitrogen donor ligands. *Coord. Chem. Rev.* 2008;252(18–20):1996–2025. <https://doi.org/10.1016/j.ccr.2007.10.029>

23. Savastano M. Words in supramolecular chemistry: the ineffable advances of polyiodide chemistry. *Dalton Trans.* 2021;50(4):1142–1165. <https://doi.org/10.1039/D0DT04091F>

19. Shi X., Bao W. Hydrogen-bonded conjugated materials and their application in organic field-effect transistors. *Front. Chem.* 2021;9:723718. <https://doi.org/10.3389/fchem.2021.723718>

20. Galantsev A.V., Drobot D.V., Dorovatovsky P.V., Khrustalev V.N. Lanthanum complex with neridronic acid: synthesis and properties. *Tonk. Khim. Tekhnol. = Fine Chem. Technol.* 2019;14(2):70–77. <https://doi.org/10.32362/2410-6593-2019-14-2-70-77> (in Russ.).

21. Nour E.M., Chen L.H., Laane J. Far-infrared and Raman spectroscopic studies of polyiodides. *J. Phys. Chem.* 1986;90(13):2841–2846. <https://doi.org/10.1021/j100404a014>

22. Mishra S. Anhydrous scandium, yttrium, lanthanide and actinide halide complexes with neutral oxygen and nitrogen donor ligands. *Coord. Chem. Rev.* 2008;252(18–20):1996–2025. <https://doi.org/10.1016/j.ccr.2007.10.029>

23. Savastano M. Words in supramolecular chemistry: the ineffable advances of polyiodide chemistry. *Dalton Trans.* 2021;50(4):1142–1165. <https://doi.org/10.1039/D0DT04091F>

#### About the authors:

**Aleksandr D. Kornilov**, Master Student, N.A. Preobrazhensky Department of Chemistry and Technology of Biologically Active Compounds, Medicinal and Organic Chemistry, M.V. Lomonosov Institute of Fine Chemical Technologies, MIREA – Russian Technological University (86, Vernadskogo pr., Moscow, 119571, Russia). E-mail: sashakornilov@bk.ru. <https://orcid.org/0000-0001-6164-8650>

**Mikhail S. Grigoriev**, Dr. Sci. (Chem.), Chief Researcher, Head of the Laboratory of Analysis of Radioactive Materials, A.N. Frumkin Institute of Physical Chemistry and Electrochemistry, Russian Academy of Sciences (31, b. 4, Leninskii pr., Moscow, 119071, Russia), E-mail: grigoriev@ipc.rssi.ru. ResearcherID U-8572-2017, <https://orcid.org/0000-0002-6363-5535>

**Elena V. Savinkina**, Dr. Sci. (Chem.), Professor, A.N. Reformatskii Department of Inorganic Chemistry, M.V. Lomonosov Institute of Fine Chemical Technologies, MIREA – Russian Technological University (86, Vernadskogo pr., Moscow, 119571, Russia). E-mail: savinkina@mirea.ru. Scopus Author ID 8419176500, ResearcherID G-2949-2013, <https://orcid.org/0000-0002-2088-5091>

#### Об авторах:

**Корнилов Александр Денисович**, магистрант кафедры технологии биологически активных соединений, медицинской и органической химии им. Н.А. Преображенского Института тонких химических технологий им. М.В. Ломоносова ФГБОУ ВО «МИРЭА – Российский технологический университет» (119571, Россия, Москва, пр-т Вернадского, д. 86). E-mail: sashakornilov@bk.ru. <https://orcid.org/0000-0001-6164-8650>

**Григорьев Михаил Семёнович**, д.х.н., главный научный сотрудник, заведующий лабораторией анализа радиоактивных материалов, Институт физической химии и электрохимии им. А.Н. Фрумкина Российской академии наук (119071, Россия, Москва, Ленинский проспект, 31, корп. 4). E-mail: grigoriev@ipc.rssi.ru. ResearcherID U-8572-2017, <https://orcid.org/0000-0002-6363-5535>

**Савинкина Елена Владимировна**, д.х.н., профессор кафедры неорганической химии им. А.Н. Реформатского Института тонких химических технологий им. М.В. Ломоносова ФГБОУ ВО «МИРЭА – Российский технологический университет» (119571, Россия, Москва, пр-т Вернадского, д. 86). E-mail: savinkina@mirea.ru. Scopus Author ID 8419176500, ResearcherID G-2949-2013, <https://orcid.org/0000-0002-2088-5091>

*The article was submitted: December 17, 2021; approved after reviewing: February 22, 2022; accepted for publication: April 14, 2022.*

*Translated from Russian into English by H. Moshkov.  
Edited for English language and spelling by Quinton Scribner, Awatera.*

---

MIREA – Russian Technological University  
78, Vernadskogo pr., Moscow, 119454, Russian Federation.  
Signed to print on *April 30, 2022*.  
Not for sale

МИРЭА – Российском технологическом университет  
119454, РФ, Москва, пр-кт Вернадского, д. 78.  
Дата опубликования *30.04.2022*.  
Не для продажи

***[www.finechem-mirea.ru](http://www.finechem-mirea.ru)***

